Université de Bourgogne
Ecole doctorale Image et Modélisation des objets naturels

Mémoire d'
Habilitation à Diriger des Recherches
de

Marc Pansu

Chimie du sol et modélisation du cycle du carbone et de l'azote

Soutenu le 17 Février 2006

Devant le Jury

Luc Abbadie, Professeur Université Pierre et Marie Curie Paris, Rapporteur,
Francis Andreux, Professeur Université de Bourgogne, Président,
Jean Luc Chotte, Directeur de Recherche IRD, Examinateur,
Etienne Dambrine, Directeur de Recherche INRA, Rapporteur,
Catherine Hénault, Chargée de Recherche INRA, Examinatrice,
Bernard Saugier, Professeur Emérite Université Paris-Sud, Examinateur,
Christian Walter, Professeur Université de Rennes, Rapporteur.

SOMMAIRE

Curriculum vitae

Curriculum Vitae

Etat civil

Marc PANSU
Date de naissance : 26-04-1947,
Marié, 3 enfants,
Ingénieur de Recherche (INR hors classe), IRD, Montpellier

Parcours professionnel

- Depuis 2004 : ingénieur de recherche, UR séquestration du carbone et biofonctionnement des sols tropicaux (IRD Montpellier) et laboratoire Matière Organique des Sols Tropicaux (MOST, IRD-CIRAD, Montpellier), Recherche pédologique, agronomique et environnementale particulièrement sur modélisation cycle C et N, version anglaise ouvrage « L'analyse du sol – minéralogique, organique, minérale»
- 2001-2004 : ingénieur de recherche, UR séquestration du carbone dans les sols tropicaux (IRD Montpellier) et laboratoire Matière Organique des Sols Tropicaux (MOST, IRD-CIRAD, Montpellier), Recherche pédologique, agronomique et environnementale particulièrement sur modélisation cycle C et N, ouvrages analytiques de synthèse « L'analyse du sol »
- 1988-2000 : ingénieur de Recherche, Laboratoire de Comportement des Sols Cultivés, IRD Montpellier, Recherche pédologique et agronomique, développements analytiques, ouvrages analytiques de synthèse, modélisation cycle C et N.
- 1984-1988 : ingénieur, responsable du Laboratoire Matière Organique (6 Ingénieurs et Techniciens), IRD Bondy, Analyses et recherche analytique sur les matières organiques.
- 1976-1984 : ingénieur au laboratoire de Spectrographie, IRD Bondy, développements analytiques particulièrement en chimiométrie, éléments trace, et analyse organique.
- 1975-1976 : ingénieur au laboratoire IRD d'Adiopodoumé (RCI) d'analyses de sol, eau et végétaux, encadrement du laboratoire (25 Techniciens et Laborantins).
- 1972-1974 : allocataire de recherche au laboratoire de l'Energie Solaire CNRS de Font-Romeu, recherches sur la purification d'oxydes réfractaires au four solaire.
- 1967-1969 : assistant-ingénieur au laboratoire de l'ENSEE de Grenoble, recherches sur accumulateurs électrochimiques.

Recherche actuelle

- Modélisation du cycle du carbone et de l'azote dans les sols,
- Application à la modélisation de la fertilisation organique,
- Application à la modélisation du fonctionnement d'écosystèmes,

Valorisation et synthèse

- Secrétaire scientifique et premier auteur de livres de synthèse sur « L'analyse du sol » : un livre en français aux éditions Masson (Paris, Milan, Barcelone), un livre en anglais aux éditions Balkema (Lisse, Abingdon, Exton, Tokyo), un livre en français aux éditions Springer (Paris, Berlin, Heidelberg, New York, Hong Kong, Londres, Milan, Tokyo), un livre en anglais sous presse chez Springer.
- auteur de deux rubriques encyclopédiques sur le sol (encyclopédie sur internet http://webencyclo.com, rubrique « sol », éditions Atlas)

Expertise et animation scientique

- Expert « rewiever » revues scientifiques « Soil Biology & Biochemistry (Elsevier) », « Etude et gestion des sols (AFES) », « Nutrient cycling in agro-ecosystems (Kluwer) », « Waste management (Elsevier) », « Forest ecology and management ».
- conférences sur l'analyse du sol et expertise de laboratoires d'analyse au Pérou et en Bolivie (2000),
- membre de la Commission scientifique sectorielle 1 de l'IRD : physique et chimie de l'environnement planétaire,
- expertise de dossiers de carrières, jury de concours, évaluation d'unités de recherche,
- organisateur de séminaires scientifiques mensuels (troisième Jeudi de chaque mois depuis 2001) sur la communauté scientifique Agropolis de Montpellier (IRD, CIRAD, CNRS, INRA, ENSAM, Université Montpellier II, CNEARC, CEMAGREF, ENGREF). Le thème des exposés concerne toutes les disciplines en relation avec les sols. Une large part consacrée à la discussion favorise les échanges et coopérations entre scientifiques de la communauté.

Enseignement

- Participation à l'encadrement de 40 stagiaires au laboratoire de spectrographie de l'IRD Bondy (dont co-encadrement de 5 thèses), 20 stagiaires au laboratoire Matières Organiques de l'IRD Bondy (dont co-encadrement d'une thèse), 45 stagiaires au laboratoire LCSC de l'IRD Montpellier (dont co-encadrement de 5 thèses et responsable principal de 8 stagiaires), 20 stagiaires au laboratoire MOST de l'IRD Montpellier (dont co-encadrement de 3 thèses et responsable principal de 9 stagiaires).
- Organisation et participation à des enseignements pour adultes dans le cadre du CNRS-Formation, Groupement pour l'Avancement des Méthodes Spectroscopiques (GAMS), IRD-formation : chimiométrie, outil informatique en chimie analytique, plans d'expériences, méthodes d'optimisation.
- Conférences à publics scientifiques : universités de Syrie, Bolivie, Pérou, cycle mensuel Agropolis Montpellier.
- Conférences grand public et lycée : fête de la science, festival « L'avenir au naturel » (L'Albenc, Isère).
- Participation à l'enseignement de la filière Ecosystèmes, Ecole doctorale Sibaghe, université Montpellier II.

Coopération

Programmes et projets internationaux

1998-2003 – Partenaire du programme Européen Tropandes INCO-DC ERBIC18CT98-0263, Fertility management in the tropical andean mountains : agroecological bases for a sustainable fallow agriculture, union de partenaires boliviens, vénézuéliens, espagnols, hollandais et français (IRD, CNRS, Université).

Partenaire du projet DUSSOL par le programme ANR ECCO 2005 "Recyclage des déchets urbains solides dans les zones agricoles péri-urbaines (Ouagadougou, Burkina Faso): bio-indicateurs de qualité des sols et compostage des résidus organiques", Coordinateur D. Masse, accepté pour 2006.

Soumission 2006 : projet ECOS-Nord France- Vénézuela : Dynamique de la matière organique du sol dans les écosystèmes vénézuéliens et son importance dans le controle de l'érosion.

En prévision : programmes ECO-PNBC et INCO-DEV

Partenaires scientifiques

CEFE-CNRS Montpellier, France,
CIRAD Montpellier, France,
INRA Montpellier, France,
Entreprise Phalippou Frayssinet (Fertilisants organique, Tarn, France),
IRD et INERA, Ouagadougou Burkina Faso,
Laboratoire d'Ecologie microbienne des sols tropicaux, IRD Sénégal
EMBRAPA, Sao Paulo, Brésil ;
Instituto de Investigaciones Agrobiologicas de Galicia, Santiago de Compostella, Espagne,
Instituto de ciencias ambientales y ecologicas, Facultad de ciencias, Merida, Venezuela,
Universidad mayor de San Andres, Instituto de Ecologia, La Paz, Bolivie,
Plant Research International, location born Zuid Wageningen, Pays Bas,
Laboratoire d'écophysiologie végétale, Université de Paris-Sud, Orsay, France

Formation

Diplomante

- Habilitation à Diriger des Recherches de l'Université de Bourgogne « Chimie du Sol et Modélisation du cycle du Carbone et de l'Azote », soutenu le 17 Février 2006 à Dijon.
- Doctorat de l'Université Montpellier II, « Chimie du sol et cycle du carbone et de l'azote » soutenu le 28 Janvier 2005, Ecole Doctorale Biologie Intégrative, Procédure Validation des Acquis de l'Expérience
- Ingénieur diplômé de l'Ecole Nationale Supérieure de Chimie de Toulouse (ENSCT, 1972),
- Admission à l'ENST par la voie du Centre Universitaire d'Education et de Formation des Adultes (CUEFA Grenoble, 1969),
- DEST par CUEFA Grenoble (1968),
- BTS par Lycée Technique d'Etat de Vizille (1967),

Stages

- Caractérisation moléculaire de substances naturelles, Faculté de pharmacie Châtenay-Malabry, 1 mois en 1984
- Plans d'expérience et Méthodes d'optimisation, CACEMI (arts et métiers, Paris) 1 semaine en 1984
- Modélisation du cycle du carbone (modèle de Rothamsted, GB), Laboratoire de radio-agronomie CEA Cadarache, 1 semaine en 1986
- Méthodologie de la recherche expérimentale, Université Aix-Marseille, 1 semaine en 1988
- Simulation des systèmes complexes, IRD-Université d'Orléans, 2 semaines en1996

Langues

- Langue maternelle : Français
- Autres langues : Anglais (écrit et parlé), Espagnol (notions)

Publications des 5 dernières années

Revues à comité de lecture

L. Thuriès, M. -C. Larré-Larrouy et M. Pansu, 2000. - Evaluation of three incubation designs for mineralization kinetics of organic materials in soil. *Communications in Soil Science and Plant Analysis*, 31, 289-304

L. Thuries, A. Arrufat, M. Dubois, C. Feller, P. Herrmann, M.C. Larre-Larrouy, C; Martin, M. Pansu, J.C. Remy et M. Viel, 2000. – Influence d'une fertilisation organique et de la

solarisation sur la productivité maraîchère et les propriétés d'un sol sableux sous abri. *Etude et Gestion des sols*, 7, 73-88.

L. Thuriès, M. Pansu, C. Feller, P. Hermann, et J.C. Rémy. 2001 – Kinetics of added organic matter decomposition in a mediterranean sandy soil. Soil Biology & Biochemistry 33, 997-1010.

L. Thuriès, M. Pansu, M.C. Larre-Larrouy et C. Feller. 2002 – Biochemical composition and mineralization kinetics of organic inputs in a sandy soil. Soil Biology & Biochemistry 34, 239-250.

M. Pansu et L. Thuriès 2003 – Kinetics of C and N mineralization, N immobilization and N volatilization of organic inputs in soil. Soil Biology & Biochemistry, 35, 37-48.

M. Pansu, L. Thuriès, M.C. Larré-Larrouy et P. Bottner, 2003 – Predicting N transformations from organic inputs in soil in relation to incubation time and biochemical composition. Soil Biology & Biochemistry, 35, 353-363.

M. Pansu, P. Bottner, L. Sarmiento, et K. Metselaar, 2004 - Comparison of five soil organic matter decomposition models using data from a ^{14}C and ^{15}N labeling field experiment, Global Biogeochemical Cycles, 18, GB4022, doi:10.1029/2004GB002230.

P. Bottner, M. Pansu, R. Callisaya, K. Metselaar, D. Hervé, 2005 - Modelización de la evolución de la materia orgánica en suelos en descanso (Altiplano seco boliviano). Ecologia en Bolivia, sous presse.

L. Thuriès, D. Bastianelli, F. Davrieux, L. Bonnal, R. Oliver, M. Pansu, and C. Feller, 2005 - Prediction by NIRS of the composition of plant raw materials from the organic fertiliser industry and of crop residues from tropical agrosystems. J. of Near Infrared Spectroscopy, 13, 187-199.

M. Pansu, L. Sarmiento, K. Metselaar, D. Hervé and P. Bottner, 2006 - Dynamics of transformations and sequestration of soil organic matter in two contrasting ecosystems. European J. of Soil Science, in correction.

P. Bottner, M. Pansu, L. Sarmiento, D. Hervé, R. Callisaya-Bautista, K. Metselaar, 2006 - Factors controlling decomposition of soil organic matter in the fallow systems of the high tropical Andes: a field simulation approach using ^{14}C and ^{15}N labelled plant material. Soil Biology & Biochemistry, in press.

Livres

M. Pansu, J. Gautheyrou et J.Y. Loyer, 2001 - *Soil analysis* - sampling, *instrumentation and quality control*, translated from French by V.A.K. Sarma, Balkema, Lisse Abingdon, Exton, Tokyo, New Delhi, Calcutta, 489 p.

M. Pansu et J. Gautheyrou, 2003 - *L'analyse du sol* – minéralogique, organique et minérale, Springer, Paris, Berlin, Heidelberg, New York, Hong Kong, Londres, Milan, Tokyo, 995 p.

M. Pansu et J. Gautheyrou, 2006 – Soil analysis – mineralogical, organic and inorganic, Springer, in press.

Communication à congrès internationaux

L. Thuriès and M. Pansu, 2001 - Classification and modelling of added organic matter decomposition in a sandy soil. Proceeding of 11th Nworkshop, Reims, France, 9-12 Sept. 2001.

M. Pansu, L. Thuriès, M.C. Larré-Larrouy et C. Feller, 2002 – Kinetics of organic inputs in soil carbon model. Proceeding of 17th World Congress of soil science, Bangkok, 14-21 August 2002, Oral communication 1502, symposium10.

M. Pansu et P. Bottner, 2002 – Modélisation de l'effet des racines actives sur les transferts de C organique dans les sols. Proceeding of congress Gestion de la biomasse, erosion et sequestration du carbone, Agropolis Montpellier, 23-28 Septembre 2002.

L. Thuriès et M. Pansu, 2002 – Classification et modélisation de la décomposition de matières organiques ajoutées au sol. Proceeding of congress Gestion de la biomasse, erosion et sequestration du carbone, Agropolis Montpellier, 23-28 Septembre 2002.

Communication à congrès nationaux

M. Pansu and P. Bottner, 2001. – Modélisation de l'effet des racines actives sur les transferts de carbone organique dans les sols. Actes 3° colloque rhizosphère, Dijon, 26-28 Nov. 2001

M. Pansu, L. Thuriès, MC Larre-Larrouy et C. Feller, 2002. – Dynamique de minéralisation d'apports organiques dans les modèles carbone du sol. *Actes Journées Nationales d'Etude des Sols AFES*, 22-24 Octobre 2002, Orléans.

Marc Pansu et Pierre Bottner, 2004 - Comparaison de modèles de décomposition de matière organique du sol à l'aide de données expérimentales *in situ* de traceurs ^{14}C et ^{15}N. Communication orale aux *Journées Nationales d'étude des sols AFES* de Bordeaux, France, 26-28 Octobre 2004

Marc Pansu et Pierre Bottner, 2004 - Dynamique des matières organiques du sol. Séminaire, IFR Ecosystems, Agropolis international, Montpellier, 16 Décembre 2004.

Marc Pansu et Pierre Bottner, 2005 - Marquage isotopique 14C et 15N *in situ* et modèles de décomposition de matière organique du sol. Journée des isotopes stables, Vendredi 21 Octobre 2005, Muséum d'histoire naturelle, Paris.

L. Thuriès, R. Oliver, F. Davrieux, D. Bastianelli et M. Pansu, 2006 - Transformations des apports organiques : application du modèle TAO à des matières de l'agro-industrie à partir de leur analyse biochimique mesurée ou estimée par Spectrométrie Proche Infra-Rouge (SPIR). Communication au séminaire "Les matières organiques en France" « Réseau Matières Organiques » et Groupe Français de l'International Humic Substance Society, 22-24 janvier, Côte d'Azur, France

Marc Pansu[1] et Pierre Bottner[2], 2006 - Mise au point de modèles de dynamique des matières organiques du sol. Communication au séminaire "Les matières organiques en France" « Réseau Matières Organiques » et Groupe Français de l'International Humic Substance Society, 22-24 janvier, Côte d'Azur, France

Information scientifique

M. Pansu, 2000. – Le sol et son analyse. *Fréquence Chimie*, 28, 2-9.

M. Pansu et F. Doumenge, 2000. – Modélisation des transferts de carbone et d'azote dans les sols, poster fête de la science.

M. Pansu, 2001. – Le sol : formation, fonctions et composition. In Encyclopédie francophone sur Internet Webencyclo http://webencyclo.com, rubrique «sol »editions Atlas

M. Pansu, 2001. – Le sol : méthodes d'analyse. In Encyclopédie francophone sur Internet Webencyclo http://webencyclo.com, rubrique «sol »editions Atlas

Conférences

M. Pansu et J.P. Rossignol, 2001. Le sol - formation, fonctions, composition, dégradation. Application aux formations en terrasses de la basse vallée de l'Isère. Grand public, 5° Festival « L'avenir au naturel » L'Albenc Isère, 1 Sept. 2001.

M. Pansu, 2001. Le sol - formation, fonctions, composition, dégradation. Public BTS, Fête de la science, 16 Oct. 2001.

Pansu M, 2001. Modélisation de la dynamique des matières organiques des sols, Cycle mensuel Agropolis Montpellier, coordinateur M. Pansu, 15 Mars 2001.

Pansu M, 2002. Cinétique des entrées organiques dans les modèles de décomposition. Cycle mensuel Agropolis Montpellier, coordinateur M. Pansu, 17 Septembre 2002

M. Pansu, 2002. Modélisation de la dynamique des matières organiques dans les sols. Public scientifique et enseignement supérieur, étudiants INA-PG, 4 Décembre 2002.

M. Pansu, 2003. Modélisation de la transformation des apports organiques dans les sols. Public scientifique et enseignement supérieur, étudiants INA-PG, Décembre 2003.

L. Thuriès et M. Pansu, 2006. La fertilisation organique et sa modélisation. Etudiants master2 pro, DEA Fennec, ENSAM Montpellier, 30 Janvier 2006, 5 h.

Activité de synthèse, animation, expertise, enseignement

Valorisation et synthèses

L'analyse du sol

Ce livre de synthèse a été entrepris à la demande des Commissions scientifiques 2 et 7 et de la Direction Générale de l'IRD en 1991. Il constitue maintenant un outil de travail performant pour le laboratoire MOST et le laboratoire central d'analyses du CIRAD, notre partenaire à Montpellier.

Auteurs : M. Pansu, J Gautheyrou et JY Loyer (in Memoriam, J.Susini, décédé en 1994), ainsi que des collaborateurs pour compléments et corrections,

Secrétaire scientifique : M. Pansu,

Objectif : pour chaque chapitre, il s'agissait de réunir une compilation d'une expérience collective de laboratoire et d'une analyse bibliographique s'appuyant sur les normes internationales et françaises et comportant souvent de très nombreuses références ; il s'agissait aussi de combler une lacune, les ouvrages sur ce thème étant assez peu nombreux surtout en Français,

Résultats : deux ouvrages en français et un deux en anglais sous les références qui suivent.

M. Pansu, J. Gautheyrou et J.Y. Loyer, 1998 –L'analyse du sol – *échantillonnage, instrumentation et contrôle*, Masson, Paris, Milan, Barcelone, 489 p.

M. Pansu, J. Gautheyrou et J.Y. Loyer, 2001 - *Soil analysis - sampling, instrumentation and quality control*, translated from French by V.A.K. Sarma, Balkema Publishers, Lisse, Abington, Exton, Tokyo, 489 p.

M. Pansu et J. Gautheyrou, 2003 - *L'analyse du sol – minéralogique, organique et minérale*, Springer, Paris, Berlin, Heidelberg, New York, Hong Kong, Londres, Milan, Tokyo 995 p.

M. Pansu et J. Gautheyrou, 2006 – Soil analysis – mineralogical, organic and inorganic. Springer, sous presse.

Impact : les deux éditions en Français ont été rapidement épuisées; des discussions sont en cours pour nouvelle édition en Français; les témoignages montrent que ces ouvrages sont devenus une référence pour les laboratoires.

Rubriques encyclopédiques

- auteur en 2001 de deux rubriques encyclopédiques sur le sol (Encyclopédie francophone Webencyclo sur internet http://webencyclo.com, rubrique « sol », éditions Atlas) :

– Le sol : formation, fonctions et composition

– Le sol : méthodes d'analyse

NOUVEAUTE

L'ANALYSE DU SOL

ÉCHANTILLONNAGE, INSTRUMENTATION ET CONTRÔLE

Marc PANSU,
Jacques GAUTHEYROU,
Jean-Yves LOYER

Préface de M. Pinta et A. Herbillon

Recherche
1997, 512 pages
395 F.

Mieux connaître les outils de l'analyse des sols pour mieux les utiliser: tel est l'objectif de cet ouvrage.

Face aux méthodes et techniques d'analyse de plus en plus nombreuses, ce volume a été Conçu Comme un guide qui permettra d'abord de choisir la méthode adaptée au problème et ensuite de la mettre en oeuvre.

La première partie est consacrée aux problèmes d'échantillonnage, qu'il s'agisse du choix des échantillons, de leur prélèvement ou de leur conditionnement et fractionnement.

Les questions liées à l'analyse proprement dite et au contrôle des résultats font l'objet de la seconde partie. Les principales méthodes physico-chimiques, notamment spectroscopiques et chromatographiques, y sont présentées successivement de manière détaillée. Les techniques d'automatisation au laboratoire et de contrôle statistique de la qualité des résultats sont exposées en fin d'ouvrage.

Ce manuel de référence dresse l'inventaire des outils d'échantillonnage, d'analyse et de contrôle dont disposent aujourd'hui les « sciences du sol ».

LE PUBLIC

Les chimistes spécialisés en physico-chimie analy- tique. les ingénieurs, les chercheurs et les techni- ciens concernés par les sciences du sol que ce soit dans le domaine de l'agronomie, de la climatologie, de la géologie, de l'environnement, du génie civil ou de l'industrie minérale et organique associée au sol.

LES AUTEURS

Marc Pansu et Jacques Gautheyrou sont ingénieurs de recherche spécialisés en sciences du sol à l'institut français de recherche scientifique pour le développement en coopération (OrstomJ.

Jean- Yves loyer est pédologue, directeur de recherche à l'Orstom.

L'ANALYSE DU SOL

CONTENU

Prélèvement d'échantillons

Premiers tests de terrain

Préparation des échantillons

Matériels de broyage et tamisage

Premiers tests qualitatifs au laboratoire

Balances analytiques

Séparations sur filtres et membranes

Présentation des techniques analytiques

Spectrométrie moléculaire, d'absorption atomique, d'émission

Ionométrie

Techniques chromatographiques

Chromatographie en phase gazeuse, en phase liquide

Analyse élémentaire CHN-OS

Automatisation et robotique au laboratoire

Contrôle de qualité des résultats analytiques

BON DE COMMANDE

Je désire commander: ..... exemplaire(s) de **L'ANALYSE DU SOL - Échantillonnage, instrumentation et contrôle de M. Pansu, J. Gautheyrou etJ.-Y.Loyer**, au prix de 375 F* au lieu de 395 F. (ISBN 2 225 831 30 0)

Frais d'envoi: pour 1 vol. 20 F (étranger : 30 F), pour chaque volume supplémentaire 10 F.

Envoi par avion: nous consulter. Franco de port pour toute commande supérieure à 1 000 F .

Ci.ioint mon chèque .....F libellé à l'ordre de MASSON Éditeur

NOM.....Prénom.....

Adresse.....

Code postal..... Ville..... Pays.....

à ***compléter et*** à ***retourner*** à

MASSON Éditeur

5, rue laromiguière -75005

Paris

•Prix public TTC au 01.12.97

MASSON

SOIL ANALYSIS

Sampling, instrumentation and quality control

by

M.PANSU, J.GAUTHEYROU & J.-Y.LOYER

24 cm, 500 pp., EUR 85.00/ $85.00/ £57
ISBN 90 5410 7162

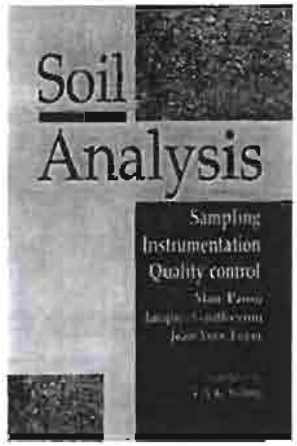

A translation of *L'analyse du sol: Echantillonnage, instrumentation et contrôle*, Masson, Paris, 1998. The objective of this book is to provide a better understanding of soil-analysis tools in order to use them more efficiently. Given the increasing number of analytical methods and techniques, this book has been designed as a guide that will enable first the selection of the method appropriate to the problem and, then, its execution. The first part is devoted to sampling problems, which encompass selection, withdrawing, drying and fractionation of samples. Problems related to the actual analysis and to quality control of the results form the subject of the second part. Principal physicochemical methods, especially spectroscopic and chromatographic, are sequentially presented in detail. Techniques of laboratory automation and of statistical quality control of the results are explained at the end of the book. This reference manual presents the list of tools for sampling, analysis and quality control currently available for "soil science".

CONTENTS:

ORDER FORM

Please send me .... copies of:

o Pansu. Soil analysis, Hardback. €85.00 / US$85.00 / £57

Private customers living within the EC have to add 6% VAT to their payment

Payment by personal cheque drawn on a bank in the USA, or credit card. Master Card / VISA / American Express / Diners Club / Eurocard

Card number: ☐☐☐☐☐☐☐☐☐☐☐☐☐☐☐☐ Cvc number: ☐☐☐

Expiry date: Signature:

Name

Address:

City & Country:

A.A.Balkema Publishers, P.O. Box 1675, Rotterdam, Netherlands

Tel.: (+31.10) 41 45 822 Fax: (+ 31.10) 41 35 947 Internet: www.Balkema.nl

A Word about the Cover Illustration

I have the notion (and I enjoy persisting with this notion) that the shapes liked by living matter are everywhere the same, true for all small objects or large geographical areas. In this spirit, I have desired in these landscapes to confuse the scale in such a manner that it will be uncertain whether the painting represents a vast area of mountains or a tiny parcel of land. I feel that, having found these rhythms of matter and being provided with any object, the painter could endow that object with life.

Many persons have imagined that because of a disparaging bias I like to show unfortunate things. How I have been misunderstood! I had wished to reveal to them that these things they consider ugly or have forgotten to see are also great wonders.

Jean Dubuffet, commentary on his paintings
'Population on the soil, 1952'
and 'Fruits of earth, 1960'.

Vient de paraître

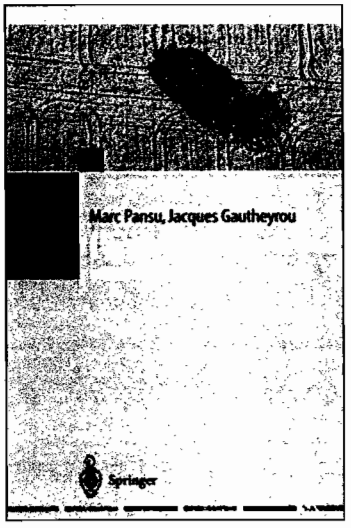

M. Pansu, J. Gautheyrou, IRD, Montpellier, France

L'analyse du sol
Minéralogique, organique, minérale

2003. XIX, 993 p. Broché **62 €***, ISBN 2-287-59774-3

Rédigé en conformité avec les normes analytiques, partie intégrante de la démarche qualité, cet ouvrage est un guide de référence pour les choix méthodologiques puis pour la mise en œuvre des nombreuses méthodes, normalisées ou non, de l'analyse du sol.

Il synthétise une multitude d'informations techniques dans des protocoles, tableaux, formules, modèles de spectres, chromatogrammes et autres diagrammes analytiques. Les modes opératoires sont diversifiés, depuis les tests les plus simples jusqu'aux déterminations les plus complexes – physico-chimie structurale des édifices minéralogiques et organiques, éléments échangeables, potentiellement disponibles et totaux, pesticides et polluants, éléments traces et isotopes.

Outil de base, il sera particulièrement utile aux chercheurs, ingénieurs, techniciens, professeurs et étudiants spécialisés en pédologie, agronomie, sciences de la terre et de l'environnement, ainsi qu'aux disciplines connexes telles que physico-chimie analytique, géologie, hydrologie, écologie, climatologie, génie civil et industries associées aux sols.

BON DE COMMANDE

à retourner à
votre libraire spécialisé
ou, à défaut, à

Springer-Verlag
Customer Service Books/
Haberstr. 7
D-69126 Heidelberg/Allemagne
Tél. : 00800 777 46437
(appel gratuit)
Fax : 00 49 6221 345 4229
e-mail : orders@springer.de

http://www.springer.de

Je désire commander :

.... Ex L'analyse du sol 2-287-59774-3 **62 €***

Nom : ..... Prénom : .....
Adresse : .....
.....
Code postal : ..... Ville : .....
Date : Signature :

Mode de règlement : ❑ chèque ❑ carte de crédit
n : ..... date de validité : .....
MONTANT TOTAL : .....

***Prix TTC en France** (livres : 5,5% TVA, produits électroniques : 19,6% TVA incl.). **Dans d'autres pays, la TVA locale est applicable.**
Participation aux frais de port : 1 ouvrage 5 € (+ 1,50 € par ouvrage supplémentaire) France métropolitaine uniquement.
Les prix indiqués et autres détails sont susceptibles d'être modifiés sans avis préalable.

Expertise et animation scientifique

Expertise

- Expert « reviewer » revues scientifiques « Soil Biology & Biochemistry (Elsevier) », « Etude et gestion des sols (AFES) », « Nutrient cycling in agro-ecosystems (Kluwer) », « Waste management (Elsevier) », « Forest Ecology and Management (Elsevier) ».
- conférences sur l'analyse du sol et expertise de laboratoires d'analyse au Pérou et en Bolivie (2000),
- membre de la Commission scientifique sectorielle 1 de l'IRD : physique et chimie de l'environnement planétaire,
- expertise de dossiers de carrières, jury de concours, évaluation d'unités de recherche,

Animation de séminaires Agropolis

- organisateur de séminaires scientifiques mensuels depuis 2001 (troisième Jeudi de chaque mois si possible) sur la communauté scientifique Agropolis de Montpellier (IRD, CIRAD, CNRS, INRA, ENSAM, Université Montpellier II, CNEARC, CEMAGREF, ENGREF). Le thème des exposés concerne toutes les disciplines en relation avec les sols et l'environnement, ils sont maintenant devenus les séminaires de l'IFR Ecosystem et Ph. Hinsinger (INRA) m'aide pour leur organisation. Une large part consacrée à la discussion favorise les échanges et coopérations entre scientifiques de la communauté. Ont déjà eu lieu les exposés suivant :

Intervenant	Date	Titre
Barthès B, IRD	25.05.00	Agrégation des sols et sensibilité au ruissellement et à l'erosion
Traoré K, U-Mali	30.06.00	Rôle du parc à karités sur le statut organique et la fertilité
Pansu M, IRD	15.03.01	Modélisation de la dynamique des matières organiques des sols
Prat C, IRD	05.04.01	Mise en valeur agricole des sols volcaniques indurés du Mexique
Babre D,Cirad	26.04.01	La certification dans les laboratoires d'analyse
Roose E, IRD	11.05.01	Evolution des stratégies de lutte anti-érosive
Larré MC, IRD	28.06.01	Utilisation des composts en agriculture: tests de maturité
Bourgeon G, Cirad	04-10-01	Niveaux d'organisation des couvertures pédologiques: applications en Inde
Feller C Manlay R, IRD	26-10-01	Concepts sur humus et durabilité au cours des trois derniers siècles
Hervé D, IRD	22-11-01	Bassin versant et usage du sol: le divorce ?
Gigou J, Cirad	17-01-02	Culture sur billons de niveau, rendements et gestion de l'eau
Braudeau E, IRD	21-02-02	La rétractométrie des sols
Warembourg F, CNRS	21-03-02	Racine vivante et flux de carbone dans les sols
Blavet D, IRD	25-04-02	La couleur des sols
Saison C, Cirad	23-05-02	Devenir des polluants organiques dans les sols contaminés

Poss R, IRD	27-06-02	La salinisation des rizières en Thaïlande
Davrieux F et Lecomte P, Cirad	20-09-02	Applications environnementales de la Spectrométrie dans le Proche Infra-Rouge (SPIR)
Pansu M, IRD	17-10-02	Cinétique des entrées organiques dans les modèles de décomposition
Saugier B, U-Paris Sud	14-11-02	Biosphère continentale, changements globaux et puits de carbone
Asseline J, IRD	19-12-02	Le drone Pixy pour l'observation aérienne rapprochée
Blanchart E. et Feller C., IRD	23-01-03	Darwin et les vers de terre
Drevon J.J., INRA	20-02-03	Phosphore et fixation symbiotique de l'azote en sols peu fertilisés
Hinsinger Ph., INRA	27-03-03	Interactions chimiques sol-racines dans la rhizosphère
Browers M., CIRAD	24-04-04	La compaction des sols
Rollin D., CIRAD	15-05-03	Le semis direct sous couvert végétal : intérêt et limite
Peoples M., CSIRO Australie	10-07-03	N dynamics in Australian pasture systems : Nfixation, Nmineralisation and crop uptake of pasture N
Hamel O, CIRAD Epron D., U Nancy 1	18-09-03	Flux de CO_2 et H_2O et séquestration de carbone sur les peuplements d'Eucalyptus du Congo
Carcaillet C., HPHE	16 10-03	Paléo-incendies et cycle du carbone.
Legros J.P. ENSAM, Sec. Gén. AFES[1]	20-11-03	Aspects actuels de la cartographie des sols
Ruellan A., ex prés. IUSS[2]	18-12-03	La formation aux sols
Swift M., ex Dir. Prog. TSBF[3], accueil IRD	22-01-04	Tropical Soil Biology and Fertility
Pinay G., Cefe-CNRS	26-02-04	Activité dénitrifiante à différentes échelles dans les paysages hétérogènes
Le Roux C, LSTM, UMR 113,IRD/CIRAD/INRA/AGRO	25-03-04	Biodiversité des bactéries fixatrices d'azote
Franche C., IRD, UMR 1098	22-04-04	La symbiose fixatrice d'azote *Casuarina-Frankia*
Eschenbrenner V., IRD, UR Seq-C	13-05-04	Le protocole de Kyoto: chronique d'une mort annoncée
Dosso M., CNEARC, UMR Sagert	16-06-04	Systèmes pédologiques et systèmes de culture: exemple d'un domaine viticole
Basile F., CNRS, UMR 5059	16-09-04	Science du sol et archéologie
Gruau G., CNRS, UMR 6118	16-10-04	Quand les eaux de surface s'enrichissent en matière organique. Causes globales ou effets locaux
Pansu M. et Bottner P., IRD-Cefe-CNRS	16-12-04	Dynamique des matières organiques du sol
Martineau Y. et Saugier B., U. Orsay	20-01-05	Modélisation de production de jachère (Faprom)
Martineau Y.	20-01-05	Outils informatiques de modélisation
Lesturgez G., IRD	10-02-05	Enracinement des cultures en sols sableux instables
Courchesne, U. Montréal	10-03-05	Cycles biogéochimiques et signaux environnementaux dans Bouclier Canadien

Noble A., IMWI, Asie du Sud-est	23-03-05	Environmentally manageable fertilizers: a new approach
Saint-André L., Cirad, UPR-80 ETP	14-04-05	Modèles de croissance en forêt et cycles biogéochimiques
Trolard F., INRA Aix en P, UR géochimie sols et eaux	19-05-05	La fougérite : des évidences de terrain à l'homologation du minéral
Munch J.C., institut écologie, GSF, Munich	25-05-05	Field site denitrification and N_2O emissions in agricultural soils
Dreyfus F., UMR 951 INRA Montpellier	23-06-05	Approche de la sociologie à partir de la notion de système –exemple du diffusionnisme
Bolger T., CSIRO, Canberra	7-07-05	Vegetation dynamics in Australian temperate grasslands: the role of N and belowground competition
Dulcire M., Cirad UPR Innov. et dynam. Expl. Agr.	29-09-05	Pour une recherche opérationnelle en partenariat
Brauman A., UR SeqBio IRD	17-11-05	Formation microbiologique par et pour la recherche en pays en voie de développement
Le Cadre-Barthelemy E, INRA Montpellier :	15-12-05	Maîtriser la volatilisation d'ammoniac après apport d'engrais

Modélisation des transferts de carbone et d'azote dans les sols

Le carbone et l'azote sont des éléments constitutifs importants des êtres vivants. La compréhension de leurs cycles – c'est-à-dire les états sous lesquels on les rencontre et les processus biochimiques qui les font passer d'un état à l'autre – est nécessaire. Étant donné la complexité de ces cycles et leurs interactions, leur modélisation est une étape incontournable. Le modèle MOMOS (MOdélisation des Matières Organiques dans les Sols), mis au point par une équipe de pédologues et chimistes, est un modèle mathématique des cycles du carbone et de l'azote dans les sols. Momos peut s'adapter aux sols du monde entier.

Domaines d'application

Le modèle Momos peut être utilisé dans les domaines des sciences du sol, de l'agronomie, la climatologie, la géologie, l'environnement et la qualité des eaux, pour :

- mieux comprendre les mécanismes microbiologiques et biochimiques dans les sols ;
- prédire l'évolution des systèmes de culture et écosystèmes, apporter des corrections ;
- quantifier les émissions atmosphériques de CO_2 et N_2O et leurs conséquences sur les changements globaux de la planète ;
- prévoir l'entraînement des nitrates dans les nappes phréatiques.

Le taux de gaz carbonique atmosphérique influence la température de la planète, la croissance des plantes et la décomposition de la nécromasse. Les pratiques culturales sont donc fortement impliquées dans les changements globaux de la planète.

Cycle du carbone organique (C)

Le carbone provenant du gaz carbonique (CO_2) atmosphérique alimente la croissance des plantes (photosynthèse) et indirectement d'autres organismes vivants de la planète (biosphère). Recueillant ces organismes après leur mort, le sol constitue le "puits de mort" de la biosphère. Il reçoit ainsi la nécromasse labile (facilement décomposable) et la [redacted]. La nécromasse sert d'aliment à la [redacted] dont la respiration restitue le gaz carbonique à l'atmosphère (minéralisation). Les premiers stades de décomposition fournissent des métabolites labiles alors qu'une faible partie du carbone est stabilisée sous forme de composés humiques (humification). Des métabolites labiles sont également apportés aux sols par les racines des plantes actives (rhizodéposition).

Un modèle à compartiments est composé d'un diagramme de flux et d'un système d'équations. Momos est un système de sept équations différentielles gouverné par douze coefficients en relation avec les données climatiques (radiation, température, pluviométrie), le type de sol, la végétation et la qualité biochimique des flux de nécromasse.

Marc Pansu (IRD), Zaher Sallih (CNRS), Pierre Bottner (CNRS)

Institut de recherche pour le développement

Diagramme Momos des flux C et N du sol, en relation avec l'atmosphère, l'hydrosphère et la biosphère

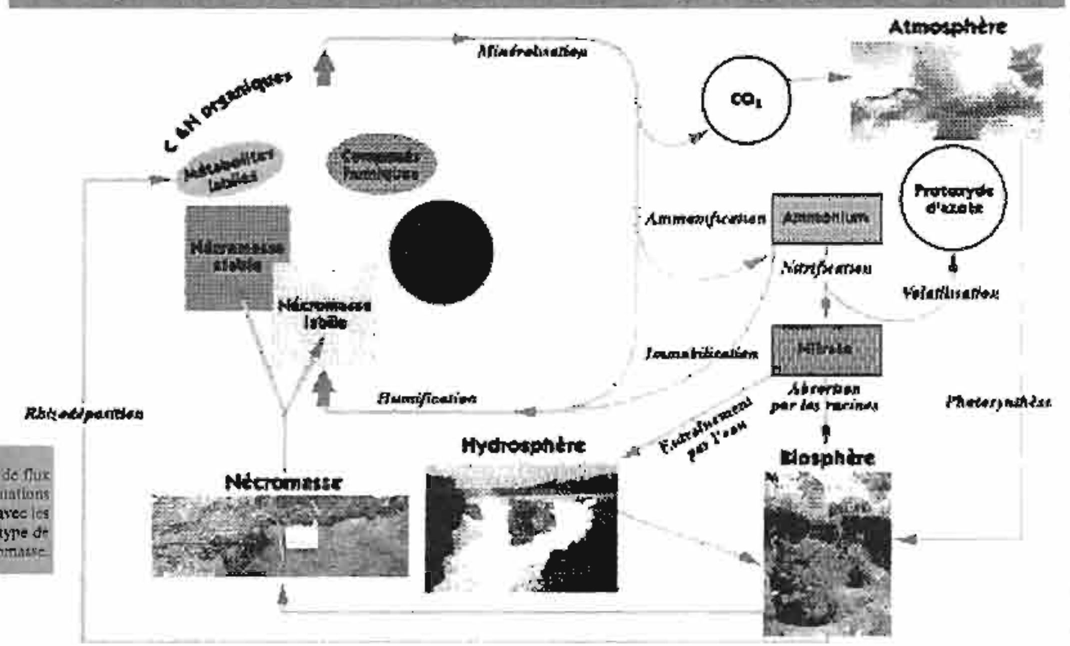

Cycle de l'azote (N)

La minéralisation fournit de l'ammonium (ammonification) qui peut être à nouveau consommé par les microorganismes (immobilisation) ou transformé en nitrates (nitrification). En milieu aéré, les nitrates sont essentiels à la croissance des plantes. L'ion nitrate est aussi le moins retenu par le complexe d'échange des sols et migre facilement dans les eaux (hydrosphère), dont il devient l'un des principaux polluants. Durant les processus de transformation de l'azote minéral en ammonium et en nitrate, une partie de N peut être perdue sous forme gazeuse (volatilisation) essentiellement en protoxyde d'azote, responsable en partie de la pollution atmosphérique.

Pour en savoir plus

- Sallih Z. and Pansu M. (1993) Modelling of soil carbon forms after organic amendment under controlled conditions. *Soil Biology & Biochemistry* 25, 1755-1762
- Pansu M., Sallih Z. et Bottner P. (1996) Modélisation des formes du carbone organique dans les sols. *Comptes Rendus Acad. Sci. Paris* 322 IIa, 401-406
- Pansu M., Sallih Z. and Bottner P. (1998) Modelling of soil nitrogen forms after organic amendment under controlled conditions. *Soil Biology & Biochemistry* 30, 19-29
- Bottner P., Pansu M. et Sallih S. (1999) Modelling the effect of active roots on soil organic matter turnover. *Plant an Soil* 216, 15-25

Enseignement

Divers

- Organisation et participation à des enseignements pour adultes dans le cadre du CNRS-Formation, Groupement pour l'Avancement des Méthodes Spectroscopiques (GAMS), IRD-formation : chimiométrie, outil informatique en chimie analytique, plans d'expériences, méthodes d'optimisation (Cf. liste bibliographique en Annexe). Parmi celles-ci :
  - La programmation des microrordinateurs, le langage Basic et son utilisation au laboratoire, GAMS PARIS, cycle "l'outil informatique en chimie analytique", 1984, 1985, 1986, 1987.
  - Gestion de fichiers de données : exemples d'applications au laboratoire, GAMS PARIS, cycle "l'outil informatique en chimie analytique", 1984, 1985, 1986, 1987.
  - Méthodes d'optimisation des conditions expérimentales en spectrométrie atomique : principes, informatisation, applications, CNRS-formation-IVRY, cycle "Spectrométrie atomique par émission et absorption : application à l'analyse", 1986.
  - Optimisation des conditions expérimentales en spectrométrie atomique : plans d'expériences et méthodologie des surfaces de réponse", CNRS-Formation-BONDY, cycle "Spectrométrie d'émission et d'absorption atomique", 1986, 1987, 1988, 1989, 1990, 1991, 1992, 1993, 1994, 1995, 1996, 1997.
  - La mesure chimique, son intervalle de confiance et quelques tests liés à l'étude de sa précision, ORSTOM-DIVA-Formation, cycle "Valorisation informatique des données des laboratoires d'analyses physico-chimiques", 1987.
  - Aperçu des méthodes d'optimisation en physico-chimie analytique, ORSTOM-DIVA-Formation, cycle "Valorisation informatique des données des laboratoires d'analyses physico-chimiques", 1987.

- Conférences à publics scientifiques : universités de Syrie, Bolivie, Pérou, cycle mensuel Agropolis Montpellier (Cf. liste bibliographique en Annexe). Parmi celles-ci :
  - Caractérisation des matières organiques des sols en liaison avec leur dynamique d'évolution, Faculté d'agronomie, DAMAS, 1986.
  - M. Pansu, 1999. El analysis de suelo. Université de Lima, Puno, La Paz, Cochabamba. 20 transparents, 1 h de conférence + 1 h de discussions. Collaboration avec Dominique Hervé pour la traduction préalable du texte en espagnol et pour la traduction des questions.
  - M. Pansu, 2001. Modélisation des transferts de carbone et azote dans les sols. Public scientifique et enseignement supérieur, séminaires Agropolis, M. Pansu, organisateur

- Conférences grand public et lycée : fête de la science, festival « L'avenir au naturel » de L'Albenc, Isère (Cf. liste bibliographique en Annexe).

- Formation par la recherche :40 stagiaires au laboratoire de spectrographie de l'IRD Bondy (dont co-encadrement de 5 thèses), 20 stagiaires au laboratoire Matières Organiques de l'IRD Bondy (dont co-encadrement d'une thèse), 45 stagiaires au laboratoire LCSC de l'IRD Montpellier (dont co-encadrement de 5 thèses et responsable principal de 8 stagiaires), 20 stagiaires au laboratoire MOST de l'IRD Montpellier (dont co-encadrement de 3 thèses et responsable principal de 9 stagiaires).

Encadrement de stagiaires pour les cinq dernières années

Encadrant principal

- Thuriès Laurent, 2000 - (direction M. Pansu et Francis Ganry, Cirad) Transformation des apports organiques dans les sols, participation aux essais interlaboratoire de normalisation AFNOR. Post-doctorat.
- Garcia Léa, 2000 – (direction M. Pansu) Echantillonnage du carbone dans les sols. Stage DUT 2° année, IUT de Perpignan
- Garcia Léa, 2001 (direction M. Pansu). Hétérogénéité du carbone dans la matrice texturale des sols. Stage de MST, université de Pau.
- Donneaud Fanny, 2002 (direction M. Pansu et L. Thuriès) Comparaison de méthodes de dosage de CO_2 pour les cinétiques de minéralisation dans les sols. DUT Génie biologique, IUT de Montpellier, 35 p.
- Ginestet Elodie, 2002 (direction M. Pansu, L. Thuriès et M.C. Larré-Larrouy). Comparaison statistique de trois méthodes de détermination des teneurs en fibres et contenus cellulaires de différents apports organiques. DUT Génie biologique, IUT de Montpellier, 37 p.
- Cayeux Léo, 2003 (direction L. Thuriès et M. Pansu). Caractérisation de matières premières végétales : calibrage de la méthode « Near Infra Red Spectroscopy » (NIRS) à partir des résultats des méthodes classiques de dosage des constituants pariétaux et des polyphénols totaux. Mémoire de DUT Génie biologique, Option Industries alimentaires et biologiques, Université Montpellier II.
- Petit Fabien, 2003 (direction M. Pansu et L. Thuriès). Caractérisation de matières premières végétales par méthodes biochimique et spectroscopique (NIRS). Rapport de stage de 1^{e} année, Ecole Nationale Supérieure d'Ingénieurs en Arts Chimiques et Technologiques, Toulouse, 71 p.
- Lair Maïté, 2005 (direction M. Pansu). Transformation des Apports Organiques dans les Sols : validation du modèle TAO-C et TAO-N. Master M1 FENEC, Montpellier.

Assistance à l'encadrement (méthodes de laboratoire et traitement des données)

- Azontonde A.H., 2000 (direction C. Feller). Dynamique de la matière organique et de l'azote dans le système mucuna-maïs sur un sol ferrallitique (Terre de Barre) au Sud-Bénin. Thèse de Doctorat, ENSAM, Montpellier, 241 p.
- Diallo D., 2000 (direction E. Roose). Erosion des sols en zone soudanienne du Mali. Transfert des matériaux érodés dans le bassin versant de Djitiko (Haut Niger). Thèse de Doctorat, Université Grenoble I, 204 p.
- Manlay R., 2000 (direction C. Feller). Organic matter dynamics in mixed-farming systems of the West African savanna: a village case study from south Senegal. Thèse de Doctorat, ENGREF, Paris, 278 p.
- Khamsouk B., 2001 (direction E. Roose). Impact de la culture bananière sur l'environnement. Influence des systèmes de cultures bananières sur l'érosion, le bilan hydrique et les pertes en nutriments sur un sol volcanique en Martinique (cas du sol brun rouille à halloysite). Thèse de Doctorat, ENSAM, Montpellier, 220 p.
- Fruhling F., 2001 (co-direction B. Barthès). DESS de l'Université de Corte.
- Gervillas S., 2001 (direction M.C. Larré-Larrouy). Stage.
- Bourgeais E., 2002 (direction E. Blanchart). Redélimitation de l'aire géographique AOC de la canne à sucre à la Martinique. Mémoire d'ingénieur de l'Ecole Supérieure d'Agriculture d'Angers.
- De Luca E., 2002 (direction C. Feller). Matéria orgânica e atributos do solo em sistems de colheita com e sem queima da cana-de-açúcar. Thèse Université de São Paulo (Brésil), 101 p.

- Goidts E., 2002 (direction E. Blanchart). Etude des conditions agro-pédo-climatiques nécessaires à la culture de la canne à sucre dans le cadre de la révision de l'aire d'Appellation d'Origine Contrôlée « Rhum Agricole de la Martinique ». Mémoire d'ingénieur agronome, Université Catholique de Louvain-la-Neuve, Belgique.
- Razafimbelo T., 2002 (direction C. Feller et B. Barthès). Effet du non brûlis de la canne à sucre sur la séquestration de C dans un sol ferrallitique argileux (Brésil). DEA national Science du sol, 22 p.
- Beaumont L., 2002 (co-direction L. Thuriès) DAA Ecole Nationale Supérieure Agronomique et des Industries Agro-alimentaires, Nancy.
- Belem M., 2003 (co-direction R. Manlay). Modélisation informatique de systèmes complexes: le modèle MIROT. Mémoire d'ingénieur, Ecole Supérieure d'Informatique, Bobo-Diaoulasso, 68 p.
- Lô C., 2003 (co-direction L. Thuriès). Caractérisation physico-biochimique des litières de filao (*Casuarina equisetifolia*) en vue d'une amélioration de leur potentiel de minéralisation (C/N) pour une utilisation comme amendement organique et fertilisant dans la zone des Niayes du Sénégal. DEA Sciences Agronomiques, Ecole Nationale Supérieure Agronomique et des Industries Agro-alimentaires, Nancy.
- Al Karkouri J., 2003 (co-direction E. Roose). Thèse au Maroc.
- Enjalric F., 2004 (direction R. Manlay). DEA national de Science du Sol.
- Grandière I., 2004. (direction B. Barthès, C. Feller et E. Blanchart). Effet du semis direct sous couvert végétal sur la matière organique d'un sol ferrallitique argileux (Madagascar). DEA national de Science du Sol.
- Ripoche A., 2004 (direction E. Blanchart et B. Barthès). Influence du mode de gestion des terres sur le stockage du carbone et les propriétés biologiques du sol sur trois types de sol de la Martinique. Stage de césure INA-PG.
- Freschet G., 2005 (direction R. Manlay). Séquestration de carbone et agriculture durable dans les savanes d'Afrique de l'Ouest : synergie ou antagonisme ? Master M1 FENEC, Montpellier.
- Hien Edmond, 2004 (co-direction C. Feller). Dynamique du carbone dans un acrisol ferrique du centre ouest Burkina : influence des pratiques culturales sur le stock et la qualité de la matière organique du sol. Thèse de Doctorat, ENSAM, Montpellier.
- Metay A., 2005 (direction C. Feller). Séquestration de carbone et flux de gaz à effet de serre. Comparaison entre semis direct et système conventionnel dans les Cerrados brésiliens. Thèse INA-PG, Paris.
- Razafimbelo T., 2005 (direction C. Feller). Stockage et protection de carbone sous systèmes en semis direct avec couverture végétale des Hautes Terres malgaches. Thèse de Doctorat, ENSAM, Montpellier.
- Salomé C., 2005 (direction B. Barthès et E. Blanchart). Effet du mode de gestion des agrosystèmes sur la stabilité de l'agrégation dans des sols de Martinique. Master M1 FENEC, Montpellier.
- Testard T., 2005 (direction L. Lardy et R. Lensi). Analyse de la diversité fonctionnelle de la communauté microbienne hétérotrophe et de la communauté dénitrifiante dans un sol soumis à des pratiques culturales différentes. Master M1 FENEC, Montpellier.
- Youl S., prévu fin 2005 (direction R. Manlay). Thèse de Doctorat, ENSAM, Montpellier.

Stagiaires ayant collaboré particulièrement à mes recherches de modélisation

- Sidi Hachemi (1987) Effet de l'apport de matière organique et de gypse sur la stabilité structurale de sols de région méditerranéenne (Mateur, Tunisie). Thèse de Docteur Ingénieur de l'INA-PG, série Géologie appliquée.

Hachemi Sidi a préparé sa thèse à l'unité Matières organiques que je dirigeais à l'Orstom de Bondy de 1984 à 1988. Des incubations en conditions contrôlées nous ont permis de valider le modèle de Hénin, Monnier et Turc (1959) et de proposer notre formulation de modèles à deux ou trois compartiments. Une relation a ensuite été trouvée entre l'évolution des taux d'agrégats stables au benzène du sol et l'évolution des matières humifiées labiles et stables du modèle à trois compartiments, ouvrant la voie à la prédiction de la stabilité structurale du sol en fonction de son statut organique. Notre collaboration s'est poursuivie quelques temps avec l'INES agro-vétérinaire de Tiaret en Algérie où H. Sidi avait obtenu un poste de professeur.

- Sallih Zaher (1990) Relations entre activité rhizosphérique et décomposition de la matière organique des sols au niveau de la biomasse microbienne et de la minéralisation du carbone et de l'azote. Thèse de Doctorat, université des Sciences et Techniques du Languedoc, Montpellier II.

Zaher Sallih a préparé sa thèse au Cefe-CNRS de Montpellier et notre rencontre a été le début d'une collaboration fructueuse avec cet institut. Il a collecté des données de grande qualité provenant d'incubations de mélanges sols-paille de blé doublement marquée 14C et 15N en conditions contrôlées de laboratoire. Ces données nous ont conduit à proposer en 1993 un modèle à 5 compartiments (MOMOS-1) pour le cycle du carbone, puis d'étendre ce modèle au cycle de l'azote (1998) enfin à la prise en compte de l'influence des racines actives sur le cycle du carbone (1999).

- Thuriès Laurent. (1999) Effets de fertilisants organiques sur les propriétés d'un sol sableux maraîcher. Modélisation de leurs cinétiques de minéralisation et conséquences sur leurs procédés de fabrication industrielle. Thèse de Doctorat en Sciences du Sol, Ecole Nationale Supérieure Agronomique de Montpellier, 170 p.

Laurent Thuriès a été accueilli dans notre laboratoire de 1996 à 1999 pour sa thèse dans le cadre d'une bourse CIFRE de développement régional (collaboration IRD, Cirad, INRA et Phalippou-Frayssinet (PF), fertilisants organiques) qui a abouti à son but. En effet nos résultats ont conduit la société PF à créer un secteur recherche en recrutant Laurent Thuriès d'abord sur CDD de 2000 à mi-2001 pour un post-doc, puis en CDI. Laurent Thuriès reste affecté à temps majoritaire par PF dans notre laboratoire MOST commun IRD-CIRAD. Notre collaboration a permis de préciser le fonctionnement des compartiments d'entrée des MO dans les sols. Elle a abouti à proposer le modèle TAO (transformation des apports organiques, transformation of added organics) permettant de prédire les transformations du carbone (minéralisation, TAO-C) et de l'azote (minéralisation, immobilisation, volatilisation, TAO-N) des apports en fonction de leur contenu biochimique.

- Lair Maïté, 2005 (direction M. Pansu). Transformation des Apports Organiques dans les Sols : validation du modèle TAO-C et TAO-N. Master M1 FENEC, Montpellier.

Formation à la modélisation et validation du modèle TAO sur des données provenant d'expériences différentes de l'expérience de calibration.

Modélisation du cycle du carbone et de l'azote

Résumé

Ce document résume vingt années d'étude et de modélisation du cycle du carbone et de l'azote. Il s'appuie sur onze publications sélectionnées chronologiquement selon une logique d'exploration de diverses parties des cycles. La modélisation est basée sur une recherche expérimentale de laboratoire et de terrain utilisant aussi bien des mesures relatives à la transformation du carbone et de l'azote que de leurs traceurs isotopiques ^{14}C et ^{15}N.

Dès 1985 à l'Orstom Bondy, des incubations de mélanges de sols et de paille de blé permettaient de valider le modèle de Hénin et al. (1959) à deux compartiments, d'en explorer une autre formulation et de proposer un modèle à trois compartiments. Des relations étaient trouvées entre compartiments organiques simulés et deux propriétés importantes du sol : capacité d'échange cationique et taux d'agrégats stables au benzène (indice Is de Hénin). Ces travaux ouvraient une voie de prédiction de propriétés physiques et chimiques du sol liées au complexe organique et organo-minéral.

Des expériences réalisées avec des traceurs isotopiques ^{14}C et ^{15}N en laboratoire au Cefe-CNRS de Montpellier, conduisaient à la proposition d'un modèle plus précis à 5 compartiments : débris végétaux labile et stable, biomasse microbienne, matière humifiée labile et stable (MOMOS1-C). En 1998, la proposition était étendue à la description du cycle de l'azote comportant les mêmes compartiments organiques plus un compartiment ammonium et un compartiment nitrate (MOMOS1-N).

En 1999, des données expérimentales de traceurs isotopiques et le modèle MOMOS-C permettaient d'explorer le rôle des racines actives sur la décomposition des résidus végétaux dans les sols et les flux de carbone à la racine. Une nouvelle méthode était proposée pour la quantification de ces flux : (i) ajustement du modèle à partir du devenir d'apports marqués ^{14}C, (ii) utilisation du modèle pour prédire les flux de carbone non marqué et quantifier ainsi la rhizodeposition.

Simultanément, des recherches expérimentales étaient développées à l'IRD Montpellier en coopération avec le CIRAD, l'INRA et l'industrie de la fertilisation organique, pour préciser le fonctionnement de la partie entrée du modèle MOMOS. Ces recherches comportaient l'incubation en conditions contrôlées de composts, engrais et amendements organiques, ainsi que matières premières diverses d'origine végétale et animale. L'objectif était de préciser la transformation spécifique de l'apport en négligeant l'effet sur la minéralisation de la matière préexistante. Pour la minéralisation du carbone, un travail de comparaison entre sept modèles de la littérature puis de simplification a conduit à la proposition d'un modèle à trois compartiments utilisant seulement deux paramètres (fraction de matière très labile et fraction de matière stable des apports). La formulation de liens entre ces paramètres et les données analytiques, permettait de prédire la minéralisation au moyen du seul contenu biochimique des apports (modèle TAO-C).

L'extension de TAO-C au cycle de l'azote considérait simultanément N restant à l'état organique initial, N ré-immobilisé dans le sol par les micro-organismes, N minéralisé et la perte éventuelle d'azote par volatilisation. Outre les deux paramètres TAO-C, le modèle utilisait trois nouveaux paramètres régulant l'immobilisation, la re-minéralisation des composés immobilisés, et dans certains cas, la volatilisation. Les deux premiers paramètres ont pu être remplacés par des équations liées à la composition biochimique des apports et au temps d'incubation. Pour l'agriculture organique, le modèle TAO (Transformation des Apports Organiques) est maintenant un outil de base de prédiction des transformations simultanées du carbone et de l'azote au moyen du seul contenu biochimique de l'apport organique.

La partie du cycle concernant les flux de matières organiques transformées vivantes et non vivantes du sol, était explorée plus récemment. Cinq diagrammes de flux étaient comparés à partir de données d'incubations in situ utilisant : (i) les traceurs isotopiques ^{14}C et

^{15}N, (ii) le couplage avec un modèle de fonctionnement hydrique du sol (SAHEL), (iii) des résultats acquis précédemment sur TAO-C, (iv) des analyses de sensibilités (simulations de Monte-Carlo). La nouvelle version MOMOS-6 donne maintenant une valeur centrale à la biomasse microbienne (BM). Elle est paramétrée uniquement avec des constantes de vitesse sans paramètres de partage de flux. La seule sortie CO_2 du modèle est la respiration du compartiment BM (modélisation du quotient respiratoire de BM). La formation des produits humifiés débute par la mortalité de BM.

Les études en cours ont pour but (1) de préciser les mécanismes liant la dynamique des matières organiques aux caractéristiques texturales du sol et les inclure dans MOMOS-6, (2) de préciser les liens entre fonctionnement microbien et qualité des apports organiques, de prendre en compte ces liens dans MOMOS-6, (3) de coupler MOMOS-6 avec des modèles de production végétale, permettant la modélisation C et N de tout l'écosystème.

Le champ d'application de nos prochaines études concernera :

- la validation et complémentation des travaux en cours,
- l'intégration de données spectrographiques dans les modèles,
- l'application à la simulation d'écosystèmes et agrosystèmes sur sites expérimentaux comportant des suivis organiques de longue durée, la comparaison et la recherche de synergies avec d'autres démarches prédictives,
- l'application à l'agriculture de précision utilisant la fertilisation organique,
- l'application à la transformation de déchets,
- l'intégration dans les modèles de changement global.

1. Introduction

1.1. Cycle du carbone et changement global

La couverture pédologique constitue l'interface de nombreux processus d'échange dans les grands équilibres de la planète. Dans le cycle terrestre annuel du carbone, les gros réservoirs profonds que sont les carbonates et sédiments océaniques (3×10^7 Gt) ou encore les schistes organiques et combustibles fossiles (7×10^6 Gt) semblent avoir peu d'influence sur la régulation à court terme des flux de carbone. On sait que les mécanismes de dissolution/précipitation des carbonates fournissent un bilan nul de CO_2 (autant de moles adsorbées pour la précipitation que de moles dégagées pour la dissolution). Les carbonates ne peuvent être un puits ou une source de CO_2 qu'en cas de changement assez important de l'ambiance physico-chimique (pH, pression partielle de CO_2, température) ou biologique (coraux...). D'une façon générale on distingue le cycle du carbone de la biosphère terrestre ou océanique comme le régulateur à court terme des échanges avec l'atmosphère (Fig. 1).

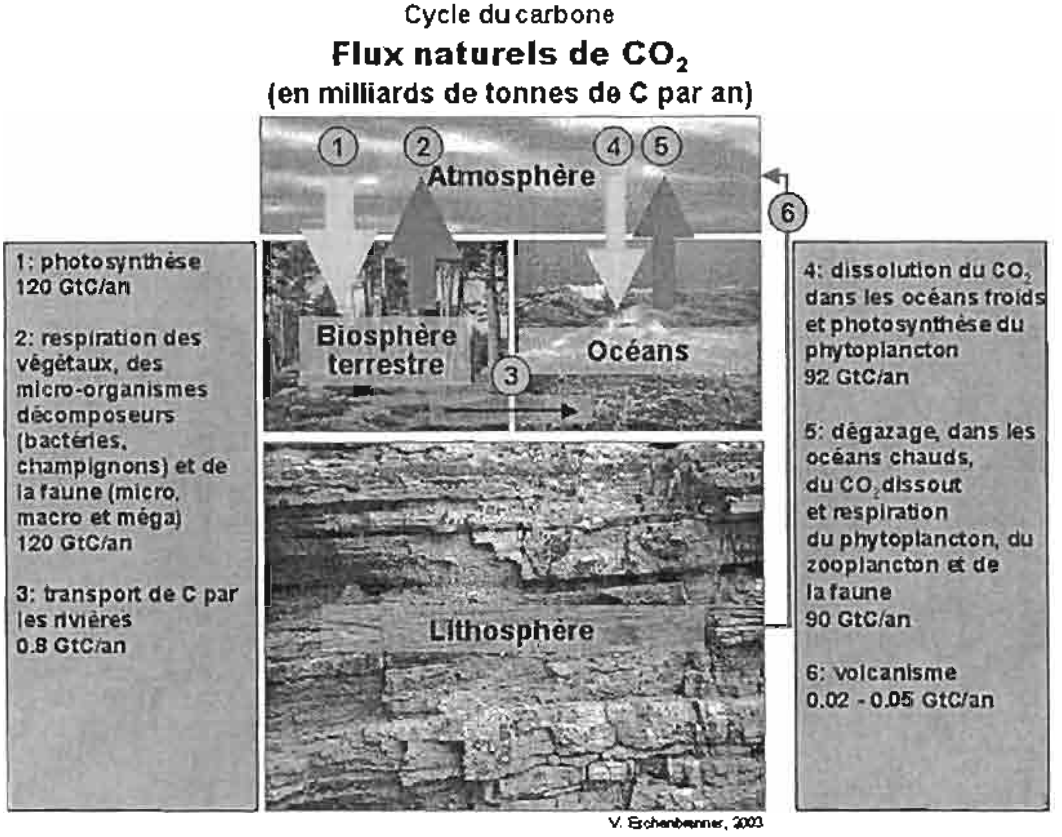

Figure 1 – Flux naturels de CO_2 en milliards de tonnes (Gt C-CO2 an^{-1}; Eschenbrenner, 2003)

Depuis la fin du XIX° siècle, ce cycle est en cours de perturbation par l'entrée non négligeable dans l'atmosphère du CO_2 provenant de la combustion des combustibles fossiles (6,3 Gt (C) an^{-1}, Fig. 2)) et résultant de changements d'usage des terres (1.6 Gt (C) an^{-1}; Fig. 2), qui s'ajoute au CO_2 en provenance de la respiration microbienne (120 Gt (C) an^{-1}, Fig 1). Le gaz carbonique atmosphérique n'est donc plus exactement équilibré par l'adsorption photo synthétique depuis les plantes. La formation des combustibles fossiles constitue un puits de C étalé sur des millénaires, alors que leur combustion par les activités

humaines est une source de CO_2 qui provoque une augmentation continue du carbone atmosphérique, contribuant au réchauffement climatique par effet de serre, même si l'augmentation s'avère partiellement tempérée par un accroissement de la production photosynthétique terrestre et océanique (Fig. 2). De nombreux programmes de recherche à travers le monde tentent de préciser la réponse de la productivité de la biosphère à ces changements atmosphériques (Saugier et al., 2001). Des programmes complémentaires tentent d'évaluer l'incidence de changements de gestion de la biomasse et des sols sur la séquestration ou la libération de C atmosphérique. La réserve de carbone organique contenue dans les sols (1 500 Gt jusqu'à la profondeur de un mètre plus 900 Gt dans la couche 1-2 m) est supérieure à celle contenue dans la biosphère (700 Gt) et l'atmosphère (750 Gt). L'UR SeqBio de l'IRD à laquelle j'appartiens s'inscrit dans ces programmes dans le cas de la gestion des sols tropicaux.

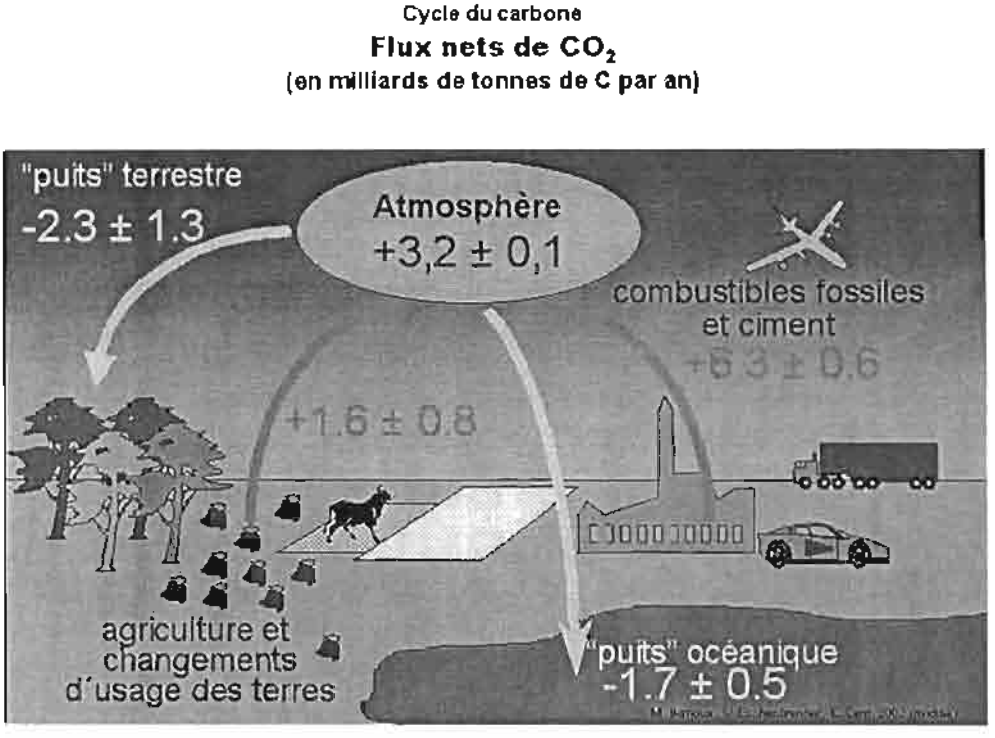

Fig. 2. Flux de gaz à effet de serre d'origine anthropique en équivalent CO_2 s'ajoutant aux flux naturels de la Fig. 1 (Gt (C-CO_2) an^{-1}). Le léger défaut de bilan est dû à la variabilité des estimations actuelles provenant de différents groupes d'experts (Eschenbrenner, 2003).

Outre ces propriétés d'échange avec l'atmosphère les matières organiques du sol ont de nombreuses autres fonctions environnementales et agronomiques. Stevenson (1982) en cite neuf :

- la couleur sombre facilite l'absorption du rayonnement solaire et le réchauffage des sols ;
- la matière organique pouvant fixer jusqu'à 20 fois son poids d'eau, améliore significativement les propriétés hydriques de certains sols, en particulier des sols sableux ;
- la combinaison avec les minéraux argileux conduit à la cimentation des particules de sol en unités structurales, appelées agrégats, qui facilitent les échanges gazeux et augmentent la perméabilité ;
- la: formation de complexes stables par chélation avec beaucoup de cations polyvalents peut réguler la disponibilité de nutriments pour les plantes ;

- la solubilité dans l'eau très réduite du fait des liens avec les argiles et certains cations polyvalents, minimise les pertes par lixiviation ;
- l'effet tampon se manifeste en milieu aussi bien légèrement acide que neutre ou alcalin ;
- l'échange de cations, 20 à 70 % de la capacité d'échange cationique de la plupart des sols serait procurée par la matière organique ;
- les combinaisons avec d'autres molécules organiques peuvent affecter l'activité biologique, la persistance et la biodégradabilité des pesticides.
- la minéralisation conduit à la libération de gaz carbonique et de formes minérales telles que NH_4^+, NO_3^-, PO_4^{3-}, SO_4^{2-} qui constituent une très importante source d'aliments pour les plantes ;

Le souci premier de l'agriculture ainsi que de la gestion sylvicole, pastorale ou environnementale a toujours été l'amélioration de la production végétale par des sélections variétales et par la mise à disposition des éléments fertilisants sous une forme absorbable par les plantes. Cette dernière fonction a souvent utilisé l'ajout de matière organique, mais aussi a cherché à favoriser la minéralisation de la matière organique afin de libérer des fertilisants adsorbables. Par exemple, le travail du sol facilite la respiration microbienne et la minéralisation. Il y aurait donc un certain antagonisme entre l'agriculture productiviste et la séquestration de carbone atmosphérique dans le sol. L'enjeu de la recherche actuelle se situe dans cette question : peut-on concilier une fonction de production végétale de niveau acceptable pour la nutrition humaine et animale, avec une fonction environnementale de séquestration de carbone.

1.2. Cycle de l'azote et changement global

Comme pour le carbone, l'azote de la planète est principalement localisé dans la géosphère avec des estimations de $1,6\times10^8$ Gt dans le noyau et le manteau (95,6 % de l'azote), 0,13 à $1,4\times10^8$ Gt dans la croute terrestre dont 0,35 à 4×10^7 Gt dans les sols et sédiments. L'atmosphère est le second plus grand réservoir terrestre avec $3,86\times10^7$ Gt soit 2,3 % de l'azote de la planète. Vient ensuite l'hydrosphère avec $2,3\times10^5$ Gt et enfin la biosphère qui contient 2.8×10^2 Gt d'azote soit seulement 0,0002 % de l'azote total de la planète. Cet azote de la biosphère se trouve principalement concentré dans le sol avec 2.2×10^2 Gt dans la matière organique et 20 Gt dans l'ammonium fixé ou adsorbé sur les feuillets d'argile.

Ainsi, bien que cet élément soit indispensable à la vie et à l'origine de la vie terrestre, les plantes et les animaux au-dessus de la surface du sol stockent seulement 40 Gt d'azote soit 0.00003 % de l'azote total de la planète.

D'un point de vue chimique l'élément azote est au numéro atomique 7 soit juste après le carbone dans la classification périodique. Il possède 5 électrons sur la couche périphérique L. Comme le carbone il peut se lier en gagnant ou perdant des électrons sur cette couche avec un caractère covalent marqué de la plupart des liaisons. Cependant, alors que le carbone peut se combiner selon 4 valences (-4, 0, +2 et +4), l'azote autorise plus de combinaisons par 9 états possibles d'oxydation (-3, -2, -1, 0, +1, +2, +3, +4, +5). Dans les êtres vivants C et N sont étroitement liés depuis l'ADN du noyau cellulaire jusqu'aux acides aminés des protéines et composés divers tels que aminosucres et amides. Les formes de l'azote trouvées dans les sols sont également très diverses depuis les formes azotées labiles des êtres vivants rapidement assimilées pour la croissance de la biomasse microbienne lors des processus de décomposition jusqu'aux atomes d'azote stabilisés dans les noyaux des molécules humiques lors des processus d'humification (Andreux, 1982). Les attaques acide à ébullition dérivées des techniques d'hydrolyse des protéines solubilisent 65 à 80% de l'azote du sol. Dans les hydrolysats, 20 à 35 % est retrouvé sous forme d'ammonium, 30 à 45 % sous forme d'acides aminés et 5 à 10 % sous forme d'amino-sucres (Bremner, 1965).

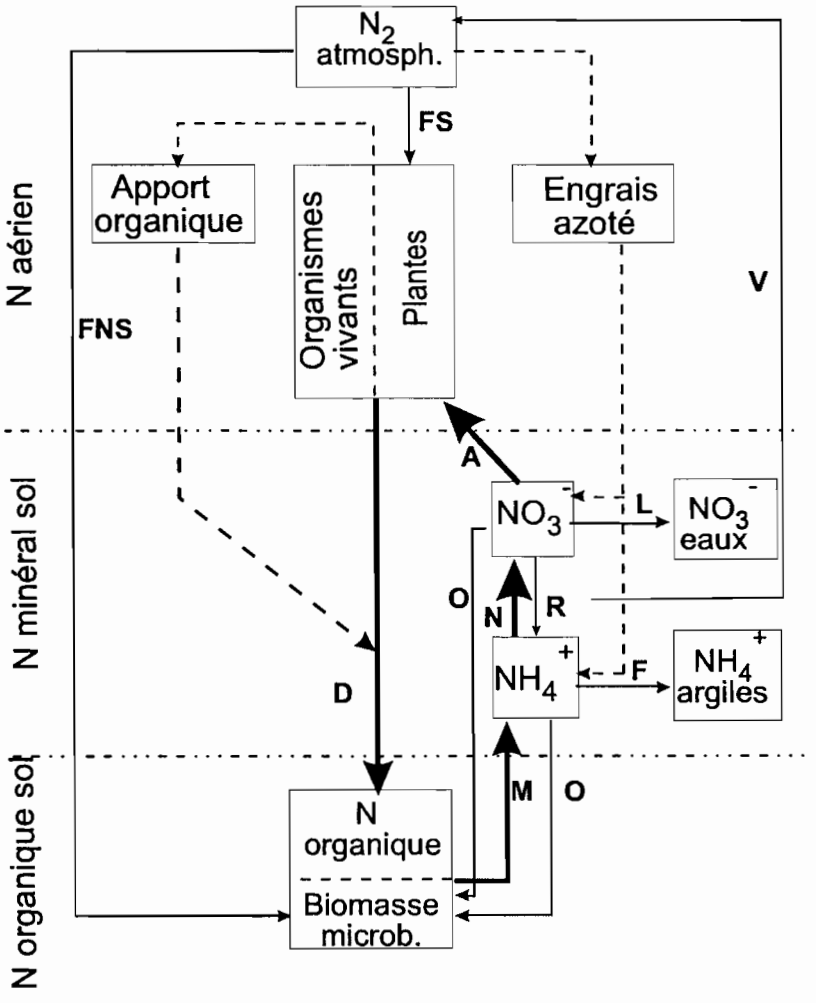

Fig. 2 - Représentation schématique du cycle de l'azote (Pansu et Gautheyrou, 2003) :
- traits pointillés = intervention de l'homme ;
- traits pleins = cycle naturel ;
- traits gras = cycle naturel principal en sol bien aéré :
  A = assimilation par les plantes,
  D = décomposition
  M = minéralisation des matières organiques du sol en ammonium,
  N = nitrification de l'ammonium,
  R = réduction des nitrates,
  O = réorganisation de l'azote minéral par les micro-organismes,
  V = volatilisations lors des processus de nitrification et dénitrification,
  F = fixation d'ammonium dans les feuillets d'argile,
  L = lixiviation des nitrates,
  FS = fixation symbiotique de l'azote atmosphérique par les plantes,
  FNS = fixation non symbiotique par la biomasse microbienne du sol.

Comme dans le cycle du carbone, l'azote stabilisé dans la géosphère participe peu au cycle rapide de transferts d'azote entre la biosphère, le sol et l'atmosphère. Ce cycle, très associé à celui du carbone, est essentiellement celui de la vie (Fig. 2) : les plantes assimilent l'azote minéral du sol et transmettent de l'azote aux autres êtres vivants par ingestion. Lors des processus de décomposition, l'azote est utilisé pour la croissance de la biomasse microbienne et transféré (i) aux matières humifiées notamment par l'intermédiaire de la

mortalité des microorganismes, (ii) en ammonium par les processus d'ammonification. Ammonium et nécromasse microbienne sont en grande partie réingérés en permanence par la biomasse microbienne. Une autre partie de l'ammonium (N^{-III}) est oxydée par des bactéries autotrophes jusqu'en nitrate (N^{+V}) en passant par divers états d'oxydation intermédiaire tels que N_2 (N^0), N_2O (N^{+I}), NO (N^{+II}), NO_2^- (N^{+III}). Les échanges avec l'atmosphère sont cependant plus limités que dans le cycle du carbone. Les entrées dans l'atmosphère proviennent des émissions gazeuses (i) d'ammoniac depuis le compartiment ammonium en présence d'élévations locales de pH, (ii) d'azote et d'oxydes d'azote lors des processus d'oxydation de l'ammonium et de réduction des nitrates. Parmi ces émissions, N_2O est un puissant gaz à effet de serre susceptible de contribuer au changement climatique (Hénault et Germon, 2000). Les sorties de l'atmosphère proviennent de fixation directe d'azote atmosphérique par des microorganismes en symbiose ou non avec les racines des plantes, et dans une moindre mesure de dépôts d'azote par les pluies acides (Ecofor, 2005). Une sortie atmosphérique plus limitée est d'origine anthropique. Elle concerne la fabrication de fertilisants azotés depuis la synthèse de l'ammoniac à partir d'azote et d'hydrogène gazeux par le procédé Georges Claude. Les sorties vers l'hydrosphère proviennent surtout de la lixiviation de l'ion nitrate, très mobile dans les sols à faible capacité d'échange anionique. Les sorties vers la géosphère proviennent surtout de fixation d'ammonium dans certains feuillets d'argile. Elles pourraient être compensées par d'autres entrées depuis la géosphère vers le cycle du vivant. (Holloway et Dahlgren, 2002).

1.3. Modèles de la dynamique des matières organiques

Les progrès de la physico-chimie analytique appliquée à l'étude du sol (Pansu et Gautheyrou, 2003), spécialement dans le domaine de l'analyse du carbone (Lal et al., 2001) et les méthodes analytiques modernes de spatialisation (Chaplot et al., 2001) ont permis des avancées importantes dans la connaissance des bilans organiques des sols terrestres. Par exemple un bilan des contenus organiques et potentiels de stockage du C a été publié pour la France (Arrouays et al., 2002) et pour le Brésil (Bernoux et al., 2002 ; General coordination on global climate change, 2004). Ces méthodes ont l'intérêt de fournir un bon état des lieux mais ne permettent d'apprécier une dynamique que pour les sites où l'on dispose de données étalées dans le temps. Elles ne permettent pas l'accès à des études prévisionnelles de simulations selon plusieurs scénarii de gestion. Enfin elles ne renseignent pas sur les mécanismes régissant les transferts entre les compartiments organiques vivants, débris et métabolites dans le sol. La modélisation de bilans à partir des flux d'entrée et de sortie organique dans le sol est une voie indispensable pour l'appréciation des dynamiques. Le modèle le plus simple dans cette voie a été proposé par Hénin et Dupuis (1945) : l'évolution du carbone du sol est régie par la différence entre les entrées et la sortie organiques (Fig. 3), une fraction k1 de l'entrée étant incorporée (coefficient isohumique) et une fraction k2 de l'humus étant minéralisée (taux de minéralisation).

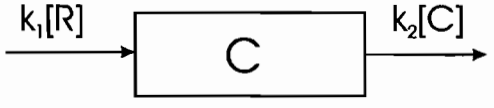

Fig. 3 – Modèle de Hénin et Dupuis (1945) : C = carbone du sol, R = résidu organique provenant de la biomasse, k1 = coefficient isohumique, k2 = taux de minéralisation.

Ce modèle a été très utilisé, par exemple par Pieri (1989) pour les terres de savane subsaharienne. Il demeure d'actualité pour les premières approximations. Cependant l'estimation des coefficients k_1 et k_2 est fortement sujette à caution car elle fournit des valeurs moyennes sur des groupes de composés extrêmement divers, tels que hydrosolubles et lignine

à l'entrée, polysaccharides microbiens et acides humiques en sortie. Le modèle de Hénin et al. (1959) était une première tentative de pallier à ces insuffisances (Fig. 4), mais il est resté longtemps une proposition théorique avant d'être validé par des essais de laboratoire (Pansu et Sidi, 1987) et de terrain (Andren et Katterer, 1997).

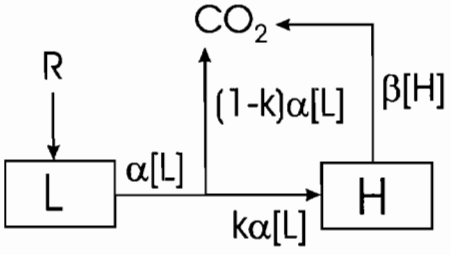

Fig. 4 – Modèle de Hénin et al. (1959) : R = résidu organique, L = matière labile, H = humus stable, α, β = taux respectifs de décomposition des matières labiles et stables, k = taux d'incorporation dans l'humus.

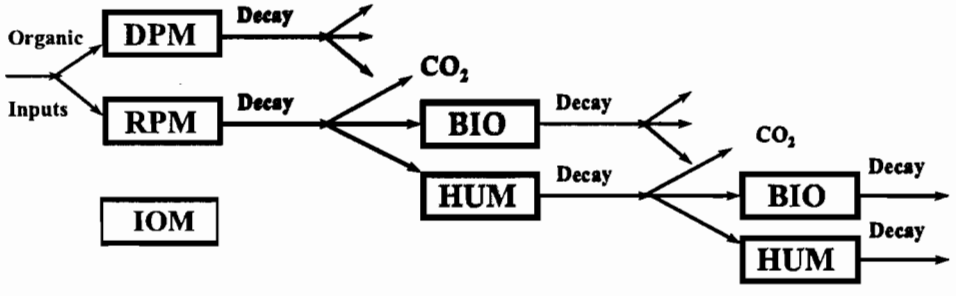

Fig. 5 – Modèle Roth-C (Jenkinson, 1990 ; Jenkinson er Rayner, 1977) : DPM = decomposable plant material, RPM = resistant plant material, BIO = biomasse microbienne, HUM = humus, IOM= inert organic matter.

Le modèle Roth-C a été proposé par Jenkinson et Rayner (1977) pour décrire le fonctionnement organique du site expérimental de Rothamsted en intégrant de nombreuses données disponibles pour certaines depuis plus d'un siècle. Roth-C constituait une première tentative de prise en compte simultanée du fonctionnement de cinq compartiments organiques : matières labiles et stables des apports, biomasse microbienne, matières humifiées labiles et stables (Fig. 5).

Les Fig. 4 et 5 définissent des modèles à compartiments, groupe de modèles le plus utilisé dans la prédiction de la décomposition et dans lesquels se situe aussi notre travail. Signalons toutefois d'autres propositions comme la théorie de la qualité continue de la matière organique (Bosatta et Ågren, 1985) ou la modélisation multi-agents des cohortes de décomposeurs (Gignoux et al., 2001). La plupart des modèles à compartiments fonctionne avec deux groupes de paramètres. Le premier groupe rassemble des constantes de vitesse du premier ordre ou taux de décomposition par unité de temps du compartiment. Par analogie avec des lois de la cinétique chimique et biologique, ces constantes peuvent être liées à la température et à l'humidité du sol pour prendre en compte l'influence climatique. Le second groupe rassemble des fractions de partage des flux (FF) à l'entrée des compartiments (par exemple k dans Fig. 4). Les FF sont plus mal définies, elles sont parfois appelées facteurs d'efficience ou rapport du taux de carbone synthétisé dans un compartiment au taux de carbone brulé pour cette synthèse. La justification des valeurs attribuées aux FF (voir Fig. 5 les chiffres indiqués sur les sorties de CO_2) est souvent absente ou imprécise.

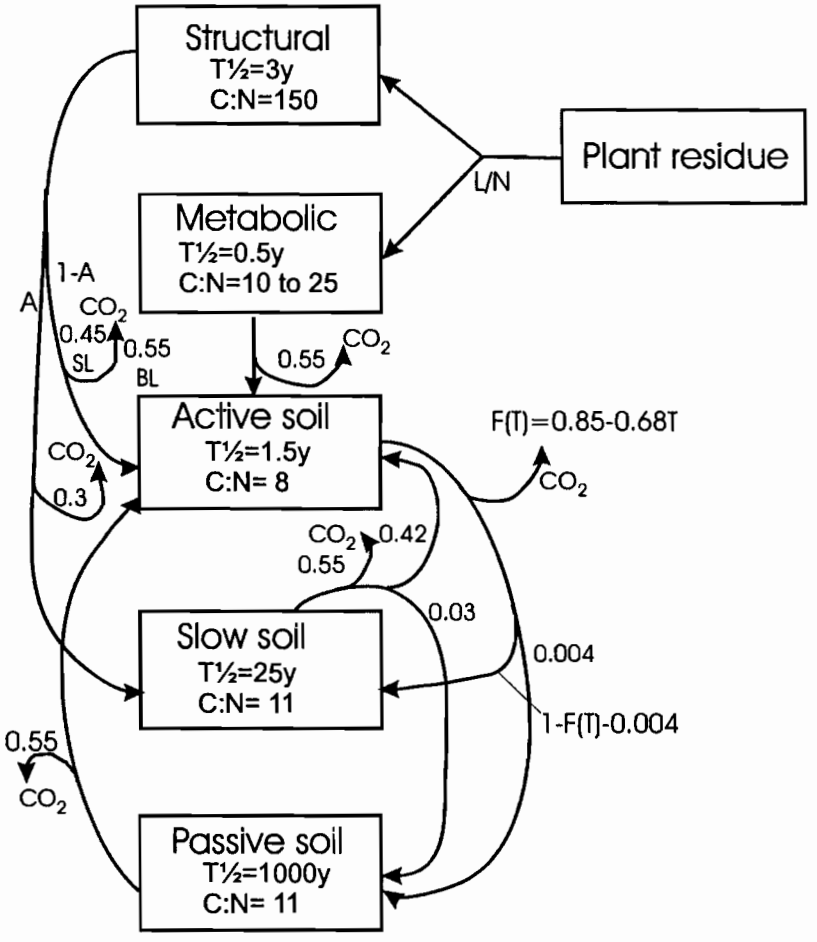

Fig. 5 – Modèle Century (Parton et al., 1987) : SL = surface litter, BL = soil litter, L/N = lignin/nitrogen ratio, A = lignin fraction, T = soil silt + clay content (fraction).

Si la biomasse microbienne (BM) est toujours considérée comme l'acteur de la décomposition, on peut distinguer les modèles qui prennent en compte explicitement BM comme un ou plusieurs compartiments, et ceux qui ne prennent en compte BM qu'indirectement dans la valeur des constantes de vitesse de décomposition. Compartiment(s) BM et paramètres FF sont une voie possible de classification des modèles de la littérature. Parmi les modèles décrivant BM dans un compartiment on peut identifier 2 FF dans *Roth-C* (Jenkinson et Rayner, 1977; Jenkinson, 1990), 6 FF dans *Turnover through MB* (Van Veen et al., 1985), au moins 4 dans *Hurley pasture* (Thornley et Verberne, 1989), 2 FF dans *MOMOS-1* (Sallih et Pansu, 1993), 1 FF dans *Candy* (Franko et al., 1995), 3 FF dans *Physical protection* (Hassink et Whitmore, 1997), 4 FF dans *Stix* (Brisson et al., 1998). *Daisy* (Hansen et al., 1991) utilise 2 compartiments pour BM et 3 FF. *Century* (Fig. 5, Parton et al., 1987) utilise un compartiment appelé sol actif et 6 FF. *Ncsoil* (Molina et al., 1983) utilise deux compartiments appelés Pool I-labile et Pool I-resistant et 4 FF. *DNDC* (Li et al., 1994) utilise deux compartiments BM et 4 FF. *Continuous quality* (Bosatta and Ågren, 1985), Somm (Chertov et Komarov, 1997), "ITE forest" (Thornley, 1991) ou Camfor (Brack et Richards, 2002) ne décrivent pas BM comme un compartiment spécifique et n'utilisent pas de FF. Les seuls modèles *Mean residence time* (Saggar et al., 1996) et *Exoenzyme activity* (Schimel et Weintraub, 2003) proposent un compartiment BM sans paramètre FF.

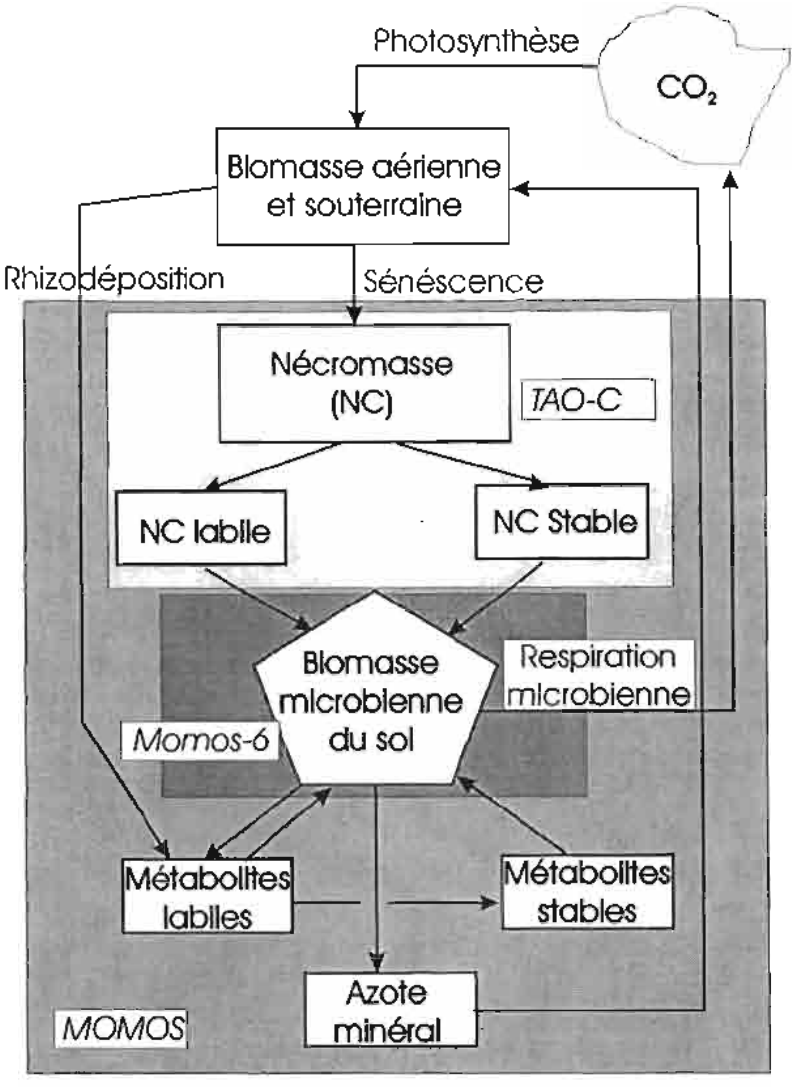

Fig. 6 – Cycle des matières organiques.

Notre travail de recherche expérimentale de ces vingt dernières années peut être situé par rapport au cycle des matières organiques représenté Fig. 6 selon l'image qui en est communément admise : (i) la biomasse aérienne et racinaire est alimentée par le gaz carbonique atmosphérique et l'azote minéral du sol lors du processus de photosynthèse, (ii) cette biomasse restitue C et N au sol selon deux voies : par exsudation de métabolites labiles et par sénescence de nécromasse labile et stable, (iii) les sorties de tous les compartiments d'origine végétale ou microbienne alimentent BM, (iv) la sortie de CO_2 du système provient de la respiration de BM, (v) la mortalité de BM produit des métabolites microbiens à nouveau consommés par BM ou stabilisés dans l'humus.

Dans un premier temps nous nous sommes intéressés à la dynamique globale (gris moyen Fig. 6) selon des modèles à deux, trois (Pansu et Sidi, 1987) puis cinq compartiments du cycle C (Pansu et Sallih, 1993) et N (Pansu et al., 1998). Les données expérimentales et les modèles nous ont aussi permis de quantifier une dynamique de la stabilité structurale (Sidi et al., 1991) et de la capacité d'échange cationique (Pansu et de Boissezon, 1989) liée à celle des matières organiques, puis de modéliser la rhizodéposition (Bottner et al., 1999). Dans un deuxième temps, nous avons précisé la partie entrée des matières organiques du modèle (rectangle gris clair, Fig. 6) selon leurs caractéristiques biochimiques pour les transformations

des formes du carbone (TAO-C ; Thuriès et al., 2001 ; Thuriès et Pansu, 2002) et de l'azote (TAO-N ; Pansu et al., 2003 a et b). Dans un troisième temps nous avons précisé les mécanismes de transferts autour de la biomasse microbienne (rectangle gris foncé Fig. 6) par comparaison de justesse et de sensibilité de cinq alternatives (Pansu et al., 2004). La suite de ce mémoire est formée des onze publications citées dans ce paragraphe.

Références de l'introduction

Andren, O. and Katterer, T., 1997. ICBM: The introductory carbon balance model for exploration of soil carbon balances. Ecological Applications, 7, 1226-1236.

Andreux, F., 1982. Genesis and properties of humic molecules. In: M. Bonneau and B. Souchier (Editors), Constituents and properties of soils. Academic Press, London, New-York, Paris, San Diego, San Francisco, Sao Paulo, Sydney, Tokyo, Toronto, pp. 109-139.

Arrouays, D., Balesdent, J., Germon, J.C., Jayet, P.A., Soussana, J.F., Stengel, P., 2002. Contribution à la lutte contre l'effet de serre. Stocker du carbone dans les sols agricoles de France ?, Rapport d'expertise collective, INRA, Orléans, 332 pp.

Bernoux, M., Carvalho, M.C.S., Volkoff, B. and Cerri, C.C., 2002. Brazil's soil carbon stocks. Soil Science Society of America Journal, 66, 888-896.

Bosatta, E. and Ågren, G.I., 1985. Theoritical analysis of decomposition of heterogeneous substrates. Soil Biology & Biochemistry, 17, 601-610.

Bottner, P., Pansu, M. and Sallih, Z., 1999. Modelling the effect of active roots on soil organic matter turnover. Plant and Soil, 216, 15-25.

Brack, C.L. and Richards, G.P., 2002. Carbon accounting model for forests in Australia. Environmental Pollution, 116: 187-194.

Bremner, J.M., 1965. Organic forms of soil nitrogen. In: Black et al. (Editor), Methods of soil analysis, Part 2 Agronomy. American Society of Agronomy, Madison, 1238-1255.

Brisson, N., Mary, B., Ripoche, D., Jeuffroy, M.H., Ruget F., Nicoullaud, B., Gate, P., Devienne-Barret, F., Antonioletti, R., Durr, C., Richard, G., Baudoin, N., Recous, S., Tayot, X., Plenet, D., Cellier, P., Machet, J.M., Meynard, J.M., Delécolle, R., 1998. STICS: a generic model for the simulation of crops and their water and nitrogen balances. I. Theory and parametrization applied to wheat and corn. Agronomie, 18, 311-346.

Chaplot, V., Bernoux, M., Walter, C., Curmi, P. and Herpin, U., 2001. Soil carbon storage prediction in temperate hydromorphic soils using a morphologic index and digital elevation model. Soil Science, 166, 48-60.

Chertov, O.G. and Komarov, A.S., 1997. SOMM: A model of soil organic matter dynamics. Ecological Modelling, 94, 177-189.

Ecofor, 2005. Pluies acides, 20 ans après. Journée d'information et de débat. Actes Ecofor, ecosystèmes forrestiers, 25 Novembre 2005, Muséum d'histoire naturelle Paris.

Eschenbrenner, 2003. Site de l'UR séquestration du carbone et biofonctionnement des sols tropicaux, IRD Montpellier, France, http://www.mpl.ird.fr/SeqBio/

Franko, U., Oelschlägel, B. and Schenk, S., 1995. Simulation of temperature-, water- and nitrogen dynamics using the model CANDY. Ecological modelling, 81, 213-222.

General Coordination on Global Climate Change, 2004. Brazil's Initial National Communication to the United Framework Convention on Climate Change, Ministry of Science and Technology, Brasilia, 275 pp.

Gignoux, J. Abbadie, L., Hall, D., House, J., Masse D., Nacro H.B., 2001. Design and test of a generic cohort model of soil organic matter decomposition: the SOMKO model. Global Ecology and Biogeography 10, 639-660.

Hansen, S., Jensen, H.E., Nielsen, N.E. and Svendsen, H., 1991. Simulation of nitrogen dynamics and biomass production in winter wheat using the Danish simulation model DAISY. Fertilizer Resarch, 27, 245-259.

Hassink, J. and Whitmore, A.P., 1997. A model of the physical protection of organic matter in soils. Soil Science Society of America Journal, 61, 131-139.

Hénault, C. and Germon, J.C., 2000. NEMIS, a predictive model of denitrification on the field scale. European Journal of Soil Science, 51, 257-270.

Hénin, S. and Dupuis, M., 1945. Essai de bilan de la matière humique du sol. Annales Agronomiques - France, 15, 17-29.

Hénin, S., Monnier, G. and Turc, L., 1959. Un aspect de la dynamique des matières organiques du sol. Compte rendu de l'académie des sciences - France, 248, 138-141.

Holloway, J.M. and Dahlgren, R.A., 2002. Nitrogen in rock: Occurrences and biogeochemical implications. Global Biogeochem. Cycles, 16, 1118. doi:10.1029/2002GB001862

Jenkinson, D.S. and Rayner, J.H., 1977. The turnover of soil organic matter in some of the Rothamsted classical experiments. Soil Science, 123, 298-305.

Jenkinson, D.S., 1990. The turnover of organic carbon and nitrogen in soil. Phil. Trans. R. Soc. Lond., B. 329, 361-368.

Lal, R., Kimble, J.M., Follet, R.F. and Stewart, B.A., 2001. Assessment methods for soil carbon. Advances in soil science. Lewis publishers, Boca Raton, London, New-York, Washington, 676 pp.

Li, C., Frolking, S. and Harriss, R.C., 1994. Modeling carbon biogeochemistry in agricultural soils. Global Biogeochemical Cycles, 8, 237-254.

Molina, J.A.E., Clapp, C.E., Shaffer, M.J., Chichester, F.W. and Larson, W.E., 1983. NCSOIL, a model of nitrogen and carbon transformations in soil: description, calibration and behavior. Soil Science Society of America Journal, 47, 85-91.

Pansu, M. and de Boissezon, P., 1990. Dynamique du carbone organique dans les mélanges sols-résidus végétaux ; influence sur la capacité d'échange cationique. In: INRA (Editor), Groupe d'études des matières organiques des sols (GEMOS). INRA, Bordeaux

Pansu, M. and Gautheyrou, J., 2003. L'analyse du sol - minéralogique, organique et minérale. Springer, Paris, Berlin, Heidelberg, New York, Hong Kong, Londres, Milan, Tokyo, 993 pp.

Pansu, M. and Sidi, H., 1987. Cinétique d'humification et de minéralisation de mélanges sols- résidus végétaux. Science du sol, 25, 247-265.

Pansu, M. and Thuriès, L., 2003. Kinetics of C and N mineralization, N immobilization and N volatilization of organic inputs in soil. Soil Biology & Biochemistry, 35: 37-48.

Pansu, M., Bottner, P., Sarmiento, L. and Metselaar, K., 2004. Comparison of five soil organic matter decomposition models using data from a ^{14}C and ^{15}N labeling field experiment. Global Biogeochemical Cycles, 18: GB4022, doi:10.1029/2004GB002230.

Pansu, M., Sallih, Z. and Bottner, P., 1998. Modelling of soil nitrogen forms after organic amendments under controlled conditions. Soil Biology & Biochemistry, 30, 19-29.

Pansu, M., Thuriès, L., Larré-Larrouy, M.C. and Bottner, P., 2003. Predicting N transformations from organic inputs in soil in relation to incubation time and biochemical composition. Soil Biology & Biochemistry, 35, 353-363.

Parton, W.J., Schimel, D.S., Cole, C.V. and Ojima, D.S., 1987. Analysis of factors controlling soil organic matter levels in great plains grasslands. Soil Science Society of America Journal, 51, 1173-1179.

Pieri, C., 1989. Fertilité des terres de savanes. Bilan de trente ans de recherche et de développement agricole au sud du Sahara CIRAD-IRAT, Montpellier.

Saggar, S., Parshotam, A., Sparling, G.P., Feltham, C.W. and Hart, P.B.S., 1996. 14C-labelled ryegrass turnover and residence times in soils varying in clay content and mineralogy. Soil Biol. Biochem., 28, 1677-1686.

Sallih, Z. and Pansu, M., 1993. Modelling of Soil Carbon Forms After Organic Amendment Under Controlled Conditions. Soil Biology & Biochemistry, 25, 1755-1762.

Saugier, B., Roy, J. and Mooney, H.A., 2001. Terrestrial Global Productivity. Academic Press, London:, 573 pp.

Schimel, J.P. and Weintraub, M.N., 2003. The implications of exoenzyme activity on microbial carbon and nitrogen limitation in soil: a theoretical model. Soil Biology and Biochemistry, 35, 549-563.

Sidi, H. and Pansu, M., 1990. Effets d'apports organiques et de gypse sur la stabilité structurale de deux sols méditerranéens. Science du Sol, 28, 237-255.

Stevenson, F.J., 1982. Humus chemistry - Genesis, Composition, Reactions. Wiley interscience publication. Wiley, New-York, Chichester, Brisbane, Toronto, Singapore, 443 pp.

Thornley, J.H.M. and Verberne, E.L., 1989. A model of nitrogen flows in grassland. Plant Cell Environment, 12, 863-886.

Thornley, J.H.M., 1991. A transport-resistance model of forest growth and partitioning. Annals of Botany, 68, 211-226.

Thuriès, L., Pansu, M., Feller, C., Herrmann, P. and Rémy, J.C., 2001. Kinetics of added organic matter decomposition in a Mediterranean sandy soil. Soil Biology & Biochemistry, 33, 997-1010.

Thuriès, L., Pansu, M., Larré-Larrouy, M.C. and Feller, C., 2002. Biochemical composition and mineralization kinetics of organic inputs in a sandy soil. Soil Biology & Biochemistry, 34, 239-250.

Van Veen, J.A., Ladd, J.N. and Amato, M., 1985. Turnover of carbon and nitrogen through the microbial biomass in a sandy loam and a clay soil incubated with [^{14}C(U]glucose and [^{15}N]$(NH_4)_2SO_4$ under different moisture regimes. Soil Biology & Biochemistry, 17, 747-756.

Cycle du carbone dans les sols

Modèles à 2 et 3 compartiments

SCIENCE DU SOL 1987 -Vol. 25/4 -pp. 247-265 -PLAISIR-FRANCE

CINETIQUE D'HUMIFICATION ET DE MINERALISATION DE MELANGES SOLS-RESIDUS VEGETAUX

M. PANSU(I), H. SIDI(2)

RESUME

Un ensemble de trois expériences d'incubation au laboratoire. de mélanges de sols {vertisol et sol salé carbonaté) et de pailles de blé, a permis la mise en équation en fonction du temps des teneurs en carbone organique total et en carbone des matières légères séparées par densimétrie.

Le carbone organique évolue comme une somme de deux exponentielles {tableau III) dont les paramètres ont été comparés aux résultats d'autres expérimentations {tableau IV). ~ *

Le carbone des matières légères décroît selon une loi hyperbolique dans deux expériences et une loi exponentielle dans la troisième {tableau VI, fig. 3).

Deux modèles prévisionnels sont proposés pour décrire I'humification et la minéralisation du carbone des sols et des résidus végétaux sous l'action des micro- organismes {lig. 1). 1 ,

-Un modèle à deux compartiments *prenant mieux en compte que celui de HENIN et al.* {1959) *les processus de renouvellement.*

-Un modèle plus précis à trois compartiments *permettant de distinguer dans les fractions labiles, le carbone resté à l'état végétal et celui provenant. à la fois de la croissance microbienne et des métabolites végétaux de faible durée de vie.*

Les modèles proposés ont été validés par nos expériences de laboratoire {tableau V, Fig. 2, *Fig.* 4).

MOTS CLES : Modélisation, Matières organiques des sols, Carbone des sols, Cinétique de minéralisation, Cinétique d'humification,

KEY WORDS : Modelisation, soil organic mater, Soil carbon, .Mineralization kinetics, Humification kinetics.

INTRODUCTION

L'évolution organique de mélanges de sols et le paille de blé a été étudiée sous un régime hydrique alterné sans lessivage. Cette expérience de laboratoire (H. SIDI, 1987) visait à préciser l'influence de l'apport de résidus végétaux sur la structure de deux sols méditerranéens de la région de Mateur (Tunisie) : un sol vertique et un sol salé carbonaté. Sur ce dernier, nous avons également étudié l'effet d'un apport simultané de gypse.

Ces.sols présentent une structure battante très dégradée. Nos précédents résultats (Sidi, 1987) ont montré que l'apport de paille procure une amélioration éphémère de la stabilité des agrégats dans les quinze premiers jours et une amélioration plus durable à partir du sixième mois.

(1) ORSTOM, 70, Route d'Aulnay, 93140 Bondy, France.
(2) INRA d'Alger, Belfort, EI-Harrach, Alger, Algérie.

Nos expériences apportent également de nombreuses mesures sur l'évolution des stocks organiques de ces sols dans des conditions expérimentales contrôlées.

Il était nécessaire de préciser parallèlement la cinétique des caractéristiques mesurées relatives aux matières organiques.

L'analyse des données « carbone organique total » et « matières légères séparées par densimétrie » avaient pour but leur mise en équations en fonction du temps d'incubation et la comparaison des résultats avec d'autres expériences du même type.

Nos données ont permis également la prise en compte du paramètre « quantité de paille apportée ».

L'ensemble des données nous a permis de proposer et valider des modèles prévisionnels d'évolution des compartiments stables et labiles des matières organiques des sols sous l'effet d'apports végétaux. Nous rappelons ci-dessous les principaux modèles en usage qui interviendront dans les discussions et qui permettent de situer nos propositions.

Le choix d'un modèle d'évolution lié à l'interprétation de données agronomiques et pédologiques dépend du volume et de la nature de celles-ci. Ainsi dans bien des cas, les auteurs se limitent à des modèles monocompartimentaux dérivés du modèle de HENIN et DUPUIS (1945). En fonction des conditions expérimentales et des mesures les auteurs ont été conduits à modifier le modèle initial selon différentes cinétiques de décroissance comme le montrent les quelques exemples du tableau I.

Tableau I : Cinétique de décroissance de modèles monocompartimentaux appliqués au carbone des sols. A = contenu carboné exprimé généralement en pour mille massique du sol sec. t est le temps exprimé en année. Ao = valeur de A au temps 0. α = coefficient de décroissance. Dans le seul cas de la décroissance exponentielle le temps de demi-vie est indépendant de la quantité de matière à détruire. Dans ce cas également appelé « mélange parfait » le temps moyen de résidence est égal au temps de renouvellement soit $1/\alpha$.

Decreasing kinetics of monocompartimental models applied to the soil carbon. *A is carbon content generaly expressed in terms of pour mille of dry soil. t is the time expressed in year. Ao is the value of A at time 0. α is decreasing coefficient. Only in case of exponential decay, the half-time is independent of the amount of matter to be destroyed. Across this so-called « well-mixed reservoir » the mean residence time is equal to the turn-over time, namely $1/\alpha$.*

Loi cinétique	Ordre 0 Linéaire	Ordre 1 exponentielle	Ordre 2 hyperbolique	Ordre n puissance
Modèle $-dA/dt$	$A \xrightarrow{\alpha}$	$A \xrightarrow{\alpha(A)}$	$A \xrightarrow{\alpha(A)^2}$	$A \xrightarrow{\alpha(A)^n}$
Dimension α M = °/°° massique T = temps	MT^{-1}	T^{-1}	$M^{-1}T^{-1}$	$M^{1-n}T^{-1}$
Evolution A	$Ao-\alpha t$	$Ao\ exp(-\alpha t)$	$Ao(1+Ao\alpha t)^{-1}$	$Ao(1+\alpha(n-1)Ao^{n-1}t)^{-1/n-1}$ $n<>1$
Demi-vie A	$Ao/2\alpha$	$Log\ 2/\alpha$	$1/\alpha Ao$	$(2^{n-1}-1)/(\alpha(n-1)Ao^{n-1})$
Exemples d'applications au carbone des sols	pour mémoire	HOFMAN et RUYMBEKE (1979) *BOIFIN et al.* (1986)	BOIFIN et FLEURY (1974)	BALESDENT (1982)

L'apparition de modèles à plusieurs compartiments de décroissances supposées homogènes est allée de pair avec l'augmentation du volume des données collectées et la qualité de leur analyse statistique.

Les compartiments correspondent très rarement à des constituants organiques définis ou à des fractions mesurables quantitativement. Les données physiques, chimiques ou biologiques permettent cependant de leur affecter une cinétique de décroissance et d'estimer les flux qui les traversent.

Ainsi, le modèle de HENIN, MONNIER et TURC (1959) permet la prise en compte des mesures densimétriques de matières légères (HENIN et TURC, 1949) assimilées alors à une fraction labile.

Le modèle de JENKINSON et RAYNER (1977) a été validé à la fois par des mesures de décroissances de matières végétales, de biomasse microbienne (JENKINSON, 1965) et de datations pour estimer les paramètres d'évolution à long terme du stock humique d'un sol soumis à un système cultural donné.

Les modèles de PAUL et VAN VEEN (1978) et JENKINSON et LADD (1981) concernent des évolutions à plus court terme. Le premier a été validé surtout par des mesures de décroissance de constituants biochimiques des plantes dans les sols, le deuxième essentiellement par des mesures de biomasse microbienne.

On peut remarquer que, contrairement aux modèls d'évolution globale de tout le carbone (tableau I), les lois cinétiques décrivant la décroissance de chaque compartiment dans les modèles multicompartimentaux ci-dessus sont toujours du premier ordre.

I. MATERIELS ET METHODES

A) Matériels utilisés et protocole expérimental

Les principales caractéristiques du sol peu évolué d'apports à tendance vertique et du sol salé carbonaté à hydromorphie de profondeur sont présentées dans le tableau II.

Tableau II : Sols utilisés pour les expériences. CE = conductivité électrique de l'extrait pâte saturée (en mmhos/cm), $CaCO_3$ = calcaire total, les valeurs du carbone organique sont indiquées dans le tableau III.

Soils under study. *CE = electrical conductivity of saturated extract (in mmhos/cm), $CaCO_3$ = total calcareous, organic carbon values are indicated in Table III.*

type de sols et horizons prélevés	pH (H20)	argile %	CE	C/N	Complexe absorbant CaCO3 %	Na	K	Ca	Mg
							meq/100g		
alluvial à tendance vertique 0-32 cm	7,2	48	0,7	13	1,2	1,1	0,39	15,18	4,44
Salé carbonaté à hydromorphie de profondeur. 0-21 cm	8,0	49	4,7	8,5	28	9,9	1,61	66,40	7,62

La paille de blé, découpée et calibrée entre 0,2 et 2 mm a été ajoutée aux sols à des doses correspondant à 0 (témoin), 2,7 et 8,1 pour mille de carbone dans le mélange sec. Des ajouts d'ammoniac mélangé à l'eau d'humectation ont permis de ramener à 15 le rapport C/N de la paille apportée.

Les échantillons de 250 g de sols amendés ou non (témoins) ont été placés dans des tubes PVC de 7,5 cm de diamètre intérieur bouchés à la partie inférieure par un grillage plastique surmonté de 2 cm de gravier.

Ces tubes ont été mis à incuber à une température constante de 28 °C avec une alternance humectation-dessiccation (teneur en eau ramenée tous les trois jours à 80 % de l'humidité équivalente à la capacité de rétention au champ) donc *sans perte par drainage*. Les prélèvements ont été effectués aux temps : 0, 15, 30, 90, 180, 270 jours d'incubation. Les essais conduits en double comprenaient donc 36 tubes pour chacune des trois expériences notées comme suit :

VE = Sol peu évolué d'apport à tendance vertique.
SA = Sol salé carbonaté.
SG = Sol salé carbonaté amendé à 1 % de gypse.

A la fin de chacune des périodes d'incubation prévues dans le plan d'expériences, les sols des 18 tubes correspondants ont été prélevés et mis à sécher avec réunion des deux répétitions. Après écrasement des mottes, tamisage à 2 mm et homogénéisation les échantillons ont été prélevés au partiteur et les teneurs en carbone organique mesurées par oxydation avec le mélange sulfochromique selon la méthode de WALKLEY et BLACK. Les teneurs en carbone des échantillons provenant du sol non carbonaté ont pu être vérifiées par combustion sous oxygène à 1 200°C et dosage du CO_2 dégagé par coulométrie.

Le coefficient de variation établi sur 15 prises d'essai d'un même sol est de 1,9 % et les intervalles de confiance au niveau de probabilité 0,95 ont été reportés sur la figure II.

Les matières végétales légères sont obtenues par séparation densimétrique avec de l'acide phosphorique 2M (DABIN, 1976). Bien que moins dense (d = 1,2) que d'autres liqueurs densimétriques (HENIN et TURC, 1949) (MONNIER et al., 1962), l'acide phosphorique est moins dangereux à manipuler, il détruit les carbonates en favorisant la libération de matières légères séquestrées et permet le dosage de matières organiques acido-solubles (acides fulviques libres) contenues dans les sols et débris végétaux.

Le carbone des particules recueillies dans le surnageant est dosé par combustion et coulométrie du CO_2.

B) Outils statistiques et informatiques

Le logiciel SPCLAS (PANSU, 1983) a permis l'extraction des données étudiées selon chacun des trois plans d'expérience, leur présentation graphique avec les intervalles de confiance et les premiers essais d'ajustement linéaires.

L'ajustement non linéaire des courbes de carbone a été réalisé au moyen du logiciel STATGRAPHICS (société UNIWARE) qui utilise la méthode analytique de l'algorithme de MARQUARDT (1963) et avec le logiciel OPTIM (CHEVILLOTTE et TOUMA, 1987) par la méthode de MARQUARDT et la méthode SIMPLEX des gradients.

Nous avons écrit un programme donnant pour chaque modèle trouvé : les résidus d'ajustement, le coefficient de détermination R2, le test F de Fisher-Snedecor, la probabilité associée Pr. de refus du modèle et l'estimation de l'écart-type s des valeurs prédites.

Le calcul des approximations de départ des modèles non linéaires est réalisé de la manière suivante :

— Estimation de l'exponentielle correspondant au compartiment stable à partir de 90 jours d'incubation.

— Déduction des valeurs prédites avec cette exponentielle aux valeurs mesurées en début d'incubation.

— Estimation de l'exponentielle correspondant au début d'incubation.

Il va de soi que pour un même phénomène, plusieurs modèles peuvent convenir. Par exemple, là où BALESDENT (1982) trouve une fonction puissance, JENKINSON (1977) trouve une somme d'exponentielles. C'est pourquoi, nous avons toujours essayé plusieurs modèles et dans ce qui suit seuls sont indiqués les ajustements les plus significatifs.

Nous avons programmé les modèles d'évolution en basic sous leur forme matricielle. Nous avons également utilisé un logiciel turbo-pascal d'intégration numérique d'équations différentielles (G. PICHON, ORSTOM, com. pers.).

II. EVOLUTION DU CARBONE ORGANIQUE TOTAL

A) Equation trouvée

Le meilleur ajustement de la teneur du carbone organique Ct en fonction du temps t que nous ayons pu observer est de la forme :

$$Ct = a \exp(-\alpha t) + b \exp(-\beta t) \qquad (1)$$

dans lesquel les constantes a et b représentent les valeurs en carbone de deux compartiments instables et stables à l'instant initial alors que α et β représentent respectivement leurs cœfficients de décroissance. Nous avons réalisé ces ajustements sur les trois séries d'essais ayant reçu les plus forts amendements en paille. Les mesures sont alors moins sujettes à des fluctuations d'échantillonnage.

Les courbes correspondant aux amendements plus faibles ont été déduites des premières en conservant les coefficients α et β des exponentielles et en posant :

$$X1 = \exp(-\alpha t)$$
$$X2 = \exp(-\beta t)$$

Une régression multiple sans constante a permis alors d'estimer les coefficients a et b des modèles :

$$Ct = a\ X1 + b\ X2$$

Les paramètres a, b, α, β sont reportés dans le tableau III avec les tests statistiques d'ajustements.

Tableau III : Décroissance du carbone organique total : α, β, a, b sont les paramètres de l'équation (1) ; m et Co représentent l'apport de carbone et la valeur mesurée au temps 0.
Les équations pour m = 8,1 pour mille sont obtenues par les méthodes non linéaires. Les autres équations sont obtenues par la méthode de régression multiple indiquée dans le texte.

Decrease of total organic carbon : α, β, a, b are the parameters of the equation (1) ; m and Co correspond to the carbon supply and the value mesured at time 0.
Equations concerning m = 8,1 pour mille are obtained with non-linear methods. The other equations are obtained with the multiple regression method mentioned in the text.

Exp.	m °/ooC	Co	$-\alpha$ -1/année	$-\beta$	a °/oo C	b	R2	F(3,3)	Pr..	s
VE	8,1	21,05	14,51	0,015	4,99	15,68	0,94	15,8	0,05	0,67
SA	8,1	27,27	16,24	0,007	9,48	17,95	0,90	60,6	0,01	0,63
SG	8,1	26,30	24,11	0,074	6,17	20,03	0,98	40,2	0,01	0,56
VE	2,7	15,60	14,51	0,015	2,23	13,23	0,79	4,0	0,28	0,61
SA	2,7	21,00	16,24	0,007	5,36	15,33	0,87	6,5	0,16	1,10
SG	2,7	20,80	24,11	0,074	6,39	14,91	0,90	9,2	0,10	1,16
VE	0	12,95	14,51	0,015	1,57	11,68	0,68	2,2	0,53	0,59
SA	0	17,75	16,24	0,007	3,47	13,97	0,94	15,2	0,05	0,47
SG	0	17,75	24,11	0,074	3,68	13,92	1,00	50,9	0,01	0,30

B) Résultats et discussion

Tableau IV : Demi-vies des compartiments labiles (A) et stables (B) selon différentes expériences d'incubation. Les ° indiquent des valeurs obtenues à partir des mesures de Carbone. Les autres valeurs sont obtenues par des mesures C14 ou N15.
Half-lives of the labile (A) and stable (B) compartements *according to differents experiments of incubation. The ° show values resulting from carbon measurements. The other values result from C14 or N15 measurements.*

Compartiments				A	B
Materiel	lieu	auteurs	durée de l'expérience (années)	T1/2 semaines	T1/2 Années
Ray-gras	Angleterre	JENKINSON (1977)	10	12,6	8,2
C14		JENKINSON (1965)			25 °
Ray-gras	Nigeria	JENKINSON et			
C14		AYABANA (1977)	2	3,7	1,8
Luzerne	Australie	LADD et Coll.			
C14		(1981)	4	1,4	4,5
			4	1,7	1,9
			4	1,6	5,3
			4	1,8	6,4
Luzerne	Australie	LADD et Coll	4	5,8	9,0
N15		(1981)	4	28	-
			4	2,6	8,0
			4	3,4	6,8
Blue Gamma	USA	NYHAN (1975)	1	5,4	
C14			1	6,9	
Paille Blé	Canada	VORONEY (1983)	10	19,1	7,6
C14			10	25,7	8,3
Paille blé	Allemagne	SAUERBECK et	9	24,5	7,6
C14		GONZALEZ (1977)	9	20,1	6,9
			4	11,1	3,5
			4	9,4	4,6
			4	7,6	4,8
			4	9,7	4,5
			4	8,0	4,4
			4	8,2	4,5
Paille blé	Costa Rica	SAUERBECK et			
C14		GONZALEZ (1977)	1	6,1	-
Paille blé	laboratoire	PAUL et	1	2,4	-
		VAN VEEN (1978)			
Paille blé	laboratoire	Present VE	1	2,5	46 °
		travail SA	1	2,2	90 °
		SG	1	1,5	9 °

Dans le tableau IV, les résultats obtenus sont comparés à ceux présentés par JUMA et MAC GILL (1986) selon un modèle à deux exponentielles et relatifs à la décomposition de matériel végétal marqué.

Dans ce tableau nous avons ajouté les ajustements que nous avons réalisés sur les données de NYHAN (1975), les résultats de PAUL et VAN VEEN (1978) en laboratoire et ceux de JENKINSON (1965) sur le compartiment stable non marqué des sols de Rothamsted.

1. Compartiment labile

Nos estimations des temps de demi-vie sont inférieures à celles obtenues dans les conditions naturelles avec la paille de blé. Elles sont proches de celles enregistrées par PAUL et VAN VEEN (1978) au laboratoire, sans correction de croissance de la biomasse. Ceci confirme les observations de ces auteurs au sujet des différences existant entre les expérimentations de laboratoire et celles en conditions naturelles.

Nos valeurs sont également proches de celles trouvées par JENKINSON et AYABANA (1977) et LADD et Coll. (1981), avec d'autres matières végétales dans des conditions naturelles de température et d'humidité élevées donc favorables à une décomposition rapide des résidus végétaux (Nigéria, Australie).

Contrairement aux hypothèses de VAN VEEN et PAUL (1981), la forte quantité d'argiles de nos sols ne renforce donc pas la stabilité des matières labiles.

2. Compartiment stable

Les temps de demi-vie du compartiment stable, sont, en revanche, beaucoup plus importants que ceux observés par les auteurs (tableau IV) pour des expériences au champ.

Il faut signaler que la plupart des expériences sont conduites sur des durées plus grandes que les nôtres, et que par contre, les données en début d'incubation qu'ils ont collectées sont peu nombreuses.

A ce sujet, JUMA et Mac GILL (1986), signalent un net aplatissement de la courbe de décomposition provenant des données de SAUERBECK et GONZALEZ (1977) au Costa Rica, pour une durée d'expérimentation d'une année, Nous avons observé le même phénomène sur les données de NYHAN (1975), également pour une durée d'expérience d'un an. On peut donc supposer l'existence d'une stabilisation temporaire des matières organiques résistantes qui peut disparaître après un an. Toutefois la durée limitée de nos expériences ne permet pas d'extrapoler au delà de la première année et l'expérience de JENKINSON et AYABANA (1977), conduite sur deux ans au Nigéria, semble infirmer cette hypothèse.

3. Hypothèse concernant la stabilité des matières humifiées

La décroissance observée du compartiment stable est, dans notre cas, beaucoup plus proche de celle du carbone initialement présent dans les expériences de JENKINSON (1965) que de celles trouvées pour les compartiments stables provenant des enfouissements de matériaux marqués.

Ces faits suggèreraient un temps moyen de résidence différent du temps de renouvellement pour les matériaux entrant dans le compartiment stable en contradiction avec les hypothèses de décroissance exponentielle (tableau I). A moins que, comme le suggèrent JENKINSON et AYABANA (1977), il existe un compartiment possédant une durée de vie plus grande que caux identifiés dans les expériences réalisées avec du carbone marqué.

Les doses de pailles enfouies dans nos expériences sont plus importantes que celles utilisées par les autres auteurs du tableau IV. Elles peuvent engendrer une formation d'acide acétique après une dizaine de jours d'incubation pouvant conduire à une diminution de l'activité biologique et de la minéralisation (LYNCH, 1979).

Cette hypothèse est peu vraisemblable dans le cas du sol carbonaté où on enregistre une augmentation des carbonates correspondant à une fixation du CO_2 les 15 premiers jours puis une diminution correspondant à une neutralisation des acides (H. SIDI, 1987).

Des observations de JENKINSON (1977) et JENKINSON et AYABANA (1977) il ressort qu'en l'absence de stress hydrique, les seuls paramètres identifiés intervenant fortement sur les cœfficients cinétiques sont la température (qui dans le domaine étudié agit sur les cœfficients selon la loi de VAN'T HOFF) et la quantité d'argile du sol.

Ce dernier paramètre intervient sans doute fortement dans notre expérience puisque les sols sont très argileux, avec des argiles 2:1 gonflantes alors que l'essai de JENKINSON et AYABANA a été réalisé sur des sols sableux avec des argiles kaolinitiques.

Nous avons tenté d'utiliser nos données pour valider des modèles prévisionnels ne différenciant pas carbone apporté et carbone présent stabilisé ou non.

III. VALIDATION DES MODELES A DEUX COMPARTIMENTS

A) Le modèle de HENIN et al. (1959) et sa validation par nos mesures de carbone total

Le modèle I de HENIN, MONNIER et TURC (1959) reporté dans la figure 1 distingue les matières organiques labiles A alimentées par les apports végétaux m et les matières humifiées B formées d'un apport provenant des précédentes, et qui se minéralisent beaucoup plus lentement.

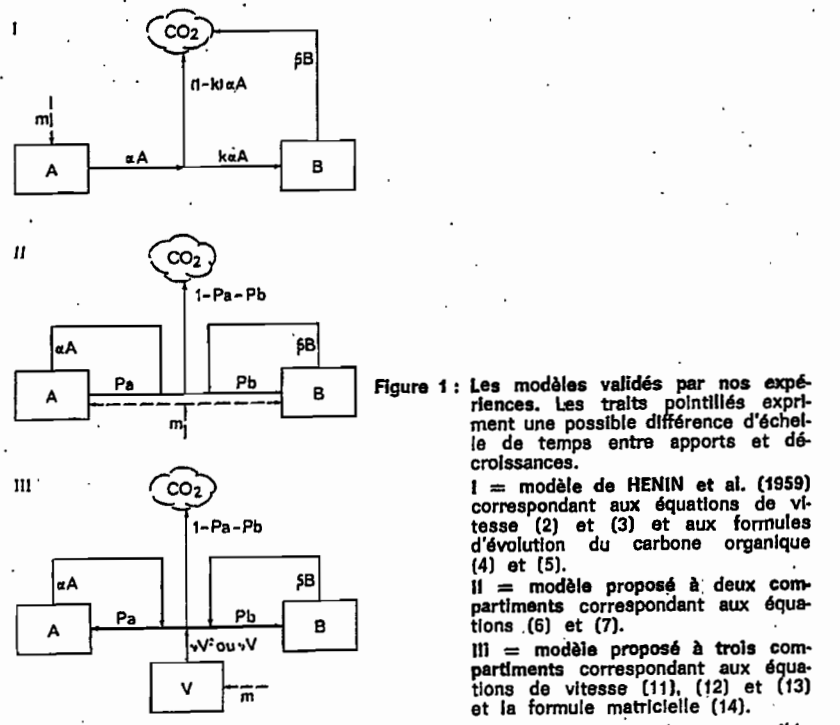

Figure 1 : Les modèles validés par nos expériences. Les traits pointillés expriment une possible différence d'échelle de temps entre apports et décroissances.

I = modèle de HENIN et al. (1959) correspondant aux équations de vitesse (2) et (3) et aux formules d'évolution du carbone organique (4) et (5).

II = modèle proposé à deux compartiments correspondant aux équations (6) et (7).

III = modèle proposé à trois compartiments correspondant aux équations de vitesse (11), (12) et (13) et la formule matricielle (14).

The models validated with our experiments. *Dotted lines show a possible time scale difference between carbon amendments and decay.*

I = HENIN et al. model (1959) *corresponding to differential equation (2) and (3) and organic carbon evolution formula (4) and (5).*

II = Suggested two compartment model *corresponding to equations (6) and (7).*

III = Suggested three compartments model *corresponding to differential equations (11), (12), (13) and matricial formula (14).*

Pour l'ajustement à nos données, nous avons modifié un peu l'expression des équations présentées initialement.

En effet, m est un apport discontinu avec une échelle de temps différente de celle du cœfficient de décroissance.

Les équations de vitesse de décroissance de chaque compartiment s'expriment alors par :

Compartiment labile A : $d(A + m)/dt = -\alpha(A + m)$ (2)

Compartiment stable B : $d(B)/dt = k\alpha(A + m) - \beta(B)$ (3)

avec

t = temps (en année)
(A + m), (B) = carbone organique total des compartiments A et B (en pour mille)
α = cœfficient de destruction des matières labiles (en année^{-1})
k = cœfficient isohumique
β = cœfficient de minéralisation des matières stables (en année^{-1}))

La somme des deux expressions obtenues par intégration des équations (2) et (3) nous fournit la formula d'évolution du carbone organique total Ct soit :

$$Ct = [Ao(1 - k\alpha/(\alpha - \beta)) + m(1 - k\alpha/(\alpha - \beta))] EXP(-\alpha t) + [Bo + kAo\alpha/(\alpha - \beta) + mk\alpha/(\alpha - \beta)] EXP(-\beta t) \quad (4)$$

et comme β est très petit devant α :

$$Ct = [Ao(1 - k) + m(1 - k)] EXP(-\alpha t) + (Bo + kAo + km) EXP(-\beta t) \quad (5)$$

Sous cette forme, le carbone évolue comme une somme de deux exponentielles avec des cœfficients multiplicatifs linéaires en fonction de l'apport. Nous avons testé cette linéarité pour chaque expérience afin d'obtenir le modèle correspondant à l'équation (5) de la forme :

$$Ct = (ao + a_1 m) (EXP(-\alpha t) + (bo + b_1 m) EXP(-\beta t) \quad (5')$$

Les valeurs des paramètres des équations (5) et (5') sont reportées dans le tableau V, où R2a et R2b représentent les cœfficients de détermination des deux ajustements linéaires des cœfficients a et b de l'équation (1) en fonction de l'apport m. Les courbes correspondant à ces équations sont reportées dans la figure 2.

Il ressort du tableau V que la linéarité en fonction des apports est meilleure pour le compartiment stable. Elle est satisfaisante pour expliquer la décroissance carbonée selon le modèle de HENIN et al. (1959) dans les expériences VE et SA. Le modèle s'applique mal par contre à l'expérience SG.

Tableau V : Estimations des paramètres des équations 5 et 5' correspondant au modèle de HENIN et al. (1959 : k = b1, δk = écart de k avec l'estimation k = 1 — a1, Ao et Bo estimés avec k = b1, δAo et δBo = écarts de Ao et Bo avec l'estimation k + δk.

Parameters evaluations in equations (5) and (5') corresponding to the model by HENIN et al. (1959) : *k = b1, δk = difference between the evaluation k = 1 — a1, Ao and Bo are evaluated with k = b1, δAo and δBo = differences on Ao and Bo with the evaluation k + δk.*

Exp	ao	a1	R2a	bo	b1	R2b	k	δk	Ao	δAo	Bo	δBo
VE	1,36	0,43	0,98	11,77	0,49	1,00	0,49	+0,08	2,68	+0,47	10,46	-0,47
SA	3,42	0,74	1,00	13,98	0,49	1,00	0,49	-0,23	6,73	-2,13	10,68	+2,13
SG	4,49	0,26	0,71	13,47	0,78	0,98	0,78	-0,04	(20,4)	-	(-2,4)	-

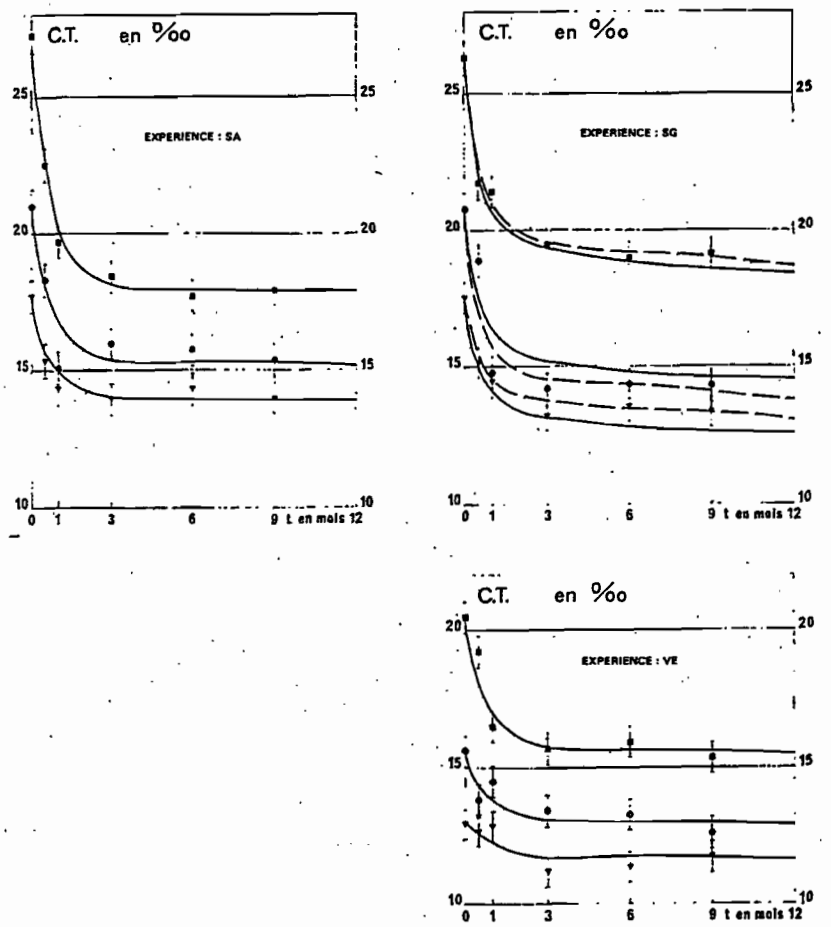

Figure 2 : **Ajustements réalisés selon les équations (5') (tableau V) du modèle de HENIN et al. (traits pleins) et selon notre modèle II (figure 1) à deux compartiments (pointillés). Les ajustements sont identiques pour les expériences VE et SA. Les points expérimentaux sont représentés avec leurs intervalles de confiance au niveau 0,95 pour les trois amendements de paille (8,1 pour mille ■, 2,7 pour mille ● et 0 ▼ de carbone).**

Fitting with the equations (5') (table V) of HENIN et al. (1959) model and our model II in figure 1 *(dotted lines). Adjustments are identical in VE and SA experiments. Experimental points are represented with their 95 % confidence intervals for the three supply of carbon straw : 8,1 pour mille ■, 2,7 pour mille ● and 0 ▼.*

B) Nouvelle présentation d'un modèle à deux compartiments

Les paramètres de l'équation (5) (tableau V) montrent que le pourcentage de carbone instable initialement présent dans le sol salé carbonaté (SA), est plus grand que dans le sol à tendance vertique (VE). L'activité biologique de ce dernier est d'ailleurs moins importante, comme le montre également la disparition moins rapide des polysaccharides (SIDI, 1987).

L'apport de gypse semble produire une augmentation simultanée des processus d'humification et de minéralisation et l'expérience SG ne permet pas de valider le modèle de HENIN et al. (1959).

Nous proposons une autre présentation d'un modèle à deux compartiments (modèle II, figure 1) prenant mieux en compte le renouvellement permanent (sauf contrainte climatique majeure) des matières organiques d'un compartiment à l'autre et la possibilité de passage des apports vers chacun des deux compartiments.

Pa et Pb représentent les proportions qui passent respectivement dans les compartiments instable A et stable B, soit de façon discontinue (traits pointillés) au moment des apports soit en permanence lors des processus de renouvellement. Les vitesses d'évolution de chaque compartiment s'expriment alors comme suit :

Compartiment instable A : $d[A]/dt = (mPa) + \alpha[A]Pa + \beta[B]Pa - \alpha[A]$ (6)

Compartiment stable B : $d[B]/dt = (mPb) + \alpha[A]Pb + \beta[B]Pb - \beta[B]$ (7)

où les parenthèses expriment une différence d'échelle de temps et les crochets, les teneurs de chaque compartiment en pour mille massique.

Dans les conditions d'état stable : $d[A]/dt = d[B]/dt = 0$

soit d'après les deux équations de vitesses :

$$[A] = [B]\ \beta Pa/\alpha Pb \quad \text{et} \quad [B] = [A]\ \alpha Pb/\beta Pa$$

Les temps de renouvellement Ta et Tb de chaque compartiment A et B s'expriment alors par $Ta = [A]/\alpha[A] = 1/\alpha$ et $Tb = 1/\beta$.

Les valeurs de carbone à l'instant initial permettent d'estimer les proportions Pa et Pb alors que les valeurs après un intervalle de temps δt fournissent une estimation de la somme Pa + Pb proche du cœfficient isohumique de HENIN et al.

Les valeurs de Pa et Pb sont respectivement de 0,3 et 0,25 pour l'expérience VE, 0,24 et 0,1 pour l'expérience SA, 0,28 et 0,32 pour l'expérience SG.

Le calcul des valeurs prédites par ce modèle (fig. 2) peut s'effectuer par deux méthodes donnant des résultats équivalents : intégration numérique des équations (6) et (7) ou sous forme matricielle de manière analogue au modèle à trois compartiments présenté ci-après.

Les courbes de la figure 2 montrent des ajustements confondus avec ceux du modèle de HENIN et al. en ce qui concerne les expériences VE et SA. Le modèle proposé permet un meilleur ajustement des données de l'expérience SG.

Les calculs montrent une moindre décroissance en fonction du temps pour le compartiment labile que dans le modèle précédent. Comme prévu, ce modèle traduit donc mieux une réalité physique : la présence de carbone facilement décomposable provenant des processus de renouvellement qui accompagnent la minéralisation de l'humus même dans les sols évolués.

IV. PRISE EN COMPTE DE LA CINETIQUE D'EVOLUTION DES MATIERES ORGANIQUES LEGERES ET PROPOSITION D'UN MODELE A TROIS COMPARTIMENTS

A) Cinétique de décroissance des matières organiques légères

Le carbone des matières légères extraites par fractionnement densimétrique en début d'incubation, juste après la première humectation, est toujours proche de 40 %

du carbone apporté par la paille. On ne peut donc assimiler ces fractions à la paille apportée. GRAFIN (1971) décrit le carbone des matières légères comme un carbone libre non remanié dans le sol alors que DABIN (1976) s'en tient au terme « matières organiques légères ».

La décroissance carbonée des matières organiques légères en fonction du temps suit une loi hyperbolique pour les expériences VE et SG alors que la loi est exponentielle dans l'expérience SA soit :

Expériences VE et SG : $V = Vo/(1 + Vo\Gamma t)$ (8)

Expérience SA : $V = Vo\ EXP(-\Gamma t)$ (9)

Avec :

t = temps (en année)

V = carbone au temps t des matières légères (en pour mille de la masse totale de sol sec)

Vo = valeur de V pour t = 0

Γ = Coefficient de décroissance du carbone des matières légères (exprimé en année^{-1} pour mille^{-1} pour l'équation (8) et année^{-1} pour l'équation (9) traduisant à la fois sa fixation dans le sol et sa minéralisation.

Dans chaque cas, les ajustements ont été trouvés en supposant que les valeurs Vo en début d'incubation sont les plus précises.

Des régressions linéaires ont permis alors d'estimer le coefficient Γ du modèle :

$$Y = \Gamma t \qquad (10)$$

avec :

Y = 1/V — 1/Vo, dans le cas de l'équation (8) et
Y = Log (V/Vo), dans le cas de l'équation (9)

Les parsmètres correspondant aux équations (8) et (9) sont présentés dans le tableau VI, et les courbes de valeurs prédites dans la figure 3.

Tableau VI : Estimation des paramètres des équations (8) et (9) décrivant la décroissance des matières organiques légères. Tous les ajustements sont significatifs au niveau 0,99 sauf pour l'apport 2,7 de l'expérience SG.

Evaluation of the parameters in equation (8) and (9) describing the decrease of light organic materials. *All fitting are significant et 0.99 level exept for the supply 1 % from the SG experiment.*

Exp.	m °/ooC	Equ. V	Vo	Γ	F(1,5)	s	T1/2
VE	0	(8)	0,24	39,86	98	0,02	5,4
VE	2,7	(8)	1,67	6,41	231	0,08	4,9
VE	8,1	(8)	2,66	1,92	163	0,15	10,2
SA	0	(9)	0,25	5,01	44	0,03	7,2
SA	2,7	(9)	1,16	2,77	53	0,14	13,0
SA	8,1	(9)	2,25	2,92	144	0,03	12,3
SG	0	(8)	0,23	38,35	40	0,03	5,9
SG	2,7	(8)	1,13	9,13	14	0,24	5,0
SG	8,1	(8)	2,19	3,19	416	0,03	7,4

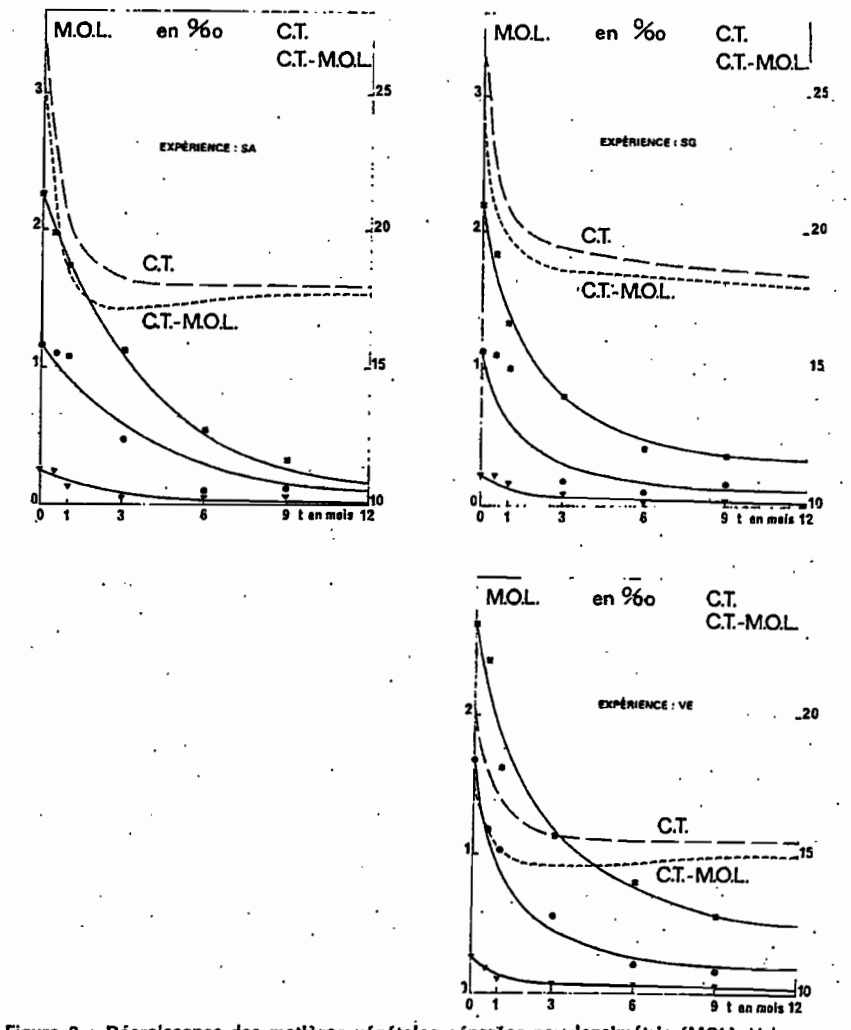

Figure 3 : Décroissance des matières végétales séparées par densimétrie (MOL). Valeurs expérimentales de 3 apports (8,1 pour mille ■, 2,7 pour mille ● et 0 ▽) et valeurs prédites par les équations (8) et (9) (tableau VI). Les courbes en pointillés représentent sur une échelle différente, les valeurs prédites du carbone total (CT), et du carbone non séparé par densimétrie (CT — MOL) pour les apports à 8,1 pour mille de carbone .

Decay of plant materials separated by densimetry MOL. *Experimental values of the three supplies (8,1 pour mille ■, 2,7 pour mille ●, and 0 ▽) and predicted values of (8) and (9) equations (table VI). The dotted curves represent on a different scale the predicted values of total organic carbon (CT) and carbon not separated by densimetry (CT-MOL) for the supplies of 8,1 pour mille carbon straw.*

B) Discussion

On ne peut pas affirmer dans le cas des expériences VE et SG que les lois de décroissance des matières organiques légères correspondent exactement à une cinétique d'ordre 2. Dans ce cas, comme nous l'indique le tableau I, les temps de demi-vie devraient dépendre de la quantité de paille apportée et le cœfficient Γ devrait être constant.

Or, nos cœfficients Γ diminuent lorsque l'apport de paille augmente, les temps de demi-vie restant relativement le paramètre le plus constant. Nous pensons que ce phénomène peut s'expliquer par une insuffisance quantitative de microorganismes par rapport à la quantité de paille enfouie. La biomasse microbienne deviendrait alors un facteur limitant.

Ces lois de décroissance des matières légères sont néanmoins très différentes de celles trouvées pour l'ensemble du carbone.

Si la vitesse de décroissance du carbone des matières légères est égale à celle du carbone de la paille enfouie, nos résultats sont en contradiction avec les hypothèses de JENKINSON et RAYNER (1977) et VAN VEEN et PAUL (1981) décrivant la décroissance des matières végétales enfouies dans les sols.

En effet, ces auteurs l'assimilent à une somme de compartiments plus ou moins décomposables à cinétique exponentielle. Or, nous ne trouvons pas de résultats expérimentaux pouvant vraiment étayer cette hypothèse. Les courbes d'évolution de végétaux marqués enfouis ne nous renseignent pas sur *l'état du carbone marqué* dans le sol au moment où il est mesuré. Par ailleurs, la décomposition d'un végétal peut-elle raisonnablement être assimilée à la somme des lois d'évolution en fonction du temps de ses constituants biochimiques ?

L'information apportée par la décroissance de nos matières légères, si imparfaites que soient nos mesures, est donc précieuse dans le débat concernant la cinétique de décroissance des végétaux dans les sols.

Nous remarquons également (tableau VI) que les temps de demi-vie du carbone de ces matières légères est supérieur au temps de demi-vie du carbone du compartiment labile (tableau VI). Ceci confirme notre hypothèse du modèle II de la figure I, c'est-à-dire que la totalité des matières végétales apportées ne peut être identifiée au seul compartiment labile de HENIN et al. (1959).

C) Présentation du modèle à 3 compartiments

Si l'on retranche des teneurs en carbone total les valeurs du carbone des matières organiques légères, les courbes obtenues (figure 3), peuvent encore être ajustées à des sommes d'exponentielles comme précédemment.

Pour prévoir l'évolution simultanée du carbone libre non remanié provenant des végétaux (compartiment V), du carbone d'origine végétale et microbienne de faible durée de vie (compartiment A) et du carbone stable de l'humus (compartiment B), nous proposons le modèle III de la figure I.

Dans *le cas d'une évolution hyperbolique des matières légères* et avec un apport m, les vitesses d'évolution de chaque compartiment s'expriment par :

$$d[V]/dt = -\Gamma[V]^2 \ (+ m) \qquad (11)$$

$$d[A]/dt = Pa\Gamma[V]^2 + Pa\alpha[A] + Pa\beta[B] - \alpha[A] \qquad (12)$$

$$d[B]/dt = Pb\Gamma[V]^2 + Pb\alpha[A] + Pb\beta[B] - \beta[B] \qquad (13)$$

avec :

t = temps (en année)

m = apport de carbone végétal en (pour mille du sol sec). Les parenthèses expriment une possible différance d'échelle de temps entre apports et décroissances.

[V,] [A], [B] = teneur carbonée de chaque compartiment (en pour mille de sol sec).

Pa, Pb = proportions de carbone entrant dans les compartiments A et B.

α, β = cœfficients de décroissance des compartiments A et B (en année^{-1})

Γ = cœfficient de décroissance hyperbolique du carbone à l'état végétal (en année^{-1} pour mille^{-1}).

Si *l'évolution des matières légères est exponentielle*, il faut remplacer $[V]^2$ par [V] dans les équations (11), (12) et (13).

Dans ce cas, le modèle fonctionne de manière analogue à celui proposé par JENKINSON et LADD (1981), pour décrire le renouvellement de la biomasse et des métabolites sous l'effet d'apports végétaux.

La principale différence réside dans le fait que notre compartiment instable A ne correspond pas à la seule biomasse microbienne mais aussi aux produits d'origine végétale facilement décomposables dont la vitesse de décomposition est souvent jugée comparable (CLARK et PAUL, 1970) (CHAUSSOT et al., 1986).

Si l'on ne tient pas compte de la différence d'échelle de temps apports/humification (suppression des parenthèses dans l'équation (11)) on peut comme JENKINSON et LADD, calculer l'apport correspondant au maintien des conditions d'état dynamique stable :

$$m = \alpha[A] \ (1 - Pa - Pb)/Pa$$

$$m = \beta[B](1 - Pa - Pb)/Pb$$

En fait, la présentation que nous donnons correspond également à une simplification du modèle de JENKINSON et RAYNER (1977) :

— Pour l'évolution à court terme, nous négligeons la fraction « Chemicaly stabilised organic matter », dans laquelle les entrées sont très faibles.

— Nous remplaçons les deux compartimenta à cinétique du premier ordre « décomposable plant material » et « Resistant plant material » par un seul compartiment dont la cinétique peut être, selon l'état du sol, exponentielle ou hyperbolique.

Pendant un intervalle de temps δt l'évolution respective de chaque compartiment peut être assimilée à :

$v = EXP(-\Gamma\delta t)$ ou $v = 1/(1 + Vo\Gamma\delta t)$ pour le compartiment végétal selon sa décroissance sans E de EXP, décroissance exponentielle ou hyperbolique.

$a = EXP(-\alpha\delta t)$ pour le compartiment instable.

$b = EXP(-\beta\delta t)$ pour le compartiment stable.

Au temps $t_i = t_{i-1} + \delta t$, l'état du sol est décrit par le vecteur :

$$Si = \begin{vmatrix} V \\ A \\ B \end{vmatrix}_i \quad \text{obtenu au moyen du produit matriciel :}$$

$$Si = M\,S_{i-1} \qquad (14)$$

où M représente la matrice d'évolution du sol :

$$M = \begin{vmatrix} v & 0 & 0 \\ Pa(1-v) & a + Pa(1-a) & Pa\,(1-b) \\ Pb(1-v) & Pb(1-a) & b + Pb(1-b) \end{vmatrix}$$

Là aussi, la méthode matricielle fournit des résultats comparables aux autres méthodes d'intégration numérique des équations de vitesses. Les courbes de la figure 4 représentent l'évolution simultanée de chaque compartiment et du carbone total pour les trois sols avec les plus forts apports de paille.

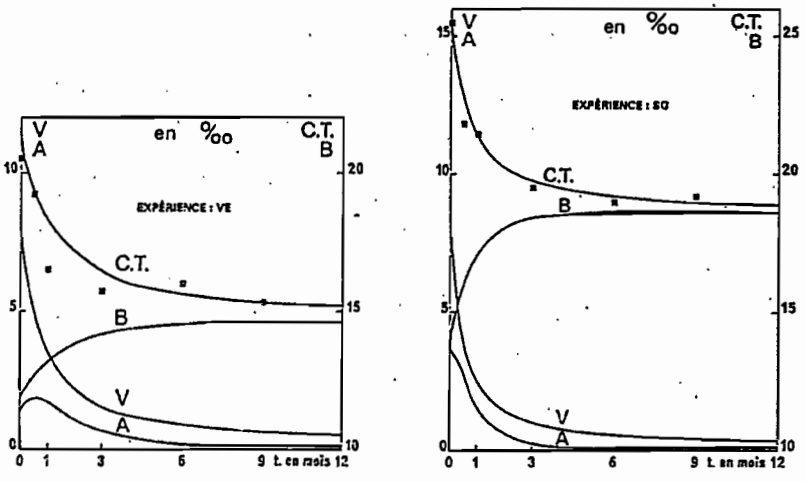

Figure 4 : Evolution simultanée des 3 compartiments du modèle III (figure 1) et du carbone total pour les apports de paille de blé correspondant à 8,1 pour mille de carbone des expériences VE et SG.

Simultaneous evolution of the three compartments of our model III (figure 1) and of total carbon for the supplies of 8,1 pour mille carbon wheat straw from the VE and SG experiments.

La validation du modèle est très satisfaisante pour l'expérience avec apport de gypse (SG). Les processus d'humification et de minéralisation sont alors plus rapides. Les mesures du carbone total des deux autres expériences s'ajustent un peu moins bien aux valeurs prédites.

On remarque une décroissance rapide du carbone végétal V accompagnée :

— d'une croissance plus lente du carbone stabilisé en B qui se rapproche du carbone total après six mois d'incubation.

— une croissance dans les premiers jours d'incubation (VE), voire dès le premier jour (SG), du carbone labile A d'origine microbienne et végétale. Ce carbone décroît ensuite rapidement et devient très peu abondant après 3 mois sans jamais atteindre une valeur négligeable.

On notera que le maximum de notre compartiment A se situe toujours à une durée d'incubation plus faible que le maximum observé (JENKINSON et LADD, 1981) pour la croissance de la biomasse en conditions naturelles. Cependant, pour l'expérience VE, il se situe au même endroit que celui noté par VAN VEEN et PAUL (1981) dans des conditions semblables.

CONCLUSIONS

Les deux modèles prévisionnels que nous proposons n'ont été validés que par des expériences de laboratoire dans des conditions contrôlées.

Le premier modèle (N° II figure 1) différencie seulement le carbone labile et le carbone stable du sol. Contrairement au modèle de HENIN et al. (1959), ce dernier ne comprend pas uniquement les fractions humifiées mais aussi une partie des fractions

végétales stabilisées dès leur incorporation. L'autre différence concerne un renouvellement du carbone labile depuis le carbone stable, même en l'absence d'apport végétal.

Le second modèle (N° III figure 1) est plus précis car il permet de tenir compte d'un répartition du carbone dans trois compartiments : fractions végétales non remaniées (V), microorganismes et métabolites végétaux labiles (A), matières organiques stables (B).

L'application des modèles à des études prévisionnelles au champ sur les sols de la région de MATEUR nécessitera la transposition sur le terrain des expériences de laboratoire avec des doses d'amendements organiques forcément plus limitées.

La possibilité de simuler avec nos modèles différents apports de pas de temps variables devrait aider à cette transposition.

Reçu pour publication : Mars 1987
Accepté pour publication : Septembre 1987

REMERCIEMENTS

Nous remercions Monsieur S. HENIN pour ses encouragements à valider et dépasser son modèle, Messieurs H. CHEVILLOTTE, J. TOUMA, B. LOUSTALAN, G. PICHON pour les discussions animées et amicales sur les méthodes numériques, Mesdames E. GAVINELLI, I. ROCHETTE, M. RICHARD, pour leur conseils en matière d'analyses chimiques et Monsieur P. de BOISSEZON qui a dirigé ce travail à l'ORSTOM.

SOIL HUMIFICATION AND MINERALIZATION KINETICS

A serie of three laboratory experiments concerning the incubation of mixtures of soils (vertisol and calcareous saline soils) and wheat straws allowed to equate as function of time total organic carbon contents and carbon contents of light plant materials separated by densimetry.

The evolution of organic carbon contents has been fitted to a sum of two exponentials (table III) whose parameters have been compared with the results obtained with other experiments (table IV).

The carbon contents in light plant materials decrease following an hyperbolic law in two experiments and following an exponential law in the third one (table VI, fig. 3).

Two models are suggested to describe the soil carbon and plant residues humification and mineralization processes by the microorganisms action (fig. 1) :

— a two compartment model which takes better account of turnover processes than the model worked out by HENIN et al. (1959).

— a more accurate three compartment model which allows to distinguish in labile fractions, plant carbon from carbon resulting both from the microbial growth and short-lived plant metabolites.

The suggested models have been confirmed by our laboratory experiments (table V, fig. 2, fig. 4).

BIBLIOGRAPHIE

BALESDENT J., 1982. — Etude de la dynamique de l'humificatoin de sols de prairies d'altitude (Haut-Jura) au moyen des datations C^{14} des matières organiques. Thèse Docteur-Ingénieur, Univ. Nancy I, 90 pages.

BOIFFIN P. et FLEURY A., 1974. — Quelques conséquences agronomiques du retournement des prairies permanentes. Ann. agron., 25 (4), p. 555-573.

BOIFFIN J., KELI ZAGBAHI J. et SEBILLOTTE M., 1986. — Systèmes de culture et statut organique des sols dans le Noyonnais : application du modèle de Hénin-Dupuis. Agronomie, 6 (5), p. 437-446.

CHEVILLOTTE H., TOUMA J., 1987. — Le logiciel OPTIM : Optimisation d'ajustements non linéaires, ORSTOM (à paraître)

CHAUSSOD R., NICOLARDOT B., SOULAS G., JOHANNES H., 1986. — Mesure de la biomasse microbienne dans les sols cultivés. II. Cinétique de minéralisation de matière organique microbienne marquée au carbone 14. Rev. Ecol. Biol. Sol, 23 (2), 119-153.

CLARK F.E. et PAUL E.A., 1970. — The microflora of grassland. Advan. Agron., 22, 375-435.

DABIN B., 1976. — Méthode d'extraction et de fractionnement des matières humiques du sol. Application à quelques études pédologiques et agronomiques dans les sols tropicaux. Cahiers ORSTOM, série pédol., 14 (4), 287-297.

GRAFFIN Ph., 1971. — Etude intégrée de la décomposition d'apports organiques dans le sol. Ann. Agron. 22, 2, 213-239.

HENIN S. et DUPUIS M., 1945. — Essai de bilan de la matière organique du sol. Ann. Agron. 15, 17-29.

HENIN S. et TURC L., 1949. — Essai de fractionnement des matières organiques du sol. C.R. Acad. Agric. Fr., 35 (1), 41-43.

HENIN S., MONNIER G. et TURC L., 1959. — Un aspect de la dynamique des matières organiques du sol. C.R. Acad. Sci. Fr., 248, 138-141.

HOFMAN G. et VAN RUYMBEKE M., 1979. — Evolution of soil humus content and calculation of global humification coefficients on different organic matter treatments during a 12-year experiment with belgian silt soils, Soil Sci., 129 (2), 92-94.

JENKINSON D.S., 1965. — Studies on the decomposition of plant material in soil. I. Losses of carbon from C^{14} labeled ryegrass incubated with soil in the field Soil Sci., 16, (1), 105-115.

JENKINSON D.S., 1977. — Study on the decomposition of plant material in soils. V. The effects of plant cover and soil type on the loss of carbon from ^{14}C labeled reygrass decomposing under field conditions J. Soil Sci., 28, 424-434.

JENKINSON D.S. et AYABANA A., 1977. — Decomposition of carbon-14 labeled plant material under tropical conditions. Soil Sci. Soc. Amer. J., 41, 912-915.

JENKINSON DS. et RAYNER J.H., 1977. — Te turnover of soil organic matter in some of the rothamsted classical experiments. Soil Sci., 123, (5), 298-303.

JENKINSON D.S. et LADD J.N., 1981. — Microbial biomass in soil measurement and turnover in « Soil Biochemistry », Marcel Dekker, New-York, 5, 415-471.

JUMA N.G. et McGILL W.B., 1986. — « Microfloral and faunal interactions in natural and agro-ecosystems ». M.J. MITCHELL et J.P. NAKAS Ed., Martinus Nijhoff Publishers, 74-136.

LADD J.N. et Coll., 1981. — Microbial biomass formed from C^{14}, N^{15} labeled plant material decomposing in soils in the field, Soil Biol. Biochem., 13, 119-126.

LYNCH J.M., 1979. — Straw residues as substrates for growth and product formation by soil micro-organisms, J. Wiley et Sons, New-York, 47-56.

MARQUARDT D.W., 1963. — An algorithm for least squares estimation of non linear parameters. Journal of the society of industrial and applied mathematics, 11 (2), 431-441.

MONNIER G., TURC L., JEANSON-LUUSINANG G., 1962. — Une méthode de fractionnement densimétrique par centrifugation des matières organiques du sol. Ann. Agron., 13 (1), 55-63.

NYHAN J.W., 1975. — Decomposition of carbon-14 labeled plant materials in a glassland soil under field conditions. Soil Sci. Soc. Amer. Proc., 39, 643-648.

PANSU M., 1983. — SPCLAS, un logiciel basic pour le calcul, le classement et la gestion des résultats d'un laboratoire d'analyses physico-chimiques, ORSTOM Bondy, 60 p.

PAUL E.A. et VAN VEEN J.A., 1978. — The use of tracers to determine the dynamic nature of organic matter. Trans. 11th Int. Congr. Soil Sci., Edmonton, Alta, 3, 61-102.

SAUERBECK D. et GONZALEZ M.A., 1977. — Field decomposition of C14 labeled plant residues in various soils of the federal republic of Germany and Costa Rica. In Soil organic matter studies, Proc. Symp. FAO/EIEA, Sept. 1976, Braunschweig, Germany, 1, 159-170.

SIDI H., 1987. — Effet de l'apport de matière organique et de gypse sur la stabilité structurale de sols de région méditerranéenne (Mateur - Tunisie). Thèse Doct. Ing. INAPG Paris, 206 p.

STEVENSON F.J., 1986. — Cycles of soil : carbon, nitrogen, sulfur, micronutients. J. Wiley et Sons Ed., New-York, 1-44.

VAN VEEN J.A. et PAUL E.A., 1981. — Organic carbon dynamic in glassland soils. 1. Background information and computer simulation. Can. J. Soil Sci. 61, 185-201.

VORONEY R.P., 1983. — Decomposition of plant residues. Ph. D. Thesis. University of Saskatchewan, Saskatoon.

Cycle du Carbone et propriétés physiques et chimiques du sol

Cycle C et stabilité structurale du sol

Extrait de Sidi et Pansu (1990)

E) STABILITÉ STRUCTURALE ET CINETIQUE D'ÉVOLUTION DES COMPARTIMENTS ORGANIQUES

Les trois compartiments du modèle de le figure I rcpr6scntcnt des ensembles organiques caractérisés par leur vitesse de décroissance (PANSU, 1989).

- Un compartiment végétal V servant d'aliment aux microorganismes. Son contenu en carbone décroît selon une cinétique hyperbolique (VEct SG) ou exponentielle (SA) à la fois par minéralisation et par répartition dans les deux autres compartiments. Nous avions estimé sa demi-vie respectivement à 7, 11 et 6 semaines pour les expériences VE, SA et SG (PANSU et SIDI. 1987). Il n'exerce pas d'influence directe sur la stabilité structurale.
- Un compartiment labile A dont le contenu carboné se trouve très rapidement renforcé en début d'incubation, en partie par solubilisation de carbone d'origine végétale mais surtout sous l'effet de la croissance des populations de microorganismes alimentés par les matières biodégradables de l'apport. Ce compartiment contient la plupart des substances bien connues pour leur effet sur la stabilisation des macro-agrégats: polysaccharides, filaments mycéliens, mucus bactériens. Sa demi-vie avait été trouvée moins importante que celle du compartiment végétal (2,5 semaines pour VE, 2,2 pour SA et 1,5 pour SG), c'est à dire qu'il est capable de s'auto-consommer avec un processus de renouvellement, avant que ne soient totalement décomposées les fractions résistantes des végétaux. Les taux de carbone de ce compartiment à la fois microbiologique et chimique, sont estimés par simulation numérique.
- Un compartiment stable B formé des matières organiques humifiées dont la demi-vie approximative a été estimée respectivement à 46, 90 et 9 ans pour les trois expériences VE, SA et SG. Son contenu carboné augmente lentement au cours de l'expérience pour se rapprocher de celui du carbone total en fin d'incubation. Si cette augmentation ressemble à celle des acides humiques, on ne peut pourtant pas assimiler cette fraction et ce compartiment. Ce dernier englobe sans doute en même temps certaines formes de l'humine. Les taux de carbone sont donc ici aussi probablement mieux estimés par simulation numérique que par fractionnement chimique. La croissance de ce compartiment pourrait être corrélée avec une stabilisation faible mais plus durable de la structure des sols.

Dans le cas du sol vertique, les simulations ont montré (Fig. 7) que le contenu du compartiment **A** passe par un maximum vers les 15 jours d'incubation. Ce maximum correspond à celui souvent observé de la biomasse microbienne en début d'incubation (JENKINSON et LADD,.1981; VAN VEEN et PAUL, 1981). Notons ici qu'il correspond également à celui des « acides fulviques pyrophosphate (AFP) ».

Remarquons surtout qu'il correspond à celui des taux d'aagrégats benzène (AGB). Sur la figure 7, nous avons indiqué les valeurs calculées des taux d'agrégats selon deux régressions linéaires en fonction : des valeurs simulées pour le compartiment A le premier mois d'incubation, des valeurs simulées pour le compartiment B en fin d'incubation. Le deuxième ajustement n'est pas significatif mais il serait instructif de poursuivre l'expérience sur des durées plus longues.

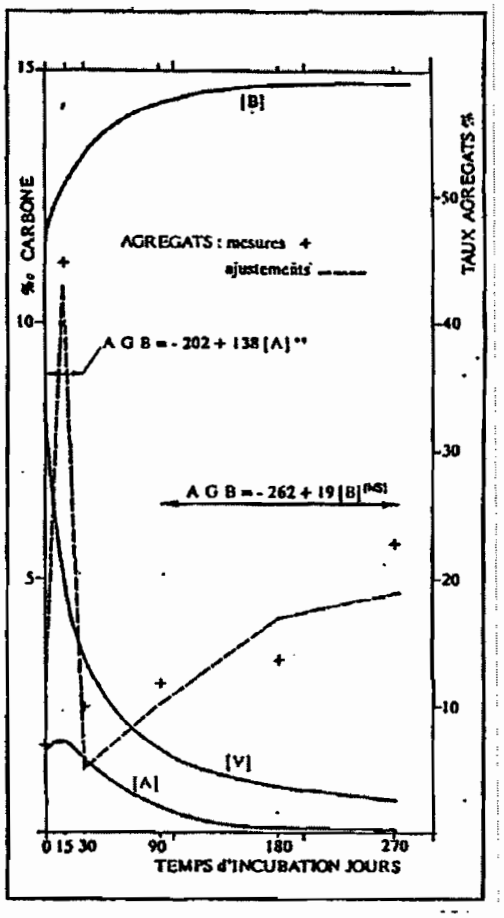

Fig.7 : Simulations de l'évolution simultanée des trois compartiments du modèle pour l'expérience VE : V = matières végétales, A = matieres organiques labiles, B = matières humifiées stables. Valeurs expérimentales des taux d'agrégats avec prétraitements au benzène (AGB, Hénin, 1938) et valeurs calculées correspondantes par ajustements sur le compartiment A durant le premier mois d'incubation, sur le compartiment B à partir de trois mois d'incubation.

Simulaled evolulion of the three compartments of the model for VE experiment: V = plant materials. A = labile *Organic matter, B = stable humified matter.*

Measured values of stable benzene aggregates (AGB) and corresponding calculated values by *adjustments on A compartment during lhe first month of incubalion. on B compartment during the last six months.*

Cycle C et capacité d'échange cationique du sol

Extrait de Pansu et de Boissezon (1989)

C - Relation avec les variations observées de la Capacité d'échange cationique

De nombreux auteurs ont montré l'existence de corrélations entre la capacité d'échange cationique des sols et leurs teneurs en matière organique, mais l'incorporation de matières organiques ne provoque pas toujours une augmentation significative de la capacité d'échange des horizons enrichis (BOISSEZON et BONZON, 1986).
Nous avons reporté dans le tableau II, les résultats d'ajustements linéaires entre la capacité d'échange cationique et les teneurs en carbone au cours des expériences, d'une part, pour chaque amendement, d'autre part pour chaque temps d'incubation, toujours selon le modèle :

$$CEC = a + b\,CT \qquad (4)$$

Tableau II : Ajustements de capacité d'échanges cationiques de l'horizon A1 correspondant à l'équation 4 pour chaque temps d'incubation (tableau de gauche) et pour chaque dose de paille ajoutée (tableau de droite).

TEMPS D'INCUBATION				DOSES DE PAILLE DE LUZERNE			
T jours	a	b	r^2	Apport C °/°°	a	b	r^2
1	18,O	0,089	0,93	0	11,I	0,346	0,57
15	17,2	0,111	0,89	10,05	15,2	0,166	0,72
30	16,6	0,122	0,85	20,I	16,7	0,118	0,84
90	15,3	0,163	0,76	30,15	17,5	0,103	0,90
180	13,4	0,242	0,57				

La capacité d'échange cationique qui est maximum en début d'incubation décroît proportionnellement à la diminution des teneurs en carbone organique dans l'horizon A1. Néanmoins, les résultats du tableau II indiquent une corrélation de plus en plus significative, pour les doses de paille les plus importantes, mais qui devient moins significative lorsque le temps d'incubation s'accroît. La pente des droites de régression varie en sens inverse : elle croît avec le temps, mais elle est divisée environ, par trois, lorsqu'on passe de l'apport nul à la dose de paille la plus forte. Ceci indique que la CEC des matières organiques résiduelles et des matières humifiées croît avec le temps tandis que la CEC due aux matières végétales ajoutées décroît d'autant moins que la dose de paille ajoutée est plus importante.
Or, notre modèle permet d'évaluer la quantité globale de carbone labile et celle de carbone stabilisé, au cours de la période d'incubation. Il était alors tentant, de calculer des ajustements linéaires de la CEC, non plus en fonction du carbone total, mais en fonction du contenu carbone des deux compartiments "A" labile et "B" stabilisé, selon un modèle du type

$$CEC = a[A] + b[B] \qquad (5)$$

Le tableau III indique les valeurs obtenues pour les deux coefficients "a" et "b", pour les quatre fumures et les coefficients de détermination correspondants. Les courbes correspondant a ces quatre ajustements sont représentées sur la figure 5 :

Tableau III : Ajustements de capacités d'échanges cationiques correspondant à l'Equation (5). sa et sb = écarts types associés a la détermination des coefficients a et b.

Apport C°/°°	a	Sa	b	Sb	R2
O	0,472	0,009	0,846	0,002	1,0000
10,05	0,303	0,014	0,787	0,005	1,0000
20,I	0,262	0,007	0,740	0,004	1,0000
30,15	0,237	0,009	0,711	0,006	0,9999

Les ajustements sont tous très hautement significatifs. Le coefficient "b" prend une valeur deux à trois fois plus forte que celle du coefficient "a", ce qui indiquerait un nombre de sites d'échange cationique également 2 à 3 fois plus fort, pour les produits humifiés que pour les matières organiques labiles. Le coefficient "a" diminue fortement lorsque la dose de paille ajoutée augmente. Avec l'apport le plus fort, la valeur devient moitié de celle sans apport. Ceci est probablement, en rapport avec la grande hétérogénéité du compartiment A. Celui-ci englobe tout le carbone des matières labiles, qu'il provienne des micro-organismes, de métabolites ou de résidus de végétaux non décomposés. Les matières labiles initialement présentes dans le sol possèdent plus de sites d'échange que les matières labiles provenant de la paille.
Le coefficient "b" diminue très faiblement lorsque la dose de paille ajoutée augmente. Les produits d'humification récente, provenant de la transformation de la paille, auraient donc un nombre de sites d'échanges légèrement moins importants que les produits humifiés antérieurement.

Modèle C à 5 compartiments (MOMOS-1-C)

Soil Biol. Biochem. Vol. 25, No. 12, pp. 1755–1762, 1993
Printed in Great Britain.

0038-0717/93 $6.00 + 0.00

MODELLING OF SOIL CARBON FORMS AFTER ORGANIC AMENDMENT UNDER CONTROLLED CONDITIONS

Z. SALLIH[1] and M. PANSU[2]*

[1]CEFE-CNRS, BP 5051, F-34033 Montpellier Cedex and [2]ORSTOM, BP 5045, F-34032 Montpellier Cedex, France

(Accepted 17 June 1993)

Summary—Two different soils were amended with ^{14}C-labelled plant material and incubated under controlled laboratory conditions for 2 yr. The dynamics of labelled and total (labelled + unlabelled) C remaining in the soil, in the microbial biomass and in the plant residue, were monitored throughout the experiment.

In order to fit these results simultaneously, a model was defined including five compartments with functioning concepts according to earlier proposals and with a relatively simplified mathematical presentation among those used to describe the soil C cycle. The simultaneous fitting of microbial, plant and total labelled C appears satisfactory in the two soils, with a plausible simulation of the humification process.

This model, focusing on the labelled C (added form), has allowed to fit the evolution of soil total C (labelled + unlabelled). The two fittings reveal the presence of a stable form of carbon with a half-life longer than that stabilized since the addition of plant material, but shorter than the 'chemically stabilized organic matter' named by Jenkinson and Rayner (*Soil Science* 123, 298–303, 1977).

Mineralization and humification kinetics were different in the two types of soils. These differences are expressed by model parameters and discussed with the presentation of results. In this way, hypothesis were derived in agreement with the soil mineral status and the soil carbon forms. Nevertheless, complementary investigations are necessary to verify these hypotheses and perhaps take into account newly endogenous variables in kinetic equations.

INTRODUCTION

Different models of the soil carbon cycle have been developed using data from natural conditions (Jenkinson and Rayner, 1977; Anderson and Coleman, 1985; Parton *et al.*, 1988; Molina *et al.*, 1983; Houot *et al.*, 1989). They take into consideration more and more main factors that influence the dynamics of organic matter, such as nitrogen contents (Molina *et al.*, 1983; Hadas *et al.*, 1987), climatic conditions (Parton *et al.*, 1987), soil temperature (Parton, 1984), and soil texture, particularly the clay content (Sorensen, 1981; Parton *et al.*, 1987).

Except for some particular approaches on mineralization and humification (Parnas, 1974; Brunner and Focht, 1984; Ionenko *et al.*, 1986), most of the proposed models classify the soil organic matter into compartments according to a decreasing rate which follows first order kinetics (Pansu, 1989).

Parton *et al.* (1987) proposed a model using concepts similar to those of Paul and Van Veen (1978). Following Jenkinson and Rayner (1977), it consists of five compartments that seem to correspond with analogous substance groups. Plant residue is divided into two compartments: 'metabolic' or 'decomposable plant material' and 'structural' or 'resistant plant material'. The soil C is divided into three compartments: 'active soil' or 'biomass', 'slow soil' or 'physically stabilized organic matter' and 'passive soil' or 'chemically stabilized organic matter'. The flow diagram of the Parton *et al.* model appears to be more complex and needs a larger number of parameters than that of Jenkinson and Rayner.

The NCSOIL model (Molina *et al.*, 1983) is equally more complex since the decomposition products POOL1 and POOL2 are both divided into two compartments, as plant residue.

Pansu and Sidi (1987) proposed two models, containing two and three compartments respectively, to describe the mineralization and humification kinetics in amended soil. These models were situated between those of Henin *et al.* (1959) and of Jenkinson and Rayner (1977), with the same type of working concepts (Pansu, 1988). These preceding studies have led us to maintain the same logic in this present proposition.

Our aim was to develop the most simple and suitable model to describe data that were obtained from a laboratory experiment (Z. Sallih, unpubl. Ph. D. thesis Université Montpellier, 1990). Some of these data have been published in two papers concerning carbon metabolism in relation to the presence of roots (Sallih and Bottner, 1988) and to microbial activity (Bottner *et al.*, 1988). The present study takes

*Author for correspondence.

into account the results of C evolution in two soils incubated without plants. In addition, labelled C found both in the light plus coarse organic particles was measured and assimilated into non-humified plant residue. Thus, to fit our model, we used more detailed results in comparison to studies carried out by Jenkinson and Ladd (1981), who considered the microbial biomass, and by Van Veen *et al.* (1985) who considered both microbial biomass and total labelled carbon simultaneously.

MATERIALS AND METHODS

Soils

The two soils used had developed under humid Mediterranean climatic conditions in southern France. Both were taken from the A1 horizon (0–15 cm) and classed according to CPCS (1976):

—soil 1: a fersiallitic calcic soil recently fallowed
—soil 2: a typical brown soil under grassland (*Brachypobium ramosum*).

The major characteristics of each soil are shown in Table 1. Main differences between the two soils were organic matter content, pH value and clay content. Illites are prevailing in soil 1, the most clayey one.

Experimental procedure

The experimental procedure was described by Sallih and Bottner (1988). Briefly, dried soil samples (5 mm) were split into portions of 800 g, mixed with 7 g mature uniformly ^{14}C-labelled wheat straw and then put in pots. The straw contained 1% N and 43% C with a specific activity of 2.59 MBq g^{-1} C; which corresponds to 3745 μg plant material ^{14}C g^{-1} soil. The procedure to obtain the labelled straw was described by Bottner (1982).

Pots were kept for >2 yr under controlled conditions in a growth chamber (daylight, 16 h at 25 ± 4°C; night 8 h at 15 ± 3°C). During this period, soil moisture was maintained at 75% WHC. Seven samplings were carried out at days 16, 29, 85, 121, 247, 422 and 690. At each sampling, the whole content of one pot was used for the analysis; 6–10 sub-samplings were carried out according to the type of analysis.

Analytical methods

Total carbon (organic plus inorganic) and labelled carbon (^{14}C) were measured using dry and wet combustion (Bottner and Warembourg, 1976).

Carbon of the microbial biomass (C-BM) was determined following the fumigation–incubation technique (Jenkinson and Powlson, 1976), using a K_c factor of 0.41.

The remaining plant material was separated from the soil using the procedure of Ladd *et al.* (1977) modified as below. Soil samples were shaken with 0.2 mol ($NaHCO_3$) L^{-1} (pH 8.3), centrifuged (12,000 rev min^{-1}) and filtered. The floating material was collected. The filtrate was concentrated and considered as the hydrosoluble fraction. The sediment was suspended again and fractionated into two parts by water sieving through a 50 μm mesh sieve. Within the fraction >50 μm, the sequestrated plant material was separated densimetrically by $ZnSO_4$ solution (density 1.4) and then added to the previous fraction. The total and labelled C of this fraction was determined by dry combustion. This procedure is detailed by Cortez (1989).

In our study, this fraction (light and coarse matter) is assumed to be the residual plant carbon.

Mathematical model

Figure 1 shows our present model compared with two other models (Pansu and Sidi, 1987; Jenkinson and Rayner, 1977). According to three principal types of organic matter, differences between these models are:

(1) Plant material: the present model separates this matter into two compartments; labile (V_L) and stable (V_R) which may correspond to the compartments 'decomposable plant materials (DPM)' and 'resistant plant materials (RPM)' of Jenkinson and Rayner. This approach is in agreement with that of Paul and Van Veen (1978), Molina *et al.* (1983) and Parton *et al.* (1987), but contrary to our earlier one which grouped these two organic fractions in one compartment with a variable kinetic order.
(2) Labile organic matter: the present model makes a distinction between microbial biomass (B) and other labile compounds (A). This is not the case in the model of Jenkinson and Rayner which takes into account only the microbial compartment (BIO), and in our earlier model which considered the sum of these two compartments (L).
(3) Stable organic matter: our data do not allow to take into account the 'chemically stabilized organic matter' (COM), obtained by Jenkinson and Rayner from dating measurements. But in short and medium term study

Table 1. Main characteristics of soils used

Soils	Particle size distribution (%) 2–0.2 mm	200–50 μm	50–20 μm	20–2 μm	<2 μm	Organic C (%)	N (%)	$CaCO_3$ (%)	pH(H_2O)
1	7	18	24	21	29	1.2	0.12	2.2	7.9
2	45	12	11	18	11	2.7	0.2	<0.1	6.5

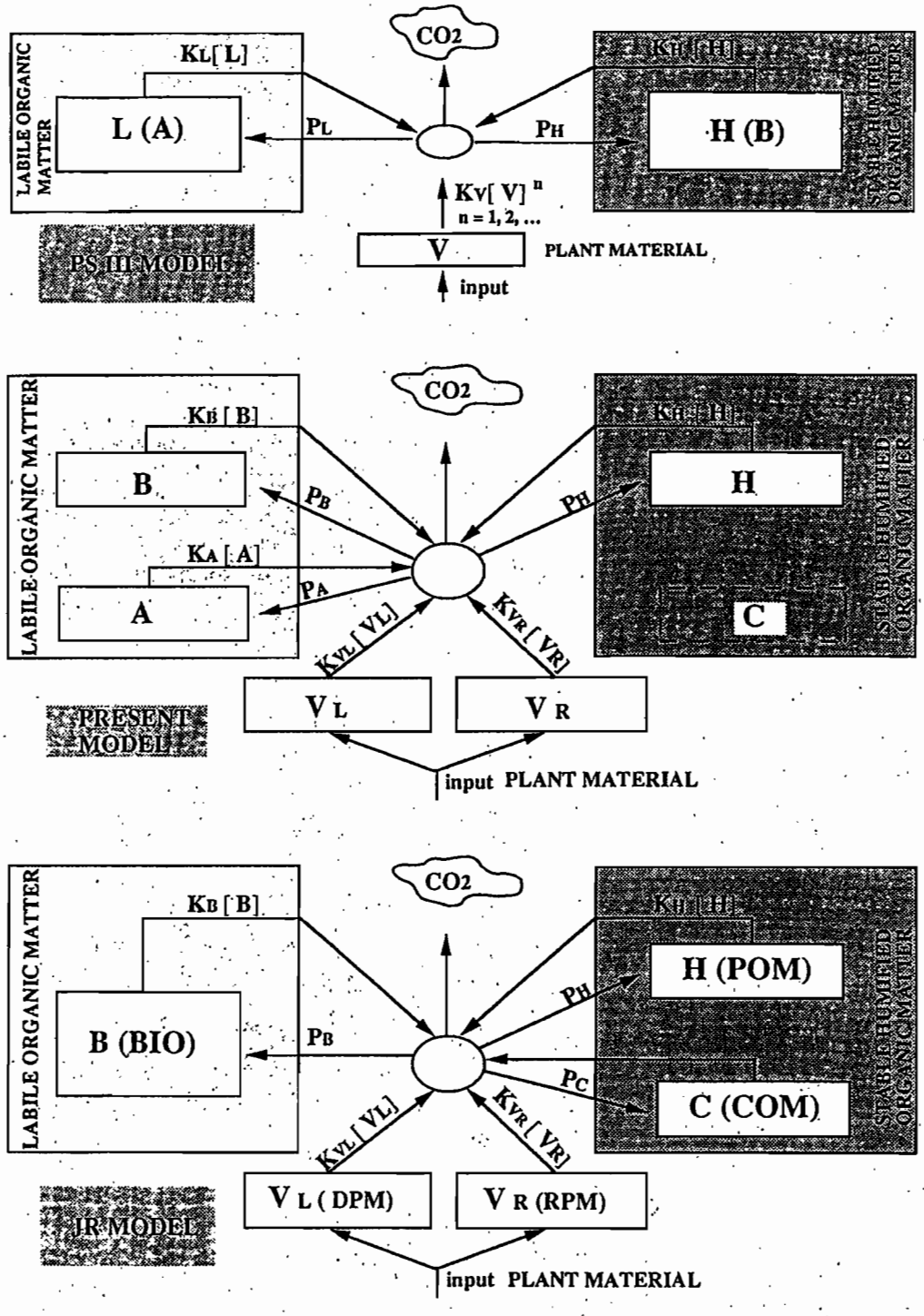

Fig. 1. Flow diagram for the present model compared to the propositions of Pansu and Sidi (1987; PSIII model) and Jenkinson and Rayner (1977; JR model). m = Organic input; V, V_L, V_R = plant material (PSIII), Labile plant material, Resistant plant material (JR and present model); B = microbial biomass (JR and present model); H = stable humified organic matter (present model, last called B in PSIII, last called 'Physically stabilized Organic Matter POM' in JR); C = chemically stabilized organic matter (COM in JR); A = labile soil organic matter, except microbial biomass and plant fragments (present model); L = labile soil organic matter, except plant fragments (PSIII model, last called A); P_L, P_A, P_B, P_H, P_C = input proportion in L, A, B, H, C compartments; Kv, Kv_L, Kv_R, K_A, K_B, K_H, K_C = kinetic coefficients of decays in the compartments V, V_L, V_R, A, B, H, C; n = kinetic order of decay in V compartment (PSIII).

of soil biochemical functioning, we can, as Molina *et al.* (1983) did, not take into account the 'passive organic phase'. In our model, the humified compartment (H) is analogous to that of our preceding model and similar to the 'physically stabilized organic matter' (POM) named by Jenkinson and Rayner.

Carbon dynamics vs time 't' is fitted according to a system of five first order differential equations. For any compartment 'm' among i compartments, this evolution is directed by:

$$\frac{dC_m}{dt} = -k_m C_m + P_m \sum_{i=1}^{5} k_i C_i \qquad (1)$$

$$m, i \in [V_L, V_R, A, B, H]$$

where:

C_m, C_i = carbon contents of compartments
k_m, k_i = rate constants of compartments (t^{-1})
P_m = proportion of carbon input into m compartment.

The equation of mineralization of carbon (C_T) is assumed to be:

$$\frac{dC_T}{dt} = -\sum_i k_i C_i \left(1 - \sum_i P_i\right) = -M \sum_i k_i C_i \qquad (2)$$

We defined M as the mineralization coefficient of the amended soil. From this, $I = \Sigma_i P_i = 1 - M$ is the renewed proportion of soil C.

Calculations were made using Turbo–Pascal Toolbox numerical methods (Borland).

RESULTS AND DISCUSSION

Study of different measurements

In preceding publications, we described:

—the decrease of added carbon according to the sum of two negatively exponential functions (Sallih and Bottner, 1988).
—the dynamic of microbial biomass and the respiratory quotient (Bottner *et al.*, 1988).

The best fitting for the non-transformed organic matter (separated by water sieving and densimetry) was obtained using the sum of two negative exponential terms. Parameters of these equations were supplied entering values for V_{L0}, V_{R0}, K_{VL} and K_{VR} (Fig. 2, Table 2). This type of fitting is different from that used by Pansu and Sidi (1987) where the light matter decreased according to an exponential or an hyperbolic function. However, preceding data are different and possibly not so accurate because they were obtained by densimetry only and from an unlabelled plant material.

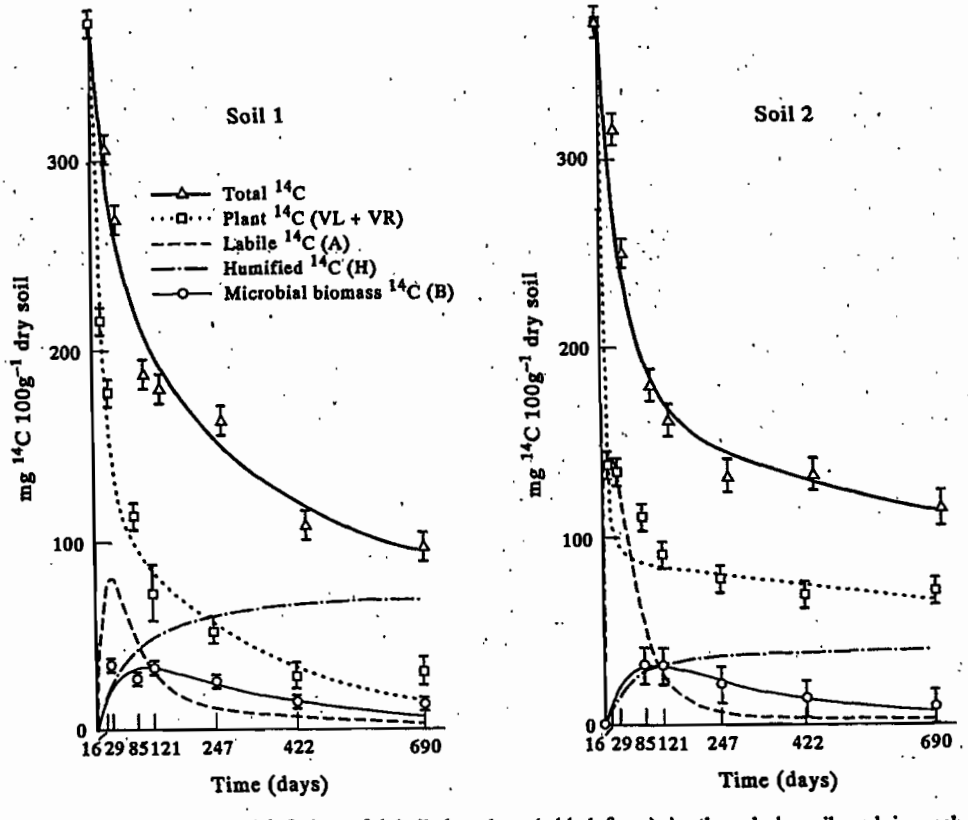

Fig. 2. Simultaneous model fitting of labelled carbon (added form) in the whole soil and in each compartment (confidence intervals of experimental data at 95%).

Table 2. Parameters of the model for labelled and total carbon of two soils

Compt.	Soil 1 I.V.	Soil 1 K_I	Soil 1 P_I	Soil 2 I.V.	Soil 2 K_I	Soil 2 P_I
			Labelled carbon			
V_L	246	0.05	0.0	283	0.1	0.0
V_R	125	0.0031	0.0	91	0.00043	0.0
A	0	0.05	0.58	0	0.1	0.79
B	0	0.006	0.08	0	0.004	0.033
H	0	0.0004	0.08	0	0.0001	0.025
			Total carbon			
V_L	246	0.05	0.0	283	0.1	0.0
V_R	125	0.0031	0.0	91	0.00043	0.0
A	9	0.05	0.58	220	0.1	0.79
B	60	0.006	0.12	120	0.004	0.033
H	1153	0.00005	0.08	2390	0.00002	0.025

I.V. = initial value of each compartment in mg C 100 g^{-1} dry soil.
K_I = kinetics constant in day^{-1}.
P_I = turnover proportion.
V_L = labile plant material.
V_R = resistant plant material.
A = labile soil organic matter (except microbial biomass and plant fragments).
B = microbial biomass.
H = humified organic matter.

Model fitting

The parameters of Table 2 and Fig. 2 show the simultaneous fitting of total-labelled C, plant-labelled C ($V_L + V_R$) and microbial-labelled C (B). The dotted lines represent the simulation of labile (A) and stable (H) humified labelled C. These two compartments were not measured but must be taken into account to equilibrate the balance of 'total-labelled C' minus 'plant-C plus microbial C'.

Moreover, the measurement of labelled C in the hydrosoluble fraction (unpubl. data) is closely correlated with the simulation of labile carbon (A) ($r = 0.89^{***}$ for soil 1 and $r = 0.73^{*}$ for soil 2), with a maximum towards day 15–30. This is clearly earlier than the maximum for microbial development. Nevertheless, the water-soluble fraction represents only about 10% of the simulated labile C, so it would be necessary to search for other labile products principally amongst the polysaccharides in the range between cellulose and simple sugars.

In the two soils, the labile compartment (A) decreased at the same rate as the plant labile compounds. This shows a very rapid incorporation of these compounds into the soil in such a way that it becomes impossible to distinguish them by granulometry or by densimetry. Both types of labile compounds are used to feed the microorganisms which reach their maximum growth after *ca* 3 months of incubation. Most of the labile compounds are consumed after 6 months, so microbial biomass decreases gradually.

Humified compounds increased progressively during the experiment to approach, at the end of the incubation, the level of the remaining added C. Nevertheless, as the degradation of the labile compounds, the major part of the humification process seemed to stabilize after 6 months of incubation.

The fitting of the model is as good as that of individual simulation of total-labelled C (Sallih and Bottner, 1988), and microbial biomass (Bottner *et al.*, 1988). A slight discrepancy of the microbial compartment fitting is noticed at the end of the experiment in soil 1. However, new experiments are necessary to define the cause of this deficit: experimental errors or a defect of model linearity would need a correction of the mathematical formulation.

Concerning the plant C, since renewal proportion P_I is zero for V_L and V_R compartments, the fitting is the same as that obtained by the sum of two exponential terms. The greater lack of fitting was noted at the end of experiment in soil 1 (as for microbial biomass), and at day 84 in soil 2. In each soil, the slope of plant C curve became close to that of total-labelled C when the labile fraction is already consumed. Then, the role of resistant plant C (V_R) becomes preponderant in the evolution of the system.

Soil type and evolution kinetics

Important differences in the mineralization process were found between the two types of soil. Mineralization is more intense in soil 1 than in soil 2; M (mineralization coefficient, equation 2) is 0.26 and 0.15 for the two soils respectively.

However, at the beginning of the experiment this order was reversed. At this time, more intensified mineralization occurred in soil 2. Conversion of rate constant of V_L and A compartments in half-life, according to Jenkinson and Rayner (1977), gives a value of 2 weeks for soil 1 but only 1 week for soil 2. This could be explained by the recent history of each soil. Soil 2 has been developed under grassland. Root input induces more labile organic matter and a microflora adapted to metabolize these substances or other labile products like the cellulose and polysaccharides of added plant material. Another explanation could be in relation to the stabilization of labile plant matter due to clay content (Van Veen and Paul, 1981) which is highest in soil 1.

When labile material was completely decayed after 2–3 months, the decrease in mineralization rate was particularly clear in soil 2. Half-life of the V_R compartment would be about 7 months in soil 1 but >4 yr in soil 2. So, at the end of the experiment, about 18% of the added plant material was not degraded in soil 2, whereas only 4% in soil 1.

The simulation by the model of the humification process (H compartment) is notably higher in soil 1 than in soil 2. This is consistent with former hypotheses about the role of clays in humification (Martin and Haider, 1986). The isohumic coefficient, calculated according to the original definition of Henin and Dupuis (1945) from 'H' compartment simulation, is equal to 0.18 for soil 1 and 0.11 for soil 2. We note here the importance of the compartmented simulation in the calculation of this coefficient, because calculations considering added carbon decrease only, may have led to an inverse conclusion

concerning humification. Effectively, at the end of the experiment, the ratio of remaining ^{14}C to initially added ^{14}C is equal to 0.25 in soil 1 and 0.31 in soil 2; the isohumic coefficient seems to be more important in sandy soil than in clay soil.

After 2 yr of incubation, and in spite of a relatively stabilized curve of global labelled C, we are still far from the equilibrium in soil 2, whereas in soil 1, the residual added C becomes close to humified carbon. The initially greater C content of soil 2 is originated probably from the preponderance of plant C that is incompletely transformed.

Finally, both mineralization and humification process are more important in soil 1 (clay soil), and express an intense biological functioning, except at the beginning of the experiment. The model shows this phenomenon by the parameters that characterize the microbial biomass. Although global aspects of microbial dynamic curves appear similar in the two soils, half-life of microbial biomass is slightly shorter in soil 1 than in soil 2 (about 4 months instead of 6 months) and the renewal proportion in soil 1 is more than twice. This higher turnover of the microbial compartment may suggest an important availability of nitrogen in soil 1, but this hypotheses must be verified.

Moreover, if humification is less intense in soil 2 (sandy soil) than in soil 1 (clayey soil), it suggests that formed humus in soil 2 is more stable; with a half-life of 'H' compartment about 19 yr against only 5 yr in soil 1.

Total carbon simulation

Before the model can be tested in natural conditions, we must verify if it is possible to fit the dynamics of total soil C (labelled + unlabelled) without major modifications in parameters. This may allow to check the validity of the model: does pre-existing organic matter in the soil behave in the same way as added matter?

Parameters of Table 2 and Fig. 3 show the simultaneous fitting of total C, plant C and microbial C. As above, the simulation of humified total C of compartments labile (A) and stable (H) are represented by dotted lines. The model seems satisfactory because similar results were obtained after changing the initial values of A, B and H compartments.

The rate constants are the same as above, except that of stable compartment (H) whose half-life would pass from 5 to 38 yr in soil 1 and from 19 to 95 yr in soil 2. This difference could be explained by the fact that the very stable compartment (COM) of soil organic matter has not been taken into account in the calculation.

With these data, we tried to estimate the stability of this compartment; assuming that K_H, k_H^*, k_H^0 are the rate constants of humified total, labelled and native carbon respectively, the [H], [H*] and [H⁰] are their corresponding contents, then the equation of the flow between these compartments is:

$$k_H[H] = k_H^0[H^0] + k_H^*[H^*] \quad (3)$$

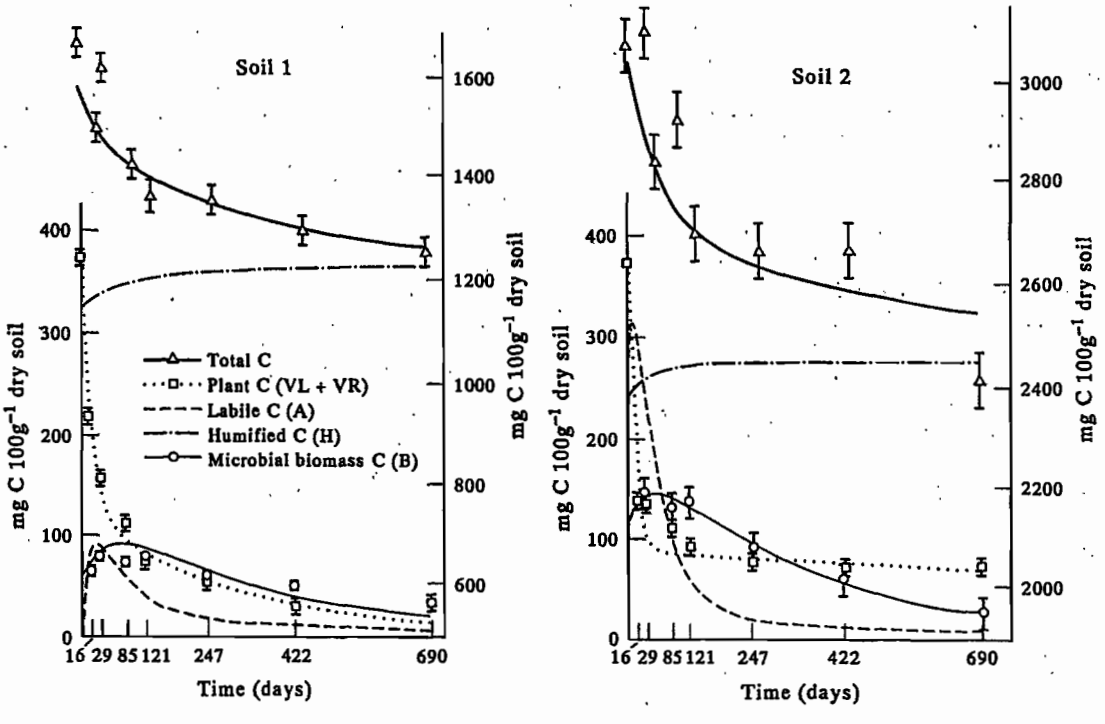

Fig. 3. Simultaneous model fitting of total carbon in the whole soil and in each compartment (plant, labile and microbial carbon on the left scale, total and humified carbon on the right scale; confidence intervals of experimental data at 95%).

If we take for [H], [H*] and [H^0], the values at the end of the experiment (with simulation of non-addition for [H^0]), equation 3 gives a k_H^0 of 0.00003 d^{-1} for soil 1 and of 0.000019 d^{-1} for soil 2; this corresponds to a half-life of 63 and of 102 yr for the two soils respectively. These half-lives are considerably smaller than that of 1980 years found by Jenkinson and Rayner for their [COM] compartment. So it is illusory to try to estimate this compartment from this type of experimentation. But it seems that it exists a part of soil C with an intermediary half-life between [H] and [COM]. This could explain the often observed decrease of native C in comparison to added C, and confirms some preceding suggestions (Jenkinson and Ayanaba, 1977; Pansu and Sidi, 1987). However, we must be careful with the estimation of stable compounds from a short-term experiment.

Renewal proportions P_i are all the same as those used for ^{14}C, except that of the microbial biomass of the soil 1, which had been increased slightly. This would confirm our preceding remarks that suggest a little anomaly of the model in this soil which have an intense biological activity, but complementary investigations will be necessary to determine precisely this observation.

On the other hand, in soil 2 the fitting of the microbial biomass by our model seems still more precise than the fitting of this only compartment (Bottner *et al.*, 1988). A choice of high initial values of both microbial and labile (A) compartments was necessary for the realization of the adjustment. This is in agreement with one of the above hypotheses about the intense mineralization activity at the beginning of the experiment in this soil from grassland.

The fitting of soil total C is acceptable despite the relatively important variability of the measurements, especially in soil 2. This variability would confirm the above hypothesis about the presence in this soil of incompletely decomposed fragments of plant C.

In spite of these restrictions, the transposition of the model on the soil total C is satisfactory. This gives a validation to the model in our experiment. The number and the type of proposed compartments appear necessary and sufficient to explain globally the soil C cycle (added or native).

Perspectives

This model, tested by experimental data, is interesting by its relative simplicity as only one equation (equation 1) can describe the evolution of every compartment. It can also be adapted to obtain the more suitable description of the soil C cycle at a given situation. For example, the model with two or three compartments (Pansu and Sidi, 1987) could be described by a similar equation with $i = 2$ or $i = 3$ (if $n = 1$ for PS III, Fig. 1) and a new definition of the compartments. The model can be used in predicting studies of the organic pools dynamics for one soil type (where organic inputs could be estimated as well as k_i and P_i). The influence of climate could be expressed by changing the k_i constants of formula (1) by k_i^{eff} such as:

$$k_i^{eff} = k_i l_{(T)} m_{(M)} \quad (4)$$

with $l_{(T)}$, $m_{(M)}$ = correcting factors for temperature and moisture which could be those provided by Van Veen and Paul (1981) or Parton *et al.* (1987). Moreover, experimental data should be of interest for a precise fitness of the model.

In addition, data provided from various experiments, comparable with ours, would be of great significance in considering the edaphic factors (nitrogen, clays, cultivation and biomass ...) which may influence the model parameters in order to make progress towards its generalization.

REFERENCES

Anderson D. W. and Coleman D. C. (1985) The dynamics of organic matter in grassland soils. *Journal of Soil and Water Conservation*, **40**, 211–216.

Bottner P. (1982) Biodégradation du matériel végétal en milieu herbacé. *Acta OEcologica/OEcologa Generalis* **3**, 155–182.

Bottner P. and Warembourg F. (1976) Method for simultaneous measurement of total and radioactive carbon in soils, soil extracts and plant material. *Plant and Soil* **45**, 273–277.

Bottner P., Sallih Z. and Billes G. (1988) Root activity and carbon metabolism in soils. *Biology and Fertility of Soils* **7**, 71–78.

Brunner W. and Focht D. (1984) Deterministic three-half-order kinetic model for microbial degradation of added carbon substrates in soil. *Applied and Environmental Microbiology* **47**, 167–172.

Cortez J. (1989) Effect of drying and rewetting on mineralization and distribution of bacterial constituents in soil fractions. *Biology and Fertility of Soils* **7**, 142–151.

CPCS (1967) Classification des sols. Ecole Nationale Supérieure d'Agronomie (E.N.S.A), 87 pp., Grignon.

Hadas A., Molina J. A. E., Feigenbaum S. and Clapp C. E. (1987) Simulation of Nitrogen-15 immobilization by the model NCSOIL. *Soil Science Society of America Journal* **51**, 102–106.

Henin S. and Dupuis M. (1945) Essai de bilan de la matière organique du sol. *Annales Agronomiques* **15**, 17–29.

Henin S., Monnier G. and Turc L. (1959) Un aspect de la dynamique des matières organiques du sol. *Comptes Rendus de l'Académie des Sciences-France* **248**, 138–141.

Houot S., Molina J. A. E., Chaussod R. and Clapp C. E. (1989) Simulation by NCSOIL of net mineralization in soils from the Deherain and 36 Parcelles fields at Grignon. *Soil Science Society of America Journal* **53**, 451–455.

Ionenko V. I., Batsula A. A. and Golovachev Ye. A. (1986) Kinetics of humification. *Soviet Soil Science* **18**, 33–42.

Jenkinson D. S. and Ayanaba A. (1977) Decomposition of carbon-14 labelled plant material under tropical conditions. *Soil Science Society of America Journal* **41**, 912–915.

Jenkinson D. S. and Ladd J. N. (1981) Microbial biomass in soil; measurement and turnover. In *Soil Biochemistry* (E. A. Paul and J. N. Ladd, Eds), Vol. 5, pp. 415–471. Dekker, New York.

Jenkinson D. S. and Powlson D. S. (1976) The effect of biocidal treatments on metabolism in soil: V. a method for measuring soil biomass. *Soil Biology & Biochemistry* **8**, 209–213.

Jenkinson D. S. and Rayner J. H. (1977) The turnover of soil organic matter in some of the Rothamsted classical experiments. *Soil Science* **123**, 298–303.

Ladd J. N., Parsons J. W. and Amato M. (1977) Studies of nitrogen immobilisation and mineralization in calcareous soils. I. Distribution of immobilised nitrogen amongst soil fractions of different particle size and density. *Soil Biology & Biochemistry* **9**, 309–318.

Martin J. P. and Haider K. (1986) Influence of mineral colloids on turnover rates of soil organic carbon. *Soil Science Society of America* **17**, 283–303.

Molina J. A. E., Clapp C. E., Shaffer M. J., Chichester F. W. and Larson W. E. (1983) NCSOIL, a model of nitrogen and carbon transformation in soil: description, calibration and behaviour. *Soil Science Society of America Journal* **47**, 85–91.

Pansu M. (1988) Proposition de modèles descriptifs de la dynamique des matières organiques des sols. (C. R. Journée de pédologie ORSTOM Sep. 1988), Cahiers ORSTOM Série Pedologie XXIV (4).

Pansu M. (1989) Cinétique chimique et modèles compartimentaux: application à l'étude de l'évolution du stock organique des sols. In *SEMINFOR 2: La Modélisation Aspects Pratiques et Méthodologie, 2° Séminaire Informatique ORSTOM, Sep.* 1988. ORSTOM, Paris.

Pansu M. and Sidi H. (1987) Cinétique d'humification et de minéralisation de mélanges sols-résidus végétaux. *Science du Sol* **25**, 247–265.

Parnas H. (1974) Model for decomposition of organic material by microorganisms. *Soil Biology & Biochemistry* **7**, 161–169.

Parton W. J. (1984) Predicting soil temperature in a short-grass steppe. *Soil Science* **138**, 93–101.

Parton W. J., Stewart J. W. B. and Cole C. V. (1988) Dynamic of C, N, P and S in grassland soils: a model. *Biogeochemistry* **5**, 109–131.

Parton W. J., Schimel D. S., Cole C. V. and Ojima D. S. (1987) Analysis of factors controlling soil organic matter levels in great plains grasslands. *Soil Science Society of America Journal* **51**, 1173–1179.

Paul E. A. and Van Veen J. A. (1978) The use of tracers to determine the dynamic nature of organic matter. *Transactions of the 11th International Congress of Soil Science Edmonton, Alta* **3**, 61–102.

Sallih Z. and Bottner P. (1988) Effect of wheat (*Triticum aestivum*) roots on mineralization rates of soil organic matter. *Biology and Fertility of Soils* **7**, 67–70.

Sorensen L. H. (1981) Carbon–nitrogen relationships during the humification of cellulose in soils containing different amounts of clay. *Soil Biology & Biochemistry* **13**, 313–321.

Van Veen J. A. and Paul E. A. (1981) Organic carbon dynamics in grassland soils. I. Background information and computer simulation. *Canadian Journal of Soil Science* **61**, 185–201.

Van Veen J. A., Ladd J. N. and Amato (1985) Turnover of carbon and nitrogen through the microbial biomass in a sandy loam and clay soil incubated with [^{14}C(U)]glucose and [^{15}N]$(NH_4)_2SO_4$ under different moisture regimes. *Soil Biology & Biochemistry* **17**, 747–756.

Cycle de l'azote dans les sols, modèle MOMOS-N

Pergamon

66 Soil Biol. Biochem. Vol. 30, No. 1, pp. 19–29, 1998

Printed in Great Britain
PII: S0038-0717(97)00087-4 0038-0717/98 $19.00 + 0.00

MODELLING OF SOIL NITROGEN FORMS AFTER ORGANIC AMENDMENTS UNDER CONTROLLED CONDITIONS

M. PANSU,[1]* Z. SALLIH[2] and P. BOTTNER[2]

[1]ORSTOM, BP 5045, 911 Avenue d'Agropolis, F-34032, Montpellier Cedex, France and [2]CEFE-CNRS, BP 5051, Route de Mende, F-34033 Montpellier Cedex, France

(Accepted 10 March 1997)

Summary—This N model is derived from the C model (MOMOS) published by Sallih and Pansu (1993). Both models were fitted to experimental data obtained from an incubation experiment of ^{14}C- and ^{15}N-labelled plant material in two soils with contrasting characteristics over 2 y under controlled laboratory conditions. The N model uses the same structure as the C model with five organic compartments: labile plant material (V_L); stable plant material (V_R); microbial biomass (B); labile humified material (A); and stable humified material (H). Two additional compartments are included: exchangeable NH_4-N and NO_3-N. The transfers of N between the organic compartments are described according to first-order kinetics. Nitrogen transferred to the NH_4 compartment results from the balance between the output and input of all the organic compartments. Ammonium N output is split between nitrification and immobilisation into B (77%) and H (23%). Nitrification is controlled by a microbial growth law. The N model uses the parameters defined in the C model, with a constant multiplying factor for the N kinetic constants (fn = 1.4 and 1.9 in soil 1 and 2, respectively). The additional parameters defined for inorganic pools are comparable in both soils. The predicted ^{14}C-to-^{15}N ratios of each organic compartment agree with the experimental data, showing a rapid incorporation of ^{15}N into microbial biomass and a gradual build-up into stable humified compounds. The model was adjusted to ^{15}N experimental data from five time series (each series containing from five to eight sampling occasions), and was validated using five series of corresponding total N data. MOMOS-C and -N formulation is relatively simple, combining mechanistic first-order kinetic models and growth models. The predictions are in agreement with 16 data sets including different forms of organic ^{14}C (three series), total C (three series), organic and inorganic ^{15}N and total N. © 1997 Elsevier Science Ltd

INTRODUCTION

Though "azote", the French name for nitrogen given by Lavoisier, means "lifeless" and inert, this element is a major constituent of living organisms which catalyse key steps in biogeochemical cycling. Several indices, relying on chemical or biological field (Greenwood *et al.*, 1985) or laboratory tests to estimate soil nitrogen availability for plants have been proposed. Kinetic expressions for mineralization proposed by Stanford and Smith (1972) are based on a potentially labile N pool (N_0), which mineralizes according to first-order kinetics (k constant). Mary and Rémy (1979) proposed kN_0 as a potential mineralization index, but other equations have been suggested: double exponential (Deans *et al.*, 1986; Matus and Rodrigez, 1994); linear (Addiscott, 1983); or parabolic (Broadbent, 1986) functions. The concept itself of defined mineralizable N pools was critically discussed by Broadbent (1986) and Sierra (1990).

To improve empirical descriptions, mechanistic models try to integrate the N cycle processes with the inconvenience of increasing the number of parameters. Process-based models have been regularly reviewed: Neeteson and van Veen (1988), Hétier *et al.* (1989), Addiscott (1993), Beckie *et al.* (1994), Hansen *et al.* (1995). Some models describe particular mechanisms, for instance mineralization-immobilization processes (van Veen and Frissel, 1981), nitrification (Laudelout *et al.*, 1974) or denitrification (Bergstrom and Beauchamp, 1993). The N cycle is described separately (Jenkinson and Parry, 1989) or is linked to the carbon cycle, e.g. McGill *et al.* (1981), Molina *et al.* (1983), van Veen *et al.* (1984), Parton *et al.* (1987), Bradbury *et al.* (1993).

The carbon part of the MOMOS model (MOdélisation de la Matie(c)re Organique des Sols, Modelling of Organic Matter Of Soils) has already

*Author for correspondence. (Tel: +046-741-6228; Fax: +046-741-6294; e-mail: pansu@mpP.orstom.fr).

been presented in former publications (Pansu and Sidi, 1987; Sallih and Pansu, 1993; Pansu *et al.*, 1996). The C and N parts were built using data from laboratory incubation experiments performed over 2 y with ^{14}C- and ^{15}N-labelled plant material. The N model is linked to the C model, which has the same structure for organic compartments. The aim was to develop the most simple and suitable model to fit the experimental data.

MATERIALS AND METHODS

Data acquisition

Data were collected from incubation experiments, conducted under laboratory conditions, with two Mediterranean soils: a fersiallitic calcic soil (soil 1: pH = 7.9, organic C = 1.2%, N = 0.12%, and clay content =29%), and a typical brown soil (soil 2: pH = 6.5; organic C = 2.7%, N =0.2%, and clay content = 11%) (CPCS, 1967). The analyses of soils and the experimental procedure were described by Sallih and Bottner (1988), Bottner *et al.* (1988) and Sallih and Pansu (1993). Briefly, soils were mixed with ^{14}C- and ^{15}N-labelled mature wheat straw (Bottner, 1982), incubated over 710 d under controlled temperature and moisture conditions and sampled on seven occasions. The following analyses were performed on two replicates:

(1) C and ^{14}C in the whole soil, (2) C and ^{14}C in plant debris separated from the soil by physical fractionation, and (3) C and ^{14}C in microbial biomass (fumigation-incubation method; Jenkinson and Powlson, 1976); this data was used to validate the C model (Sallih and Pansu, 1993).

N and ^{15}N of: (1) the whole soil; (2) the plant debris; (3) the microbial biomass; (4) K_2SO_4 extractable ammonium; and (5) K_2SO_4 extractable nitrate. This data is used in the present N model.

For physical fractionation, the samples were first shaken with a 0.2 mol $NaHCO_3$ l^{-1} solution to separate floating material (F0). The sediment was then fractionated by wet sieving to give a >50 μm fraction. This coarse fraction was separated densimetrically ($ZnSO_4$ solution) into a sandy (F1) and a light fraction (F2). As for the C model, the sum F0 + F1 + F2 was considered as the residual plant material. Ammonium and NO_3^- were extracted from unfumigated and fumigated subsamples with a 0.5 mol K_2SO_4 l^{-1} solution. Ammonium was separated by steam distillation with MgO; NO_3^- was distillated after reduction by Devarda reagent. In the distillates, N was measured by automated colorimetry and ^{15}N by mass spectrometry. Total N and ^{15}N in soil and plant material, were determined by automated colorimetry and mass spectrometry on Kjeldhal-mineralization distillates.

Mathematical model

MOMOS describes N transformations using the structure and parameters defined in the C model, with additional N specific parameters. Figure 1 shows the causal diagram and the main flows of N described by MOMOS. The following abbreviations were used in Fig. 1, the equations and in the text: *oN*, *aN*, *nN* = organic N, ammonium N, and nitrate N, respectively.

The model formulation is relatively simple. The state variable *oN* (Fig. 1) represents the five organic compartments as subscripts: V_L = labile plant material; V_R = resistant plant material; A = labile soil organic matter; B = microbial biomass; and H stable humified organic matter. As described by Sallih and Pansu (1993) for carbon, the input of a given organic compartment m (oN_m) includes a fraction (P_m) of the outputs of organic compartments (oN_i) and immobilization from ammonium (aN). This is directed by:

$$\frac{doN_m}{dt} = f_n\left(-k_m oN_m + P_m \sum_i k_i oN_i \right)$$

$$+ f(m)\left(aN\left(1 - k_{n1}\left(k_{n2} - aN\right)\right)\right) \qquad (1)$$

where k_i, k_m (time^{-1}) are kinetic constants of the organic compartments; P_m is the proportion of N input from compartments i into compartment m. These parameters were previously defined by Sallih and Pansu (1993). The multiplying factor f_n increase

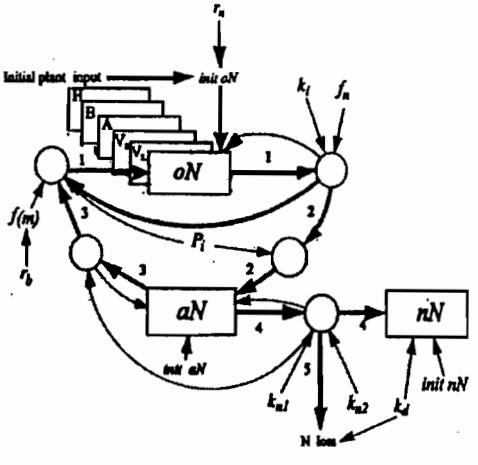

Fig. 1. Causal diagram of the N model. The state variable *oN* includes the five organic compartments as subscripts. They are defined in the text: V_L, labile plant material; V_R, resistant plant material; A, labile humified material; B, microbial biomass; and H, stable humified material. The state variables *aN* and *nN* represent ammonium N and nitrate N, respectively. Wide arrows indicate N flows. Numbers (1–5) associated with the wide arrows represent: (1) organic N transfers between the five organic compartments; (2) ammonification; (3) immobilisation of NH_4-N; (4) nitrification; and (5) N loss during nitrification process. The function $f(m)$ and the constants k_i, P_i, r_n, r_b, f_n, k_{n1}, k_{n2}, k_d are defined in the text and in Table 1.

the rate of N transformation compared with that of C. The flow of aN toward oN (arrow 3, Fig. 1) is distributed by $f(m)$: $f(m) = 0$ for $m \in \{V_L, V_R, A\}$, $f(m) = r_b$ for $m = B$ (r_b is the proportion of NH_4-N immobilized in microbial biomass), $f(m) = 1 - r_b$ for $m = H$. k_{n1} and k_{n2} represent two nitrification rate constants.

The ammonium N (aN) balance is directed by:

$$\frac{daN}{dt} = f_n\left(1 - \sum_i P_i\right)\sum_i k_i oN_i - aN \qquad (2)$$

i.e. aN is nitrified, lost or immobilized; exchangeable ammonium represents the balance between ammonification and these outputs. Nitrate (nN) production is directed by:

$$\frac{dnN}{dt} = (1 - k_d)k_{n1}aN(k_{n2} - aN)$$

$$\text{when } aN \le k_{n2}, \text{ otherwise } \frac{dnN}{dt} = 0. \qquad (3)$$

Equation 3 states that the nitrate production rate is proportional to the mass of depleted substrate (ammonium). Parameters k_{n1} and k_{n2} are the same as in eq.(1); k_d represents the fraction of N which is lost. Alternately, the more precise law of Monod (1941) can be used with the inconvenience of an additional parameter k_{n3} giving:

$$\frac{dnN}{dt} = (1 - k_d)\frac{k_{n1}aN}{k_{n3} + aN}(k_{n2} - aN)$$

$$\text{when } aN \le k_{n2}, \text{ otherwise } \frac{dnN}{dt} = 0 \qquad (3')$$

The process can also be described by enzyme kinetics:

$$\frac{dnN}{dt} = (1 - k_d)\frac{k_{n1}aN}{k_{n3} + aN} \qquad (3'')$$

Equations (3') and (3'') imply corresponding modifications of equation (1). The nitrification kinetic constants k_{n1}, k_{n2} and k_{n3} are discussed below.

Calculations were made according Press *et al.* (1992) by numerical integrations using Euler's method and by optimizations of the parameters for the N part of MOMOS using Powell's method, with the minimized criterion:

$$SSK = \sum_k p_k^2 \sum_j (y_{kj} - \hat{y}_{kj})^2 \qquad (4)$$

where j identifies the number of sampling points, k is the number of data series and y_{kj} and $\hat{y}_{kj}$ are the measured and predicted value of each data point, respectively; p_k are weight coefficients for each data series. In this work p_k values are 0.5, 0.3, 1, 1, 1 for total-^{15}N, plant-^{15}N, oN[B]-^{15}N, aN-^{15}N, and nN-^{15}N, respectively.

RESULTS AND DISCUSSION

Inorganic N

Measured exchangeable NH_4-^{15}N (Fig. 3) and NH_4-N (Fig. 7) concentrations were always low and varied irregularly with time. It was possible to simulate chaotic variations of ammonium by introducing a kinetic constant for ammonium immobilization. The proportion of ^{15}N in NH_4-N decreased with time in both soils, from 1/10 to about 1/50 at the end of experiment. Labelled NH_4-N concentrations were of the same order of magnitude in both soils, as well as total NH_4-N.

The accumulation of NO_3-^{15}N and NO_3-N was more regular and could be expressed using linear functions, reflecting zero-order kinetics. A linear function for nitrification was also found by Addiscott (1983), while first-order kinetic functions were calculated by Stanford and Smith (1972), from experiments where inorganic N was regularly extracted from the same soil sample. Zero-order kinetics of nitrification were used by Nicolardot *et al.* (1994) in the NCSOIL model (Molina *et al.*, 1983) to simulate data from a laboratory incubation experiment. Zero-order functions which indicate no substrate (NH_4-N) limitation for nitrifiers are not realistic for long-term incubations of unfertilized soils. The use of only one nitrification parameter (slope) could simplify the model, but this parameter was specific for each soil type and was different for labelled and total N.

First-order kinetics (van Veen *et al.*, 1984; van der Linden *et al.*, 1987; Parton *et al.*, 1987; Bradbury *et al.*, 1993) did not fit the measured nitrate values. Introduction of a state variable between aN and nN (arrow 4, Fig. 1), representing nitrite and other intermediates forms, improved the first-order kinetic predictions. However, the intermediate compartment became too large. Integrating the fixation of ammonium by clays also resulted in a good fit, but the simulated pool of fixed NH_4 was too important.

Nitrification can also be described taking into account its control by the growth of nitrifiers or by enzymatic kinetics. Several models (Smith, 1979; van Veen and Frissel, 1981; McGill *et al.*, 1981; Knapp *et al.*, 1983; Grant *et al.*, 1993) use exclusively kinetic equations for microbial growth but they are rather complex compared to the MOMOS model. The growth model of Laudelout *et al.* (1974) for ammonium nitrification in water, necessitates 10 parameters which cannot easily be estimated in soils.

Enzymatic kinetics [equation (3'')] become zero-order kinetics, when the Michaelis constant k_{n3} is near 0, i.e. when nitrification is always at a maximum rate ($V_{max} = k_{n1}$). Enzymatic law was used for soil nitrification by Franko *et al.* (1995) and Svendsen *et al.* (1995). This formulation is valid for constant enzyme concentrations and does not con-

Table 1. Parameters used in the model for labelled and total nitrogen. k_{n1}, k_{n2}, k_{n3}: nitrification parameters; k_d: volatilisation parameter; r_n: labile fraction of the plant material input; r_b and f_n are an immobilisation parameter and a multiplicative parameter defined in the text. Parameters k_l and P_l associated with organic compartments (V_L = labile plant material, V_R = resistant plant material, A = labile humified material; B = microbial biomass; H = stable humified material) are defined in Sallih and Pansu (1993) for the carbon model. For labelled N, initial values of compartments A, B, H, NH_4, and NO_3 = 0

	Soil 1			Soil 2		
	Labelled N					
Nitrification equation	3	3′	3″	3	3′	"3
k_{n1} (d^{-1})	7.8	0.26	0.0054	6.3	0.22	0.009
k_{n2} (mg kg^{-1})	0.6	0.7	No	0.8	1.1	No
k_{n3} (mg kg^{-1})	No	0.2	0	No	0.34	0.08
k_d (no dimension)		0.1			0	
r_b (no dimension)		0.77			0.77	
f_n (no dimension)		1.4			1.9	
r_n (no dimension)		0.5			0.5	
SSK (equation 4)	830	830	880	280	290	310
	Total N (nitrification equation 3)					
k_{n1} (d^{-1})		7.8			6.3	
k_{n2} (mg kg^{-1})		1.16			2.22	
k_d (no dimension)		0.1			0	
r_b (no dimension)		0.77			0.77	
f_n (no dimension)		1.4			1.9	
r_n (no dimension)		0.5			0.5	
k[H] (d^{-1})		0.00015			0.00005	
		Initial values (mg kg^{-1})				
A (labile humified material)		0			0	
B (microbial biomass)		160			320	
H (stable humified material)		950			1930	
aN (ammonium N)		0			0	
nN (nitrate N)		0			0	

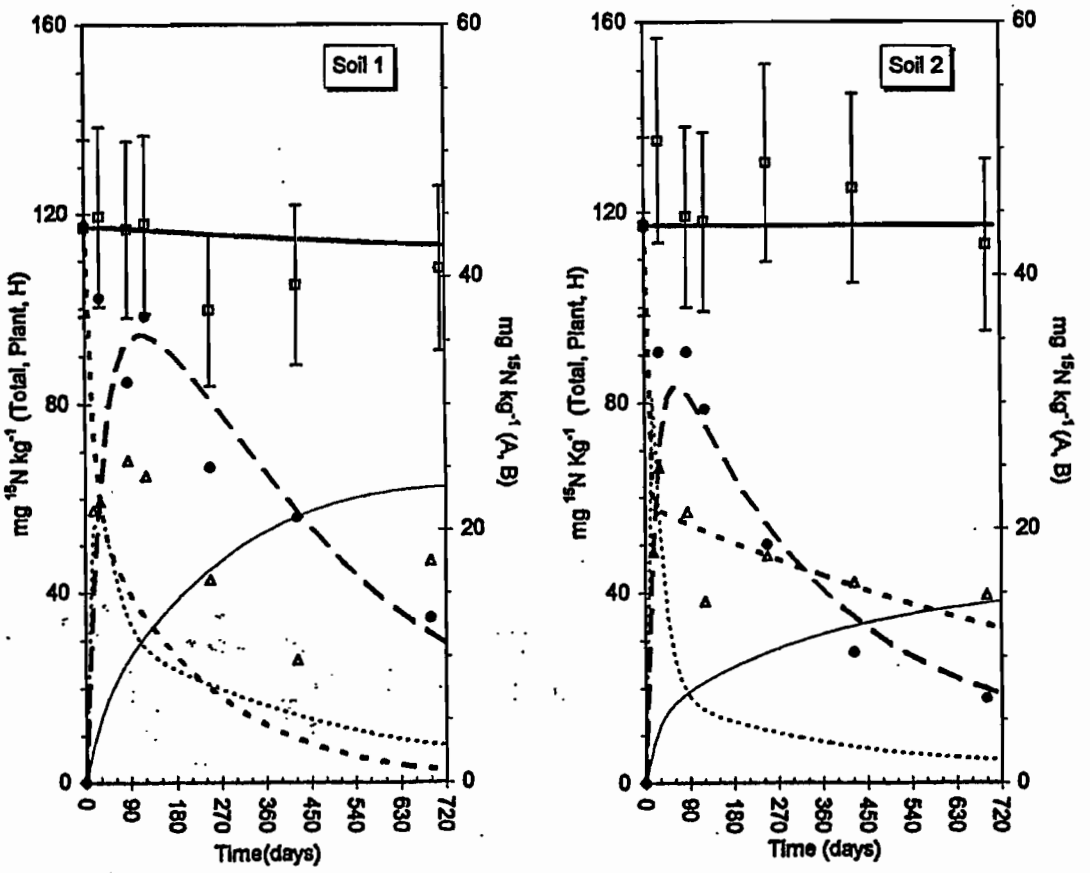

Fig. 2. Observed and predicted total ^{15}N and organic compartment-^{15}N, in both soils: total □ ———, microbial biomass (B) ● — — —, plant material (labile V_L + resistant V_R) △- - - -, labile humified material (A) - - - -, stable humified material (H) ——.

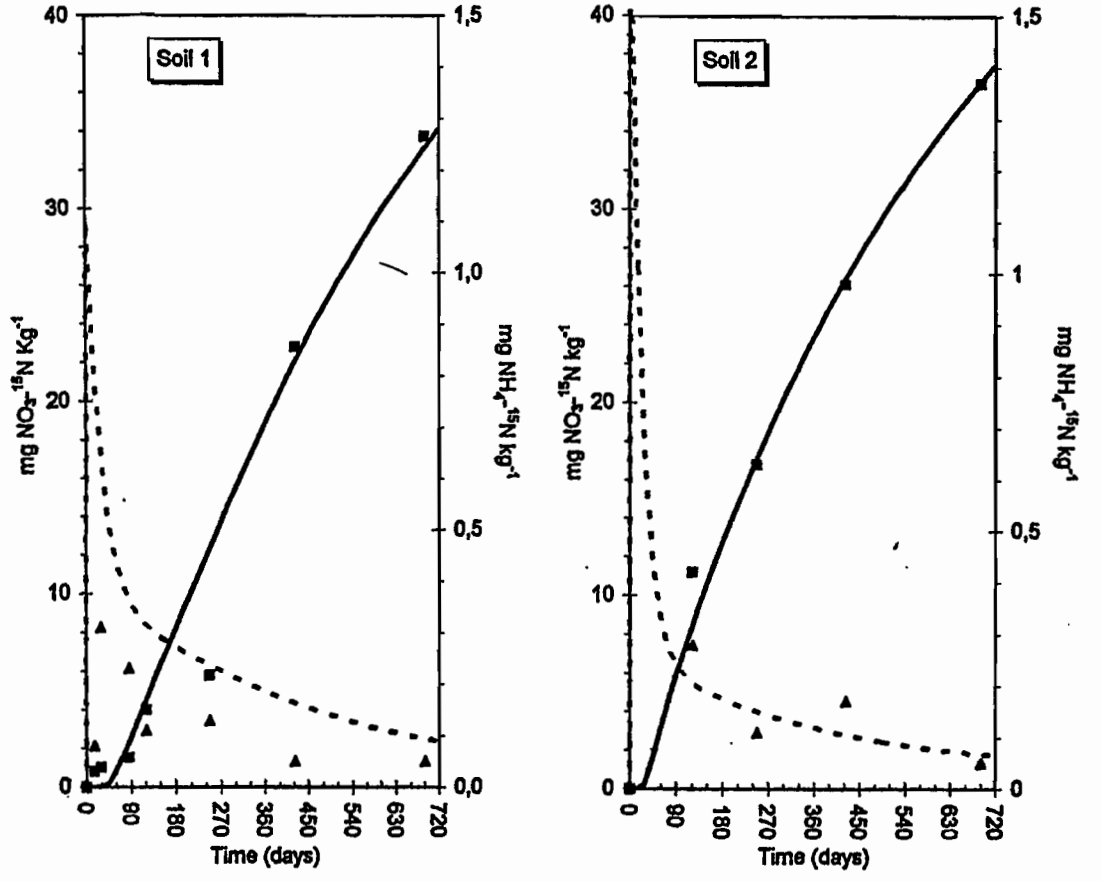

Fig. 3. Observed and predicted inorganic ^{15}N in both soils: NH_4-^{15}N (*aN*) ▲-----, NO_3-^{15}N (*nN*)

sider the growth of nitrifying bacteria. If we express the Monod (1941) equation in terms of substrate (NH_4-N) decrease, then k_{n1} in formula 3′ represents the growth rate, k_{n3} is Monod's constant and k_{n2} depends on the initial population of nitrifying bacteria and the concentration of substrate. The dimension of k_{n1} is time^{-1}, while parameters k_{n2} and k_{n3} express concentrations. It is assumed that for a given soil, k_{n1} has the same value for labelled and total NO_3-N. This is not the case for the two other constants.

Both equations (3) and (3′) gave a similar prediction accuracy [*SSK* equation (4); Table 1]. However equation (3′) required three parameters instead of two for equation (3). A similar precision was obtained with equation (3″) (two parameters). As the maximum reaction rate [k_{n1}, equation (3″)], necessitates separate values for labelled and total $-NO_3$-N (*nN*), we choose equation (3).

Modelling labelled nitrogen forms

The parameters k_l and P_m [equation (1)] were defined for the carbon model (Sallih and Pansu, 1993). For the N model (Table 1; Figs 2 and 3) new kinetic constants were added: k_{n1}, k_{n2} [equation (3) version] and/or k_{n3} [equations (3′) and (3″)]. It is assumed that microorganisms use NH_4^+ preferably to NO_3^- for inorganic N immobilization (Dommergues and Mangenot, 1970; Stevenson, 1986). Gazeous N loss during nitrification (N_2O release) and denitrification (N_2O and N_2) are regulated by k_d. Both soils were maintained under aerobic macro-conditions. The N loss (estimated by total ^{15}N balance) from soil 2 was not significant, thus $k_d = 0$. In soil 1, about 10% of the N flux between NH_4^+ and NO_3^- ($k_d = 0.1$) was lost after the onset of nitrification. This difference may be explained by the higher clay content in soil 1 compared with soil 2, creating temporarily anaerobic microsites (Nevison *et al.*, 1996).

Contrary to Nicolardot *et al.* (1994) using the NCSOIL model and Yevdokimov and Blagodatsky (1993), the kinetic constants were not modified during the incubation time. For the N model, the kinetic constants of the C model were multiplied by f_n, for the five organic compartments. The positive value of f_n, (1.4 and 1.9 for soil 1 and 2, respectively) indicates that N transformations were faster than C transformations for all organic compartments.

For each soil, the parameter r_b indicated that 77% of the flux of *aN* to *oN* compartments (arrow

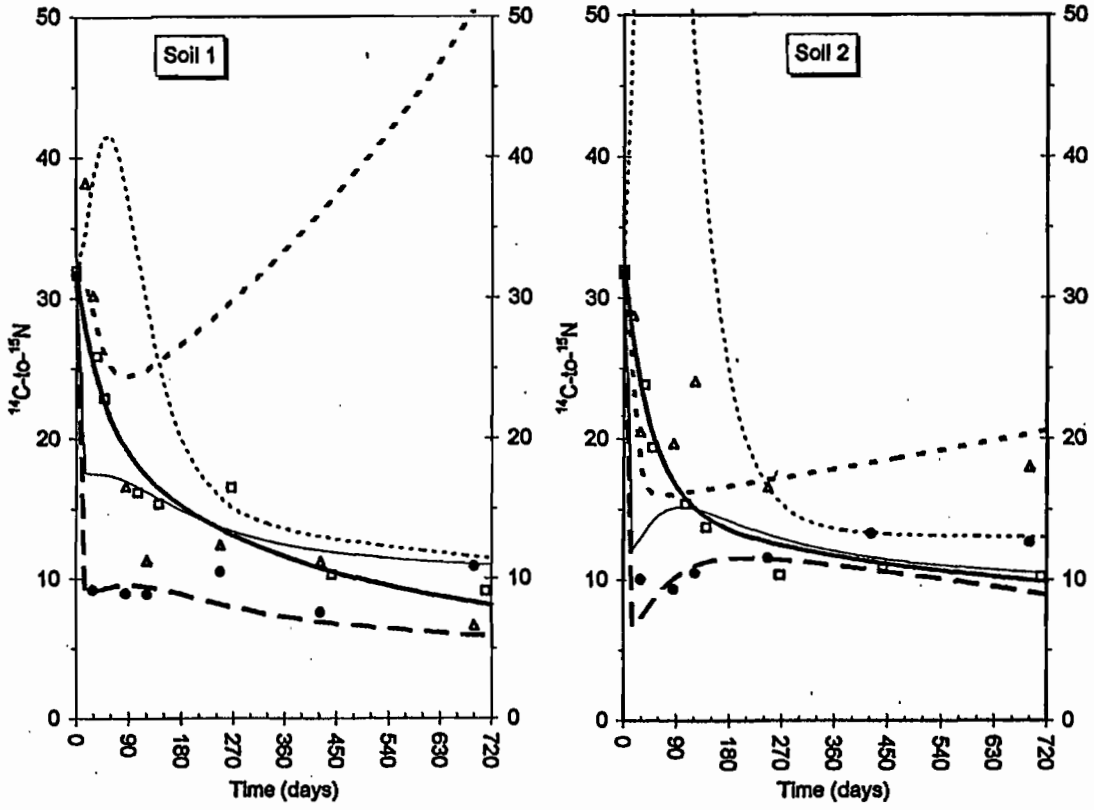

Fig. 4. Observed and predicted ^{14}C-to-^{15}N ratios of the whole soil and organic compartments for both soils: total □———, microbial biomass (B) ● — — —, plant material (labile V_L + resistant V_R) △- - - -, labile humified material (A) - - - -, stable humified material (H) ——.

3, Fig. 1) was incorporated into the microbial biomass (B compartment) and the remaining 23% directly into stable humified material (H compartment). The parameter r_n is the proportion of labile N of the initially added plant material N (0.5 for each soil).

The optimized parameter values were approximately the same for both soils, except for f_n. The small difference observed between the two soils for k_{n2} was not surprising, since this value expresses a concentration. The k_{n1} values found with equation (3') are similar to the growth rates given by Laudelout *et al.* (1994) for *Nitrosomonas* (0.20) and *Nitrobacter* (0.22) for soils incubated at 30°C. Nevertheless, the Monod constants [k_{n3} in equation (3')] are different. Equations (3) and (3') were established by Monod (1941) for a fixed initial amount of substrate, while in soils the NH_4-N concentration results from the balance between continuous and simultaneous NH_4-N production and depletion.

Amounts of ^{15}N incorporated into microbial biomass (Fig. 2) and inorganic ^{15}N (Fig. 3) were similar for both soils and predictions were in agreement with experimental data (except for plant material N and exchangeable NH_4 (aN) in soil 1). The measured plant material ^{15}N was probably overestimated for soil 1, since the high clay content of this soil tended to increase the coarse material ^{15}N by incomplete particle size dispersion and separation. The small overestimation of aN-^{15}N by the model for soil 1 could indicate that in this clay soil part of the non-exchangeable NH_4 is accessible to microorganisms.

Observed nitrate accumulation began after 1 month of incubation in both soils (Fig. 3) when the NH_4-^{15}N concentration fell below k_{n2}. N-uptake by microorganisms (B compartment, Fig. 2) and N humification (H compartment) occurred from the beginning of the experiment independently of nitrification. Immobilization was about twice as high in soil 1 compared with soil 2, although parameter r_b was similar for both soils. This is consistent with published results: humified C (H compartment) was higher in soil 1 than in soil 2 (Sallih and Pansu, 1993).

C-to-N ratios

MOMOS described the ^{14}C-to-^{15}N ratio evolution of each organic compartment (Fig. 4). At time 0, all ^{14}C-to-^{15}N ratios $=31.7$ i.e. that of the initial labelled straw. Nitrogen was quickly incorporated into microbial biomass, resulting in predicted ^{14}C-to-^{15}N ratios ≤ 10 for the B compartment, in accordance with the measured values. In the Century

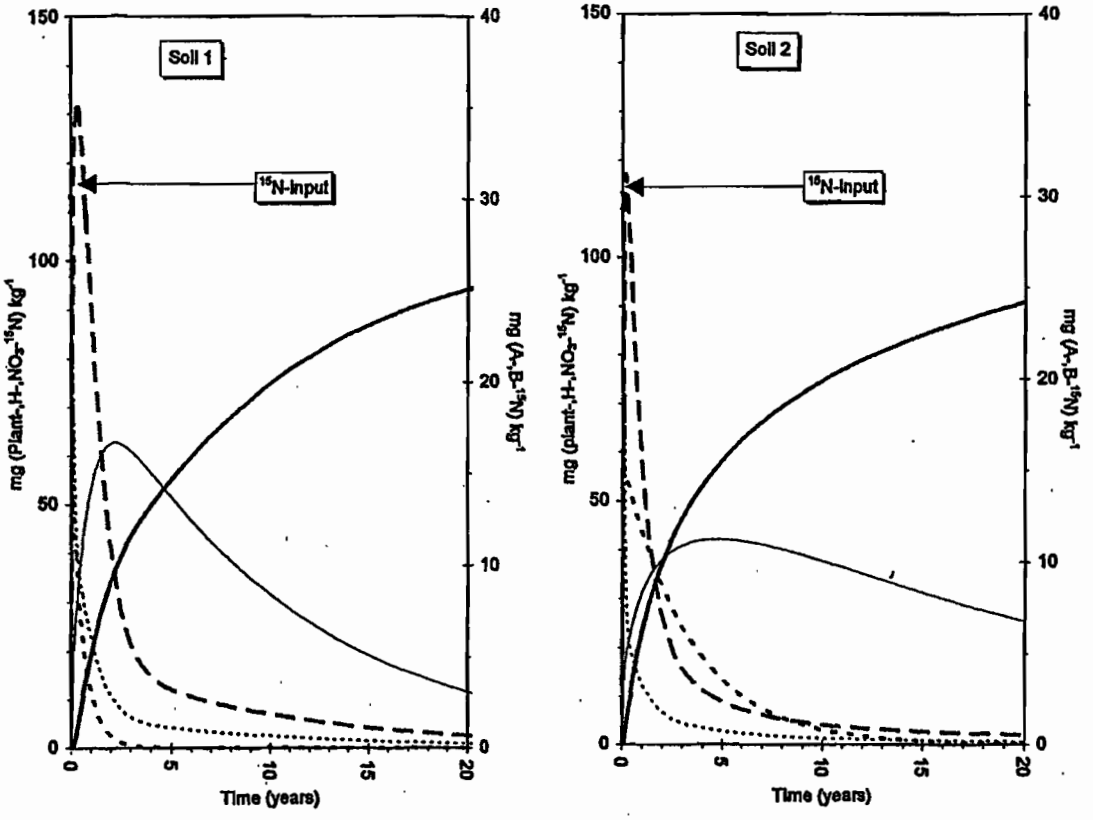

Fig. 5. Predicted long term transformation of the initial ^{15}N input in both soils: NO_3-N (*nN*) ———, microbial biomass (B) — — —, plant material (labile V_L + resistant V_R) - - - - -, labile humified material (A) - - - - -, stable humified material (H) ——.

model (Parton *et al.*, 1987) the C-to-N ratio of microbial compartment was fixed at a constant value of 8. In contrast, the ^{14}C-to-^{15}N of the A-compartment was high, mainly due to an abundance of labile C compounds (carbohydrates), the main energy source for microorganisms. The predicted ^{14}C-to-^{15}N ratio of plant debris decreased to about two-thirds of the initial value during the first 3 months; this can be explained by a rapid initial exhaustion of labile C compounds. After this time, the plant material C-to-N ratio increased constantly. The similarity between predicted and calculated plant debris values is acceptable for soil 2 but not for soil 1. This is probably due to the inaccuracy of the fractionation method for clay soils (soil 1), as explained above. Except for plant fragments, all the labelled C-to-N values approached 10 at the end of the incubation. Nitrogen was progressively incorporated into the stable humified H compartment, which was the major ^{15}N reservoir at the end of the experiment. For the ^{14}C-to-^{15}N ratio of the total soil, the prediction agrees with the experimental data at each sampling occasion for both soils. Thus, taking into account the propagation of random errors when calculating the ratios, the model predictions are acceptable except for the remaining plant debris in the clay soil.

Some important differences appeared between the two soils. At the end of the incubation, total ^{14}C-to-^{15}N was lower in soil 1 compared with soil 2. This was because: (i) despite the fact that the same amount of plant material was initially added to both soils, the proportion of plant debris remaining in soil 2 (Fig. 2) was higher than in soil 1 (near 0); (ii) the size of labelled microbial biomass remaining at the end of the experiment was higher in soil 1 compared with soil 2. The higher clay content of soil 1 may have had a protecting effect on microbial survival. In soil 2, a high proportion of plant fragments remained undecomposed and acted as a nitrogen source for a prolonged period, while in soil 1 a larger proportion of ^{15}N was incorporated into humified materials (H compartment) and into microbial biomass which remained until the later stages of decomposition (B compartment).

Long-term decomposition of the plant residues

Figure 5 shows the predicted transformation of the initial ^{15}N input over 20 y, assuming a steady state organic matter content. During the early stages of decomposition, the labile plant material N (V_L) is the major source of inorganic N. Simultaneously, N is transferred to microbial biomass, which becomes the essential source during the

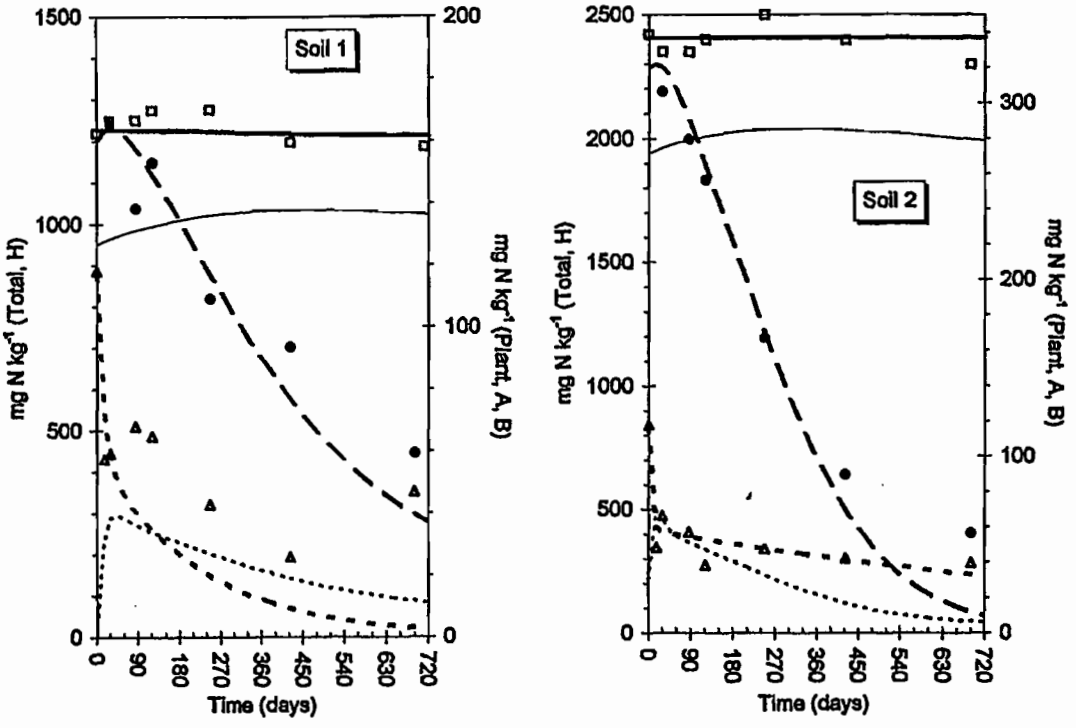

Fig. 6. Observed and predicted total N in the whole soil and in organic compartments for both soils: total □ ——— microbial biomass (B) ● — — —, plant material (labile V_L + resistant V_R) △ - - - -, labile humified material (A) -----, stable humified material (H) ——.

first 2 y of incubation. Ammonium is reorganized into organic compartments with a progressive storage in stable H compartment, which becomes the main mineralization pool after 3 or 4 y. Since this stable compartment decays according first-order kinetics, the release of inorganic N decreases progressively. The model predicts a NO_3-^{15}N release from initial labelled wheat straw over 30 y for soil 1 and over more than 40 y for soil 2. During the first 10 y in soil 2 the stable plant N (V_R compartment) is an important source of inorganic N, whereas in soil 1 this compartment is exhausted after 2 y.

Modelling of total N forms

Predicted and observed total N pools (soil native N + labelled N) are presented in Figs 6 and 7. The initial values of the compartments A, B, H (0 for labelled N) were modified as well as k_{n2} (which expresses a concentration). The other parameters for total N (Table 1) were the same as for labelled N. However, for total N as for total C, k_H constant had to be reoptimized. Values of k_H for the stable N compartment were more accurate than those of k_H for the stable C compartment (Sallih and Pansu, 1992), since the N model is more sensitive to k_H than the C model. The k_H values for stable C and N were lower compared to stable ^{14}C and ^{15}N, indicating that the long-term evolution of these stable compartments cannot completely be predicted from short-term descriptions based on tracer techniques. Total N predictions were in agreement with the experimental data. As for the C model, total N allowed to check the validity of the N model built from ^{15}N data.

High nitrification rates of native soil N were observed, particularly in soil 2. At the end of the experiment, NO_3-^{15}N amounted to about 35 mg ^{15}N kg^{-1} for each soil (Fig. 3), representing 30% of added labelled N and only 2.7 and 1.7% of total N (soil + plant) for soils 1 and 2, respectively. Total NO_3-N was about 130 and 350 mg kg^{-1} corresponding to 11 and 18% of total N for soils 1 and 2, respectively. The model predictions agreed with the observed data for both soils, showing high mineralization rates of native soil N for soil 2 and lower rates for soil 1. Microbial biomass N was the major source of inorganic N and was about twice as high for soil 2 compared with soil 1 at the beginning of the experiment. This difference between the two soils has been observed already and predicted for C and is probably explained by the recent history of both soils (Sallih and Pansu, 1993). Despite great changes in all labile compartments, variations of total N and of stable humified N (H compartment) were not significant during the incubation (Fig. 6).

Conclusion

The MOMOS N model combines the concept of first-order kinetics used in most actual process-based models with concepts used in microbial

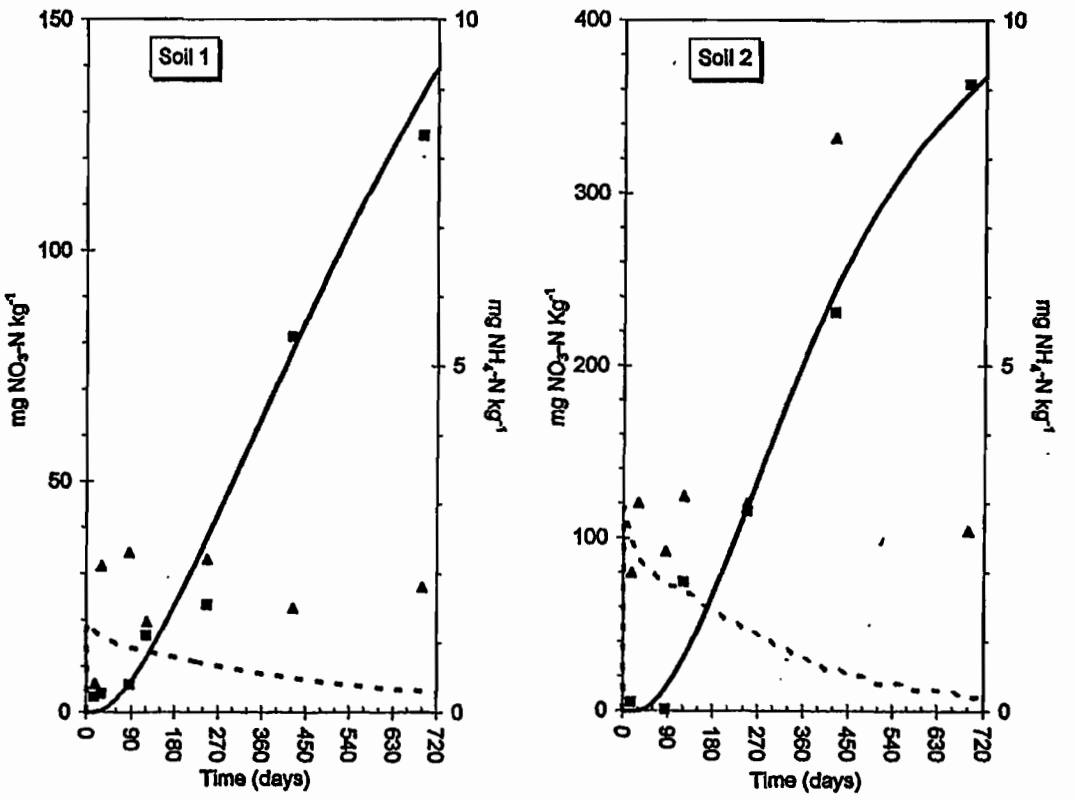

Fig. 7. Observed and predicted inorganic total N in both soils: NH_4-N (*aN*) ▲- - - - -, NO_3-N (*nN*) ■——.

growth models. Transfers between organic compartments and mineralization are explained by first-order kinetics. This is not surprising, since these processes are associated with a wide range of diversified microbial species. In contrast nitrification, which is associated principally with only two microbial genera, can be described by a growth function. Nitrate was not detectable at the beginning of the experiment. At this stage, when labile organic C compounds are available, most NH_4-N is reincorporated into the internal cycle (three-quarters in microbial biomass and one-quarter in stable humus compounds).

The MOMOS formulation is relatively simple and based on data obtained under controlled conditions. The model was able to describe the transformation of labelled C and N as well as total C and N. For each labile organic compartment, the model used the same parameters for C and N (adjusted for N using the constant f_n). For the stable native humified C and N, the kinetic constants k_H were lower than for the stable humified ^{14}C and ^{15}N material, indicating storage of C and N into very stable compartments. The N model was more sensitive to k_H than the C model, indicating that the estimation of k_H for soil native compounds was more accurate for N than for C. The parameters describing the behaviour of the inorganic N compartments have the same value for labelled and total N (except for the nitrification constant k_{n2}, which expresses a concentration) and they were similar for both soils, except for k_{n2} and f_n. Simulated values of ^{14}C-to-^{15}N in organic compartments agreed with experimental data. They showed: (i) a rapid incorporation of N in the microbial biomass, with ^{14}C-to-^{15}N values <10; (ii) a rapid exhaustion of N from the labile humified compartment (energetic substrate); and (iii) a progressive incorporation of N in stable humified compounds with C-to-N near 10 at the end of the experiment.

The link between the C model and the N model was established by using the same five organic compartments and by using the same input and output parameters with a constant multiplicative factor for N kinetic constants.

Acknowledgements—The authors wish to express their gratitude to Professor H. Laudelout (U C Louvain-la-Neuve B), and to Dr M. J. Whealan (University of Exeter UK) for critically reading the manuscript and for linguistic corrections

REFERENCES

Addiscott T. M. (1983) Kinetics and temperature relationships of mineralization and nitrification in Rothamsted

soils with differing histories. *Journal of Soil Science* **34**, 343–353.

Addiscott T. M. (1993) Simulation modelling and soil behaviour. *Geoderma* **60**, 15–40.

Beckie H. J., Moulin A. P., Campbell C. A. and Brandt S. A. (1994) Testing effectiveness of four simulation models for estimating nitrates and water in two soils. *Canadian Journal of Soil Science* **75**, 135–143.

Bergstrom D. W. and Beauchamp E. G. (1993) An empirical model of denitrification. *Canadian Journal of Soil Science* **73**, 421–431.

Bottner P. (1982) Biodégradation du matériel végétal en milieu herbacé. *Acta Oecologica/Oecologa Generalis* **3**, 155–182.

Bottner P., Sallih Z. and Billes G. (1988) Root activity and carbon metabolism in soils. *Biology and Fertility of Soils* **7**, 71–78.

Bradbury N. J., Whitmore A. P., Hart P. B. S. and Jenkinson D. S. (1993) Modelling the fate of nitrogen in crop and soil in the years following application of ^{15}N labelled fertiliser to winter wheat. *Journal of Agricultural Science* **121**, 363–379.

Broadbent F. E. (1986) Empirical modelling of soil nitrogen mineralization. *Soil Science* **141**, 208–213.

CPCS (1967) *Classification des Sols*. Ecole Nationale Supérieure d'Agronomie, Grignon, France.

Deans J. R., Molina J. A. E. and Clapp C. E. (1986) Models for predicting potentially mineralizable nitrogen and decomposition rate constants. *Soil Science Society of America Journal* **50**, 323–326.

Dommergues, Y. and Mangenot, F. (1970) Cycle de l'azote. In *Ecologie Microbienne du Sol*. Masson, Paris, pp. 155–232.

Franko U., Oelschlägel B. and Schenk S. (1995) Simulation of temperature-, water- and nitrogen dynamics using the model CANDY. *Ecological Modelling* **81**, 213–222.

Grant R. F., Juma N. G. and McGill W. B. (1993) Simulation of carbon and nitrogen transformations in soil. *Soil Biology & Biochemistry* **25**, 1317–1338.

Greenwood D. J., Neeteson J. J. and Draycott A. (1985) Response of potatoes to N fertiliser: dynamic model. *Plant and Soil* **85**, 185–203.

Hansen S., Jensen H. E. and Shaffer M. J. (1995) Developments in modeling nitrogen transformations in soil. In *Nitrogen Fertilization in the Environment* (P. E. Bacon, Ed.), pp. 83–107, Dekker, New York.

Hétier J. M., Zuvia M., Houot S. and Thiéry J. M. (1989) Comparaison de trois mode(c)les choisis pour la simulation du cycle de l'azote dans les agro-syste(c)mes tropicaux. *Cahiers ORSTOM série Pédologie* **25**, 443–451.

Jenkinson D. S. and Parry L. C. (1989) The nitrogen cycle in the broadbalk wheat experiment: a model for the turnover of nitrogen through the microbial biomass. *Soil Biology & Biochemistry* **21**, 535–541.

Jenkinson D. S. and Powlson D. S. (1976) The effect of biocidal treatments on metabolism in soil: V. A method for measuring soil biomass. *Soil Biology & Biochemistry* **8**, 209–213.

Knapp E. B., Elliott L. F. and Campbell G. S. (1983) Carbon, nitrogen and microbial biomass interrelationships during the decomposition of wheat straw: a mechanistic simulation model. *Soil Biology & Biochemistry* **15**, 455–461.

Laudelout H., Cheverry C. and Calvet R. (1994) *Modélisation Mathématique des Processus Pédologiques*. Actes Editions, Rabat.

Laudelout H., Lambert R., Fripiat J. L. and Pham M. L. (1974) Effet de la température sur la vitesse d'oxydation de l'ammonium en nitrate par des cultures mixtes de nitrifiants. *Annales de Microbiologie (Institut Pasteur)* **125B**, 75–84.

Mary B. and Rémy J. C. (1979) Essai d'appréciation de la capacité de minéralisation de l'azote des sols de grande culture. I— Signification des cinétiques de minéralisation de la matie(c)re organique humifiée. *Annales Agromiques, France* **30**, 513–527.

Matus F. J. and Rodrigez J. (1994) A simple model for estimating the contribution of nitrogen mineralization to the nitrogen supply of crops from a stabilized pool of soil organic matter and recent organic input. *Plant and Soil* **162**, 259–271.

McGill W. B., Hunt H. W., Woodmansee R. G., Reuss J. O. and Paustian K. H. (1981) Formulation, process controls, parameters and performance of PHOENIX: a model of carbon and nitrogen dynamics in grassland soils. In *Simulation of Nitrogen Behaviour of Soil Plant Systems* (M.J. Frissel and J.A. van Veen, Eds), pp. 171–191. Centre for Agricultural Publishing and Documentation, Wageningen, The Netherlands.

Molina J. A. E., Clapp C. E., Shaffer M. J., Chichester F. W. and Larson W. E. (1983) NCSOIL, a model of nitrogen and carbon transformation in soil: description, calibration and behaviour. *Soil Science Society of America Journal* **47**, 85–91.

Monod J. (1941) Recherches sur la croissance des cultures bactériennes. The(c)se faculté des sciences Paris, Hermann et Cie, pp. 1–137.

Neeteson J. J. and Van Veen J. A. (1988) Mechanistic and practical modelling of nitrogen mineralization–immobilization in soils. In *Advances in Nitrogen Cycling in Agricultural Ecosystems, Proceedings of the Symposium held in Brisbane (Australia) 11–15 May 1987* (J.R. Wilson, Ed.), pp. 145–155, C.A.B. International, Wallingford.

Nevison C. D., Esser G. and Holland E. A. (1996) A global model of changing N_2O emissions from natural and perturbed soils. *Climatic Change* **32**, 327–378.

Nicolardot B., Molina J. A. E. and Allard M. R. (1994) C and N flux between pools of soil organic matter: model calibration with long-term incubation data. *Soil Biology & Biochemistry* **26**, 235–243.

Pansu M. and Sidi H. (1987) Cinétique d'humification et de minéralisation des mélanges sols-résidus végétaux. *Science du Sol* **25**, 247–265.

Pansu M., Sallih Z. and Bottner P. (1996) Modélisation des formes du carbone organique dans les sols. *Comptes Rendus Academy of Science, Paris* **322**, 401–406.

Parton W. J., Schimel D. S., Cole C. V. and Ojima D. S. (1987) Analysis of factors controlling soil organic matter levels in great plains grasslands. *Soil Science Society of America Journal* **51**, 1173–1179.

Press W. H., Teukolsky S. A., Vetterling W. T. and Flannery B. P. (1992) *Numerical Recipes in Fortran. The Art of Scientific Computing*, 2nd edn. Cambridge University Press, Cambridge.

Sallih Z. and Bottner P. (1988) Effect of wheat (*Triticum aestivum*) roots on mineralization rates of soil organic matter. *Biology and Fertility of Soils* **7**, 67–70.

Sallih Z. and Pansu M. (1993) Modelling of soil carbon forms after organic amendment under controlled conditions. *Soil Biology & Biochemistry* **25**, 1755–1762.

Sierra J. (1990) Analysis of soil nitrogen mineralization as estimated by exponential models. *Soil Biology & Biochemistry* **22**, 1151–1153.

Smith O. L. (1979) An analytical model of the decomposition of soil organic matter. *Soil Biology & Biochemistry* **11**, 585–606.

Stanford G. and Smith S. J. (1972) Nitrogen mineralization potential of soils. *Soil Science Society of America Proceedings* **36**, 465–472.

Stevenson F. J. (1986) *Cycles of Soil: Carbon, Nitrogen, Phosphorus, Sulphur and Micronutrients*. Wiley, New York.

Svendsen H., Hansen S. and Jensen H. E. (1995) Simulation of crop production, water and nitrogen balances in two German agro-ecosystems using the DAISY model. *Ecological Modelling* **81**, 197–212.

van der Linden A. M. A., van Veen J. A. and Frissel M. J. (1987) Modelling soil organic matter levels after long term applications of crop residues, and farmyard and green manures. *Plant and Soil* **101**, 21–28.

van Veen J. A. and Frissel M. J. (1981) Simulation model of the behaviour of N in soil. In *Simulation of Nitrogen Behaviour of Soil–Plant Systems* (M. J. Frissel and J. A. van Veen Eds), pp. 126–144. Centre for Agricultural Publishing and Documentation, Wageningen, The Netherlands.

van Veen J. A., Ladd J. N. and Amato M. (1984) Turnover of carbon and nitrogen through the microbial biomass in a sandy loam and a clay soil incubated with [^{14}C(U)]glucose and [^{15}N]$(NH_4)_2SO_4$ under different moisture regimes. *Soil Biology & Biochemistry* **17**, 747–756.

Yevdokimov I. V. and Blagodatsky S. A. (1993) Nitrogen immobilization and remineralization by microorganisms and nitrogen uptake by plants: interactions and rate calculations. *Geomicrobiology Journal* **11**, 185–193.

Influence des racines actives sur le cycle du carbone

Plant and Soil **216**: 15–25, 1999.

Modelling the effect of active roots on soil organic matter turnover

Pierre Bottner[1,*], Marc Pansu[2] and Zaher Sallih[1]
[1]*CEFE-CNRS, 1919 Route de Mende F-34293 Montpellier Cedex 5, France and* [2]*IRD BP 5045, 911 Avenue d'Agropolis, F-34032 Montpellier Cedex 1, France*

Received 11 March 1999. Accepted in revised form 16 August 1999

Key words: Soil organic matter, Decomposition, Carbon mineralisation, Root activity, Rhizosphere, Microbial biomass, Modelling

Abstract

The aim of this experiment was to study the effect of living roots on soil carbon metabolism at different decomposition stages during a long-term incubation. Plant material labelled with ^{14}C and ^{15}N was incubated in two contrasting soils under controlled laboratory conditions, over two years. Half the samples were cropped with wheat (*Triticum aestivum*) 11 times in succession. At earing time the wheat was harvested, the roots were extracted from the soil and a new crop was started. Thus the soils were continuously occupied by active root systems. The other half of the samples was maintained bare, without plants under the same conditions. Over the 2 years, pairs of cropped and bare soils were analysed at eight sampling occasions (total-, plant debris-, and microbial biomass-C and -^{14}C). A five compartment (labile and recalcitrant plant residues, labile microbial metabolites, microbial biomass and stabilised humified compounds) decomposition model was fitted to the labelled and soil native organic matter data of the bare and cropped soils. Two different phases in the decomposition processes showed a different plant effect. (1) During the initial fast decomposition stage, labile ^{14}C-material stimulated microbial activities and N immobilisation, increasing the ^{14}C-microbial biomass. In the presence of living roots, competition between microorganisms and plants for inorganic N weakly lowered the measured and predicted total-^{14}C mineralisation and resulted in a lower plant productivity compared to subsequent growths. (2) In contrast, beyond 3–6 months, when the labile material was exhausted, during the slow decomposition stage, the presence of living roots stimulated the mineralisation of the recalcitrant plant residue-^{14}C in the sandy soil and of the humified-^{14}C in the clay soil. In the sandy soil, the presence of roots also substantially stimulated decomposition of old soil native humus compounds. During this slow decomposition stage, the measured and predicted plant induced decrease in total-^{14}C and -C was essentially explained by the predicted decrease in humus-^{14}C and -C. The ^{14}C-microbial biomass (MB) partly decayed or became inactive in the bare soils, whereas in the rooted soils, the labelled MB turnover was accelerated: the MB-^{14}C was replaced by unlabelled-C from C derived from living roots. At the end of experiment, the MB-C in the cropped soils was 2.5–3 times higher than in the bare soils. To sustain this biomass and activity, the model predicted a daily root derived C input (rhizodeposition), amounting to 5.4 and 3.2% of the plant biomass-C or estimated at 46 and 41% of the daily net assimilated C (shoot + root + rhizodeposition C) in the clay and sandy soil, respectively.

Introduction

There is a substantial body of information reviewed by Wipps (1990) on the amounts and quality of root-derived organic compounds released in the rhizosphere and defined as rhizodeposition. More recently the effect of plant below-ground activity on nutrient mobilisation has raised new interest as a response to atmospheric CO_2 increase (Rogers et al., 1994; Van Noordwijk et al., 1998; Van Veen et al., 1991). The release of organic compounds in the rhizosphere is recognised as a major energy input to the soil, provid-

* FAX No: +33 (0)4 67412 138.
E-mail: bottner@cefe.cnrs-mop.fr

ing an essential driving force for microbial mediated processes: carbon mineralisation–humification, nutrient mobilisation, mineralisation and immobilisation, denitrification (Quian et al., 1997) and maintenance of soil structure. However some essential questions on how the root and rhizosphere activity positively or negatively affects decomposition (Dormaar, 1990) and how the rhizodeposits are used in the soil, still remain unanswered. Shields and Paul (1973) and Jenkinson (1977) demonstrated by field experiments, that decomposition of ^{14}C-labelled plant material is substantially lowered in the presence of cultivated plants or under natural grassland when compared to bare soil. In these field experiments the reduction in the decomposition rate is essentially explained by the modification of soil water balance by plant transpiration, lowering microbial activity. In addition to this indirect effect, nutrient uptake by plants, modifying the soil nutrient balance and subsequent N-mediated microbial processes, is another plant-induced modification. Thus Merckx et al. (1985, 1987) demonstrated that in N poor soils, the rhizosphere microbial biomass was controlled by N-limitation, despite the supply of available C derived from the roots. This illustrates the complexity of the response of soil net C and N mineralisation rates to the presence of active roots, resulting from the link between the C and N cycles and involving (1) the active roots as a net C source and net N sink, (2) decomposing dead plant material as a labile C supply and (3) the stabilised humus as a probable N source. In this system, the microbial biomass is the key pool linking the C and N cycles. Thus the still controversial question is: how the root and rhizosphere activity directly affects soil organic matter decomposition, modifying the energy input and nutrient balance.

In the present work, ^{14}C- and ^{15}N-labelled plant material was incubated in two contrasting soils over 2 years in pots under controlled laboratory conditions. Half of the pots were cropped with wheat, 11 times in succession, whereas the other half was treated as uncropped control bare soils. A carbon decomposition model was fitted to the results of both treatments. The aim was to describe and predict the effect of roots during a long-term incubation, involving the initial fast phase of fresh labelled plant material decomposition and the later slower phase, when the ^{14}C derived from the plant material was stabilised in humus compounds.

Materials and methods

Data acquisition

Data were obtained from an incubation experiment carried out under controlled laboratory conditions and previously described by Sallih and Pansu, (1993) and Pansu et al. (1998). Briefly, two Mediterranean soils from southern France were selected, differing mainly by their texture and organic matter content: soil 1, a clay soil (C 1.2%; N = 0.12%; clay content = 29%; total sand = 27%; pH(H_2O) = 7.9); and soil 2, a sandy soil (C = 2.7%; N = 0.20%; clay content = 11%, total sand = 66%; pH(H_2O) = 6.5). After drying, sieving (5 mm mesh) and homogenisation, the soils were split into 18 portions of 800 g dry soil. Each portion was mixed with 7 g of mature uniformly ^{14}C- and ^{15}N-labelled wheat straw (stems + leaves; C = 46%; N = 1.0%; specific activity 2.59 MBq g^{-1} C), cut in about 1–2-cm pieces and placed in 10×10×12 cm plastic pots. The pots were installed in a ventilated growth chamber with 16 h light (25±4 °C) and 8 h dark (15±3 °C), at ambient atmosphere. Half the pots were cropped 11 times in succession with spring wheat (*Triticim aestivum*, cultivar 'Florence Aurore', six seedlings to each pot). After 1.5–2 months of growth, the plants were harvested close to earing time and the roots were removed from the soil by sieving and hand sampling. The next culture started 2–5 days after each harvest, using 4–7-day-old pre-germinated seedlings. Thus in the planted pots, the soil was constantly occupied by active roots (from seedling to earing). The experiment was performed without fertilisation. The wheat variety (an old cultivar) was chosen for its low nutrient requirement. The other half of the pots remained unplanted. In all pots with or without plants, soil moisture was maintained at 75±15% of the WHC by weight adjustment. In order to reduce evaporation, soil surface was covered with a perforated aluminium sheet covering 80% of the soil surface area. At each remoistening, pots were randomly replaced in the growing chamber. Pots without plants were treated in the same ways as pots with plants, especially for the soil mixing when the roots were removed. Between harvest of culture 3 and new seeding for culture 4 and again between growth 8 and 9, all the pots were kept bare for 80 days without moistening. The soils dried out progressively.

During the 2 years of experiment, eight samplings of one paired bare and cultivated pots were collected. After harvest of plants and removal of roots, the

soil was immediately divided into several portions for analyses. The following analyses previously described (Pansu et al., 1998; Sallih and Pansu, 1993) were performed: C and ^{14}C of (1) the whole soil, (2) the undecomposed labelled plant debris separated from the soil by flotation and wet sieving, (3) the microbial biomass determined by the fumigation–incubation technique (Jenkinson and Powlson, 1976), and (4) the plant materials (shoots and roots) of the 11 wheat crops. The cumulated total loss of soil ^{14}C adhering to the roots at plant harvests did not exceed 4% of the initial ^{14}C. The statistical analyses are described in Sallih and Pansu (1993).

Mathematical model

The MOMOS-Carbon model describing C-transfer in the soil organic matter, has been previously presented by Sallih and Pansu (1993) and extended to N-transfers (MOMOS-N, Pansu et al., 1998). Five organic compartments were defined: (Figure 1): V_L, V_R are labile and resistant plant residues; A is labile microbial metabolite; B is microbial biomass; and H is stable humified materials. In the present model, two additional compartments describe the plant carbon: (1) dead plant material entering the soil (Dead Plant Material, DPM) and (2) living plant material (Living Plant Material, LPM, Fig. 1). The organic carbon (oC) dynamics of a given compartment m in relation with i compartments is given by:

$$\frac{doC_m}{dt} = -k_m oC_m + P_m \sum_i k_i oC_i + f(t)f(m,l)\,DPM + f(m)k_r LPM \qquad (1)$$

The first (1 in figure 1) and second (2 in figure 1) terms previously described in Pansu and Sallih, 1993) of Eq. (1) indicate a first-order kinetics decrease in each soil compartment with kinetic constants k_i (T^{-1}, with $k_A = k_{V_L}$); P_m (dimensionless) represents the proportion of carbon input from compartments i to the compartment m (with $P_{V_L} = P_{V_R} = 0$). The metabolised material (balance between total ^{14}C minus plant debris-^{14}C minus microbial biomass-^{14}C) could not be described with only one first-order kinetic compartment H (HUM of the model of Jenkinson, 1990). Thus compartment A was integrated as labile metabolites. The predicted total ^{14}C and microbial biomass-^{14}C were more sensitive to changes of P parameters than changes in k parameters, especially for P_A which regulates the greatest C flow. Modification of P_H (the lowest P parameter influenced only predicted total ^{14}C at the end of experiment. Changes in any k parameter modified first the C content of the corresponding compartment. The effect of k_H modifications on total ^{14}C were weak during the years of experiment but it becomes important for long-term predictions.

The third (3 in figure 1) term $(f(t)f(m,l)DPM)$ defines the C of dead plant material (DPM, g C kg^{-1} dry soil day^{-1}) entering the soil. The DPM flow is distributed into V_L and V_R by the Boolean function $f(t)$ (with $f(t) = 1$ when t = the input time, else $f(t) = 0$) and a distribution function $f(m,l)$ (with $f(m,l) = 0$ for $m \in \{A, B, H\}$, $f(m,l) = l$ for $m = V_L$, $f(m,l) = 1 - l$ for $m = V_R$; l = labile fraction of DPM input set at 0.7 from plant debris ^{14}C data).

The last (4 in figure 1) term of equation 1 $(f(m)k_r LPM)$ expresses the rhizodeposition, that is the C input derived from living roots (Living Plant Material = LPM, g plant-dw kg^{-1} dry soil) regulated by a distribution function $f(m)$ (with $f(m) = 0$ for $m \in \{V_L, V_R, B, H\}$, and $f(m) = 1$ for $m = A$). The constant k_r, defining the proportion of C derived from living roots and entering the soil was calculated in two ways: (1) at any time during plant growth, k_r (g C g^{-1} plant-dw day^{-1}) is considered as a constant proportion of plant-dw (shoots + roots; equation 1); (2) k_r (g C g^{-1} plant-dw) is a constant proportion of the plant daily net production (shoots + roots). In Eq. (1), replace LPM by $d(LPM)/dt$ (= Eq. (1′)).

In the model, the living root effect is based on two assumptions: (1) during the active root phase (in this experiment from seedling to earing time), the C-input from roots is a constant (k_r) proportion of LPM (Eq. (1)) or $d(LPM)/dt$ (Eq. (1′)); (2) C input derived from living roots is essentially composed of labile compounds (Wipps, 1990). This material is directly incorporated into compartment A (labile metabolites). Sensitivity test showed that 10% change in k_r values induced a corresponding linear modification in predicted total- (3%) and microbial biomass-C (10%).

LPM (shoots + roots) was simulated at each cultivation (Fig. 2) from the harvested plant material dry weight by a classical logistic function (Eq. (2)):

$$LPM^j = \frac{LPM^J_{\max}}{1 + e^{\alpha LPM^j_{\max}(t^j - t^j_{1/2})}} \qquad (2)$$

where $LPM^j_{\max}$ is total dry matter of the harvest j, t^j is growth time since planting of the seedlings, j, $t^j_{1/2}$ is half of the growth period, α is growth kinetic parameter set at 0.001 day^{-1} to simulate the wheat growth.

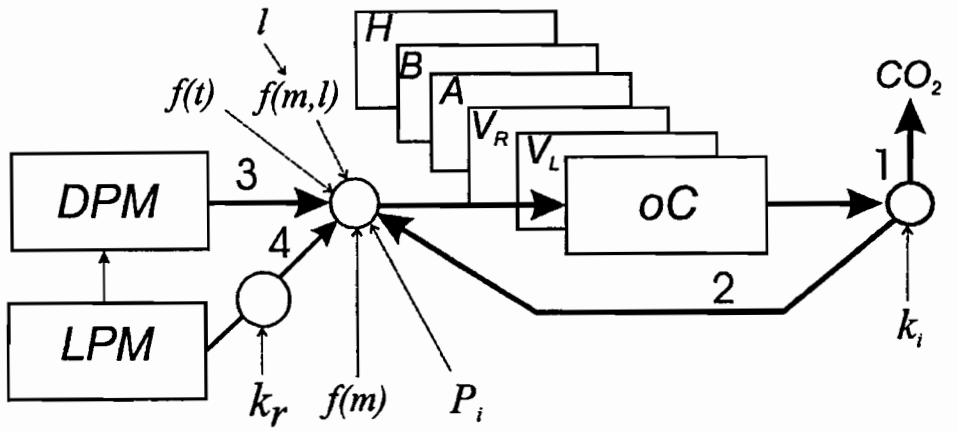

Figure 1. The MOMOS-C model. Five soil organic carbon (oC) compartments (V_L, labile plant material; V_R, resistant plant material; A, labile metabolites; B, microbial biomass; H, stable humified material). Two plant material compartments (DPM, dead plant material = above ground and root litter; LPM, living plant material). The numbers correspond to the terms in Eq. (1): 1, carbon mineralisation; 2, humification; 3, dead plant material-oC input (litter); 4, oC input from living roots (rhizodeposition). The parameters are defined in Eq. (1).

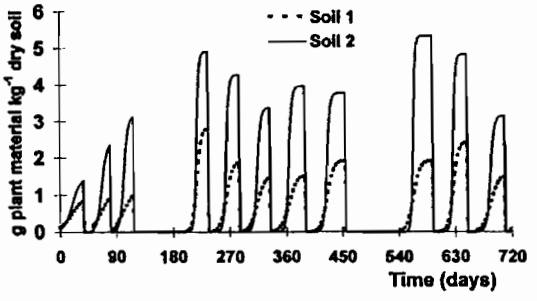

Figure 2. Simulated production of plant material over the eleven successive wheat growths (see Eq. (2)). LPM_{max} was set to the measured plant dry weight at each harvest.

The daily net plant production was simulated by the differential form of Eq. (2), giving Eq. (2′):

$$\frac{d(LPM^j)}{dt} = \alpha LPM^j \left(1 - \frac{LPM^j}{LPM^j_{\max}}\right) \qquad (2')$$

In the experiment and for the simulation, the dead (labelled) plant material (DPM) was introduced in the soil only once, at the beginning of incubation (70% directed into V_L and 30% into V_R).

The numerical integration was performed using Euler's method and the parameter optimisation using Powell's method, by minimising the following criterion:

$$SSK = \sum_q w_q^2 \sum_r (y_{qr} - \hat{y}_{qr})^2 \qquad (3)$$

where r identifies the number of sampling points; q is the number of data series and y_{qr} and $\hat{y}_{qr}$ are the measured and the predicted value of each data point respectively; w_q are weight coefficients for each data series. For these data, w_q was set at 0.3, 0.3 and 1 for total-, plant material- and microbial-^{14}C, respectively.

Results and discussion

Mineralisation and humification of labelled plant material

The respective parameters describing the ^{14}C dynamics were different for the two bare soils. In contrast when the two cultivated soils are compared, the parameters were similar (Table 1).

The presence of living plants lowered the measured and predicted total ^{14}C mineralisation during the first 3 (soil 1) or 6 (soil 2) months (Fig. 3A). Nevertheless the retarding effect was weak, especially in soil 1. During the initial decomposition stages, the availability of labile labelled plant material stimulated the microbial activity and N immobilisation (Pansu et al., 1998). This active decomposition stage is illustrated by (1) high total-^{14}C mineralisation rates (Fig. 3A), (2) increasing microbial biomass-^{14}C, reaching maximum levels after 3–4 months (Fig. 3B) and (3) high microbial metabolic quotients for labelled CO_2 (qCO_2-^{14}C, Bottner et al., 1988). In the presence of living plants, the competition between roots and active micro-organisms for inorganic N lowered the total-^{14}C

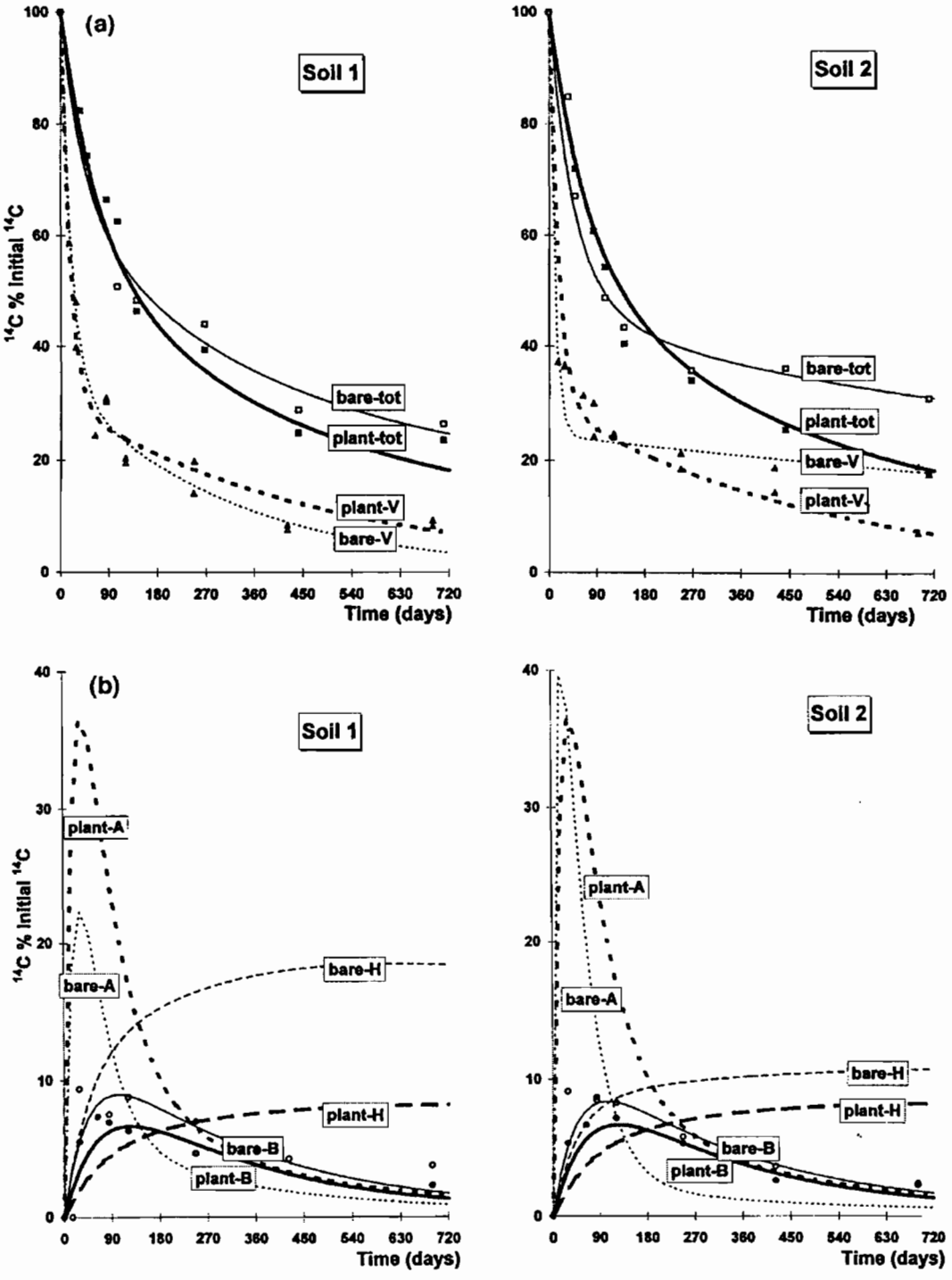

Figure 3. Measured and predicted ^{14}C distribution (in percent of total initial ^{14}C) in the soil compartments in bare and cultivated soils 1 and 2.

Table 1. Optimised model parameters for bare and cultivated soils

Compartment	Bare soil 1		Bare soil 2		Culivated soils 1 and 2	
	k_i	P_i	k_i	P_i	k_i	P_i
V_L	0.05	0.0	0.1	0.0	0.06	0
V_R	0.0031	0.0	0.00043	0.0	0.002	0
A	0.05	0.58	0.1	0.79	0.06	0.77
B	0.006	0.08	0.004	0.033	0.006	0.037
H	0.0004	0.08	0.0001	0.025	0.00025	0.02

K_i, kinetic constants (day^{-1}); P_i, proportion of compartment input. For the cultivated soils the parameters were similar.

mineralisation rates. This explanation is supported by the observations of Merckx et al. (1985, 1987) showing that in nutrient limited soils the N deficiency in the rhizosphere reduces the C metabolism. Thus the depletion of mineral nutrients by plants may limit microbial activity during active decomposition stages. The competition between micro-organisms and plants occurring during the initial decomposition stage, also resulted in a lower plant productivity (Fig. 2). The dry weight of plant material produced during the three first growths was lower than subsequent growths.

In contrast, beyond 3 or 6 months, the measured and predicted total-^{14}C mineralisation was significantly increased in both cultivated soils compared to the bare soils (Fig. 3A). The total-^{14}C remaining in the soils at the end of the experiment was 18% of the initially added ^{14}C in both cultivated soils, compared to 25 and 31% for bare soils 1 and 2, respectively. Thus, during the low activity stages, when the labile ^{14}C-compounds were exhausted, the presence of active roots stimulated the mineralisation of the more resistant ^{14}C-compounds. A similar stimulation of total-^{14}C mineralisation was observed by Cheng and Coleman (1990) as evidenced by a higher CO_2-^{14}C release and interpreted as resulting from a higher microbial metabolism.

In addition to the total-^{14}C mineralisation, the model predicts root-induced modifications of some measurable and unmeasurable organic matter compartments. In bare soils, the plant debris-^{14}C (V_L + V_R, Fig. 3A) remaining at the end of experiment was 4 and 18% of the initial ^{14}C in soil 1 and 2, respectively. In cultivated soils, this proportion was not significantly modified for soil 1, but greatly decreased to 7% for soil 2 (Fig. 3A). Thus, in soil 2 the roots accelerated the decomposition of the stable labelled plant debris, explaining partly the plant induced stimulation of total-^{14}C mineralisation.

In the presence of roots, the model predicts a decreased accumulation of the stabilised humus-^{14}C (H in Fig. 3B) especially in soil 1. At the end of incubation, the net ^{14}C accumulation in compartment H amounted to 8% of the total-^{14}C initially added for both cultivated soils, compared to 18% and 11% in bare soils 1 and 2, respectively. Thus, in soil 1, the lower total-^{14}C remaining at the end of the incubation in the cultivated soil (18%, Fig. 3A) compared to the bare soil (25%), is essentially explained in the model by a lower predicted (not measured) accumulation of stabilised humified-^{14}C in compartment H (Fig. 3B). For the bare soils, Sallih and Pansu (1993) explained the higher humification rates (accumulation in H) of the clay soil 1 (18%, Fig. 3B), compared to the sandy soil 2 (11%), by the properties of the clays to protect humified compounds (Merckx et al., 1985). The present simulation shows that this protecting effect may be counteracted in presence of roots. Thus the roots stimulate the mineralistion of recently stabilised humus fractions. Similarly, in a comparable experiment, Zagal (1994) demonstrated that the roots also liberated formerly stabilised ^{15}N compounds.

In both soils and both treatments, the microbial biomass-^{14}C increased during the initial active decomposition stage, in response to the availability of labile ^{14}C-material. Beyond this time, when the labile material was exhausted, the B compartment decreased slowly for both treatments, showing a typical shape of the microbial biomass curve (Fig. 3B) observed in many labelling experiments. Nevertheless the presence of roots slightly lowered the measured and predicted microbial biomass-^{14}C. Bottner et al. (1988) explained the ^{14}C decrease induced by the active roots by a stimulated C turnover in the microbial biomass. In the bare soils, beyond the active decomposition stage, the labelled portion of microbial biomass partly decayed (explaining the decrease of the curve) and

partly became dormant by exhaustion of available ^{14}C-substrate. In the planted systems, part of the microbial biomass, stimulated by the input of labile C derived from the roots, remained active and ^{14}C was progressively replaced by unlabelled C derived from the roots. The qCO_2-^{14}C values (microbial metabolic quotient for CO_2-^{14}C) calculated by Bottner et al. (1988) for both systems, revealed that in the rooted soils the labelled biomass was smaller but more active than in the bare soils. Thus during the slow decomposition phases, the presence of roots accelerated the turnover of the portion of microbial biomass which previously used the labelled plant material as substrate. In Table 1 for soil 1, k_B (k_i for compartment B) is similar in bare and cultivated soil, but P_B in the planted soil is half that of bare soil, illustrating the higher turnover of C in compartment B of the planted soil.

In the Rothamsted model, Jenkinson (1990) described the effect of living plants by multiplying the first order kinetic constants by a constant factor ('retainment' factor). The present experiment shows that (1) the multiplication factor of k_i (Table 1) cannot be constant and (2) the plant effect varied positively or negatively depending on the decomposition phases, as illustrated by the total ^{14}C mineralisation and the plant debris-^{14}C decomposition (Fig. 3A). In bare soils, the model parameters (k_i and P_i, Table 1) varied according to the soil properties. In contrast for the planted soils, the model parameters were found to be similar for both soils. Thus, the plant effect could not be described by simply multiplying each bare soil parameter by a constant factor. The solution was to run the model for both treatments and to compare the re-optimised parameters of each treatment (Table 1). Nevertheless in a strictly mechanistic way, this procedure is not satisfying, since the plant effect could not be intrinsically described.

Total carbon transfers

Total-C was simulated using: (1) parameters defined from ^{14}C data in cultivated soils (Table 1), (2) initial values of A, B and H compartments calculated in bare soils and (3) optimisation of the k_r parameter. Predicted values agreed closely with the experimental data (Fig. 4A, B).

The model predicted large fluctuations in compartment A (not measured), which were related to the successive plant growths (Figs. 2 and 4B). Indeed in the model, the labile C derived from the active roots (rhizosphere activity) was directed into the compartment A. Thus A is defined by two origins: (1) labile microbial metabolites derived from the decomposing (labelled) plant material. In both bare soils, these transient compounds appear in small amounts essentially during the initial active decomposition phase (Fig. 4B), (2) labile material derived from active roots (rhizodeposits). The second origin is quantitatively greater than the first (compare bare to cultivated soils, in Fig. 4B), explaining the high fluctuation of simulated A related to the successive crops.

In the unplanted soils, the microbial biomass-C decreased from the beginning to the end of experiment, by a factor of 2.5–3 for both soils (compartment B, Fig. 4B), as a result of the progressive exhaustion of labile C (Sallih and Pansu, 1993). In contrast, with plants present, the measured and predicted microbial biomass-C remained at a relatively high level until the end of the experiment, illustrating the supply to micro-organisms of labile carbon derived from the living roots (A compartment). Nevertheless, the fluctuations of B are greatly attenuated compared to A. As a matter of fact, in the model 70% of A is directly mineralised and used as energy source and only 20% is used to build new microbial biomass. At the end of experiment, bare soil microbial biomass was 3 times lower than in the cultivated soils, illustrating the C and energy input derived from the roots.

The predicted H compartment (the stabilised humus, Fig. 4A) remained relatively stable in soil 1 under both bare and cultivated soil conditions. In contrast, in soil 2 the predicted H decreased substantially in the presence of plants. Thus the presence of living roots stimulated the mineralisation of the stabilised unlabelled soil native humus. In cultivated soil 2, when the k_H value of 0.00025 obtained from the ^{14}C data was used (as for the other k_i and P_i parameters, Table 1), the predicted H values were too high to properly describe the total-C dynamics. A new optimisation gave $k_H = 0.0007$. Thus in this cultivated soil 2, the parameters describing the ^{14}C dynamics could not be used to describe the unlabelled H compartment, indicating that roots probably stimulated the mineralisation of an extra-amount of old stabilised humus whose dynamics differ from those of recently formed stabilised humus. In soil 1, the predicted stimulation of H mineralisation was weaker (Fig. 4A). For both cultivated soils, the H compartment curve declined parallel to total C, illustrating that the dynamics of total-C are essentially explained by the dynamics of H. This compartment represents the major portion of organic matter. In cultivated soil 2, almost one-third of the total C was lost

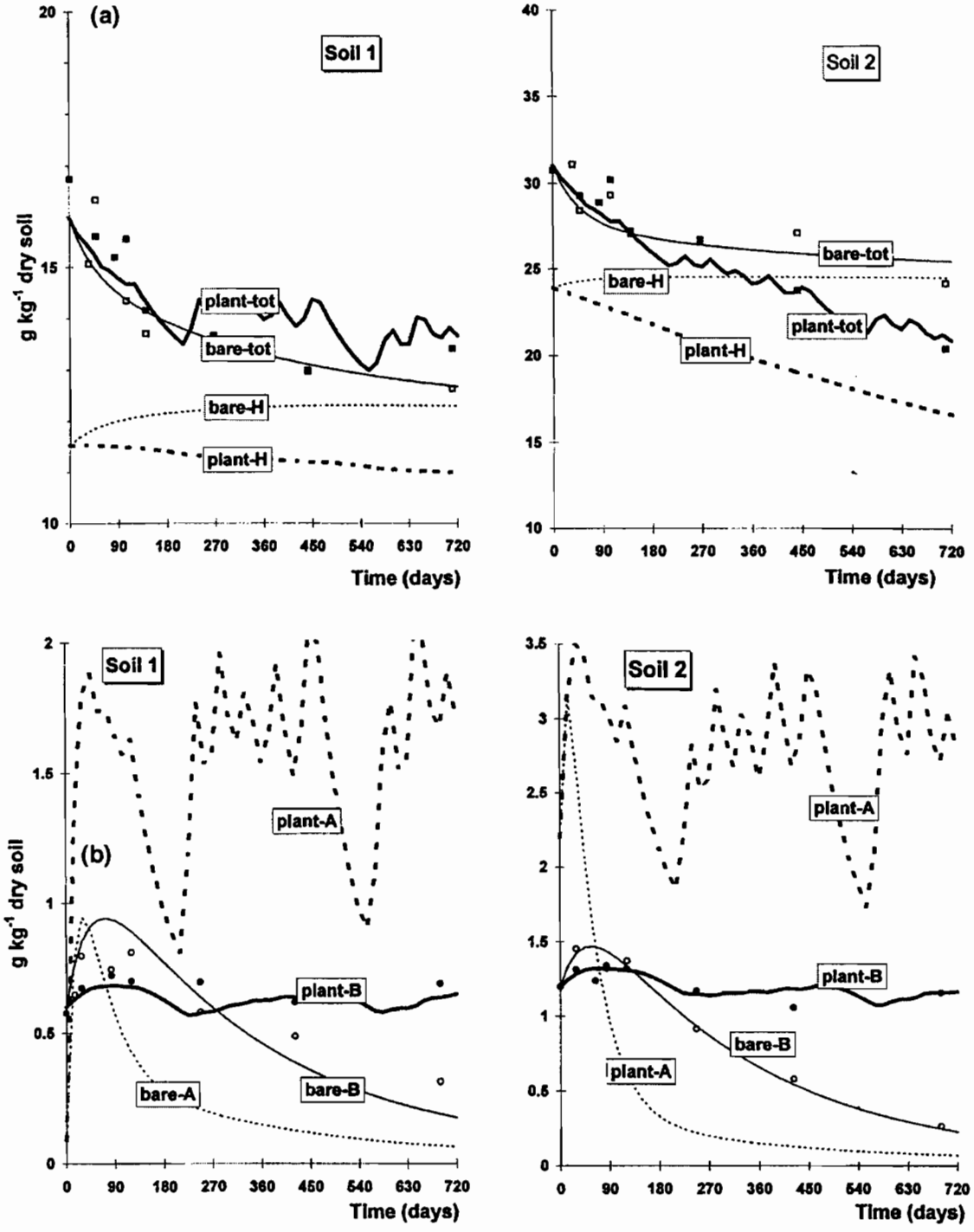

Figure 4. Measured and predicted total carbon distribution (g C kg^{-1} dry soil) in the soil compartments in bare and cultivated soils 1 and 2.

during the experiment, indicating a high instability under the experiment conditions, especially with plants (Fig. 4A).

Predicted rhizodeposition

Total N contents of soil 1 and 2 were 0.12 and 0.20%, respectively. Plant production of soil 1 was about half that of soil 2 (Fig. 2). Cumulative total N taken up by the plants of the 11 growths amounted to 173 and 366 mg N kg^{-1} dry soil for soils 1 and 2, respectively, 14 and 18% of the total soil N. The decline in productivity of both soils at the last growth (11th, Fig. 2) indicates nutrient exhaustion (this was confirmed by the 12th growth not used in the calculations). For each growth, LPM (shoots + roots) was simulated from the mass of harvested dry plant material and from a classical logistic function (formula 2; Fig. 2). Parameter k_r is the predicted proportion of C, which is derived from living roots and directed into the soil as labile material. In formula 1, k_r is defined as a constant proportion of the plant biomass (LPM) and was 0.025 and 0.015 g C g^{-1} plant dw day^{-1}, which is 0.054 and 0.032 g C g^{-1} plant-C day^{-1} (plant material-C = 46%) for soils 1 and 2 respectively. Thus the model predicts a lower proportion of labile C released from roots for the more productive soil 2 than in the less productive soil 1. Nevertheless, in absolute values, predicted C derived from roots was comparable for both soils. During the 11 growths, 10.7 and 13.8 g organic C kg^{-1} dry soil were released by plants into soils 1 and 2, respectively. The model prediction confirms results from many pulse-labelling and non-labelled experiments, pointing out an increased below ground translocation and rhizosphere activity with decreased N availability (Hansson et al., 1991). By contrast, Swinnen et al. (1995) in a pulse-labelling experiment, found that N fertilisation of a winter wheat had no effect on the proportion of ^{14}C which is translocated to the roots, calculated as a proportion of net assimilated ^{14}C. Unlike our results, Liljeroth et al. (1990) found that the proportion of net assimilated ^{14}C recovered in root/soil respiration and deposited in soil was higher with a high N fertilisation, compared to low N. These contradictory results illustrate that, beside the N fertility, other factors also control below-ground C translocation. Thus, a higher soil compaction in the clay soil 1 also may explain the higher proportion of ^{14}C released in the soil, since Barber and Gun (1974) observed a higher exudation rate in soils with increased physical resistance to roots.

In formula (1′), k_r was defined as a constant proportion of the net daily production and was 0.43 and 0.35 g C g^{-1} plant dw or 0.93 and 0.76 g C g^{-1} plant-C for soils 1 and 2, respectively. If in our calculation the 'assimilated C' is defined as the sum of shoots-C +roots-C+the organic C released from the roots as rhizodeposition, then the model predicts that the organic C released from the roots represented 48 and 43% of this 'assimilated C'. These values are high, because in the calculation the direct root respiration-C (not measured nor predicted in this experiment) is not included in the 'assimilated C'. The estimated proportion of assimilated C translocated to the roots is controversial, with a large degree of uncertainty. Approximately 10–30% of the total assimilated C is lost by the roots as root respiration and organic C release (Van Veen et al., 1991). The estimated root respiration/microbial respiration ratio ranges from 1/1 (Warembourg and Billes, 1979) to 1/4 (Van Veen et al., 1991). When the means of these values are used, then the rhizodeposited-C in soils 1 and 2 amounts to 46% and 41%, respectively, in percent of the classically defined net assimilated-C (shoot+root+direct root respiration+root exudation). These values are still high. Except under sterile conditions, the techniques (pulse labelling) seldom allow direct measurement of organic C release from the roots. Microbial respiration cannot therefore be distinguished from root respiration. The fluxes are generally calculated indirectly. Reviewing the carbon economy in the rhizosphere, Wipps (1990) reported that the CO_2 produced by the micro-organisms utilising carbon sources derived from the roots varied from 7% to at least 30% of the total C fixed by the plant. The author concluded that the majority of below-ground CO_2 respired during the growth of wheat, was derived from the respiration of micro-organisms degrading root-derived material. In addition, the root exudation varies to a large extent, depending on the age of the plants (Meharg and Killham, 1990; Warembourg 1997). The present experiment was performed only with active root systems (until earing time), generating mean values calculated from the model prediction over the 11 growths. Finally, the relatively high k_r (Eq. (1′)) values may also be partly explained by a quantity of fine roots which remained in the soil after each plant harvest and root extraction, slightly overestimating the input of organic C derived from the living roots. The cumulated soil ^{14}C adhering to the roots at plant harvests did not exceed 4% of the initial total ^{14}C, but the cumulated proportion of roots remaining in soil was probably higher.

Conclusion

The present experiment investigated the effects of active roots on decomposition of labelled plant material, throughout a complete decomposition cycle, from very fast to slow stages dominated by dormant organisms. The root effect could not be described by simple multiplying factors. This illustrates the complexity of the root effect and the difficulty to parametrise the process, when multi-compartment models are fitted to measured soil carbon pools. Thus the plant effect cannot yet be easily extended to other soil and growth conditions. The generalisation of multi-compartment models supported by measured compartments is still questionable. The controversial response of the soil processes to the presence of living roots, pointed out by many authors, is in this experiment predicted by two main processes:

(1) The competition between plants and microorganisms for inorganic N explains the negative effect of plants on total C mineralisation rates, during the initial active decomposition stage, when available labile-C stimulates microbial activity. This effect is also reflected by lower plant productivity and lower plant N uptake during the active decomposition stages compared to the subsequent growths. Nevertheless this root-induced reduction of decomposition is relatively low.

(2) By contrast, the presence of living roots stimulates the total carbon mineralisation during the later decomposition stage. During this phase, the labile-C resources are exhausted, leading to low mineralisation rates. In bare soils, part of the microbial biomass decays, and most of the surviving organisms are dormant. In the presence of living roots, the model predicts the mineralisation of an extra amount of stabilised humus or recalcitrant plant debris. The protecting effect of clays and loam on recently formed labelled humus is partly counteracted by the presence of roots, stimulating its mineralisation. The model also predicts a stimulated mineralisation of old soil native stabilised organic fractions; they are not governed by the same mineralisation rates as the freshly formed compounds derived from the labelled material. The total soil native-C dynamics are essentially explained by the humus compartment, since this fraction is largely dominant. The presence of roots led to a progressive replacement of the labelled microbial biomass derived from the initial plant material by unlabelled microbial biomass derived from the root deposited carbon. During the slow decomposition phase, in the bare soils, the biomass decreased 2.5-to 3-fold by progressive energy exhaustion. By contrast in the cultivated soils, high biomass levels were maintained until the end of the experiment.

To maintain this high biomass level in the cultivated soils and to sustain its activity, the model predicts an input of labile C derived from the roots and related to the plant growth. This predicted organic rhizodeposition was described as a mean proportion of the living biomass: (shoots+roots) or as a mean proportion of the daily plant production. At each day, the mean value of C released by the roots into the soil amounted to 5.4 and 3.2% of the plant biomass present or 48 and 43% of the daily plant 'net production' for soils 1 and 2, respectively. These calculated values are relatively high but within the range of some published data.

References

Barber D A and Gunn K B 1974 The effect of mechanical forces on the exudation of organic substances by the roots of cereal plants grown under sterile conditions. New Phytol. 73, 39–45.

Bottner P, Sallih Z and Billes G 1988 Root activity and carbon metabolism in soils. Biol. Fertil. Soils 7, 71–78.

Cheng W X and Coleman D C 1990 Effect of living roots on soil organic matter decomposition. Soil Biol. Biochem. 22, 781–787.

Dormaar J F (1990) Effect of active roots on the decomposition of soil organic materials. Biol. Fertil. Soils 10, 121–126.

Hansson A C, Andren O and Steen E 1991 Root production of four arable crops in Sweden and its effect on abundance of soil organisms. *In* Plant Root Growth an Ecological perspective. Ed. D Atkinson. pp 247–266. Blackwell Scientific Publications, Oxford.

Jenkinson D S 1977 Studies on the decomposition of plant material in soil. V. The effects of plant cover and soil type on the loss of carbon from ^{14}C labelled ryegrass decomposing under field conditions. J. Soil Sci. 28, 424–434.

Jenkinson D S 1990 The turnover of organic carbon and nitrogen in soil. Phil. Trans. R. Soc. London B 329, 361–368.

Jenkinson D S and Powlson D S 1976 The effect of biocidal treatments on metabolism in soil: V. A method for measuring soil biomass. Soil Biol. Biochem. 8, 209–213.

Liljeroth E, van Veen J A and Miller H J 1990 Assimilate translocation to rhizosphere of two wheat cultivars and subsequent utilisation by microorganisms at two soil nitrogen levels. Soil Biol. Biochem. 22, 1015–1021.

Meharg A A and Killham K 1990 Carbon distribution within the plant and rhizosphere in laboratory and field-grown *Lolium perenne* at different stages of development. Soil Biol. Biochem. 22, 471–477.

Merckx R, den Hartog A and van Veen J A 1985 Turnover of root-derived material and related microbial biomass formation in soils of different texture. Soil Biol. Biochem. 17: 565–569.

Merckx R, Dijkstra A, den Hartog A and van Veen J A 1987 Production of root-derived material and associated microbial growth in soil at different nutrient levels. Biol. Fertil. Soils 5, 126–132.

Pansu M, Sallih Z and Bottner P 1998 Modelling of soil nitrogen forms after organic amendment under controlled conditions. Soil Biol. Biochem. 30, 19–29.

Quian J H, Doran J W and Walters D T 1997 Maize plant contributions to root zone available carbon and microbial transformations of nitrogen. Soil Biol. Biochem. 29, 1451–1462.

Rogers H H, Runion G B and Krupa S V 1994 Plant response to atmospheric CO_2 enrichment, with emphasis on roots and the rhizozsphere. Environ. Pollut. 83, 155–189.

Sallih Z and Pansu M 1993 Modelling of soil carbon forms after organic amendment under controlled conditions. Soil Biol. Biochem. 25, 1755–1762.

Shields J A and Paul E A 1973 Decomposition of C-labelled plant material under field conditions. Can. J. Soil Sci. 53, 297–306.

Swinnen J, van Veen J A and Merckx R 1995 Root decay and turnover of rhizodeposits in field-grown winter wheat and spring barley estimated by ^{14}C pulse-labelling. Soil Biol. Biochem. 27, 211–217.

Van Noordwijk M, Martikainen P, Bottner P, Cuevas E, Rouland C and Dhillion S 1998 Global change and root function. Global Change Biol. 4, 759–772.

van Veen J A, Liljeroth E, Lekkerkerk L J A and Van de Geijn S C 1991 Carbon fluxes in plant-soil systems at elevated atmospheric CO_2 levels. Ecol. Appl. 1, 175–181.

Warembourg F. 1997 The 'rhizosphere effect': a plant strategy for plants to exploit and colonize nutrient limited habitats. Bocconea 7, 187–193.

Warembourg F and Billes G, 1979. Estimating carbon transfer in the rhizosphere. *In* The Soil–Root Interface. Eds J L Harley and R S Russel. pp 183–197. Academic Press, New York, USA.

Wipps J M 1990 Carbon Economy. *In* The Rhizosphere. Ed. J M Lynch. pp 59–97. Wiley and Sons, Chichester, UK

Zagal E 1994 Influence of light intensity on the distribution of carbon and consequent effects on mineralization of soil nitrogen in a barley-soil system. Plant Soil 160, 21–31.

Section editor: R Merckx

La Transformation du carbone des Apports Organiques (modèle TAO-C)

Cinétique de transformation des formes du carbone

PERGAMON

Soil Biology & Biochemistry 33 (2001) 997–1010

Soil Biology & Biochemistry

www.elsevier.com/locate/soilbio

Kinetics of added organic matter decomposition in a Mediterranean sandy soil

L. Thuriès[a,b,c], M. Pansu[a,*], C. Feller[a], P. Herrmann[b], J.-C. Rémy[b]

[a]*IRD (formerly ORSTOM), BP 5045, 34032 Montpellier Cedex 1, France*
[b]*INRA-ENSAM, 2 place P. Viala 34060 Montpellier Cedex 1, France*
[c]*Phalippou-Frayssinet S.A., Organic fertilizers, BP 42, 81270 Labastide-Rouairoux, France*

Received 17 December 1999; received in revised form 13 July 2000; accepted 6 December 2000

Abstract

Carbon mineralization kinetics of 17 organic materials were studied in a Mediterranean sandy soil. These added organic matters (AOM) used in the organic fertilizer industry differed in their origin and composition: plant residues from the agri-food industry, animal wastes, manures (plant and animal origin), composts at different composting times and organic fertilizers. The mixtures AOM-soils were incubated under aerobic conditions at 28°C during 6 months. Soil moisture was maintained at 75% water holding capacity and respired-CO_2 was regularly trapped into alkali media in closed chambers, then checked by HCl titration. Analyses of CO_2 were performed in triplicate at 17 sampling occasions. The mineralized AOM fraction (MAOMF) varied according to the AOM origin: from 12–33% of added C for composts, to 65–90% for animal-originated AOM, with many intermediate patterns for plant-originated AOM.

Seven decomposition models from the literature were fitted to actual MAOMF: (a) three consecutive models with two 1st-order-kinetic compartments and three parameters (*m*1, humification; *m*2, exchange; *m*3, decomposition), (b) three parallel models (*m*4, with two compartments and three parameters; *m*8, a 1st-order plus 0-order model with three parameters; *m*5, a three-compartment model with four parameters), and (c) *m*7, a model with one 2nd-order-kinetic compartment and two parameters. Additionally, *m*6, a simplified version of *m*5 was proposed. Models *m*2 and *m*7 did not match with actual data or gave a poor fit. By the correlation parameters, the most simple model *m*4 was chosen instead of the consecutive models *m*1 and *m*3. Residual sums of squares were always greater—but not significantly—in *m*8 than in *m*4, which confirmed the superiority of the models with two 1st-order compartments against 1st-order plus 0-order models for incubation times higher than 100 days. Model *m*5 (most of its parameters being not correlated) gave the best predictions of our data. The proposed *m*6 version gave predictions with similar precision as *m*4 and appeared powerful with only two parameters (very labile and stable fractions of the AOM). A compromise between the precision of the predictions and the simplicity of the formulae allowed the recommendation of the well-known *m*4 model, and above all the simpler *m*6 model.

Keywords: Decomposition models; Added organic matter; Organic fertilizers; Composted organic amendments; Organic carbon

1. Introduction

The utilization of organic amendments and fertilizers is increasing with the development of organic farming, and is even increasing among conventional farmers (Hartz et al., 2000). Indeed, such products are largely available due to: (a) a social need for healthy food produced under conditions that protect the environment and (b) a constant legislative pressure for recycling of organic wastes. Both manufacturers and farmers need tools for characterizing and evaluating such organic materials. Furthermore, environmental scientists need more precise parameters for modelling the decomposition of such added organic matter (AOM, Mueller et al., 1998) in soils. Up to now, many works have dealt with the carbon and/or nitrogen mineralization kinetics of crop residues (Janzen and Kucey, 1988; Mary et al., 1993; Recous et al., 1995; Kaboneka et al., 1997) and its modelling (Quemada and Cabrera, 1995; Whitmore, 1996; Gilmour et al., 1998; Henriksen and Breland, 1999). Carbon mineralization kinetics have also been studied with manures and composts (Hébert et al., 1991; Hadas and Portnoy, 1994; Paul and Beauchamp, 1994; Sørensen and Jensen, 1995; Paré et al., 1998; Hartz et al., 2000), together with modelling investigations (Levi-Minzi et al., 1990; Saviozzi et al., 1993; Kirchmann and Bernal, 1997; Hadas and Portnoy, 1997; N'Dayegamiye et al., 1997; Bernal et al., 1998). Because laboratory techniques and model standardization is lacking, these studies are difficult to compare. Laboratory

* Corresponding author. Tel.: +33-4-67-41-62-28; fax: +33-4-67-41-62-94.
E-mail address: pansu@mpl.ird.fr (M. Pansu).

0038-0717/01/$ - see front matter
PII: S0038-0717(01)00003-7

Table 1
Major characteristics (C, N, C-to-N ratio, total ashes) and doses of added organic matter (AOM) in g (C or N) kg^{-1} dry soil, and in equivalent field dose in ton per hectare

AOM origin	AOM	g kg^{-1} AOM (dry basis)				g kg^{-1} dry soil		t ha^{-1}
		C	N	Ashes	C: N	Added C	Added N	Field dose[a]
Plant	Coffk	537	20	31	27	4.999	0.184	28
	Wgrap	529	27	89	20	4.667	0.238	28
	Dgrap	494	22	71	22	4.605	0.209	28
	Olivp	469	20	88	24	4.426	0.186	28
	Kokoa	437	45	91	10	4.072	0.423	28
Manure	Shepm	379	22	281	17	3.230	0.190	28
	Chicm	376	61	323	6	3.360	0.542	28
Animal	Nfeat	545	146	38	4	1.205	0.322	7
	Featm	471	152	28	3	1.064	0.343	7
	Guano	175	156	433	1	0.392	0.350	7
Fertilizer	Gnofer	273	95	404	3	0.617	0.215	7
	Comfer	369	37	255	10	1.735	0.176	14
Compost	Compo a	362	29	322	12	2.709	0.218	28
	Compo b	363	25	344	15	3.434	0.233	28
	Compo e	288	27	404	11	2.505	0.235	28
	Compo +	339	26	321	13	3.035	0.229	28
	Compo p	449	25	402	18	2.816	0.156	28

[a] AOM bulk weight, calculated on 0–20 cm layer, mean soil bulk density (<2 mm) = 1.5, refuse (>2 mm) = 5.21% and 6.68% for the 0–10 cm and 10–20 cm layers, respectively.

protocols differ on CO_2 measurement methods, type of soil, incubation time, temperature, soil moisture, AOM amounts, decomposition of AOM alone (specific mineralization) or simultaneous addition of mineral-N (mineralization with standardized total-N content). Most of the models used for predicting CO_2-C mineralization take into account one (the whole AOM), two, or more organic compartments of the AOM (more or less resistant to microbial attack).

The first objective of this work was to test, under standard laboratory conditions, the specific carbon mineralization of a wide range of AOM in a sandy soil with low organic matter content. The second objective was to find accurate models to describe the carbon-AOM mineralization kinetics under these standard conditions, the model parameters only depending upon AOM quality.

2. Material and methods

2.1. Soil for mineralization test

The incubation test was done with the top-layer (0–20 cm) of a sandy soil (69.3% sand, 11.5% clay), previously described by Servat and Callot (1966) and classified as fluvisol (FAO-UNESCO-ISRIS, 1988) or Udifluvent (USDA, 1975). It was collected in an experimental site (Thuriès et al., 2000a) located in Théza (Eastern Pyrénées, France). This soil has $pH_{(H_2O)}$ 6.6, CEC 5.5 cmol c^+ kg^{-1} soil, total C and N 4.98 and 0.59 g kg^{-1} soil, respectively. It was partially air-dried at room temperature (20°C) until it could be crushed and sieved through a 2 mm sieve, then air-dried to constant weight.

2.2. Added organic matter (AOM)

Different kinds of AOM from agri-food industry wastes and industrial-processed fertilizers (organic amendments and fertilizers) were tested. Their major characteristics are shown in Table 1. The raw materials were from (a) plant origin: wet and dry grape berry pellicles cakes (Wgrap, Dgrap), coffeecake (Coffk), cocoacake (Kokoa), olivecake (Olivp), (b) animal origin: hydrolyzed feather meal (Featm), native fine feather (Nfeat), guano (Guano), (c) manure origin (plant and animal origin): sheep manure (Shepm), chicken manure (Chicm) and (d) fertilizers: organic composted amendments (Compo series), and organic fertilizers (Gnofer, Comfer). The composted organic amendments (Compo) were made from Shepm and Coffk in periodically-turned and aerated piles, during a 10-month composting period. Samples were taken before the composting process (Compo a), and at 40 (Compo b), 120 (Compo p), and 305 (Compo e) days. Compo + was a mixture of 75% Compo e and 25% Dgrap (used for drying the compost). Gnofer was a guano-based organic fertilizer, whereas Comfer was a Compo-based fertilizer supplemented with Chicm. The AOM were air-dried at 25°C, then finely ground.

2.3. Incubation experiment

Carbon mineralization was measured as respired CO_2-C in closed chambers (28°C ± 1°C, in an incubator) with the experimental design adapted by Thuriès et al. (2000b). An exact mass (125–500 mg AOM per container) was

homogeneously incorporated in 50 g air-dried soil. These experimental AOM amounts were chosen to correspond to realistic inputs in field conditions: 7 or 14 t ha^{-1} for animal products or fertilizers, 28 t ha^{-1} for composts, plant origin products and manures (Table 1).

The AOM-C ranged from 8 to 102% of initial soil C, and the AOM-N from 26 to 93% of initial soil N. Identical added quantities of AOM-N would have led to very low inputs of C for N-rich fertilizers and unrealistic high field doses for N-poor amendments. Recous et al. (1995) and Henriksen and Breland (1999) indicated that concentrations of available N (AOM-N + soil inorganic N) less than 1.2% of AOM dry matter significantly reduced the rate of C-mineralization and growth of microbial biomass. This risk does not exist in the present experiment since AOM-N concentrations alone were greater than 2% of AOM-dry matter (Table 1). For our study of specific AOM mineralization, we did not consider any mineral N addition simultaneously with AOM addition. During decomposition, the N pathway and dynamics of organic and inorganic N are not the same (Pansu et al., 1998b); the addition of mineral-N would not reduce the N heterogeneity linked to AOM addition.

Three replicates per AOM treatment, basal soil respiration and blanks were used for the experiment. Sample containers were placed in 1.2 l airtight glass jars containing a 50 ml vial with 20 ml aqueous NaOH solution 0,25 mol l^{-1} (Titrisol) for CO_2-C trapping and ~10 ml deionized water (moisture saturated atmosphere) to prevent soil desiccation. Soil moisture was checked by periodical weighting and maintained at ~75% water holding capacity (~ − 30 kPa or 16% dry weight basis) with deionized water. For each replicate of AOM, blank and control, 17 sampling occasions of CO_2-C measurements were done at days 1, 2, 3, 5, 7, 10, 14, 20, 28, 41, 61, 90, 100, 120, 130, 152 and 180.

2.4. Measurements

Organic carbon and total nitrogen of soil and AOM were determined by dry combustion (Carlo Erba NA 2000) with control by lost on ignition at 450°C for AOM (NFU 44160, 1985).

The respired CO_2-C was estimated by precipitating the carbonates with a solution of $BaCl_2$ and titrating the remaining NaOH (uncarbonated) with HCl 0.25 mol l^{-1}. Soil basal respiration (control unamended soil) was subtracted from the gross respiration to assess the net respiration associated to AOM mineralization (Eq. 1). The total respired CO_2-C quantities were obtained by summing the CO_2-C respired between sampling occasions (Eq. 2).

2.5. Data calculation and control

The fraction of added C mineralized from AOM at a sampling occasion i was estimated according to:

$$Cm_{i\alpha} = \frac{CO_2C^a_{i\alpha} - CO_2C^c_{i\alpha}}{TAC} \quad (1)$$

$$\bar{C}m_i = \frac{1}{n}\sum_{\alpha=1}^{n} Cm_{i\alpha} \quad (2)$$

$$\overline{MAOMF}_i = \overline{MAOMF}_{i-1} + \bar{C}m_i \quad (3)$$

Where $Cm_{i\alpha}$ = respired fraction of organic amendment at sampling occasion i and replication α, $CO_2C^a_{i\alpha}$ and $CO_2C^c_{i\alpha}$ are the amounts of C evolved from the amended and control $i\alpha$ samples respectively, TAC is total added C expressed in the $CO_2C^a_{i\alpha}$ and $CO_2C^c_{i\alpha}$ unit, $\bar{C}m_i$ = mean respired fraction of AOM at sampling occasion i ($n = 3$ replicates), $\overline{MAOMF}_i$ and $\overline{MAOMF}_{i-1}$ are mean mineralized AOM fractions (cumulated values of respired fractions with $MAOMF_0 = 0$).The expression $\overline{MAOMF}$ is very useful for practical use since it does not depend on any unit. For example, a value $\overline{MAOMF} = 0.4$ at 150 days, means (with gross approximate of comparable mineralization conditions) that for a 10 Mg C ha^{-1} AOM application, 4 Mg C ha^{-1} will be mineralized during 5 months after spreading. Hess and Schmidt (1995) pointed out that estimations with non-cumulative data were more accurate than with cumulative ones. But they used short-term experiments with a great number of sampling occasions with the same time interval. Moreover, their estimations by the two methods where not really different. Our experiment lasted for 6 months with very different time intervals between sampling occasions. The cumulative values are also the most frequently used for parameter estimations and correspond directly to the analytical solutions of differential equations (Table 2). Nevertheless, working with cumulative values necessitate careful data control during the experiments since variances are added simultaneously with mean additions. The pooled variance of Cm_i is:

$$s^2_{Cm_i} = \frac{1}{np - p}\sum_{i=1}^{p}\sum_{\alpha=1}^{n}(Cm_{i\alpha} - \bar{C}m_i)^2 \quad (4)$$

where p is the total number of sampling occasions with n samples. The cumulative confidence intervals must be calculated according to Pansu et al. (1998a):

$$MAOMF_i = \overline{MAOMF}_i \pm t^{np-p}_{0,975} \times S_{Cmi}\sqrt{\frac{i}{n}} \quad (5)$$

2.6. Mathematical models

Our main objective was to compare the efficiency of different model formulations (Table 2) in the description of cumulative CO_2-C data. The tested models can be classified in three types: one-compartment model (O in Table 2), consecutive 1st order compartment models (C in Table 2) and parallel 1st order compartment models (P in Table 2).

The first consecutive two-compartment humification model

Table 2
Model formulations for remaining AOM fraction (RAOMF = 1–MAOMF); CM = compartment model; T = model type (C = consecutive two CM, P = parallel 2 or 3 CM, O = one CM)

T No.	Name	Flow AOM = added organic matter	Analytical solution RAOMF at time *t*	Parameters
C *m*1	Consecutive humification, 1st order 2 CM, three parameters	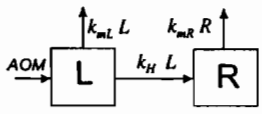	$\frac{(k_{mL}-k_{mR})}{k_{mL}+k_H-k_{mR}}e^{-(k_{mL}+k_H)t} + \frac{k_H}{k_{mL}+k_H-k_{mR}}e^{-k_{mR}t}$	k_{mL}, k_{mR}: 1st order kinetic mineralization constants of labile (L) and resistant (R) compartments k_H: humification constant
C *m*2	Exchange 1st order 2 CM	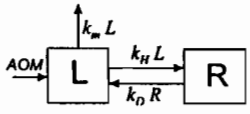	$\frac{\lambda_1+k_m}{\lambda_1-\lambda_2}e^{\lambda_2 t} - \frac{\lambda_2+k_m}{\lambda_1-\lambda_2}e^{\lambda_1 t}$	k_H, k_D: humification and decomposition constants. k_m: mineralization constant (λ_1, λ_2: roots of 2nd order linear differential equation $f(k_H, k_D, k_m)$)
C *m*3	Consecutive decomposition 1st order 2 CM, three parameters	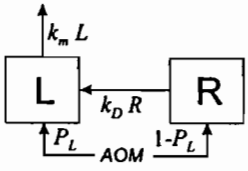	$\frac{P_L k_m - k_D}{k_m - k_D}e^{-k_m t} + \frac{(1-P_L)k_m}{k_m-k_D}e^{-k_D t}$	k_D, k_m: decomposition and mineralization constants, P_L: labile AOM fraction
P *m*4	Parallel 1st order 2 CM, three parameters	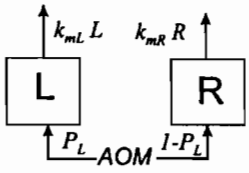	$P_L e^{-k_{mL}} + (1-P_L)e^{-k_{mR}t}$	k_{mL}, k_{mR}: see *m*1 above, P_L: see *m*3 above
P *m*5	Parallel 1st order 3 CM, 4 parameters	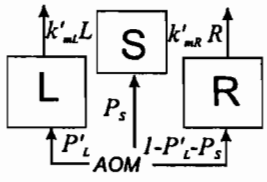	$P'_L e^{-k'_{mL}t} + (1-P'_L-P_S)e^{-k'_{mR}t} + P_S$	P'_L: very labile AOM fraction. k'_{mL}, k'_{mR}: kinetic constants of very labile and R fractions. P_S: stable AOM fraction
P *m*6	Parallel 1st order 3 CM, 2 parameters	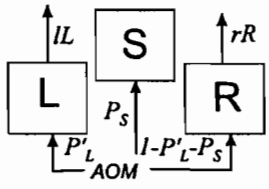	$P'_L e^{-lt} + (1-P'_L-P_S)e^{-rt} + P_S$	P'_L, P_S: see *m*5 above. *l*, *h* = constants (fixed values of k_{mL} and k_{mR} for all AOM)
O *m*7	2nd order kinetic model	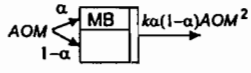	$\frac{1}{1+k\alpha(1-\alpha)t}$	*k*: 2nd order kinetic constant. α: fraction of AOM becoming microbial biomass
P *m*8	1st order plus 0 order model	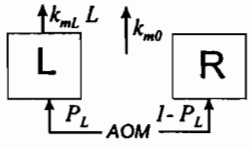	$P_L e^{-k_{mL}t} + 1 - P_L + k_{m0}t$	P_L, k_{mL}: see *m*4 above. k_{m0}: 0 order kinetic constant

(*m*1 in Table 2) was proposed by Hénin et al. (1959), used by Pansu and Sidi (1987) for a laboratory incubation experiment and extended by Andrén and Kätterer (1997) by adding an *r* parameter which combines the external effects (climate, edaphic factors).

The model *m*2 is a two-compartment version of the three-compartment model proposed by Saggar et al. (1996). Using models *m*1 or *m*2 means that a CO_2-C mineralization experiment alone cannot give a valuable information about the forms of C in soil, especially for long-term incubations. Hénin et al. (1959) and Saggar et al. (1996) presented their model with humification from organic inputs (L in Table 2) toward humified materials (R in Table 2) with consecutive direct R-mineralization (*m*1) or R-decomposition toward *L* (*m*2).

The consecutive 1st order two-compartment decomposition model (*m*3 in Table 2) was used by Andrén and Paustian (1987) to fit field decomposition data: the AOM input is split between labile AOM (L) which mineralizes and resistant AOM (R) which decomposes toward *L*.

Parallel 1st order two-compartment model (*m*4 in Table 2) is the most commonly used to interpret incubation experiments (Gilmour et al., 1998) and was used to model climate effects (Lomander et al., 1998). It is the easiest to integrate to an analytical solution. Parallel 1st order two-compartments models (labile and resistant organic materials) regulates the C-input in most of the more complex soil organic matter models such as Phoenix (McGill et al., 1981), Ncsoil (Molina et al., 1983), Century (Parton et al., 1987), Momos (Sallih and Pansu, 1993), Rothamsted (Bradbury et al., 1993). So a better knowledge of model parameters for different organic inputs are of great interest to improve all model predictions. Non-linear fittings of models *m*1, *m*3 and *m*4 analytical solutions (Table 2) are equivalent. Models *m*1 and *m*4 are related by $\{k_{mR}\}_{m1} = \{k_{mR}\}_{m4}$, $\{k_{mL} + k_H\}_{m1} = \{k_{mL}\}_{m4}$ and

$$\left\{\frac{k_{mL} - k_{mR}}{k_{mL} - k_{mR} + k_H}\right\}_{m1} = \{P_L\}_{m4}$$

but parameters of the two models do not have the same physical significance, except k_{mR}. However, if in model *m*1, $k_{mR} \ll k_L$, then

$$\frac{k_{mL} - k_{mR}}{k_{mL} - k_{mR} + k_H} \approx \frac{k_{mL}}{k_{mL} + k_H}$$

which can represent the AOM labile fraction (P_L in model *m*4). Models *m*3 and *m*4 are related by $k_m = k_{mL}$, $k_D = k_{mR}$ and

$$\left\{\frac{P_L k_m - k_D}{k_m - k_D}\right\}_{m3} = \{P_L\}_{m4}$$

when $k_D \ll k_m$, models *m*3 and *m*4 are identical.

Parallel 1st order three compartment-model (*m*5 in Table 2) was used to regulate C-input in the Verberne et al. (1990) model and in the Daisy model (Hansen et al., 1991). The compartment S corresponds to the AOM stable fractions. It was not possible to predict its mineralization during a 6-month experiment, thus we did not mention any mineralization constant for the S compartment. In order to reduce the complexity, we proposed the *m*6 model (Table 2) with only two parameters: the very labile and stable fractions in AOM.

The 2nd order kinetic model (*m*7 in Table 2) was found better than a simple 1st order kinetic (one compartment) model by Whitmore (1996). The mixed 1st-order plus 0-order kinetic model (*m*8 in Table 2) was chosen by Bernal et al. (1998) to fit CO_2-data from a 2-month laboratory incubation and by Blet-Charaudeau et al. (1990) to fit CO_2-data from field experiment.

2.7. Calculation tools

Calculations were performed using linear (*m*5 and *m*6 in Table 2) or non-linear (*m*1 to *m*4 and *m*7 in Table 2) fittings with optimization of parameters using the Marquardt algorithm to minimize residual sum of square (RSS). The choice of a model was based on the following statistical tests:

- Determination coefficient r^2 or percentage of variability explained by the model;
- Residue distributions: a model which explains the whole information in a given data series must have a normal residue distribution around residual mean = 0; residual tests can be performed in two ways: visual graphical observation (Hess and Schmidt, 1995) or auto-correlation Durbin-Watson test (DW);
- Correlations: our work with 17 data series allowed us to calculate correlation between parameters values; a positive test indicates a possible dependence between parameters which can be graphically observed;
- Residues comparison: the best model must have the lowest RSS; let RSS*a* and RSS*b* the residual sum of square of models *a* and *b* respectively; comparisons with test *F* must be performed as follows:

$$F = \frac{\text{RSS}a}{\text{RSS}b} = \frac{\sum(y_i - \hat{y}_{ia})^2/(p-m)_a}{\sum(y_i - \hat{y}_{ib})^2/(p-m)_b} \quad (6)$$

if RSS*a* > RSS*b* – otherwise:

$$F = \frac{\text{RSS}b}{\text{RSS}a}$$

if RSS*b* > RSS*a* – with p = number of sampling occasions, m = number of model parameters, y_i, $\hat{y}_{ia}$, $\hat{y}_{ib}$ = measured and predicted values with *a* and *b* models respectively, at sampling *i*. An *F* value (Eq. 3) greater than bilateral $F^{0,05}_{(P-m)_a(p-m)_b}$ (statistical table) indicates that equality hypothesis must be rejected with 5% risk: RSS*a* is greater than RSS*b* so model *b* fitting is better than *a*.

3. Results and discussion

3.1. Data from CO_2 mineralization

The patterns of C mineralization are presented in

Figs. 1–3. Most of AOM from animal origins were rapidly mineralized (Figs. 1 and 3). During 6 months, 65% (Chicm), or up to 90% (Guano) of AOM-C was respired. Mineralization from plant origin-AOM was less intensive (Fig. 1) with a large range of mineralized C: from 29% for Dgrap to more than 56% for Coffk. These discrepancies occurred during the last stages of incubation (after 2 months). Some AOM have uncommon patterns. On one hand the Kokoa mineralization curve looks like a fertilizer or an animal-originated AOM (see Featm in Fig. 1) with a large very labile fraction. On the other hand, native fine feather (Nfeat in Fig. 1) was less susceptible to microbial degradation, and behaved like a recalcitrant plant material. Nfeat is composed of native proteins arranged in lamella, and is quite recalcitrant to microbial attacks (AOM manufacturer, unpublished data). Another hypothesis is the possible presence of antibiotics since Nfeat is derived from intensive duck livestock.

After 6 months of incubation, the C mineralization of the industrial composts (Compo in Fig. 2) showed a gradient according to the time of composting: 33% for the initial mixture to 12% for the most composted material. The curve patterns were intermediary between the animal-origin AOM and plant-origin ones. The fertilizer with a compost base (Comfer in Fig. 3) combined the typical fertilizer pattern (strong early mineralization rate) with a more stable one.

The confidence intervals at 152 or 180 days of incubation (Figs. 1–3) are the greatest of the experiment since they are calculated with $i = 16$ or $i = 17$ respectively (Eq. 5). It is difficult to compare their amplitudes with other works since the calculation methods are not given, and results are very different: for example, very small intervals reported by Bernal et al. (1998) and wider ones by Paré et al. (1998).

The highest actual confidence intervals relate to the products with strong mineralization: guano-based fertilizer and guano (Fig. 3). In contrast, the third animal product with rapid mineralization (Featm in Fig. 1) gave a better repeatability. This feather meal is an industrial product, and has been treated at high temperature (120°C, autoclaved); this product is finely ground and is probably more homogenous with respect to the C- and N-repartition and active sites for microbial attack.

3.2. Comparative m1, m2, m3, m4, m7, m8 model predictions

Models *m*2 and *m*7 (Table 2) did not match with this data or gave poor fittings (determination coefficients $2\% < r^2 < 97\%$, depending on the AOM). As expected, models *m*1, *m*3 and *m*4 gave the same predictions. The 17 data series were well predicted with these two-compartment models (Figs. 1–3). The determination coefficients (in Table 3 and on each curve) were above 99% for 11 series,

Table 3
Comparison of predictions with models *m*4 (or *m*1 or *m*3), *m*5, *m*6 and *m*8 (*F*-test, Eq. 6; Durbin-Watson test, DW). Symbols represent the level of significance for *F*-test. * * * ($p < 0.01$), * ($p < 0.05$); ns = no significant difference, – = unsatisfactory prediction. ac = autocorrelated parameters, ra = randomly distributed parameters

AOM origin	AOM	*F*										DW									
		(*m*1, *m*3 or *m*4)/*m*5		(*m*1, *m*3 or *m*4)/*m*6		*m*6/*m*5		*m*6/(*m*1, *m*3 or *m*4)		*m*8/(*m*1, *m*3 or *m*4)		*m*1, *m*3 or *m*4		*m*5		*m*6		*m*8	
Plant	Coffk	3.17	ns	1.68	ns	1.90	ns	0.60	ns	1.67	ns	0.94	ac	1.90	ra	0.96	ac	0.68	ac
	Wgrap	5.35	* * *	0.69	ns	7.76	* * *	1.45	ns	1.15	ns	0.88	ac	1.89	ra	0.46	ac	0.83	ac
	Dgrap	4.02	*	1.05	ns	3.81	*	0.95	ns	1.02	ns	0.42	ac	1.18	ac	0.51	ac	0.41	ac
	Olivp	26.57	* * *	9.65	* * *	2.75	ns	0.10	ns	1.04	ns	0.36	ac	1.12	ac	0.56	ac	0.33	ac
	Kokoa	7.34	* * *	0.71	ns	10.28	* * *	1.40	ns	1.30	ns	0.63	ac	1.51	ra	0.40	ac	0.59	ac
Manure	Shepm	1.57	ns	0.11	ns	14.11	* * *	9.00	* * *	1.00	ns	1.05	ac	1.72	ra	0.45	ac	1.04	ac
	Chicm	4.10	*	2.52	ns	1.63	ns	0.40	ns	2.24	ns	1.04	ac	2.37	ra	1.27	ac	0.79	ac
Animal	Nfeat	–	–	0.06	ns	–	–	16.66	* * *	1.00	ns	1.64	ra	–	–	0.36	–	1.64	ra
	Featm	1.01	ns	0.23	ns	4.46	* * *	4.41	* * *	1.04	ns	0.86	ac	0.86	ac	0.41	ac	0.85	ac
	Guano	–	–	0.13	ns	–	–	7.46	* * *	0.91	ns	1.90	ra	–	–	0.49	–	1.97	ra
Fertilizer	Gnofer	–	–	0.14	ns	–	–	7.12	* * *	1.29	ns	1.35	ac	–	–	0.53	–	1.24	ac
	Comfer	12.23	* * *	2.41	ns	5.08	* * *	0.42	ns	1.05	ns	0.58	ac	2.87	ra	0.78	ac	0.57	ac
compost	Compo a	6.33	* * *	0.64	ns	9.96	* * *	1.57	ns	1.14	ns	0.66	ac	1.67	ra	0.44	ac	0.64	ac
	Compo b	16.38	* * *	3.70	*	4.42	* * *	0.27	ns	1.17	ns	0.64	ac	2.63	ra	0.85	ac	0.62	ac
	Compo e	4.00	*	3.38	*	1.18	ns	0.30	ns	1.05	ns	0.88	ac	2.04	ra	1.63	ra	0.86	ac
	Compo +	11.50	* * *	1.59	ns	7.26	* * *	0.63	ns	1.10	ns	0.60	ac	1.93	ra	0.52	ac	0.58	ac
	Compo p	1.99	ns	1.26	ns	1.57	ns	0.79	ns	1.02	ns	0.60	ac	1.18	ra	0.77	ac	0.59	ac

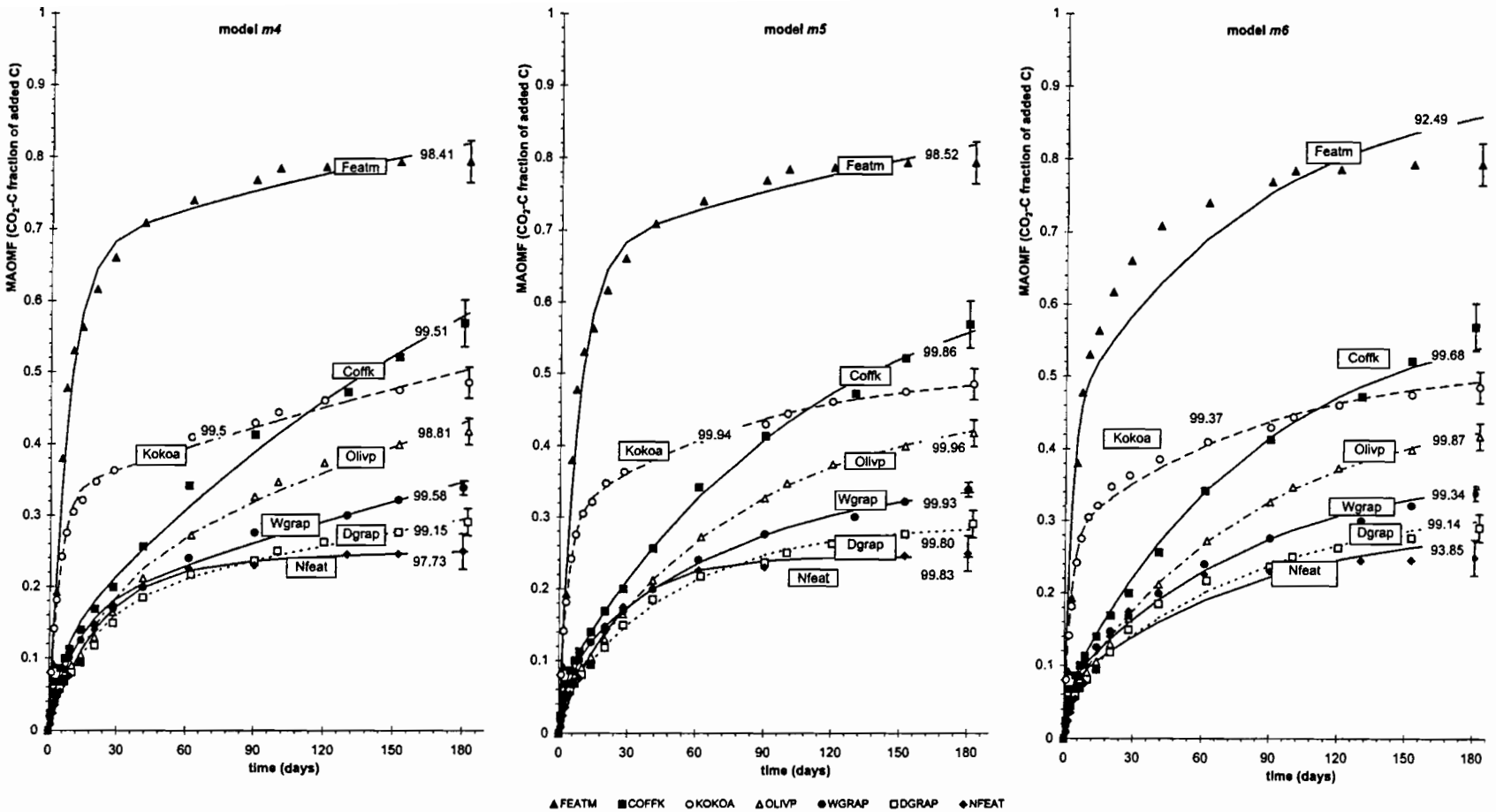

Fig. 1. Mineralized added organic matter fraction (MAOMF) of cocoa (Kokoa), dry and wet grap pellicle cake (Dgrap, Wgrap), olive pulp (Olivp), coffee cake (Coffk), native fine feather (Nfeat), feather meal (Featm). Symbols represent experimental data ($n = 3$), and plain or dashed lines represent the predictions according to models $m4$, $m5$ and $m6$ (r^2 values from Table 4 are reported on each curve). Vertical bars represent the maximum confidence intervals at 95% for cumulated values of C mineralization.

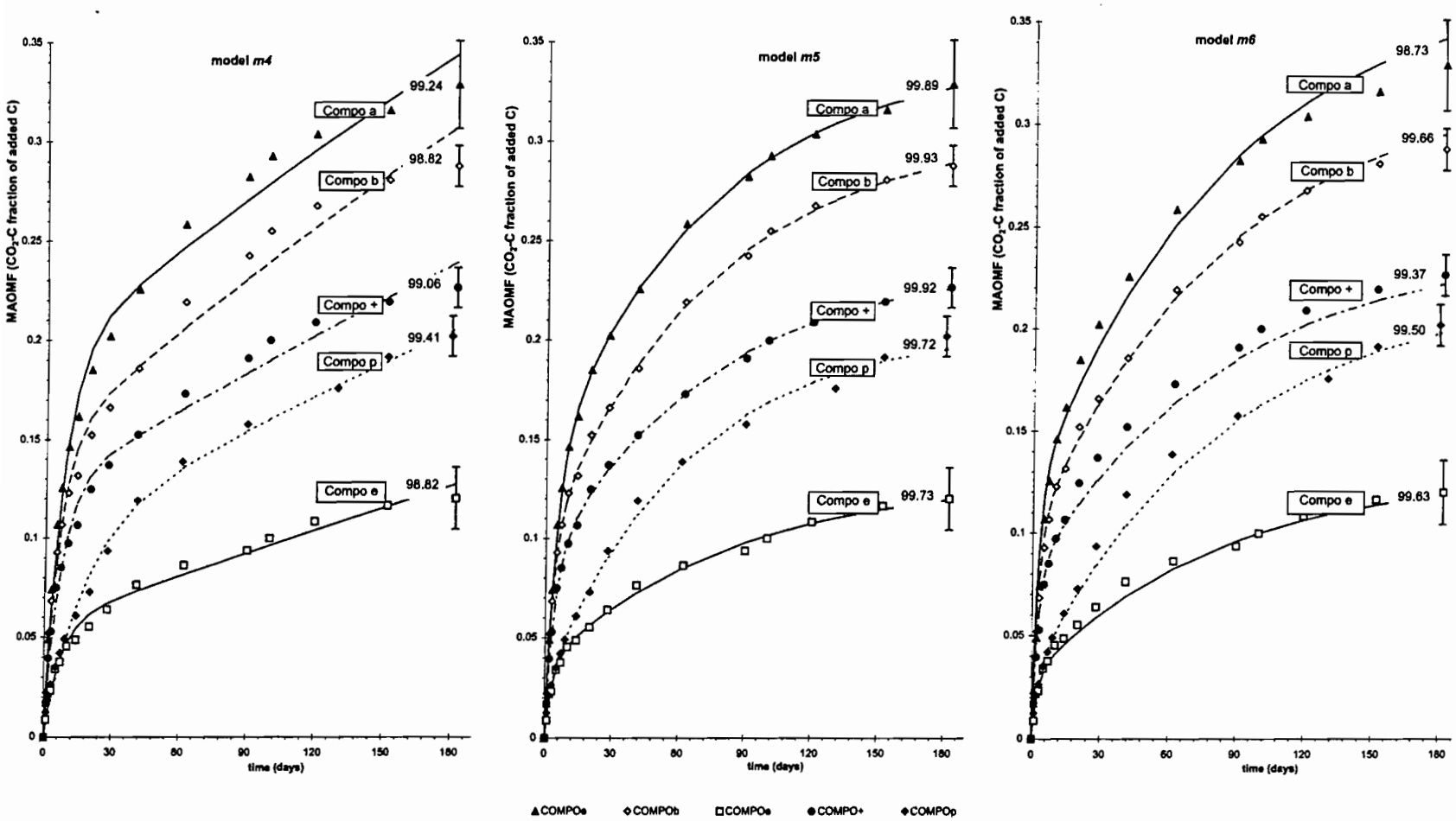

Fig. 2. Mineralized added organic matter fraction (MAOMF) of composts (Compo a, b, e, + and Compo p). Symbols represent experimental data ($n = 3$), and plain or dashed lines represent the predictions according to models *m*4, *m*5 and *m*6 (r^2 values from Table 4 are reported on each curve). Vertical bars represent the maximum confidence intervals at 95% for cumulated values of C mineralization.

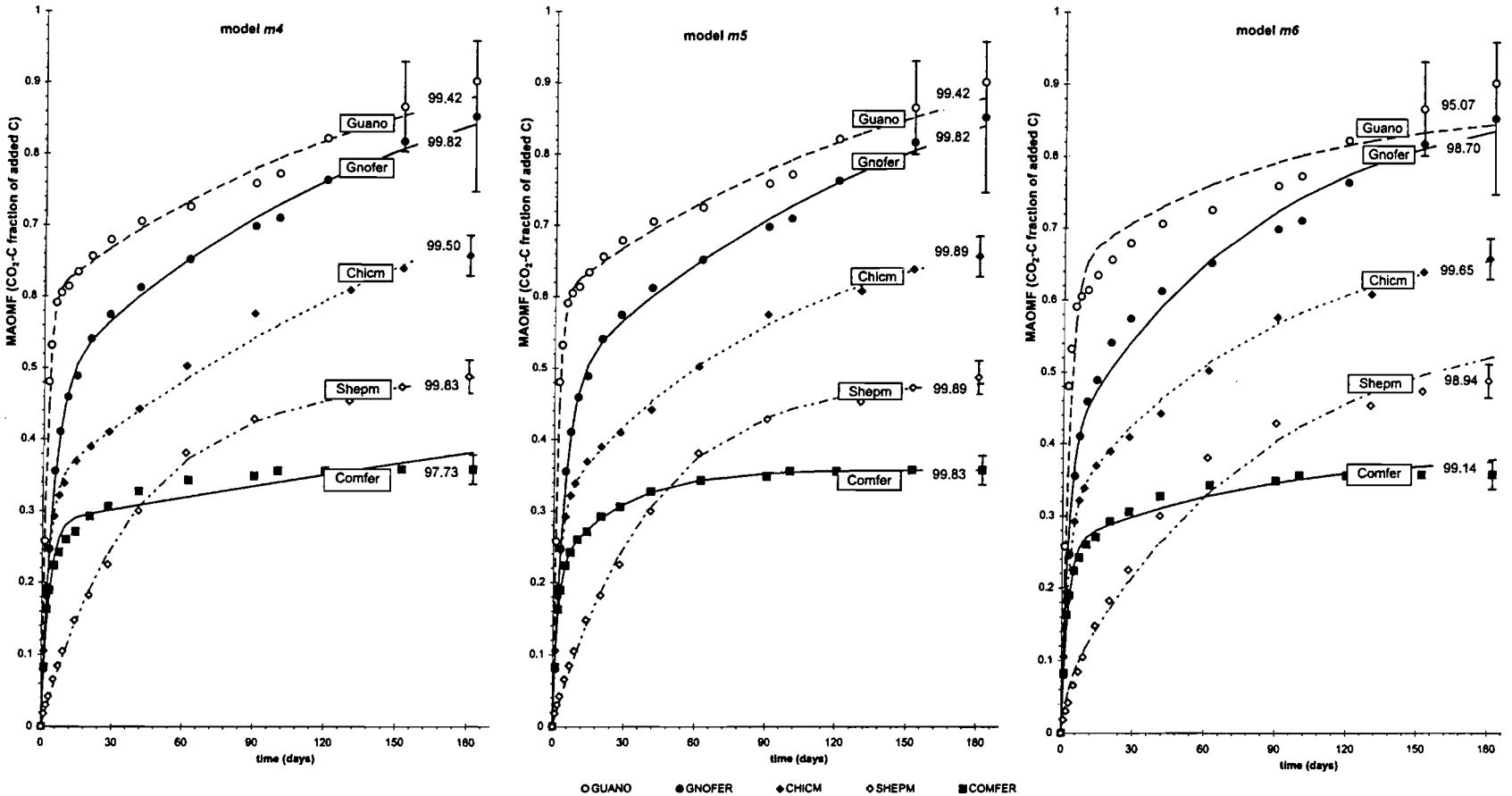

Fig. 3. Mineralized added organic matter fraction (MAOMF) of chicken manure (Chicm), guano (Guano), guano-based fertilized (Gnofer), compost-based fertilizer (Comfer), sheep manure (Shepm). Symbols represent experimental data ($n = 3$), and plain or dashed lines represent the predictions according to models $m4$, $m5$ and $m6$ (r^2 values from Table 4 are reported on each curve). Vertical bars represent the maximum confidence intervals at 95% for cumulated values of C mineralization.

Table 4
Values of the estimated parameters: P_L (no dimension), k_{mL}, k_{mR} (d^{-1}) in model *m*4, P'_L, P_S (no dimension), $k'm_L$, $k'm_R$ (d^{-1}) in models *m*5 and *m*6. In model *m*4, P_R is calculated by difference 1-P_L. In models *m*5 and *m*6, P_R is calculated by difference 1-P'_L-P_S. * = Two exponential models (*m*1 or *m*4) gave low k_{mR} values with associated confidence interval including zero value, low k_{mL} values close to k_{mR} values of most products; consequently they could be considered as particular cases of models *m*5 with labile L compartment = 0; * * = Particular cases of model *m*5 where $P_H = 0$, could be fitted with one exponential term and a constant term with two parameters k_{mL} and P_S (with $P_L = 1\text{-}P_S$); * * * = Particular cases of models *m*5 where $P_S = 0$, then fittings are those of model *m*4

AOM origin	AOM	Model *m*4 (or *m*1)					Model *m*5					Model *m*6		
		P_L	k_{mL}	k_{mR}	r^2 (%)		P'_L	k'_{mL}	k'_{mR}	P_S	r^2 (%)	P'_L	P_S	r^2 (%)
Plant	Coffk	0.114	0.164	0.0041	99.51		0.065	0.449	0.0093	0.330	99.86	0.046	0.425	99.380
	Wgrap	0.165	0.082	0.0014	99.58		0.089	0.172	0.0126	0.638	99.93	0.065	0.641	99.580
	Dgrap	0.177	0.053	0.0008	99.15		0.036	0.632	0.0199	0.711	99.80	0.053	0.686	99.470
	Olivp	0.197	0.044	0.0019	98.81		0.041	0.904	0.0127	0.538	99.96	0.041	0.556	99.780
	Kokoa	0.333	0.245	0.0016	99.56		0.298	0.293	0.0124	0.495	99.94	0.273	0.495	99.470
Manure	Shepm	0.428	0.028	0.0006	99.83	*	0		0.024	0.515	99.80	0.054	0.449	98.940
	Chicm	0.338	0.375	0.0041	99.50		0.307	0.445	0.0107	0.281	99.89	0.303	0.326	99.650
Animal	Nfeat	0.231	0.045	0.0001	99.66	*	0		0.042	0.756	99.62	0.064	0.709	94.870
	Featm	0.668	0.136	0.0033	98.41	* *	0.668	0.136	–	0.33	98.41	0.439	0.112	93.000
	Guano	0.599	0.668	0.0066	99.42	* * *	0.599	0.668	0.0066	0	99.42	0.635	0.146	95.070
Fertilizer	Gnofer	0.479	0.227	0.0065	99.82	* * *	0.479	0.227	0.0065	0	99.82	0.386	0.136	98.700
	Comfer	0.285	0.334	0.0008	97.73		0.217	0.533	0.0362	0.642	99.83	0.259	0.620	99.140
Compost	Compo a	0.191	0.130	0.0012	99.24		0.137	0.207	0.0138	0.656	99.89	0.112	0.648	99.020
	Compo b	0.148	0.161	0.0011	98.82		0.102	0.291	0.0134	0.693	99.93	0.093	0.693	99.790
	Compo e	0.057	0.139	0.0004	98.82		0.037	0.293	0.0116	0.869	99.73	0.032	0.874	99.650
	Compo +	0.125	0.144	0.0008	99.06		0.087	0.251	0.0135	0.761	99.92	0.076	0.759	99.560
	Compo p	0.102	0.058	0.0007	99.41		0.026	0.400	0.0158	0.794	99.72	0.029	0.786	99.67

between 98 and 99% for four series and between 97 and 98% for two series.

Model *m*8 gave also good predictions; differences between model *m*8 and models *m*1, *m*3 or *m*4 (Table 3) were not significant at 5% level (*F* values, Eq. 6). Nevertheless, in all cases (except the curve for Guano) the trends were the same: *F* values (Eq. 6, Table 3) greater than 1 indicated that models *m*1, *m*3 and *m*4 gave a better prediction than model *m*8. These model behaviors can be easily explained since 1st order kinetic constants for the 2nd exponential in models *m*1, *m*3 and *m*4 were found to be relatively small (Table 4). So resistant organic material (R in Table 2) mineralization curves were flattened for small incubation times, like the straight line of the zero order kinetics in model *m*8. Blet-Charaudeau et al. (1990) indicated that 'the use of the double exponential model is superfluous unless the duration of incubation experiments exceeds 100 days'; Bernal et al. (1998) found 1st-order plus 0-order kinetics from 70 days incubation experiments. Our 180 day experiments began to show a better prediction by the double exponential model but with no significant differences. The differences would become more significant for greater incubation times. Our experimental data confirmed the superiority of double exponential model compared to 1st-order plus 0-order model. This is satisfactory in mechanistic terms, since a constant R mineralization rate even when R = 0 is not realistic.

The comparison between models *m*1, *m*2, *m*3, *m*4, *m*7 and *m*8 (Table 2) indicated that the 1st order two-compartment models *m*1, *m*3 and *m*4 should be retained. Unfortunately, most of the correlation coefficients between the parameters found with models *m*1, *m*3 and *m*4 from these 17 data series were significant. But graphical representation (Fig. 4) showed that there was no evident relationship between the different parameters. Nevertheless, actual data could not allow a real choice between the three models. The model *m*4 can be selected for the relative simplicity of its formula (Table 2). The model *m*3 k_D or model *m*4 k_{mR} fitted values were found small in comparison to k_m or k_{mL} fitted values (Table 4). Model *m*3 P_L were found close to model *m*4 P_L and the two models were almost identical: the parallel 1st order two-compartment model (*m*4 in Table 2) can be seen as a *m*3 decomposition model.

3.3. Comparative m4 and m5 model predictions

Despite good predictions given by models *m*1, *m*3 or *m*4 with determination coefficients higher than 97% (Figs. 1–3), the residues (predicted minus measured values) were not randomly distributed. The DW tests (Table 3) showed significant autocorrelation in residues from all data series except for the animal products Guano, Gnofer and Nfeat: two

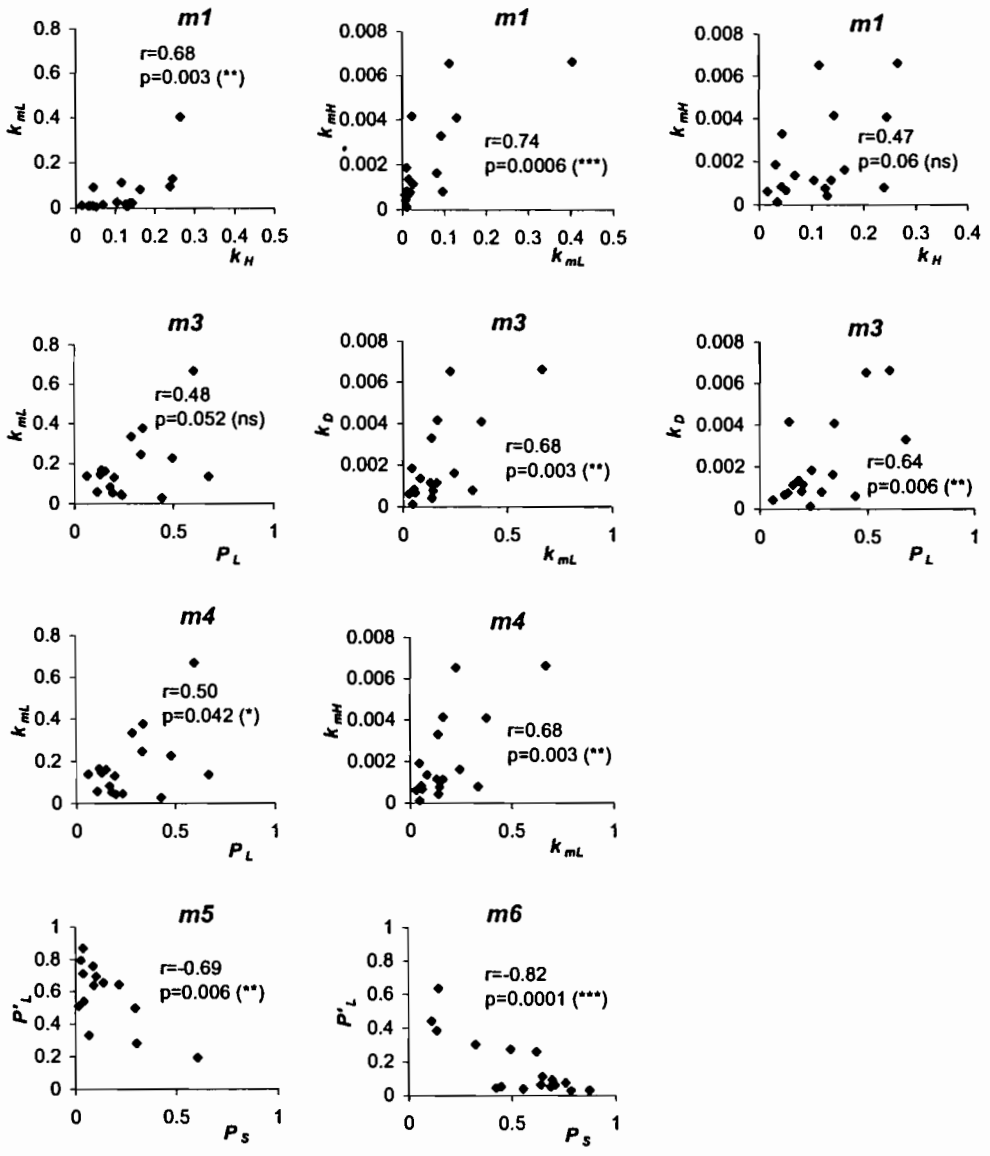

Fig. 4. Correlation between estimated parameters for models $m1$, $m3$, $m4$, $m5$ and $m6$. Only significant correlations are shown, other values (model $m5$) are $r_{kmL/PS} = -0.01$ ($p = 0.96$), $r_{kmH/PL} = 0.24$ ($p = 0.41$), $r_{kmH/PS} = 0.18$ ($p = 0.54$), $r_{kmL/kmH} = 0.11$ ($p = 0.71$), $r_{kmL/PL} = -0.40$ ($p = 0.17$).

exponential models cannot describe the whole information in most of the data.

The use of model $m5$ improved all predictions with r^2 values higher than 99.7% for 14 data series and higher than 98.4 for the three other data series (animal products with strong mineralization rates: Guano, Gnofer and Featm). Tests F (Eq. 6, Table 3) showed a significant improvement at 5% level for ten data series, at 1% level for seven data series included in the former ten series. The improvements are shown in Figs. 1–3, especially with a better fitting of the intermediate points (between 30 and 120 days) for nine curves (Kokoa, Coffk, Olivp, Wgrap, Compo a, Compo b, Compo + , Chicm, Comfer). At the end of the 6-month incubation, the slopes of model $m5$ curves were smaller than model $m4$ curve slopes, tending to the asymptotic lines given by the P_S ($m5$ in Table 2) values (Table 4).

The correlation between the four parameter values of model $m5$ predictions for the 17 data series were not significant except the correlation between P'_L and P_S values; but this correlation did not appear as an evident relation (Fig. 4). The model $m5$ explained the whole information in 11 data series as shown by DW autocorrelation test in residual values (Table 3); in three other cases residual autocorrelation in model $m5$ were smaller than in model $m4$; model $m5$ did not match for the three

other cases concerning animal products Guano, Gnofer and Nfeat. In products with high mineralization rates, Guano and Gnofer, the stable S compartment was not found. In the 3rd high mineralization animal product, Featm, models *m*4 and *m*5 gave the same predictions. In Nfeat the intermediary compartment H was not found. This may be related to the particular biochemical structure of this product.

3.4. Comparative m4, m5 and m6 model predictions

The three-compartment model *m*5 (in Table 2) gave the best predictions. But this model need four parameters against three for the two-compartment models *m*4. An examination of k'_{mL} and k'_{mR} fittings showed less variable values in model *m*5 than k_{mL} and k_{mR} values in models *m*4 (Table 4). For 14 data series (except the animal products Guano, Gnofer and Featm) the mean k'_{mL} value was 0.40 (±0.21 sd) d^{-1}, the mean k'_{mR} value was 0.014 (±0.007) d^{-1}. There was one extraneous value in k'_{mL} distribution for Olivp ($k'_{mL} = 0.90$). The elimination of Olivp gave normal distribution (kurtosis and skewness tests, normal probability plot) for k'_{mL} with a mean value = 0.36 (±0.15). There were two extraneous values in k'_{mR} distribution for Comfer ($k'_{mR} = 0.036$) and Shepm ($k'_{mR} = 0.002$). Their elimination gave k'_{mR} normal distribution with mean k'_{mR} value = 0.014 (±0.003). The corresponding half lives of the two parallel 1st order compartment models were 1.8 days for labile compounds L and 49 days for resistant compounds R.

Gilmour et al. (1998) reported for different crop residues incubated at 25°C, the first order rate constants for labile compartment in the range 0.09–0.43 d^{-1} with a mean value of 0.21 (±0.02) and for stable compartment in the range 0.0026–0.016 d^{-1} with a mean value of 0.008 (±0.0052). Vanlauwe et al. (1994) found 0.4 and 0.012 d^{-1} for labile and stable kinetic constants respectively, of maize residue incubated at 25°C.

Model *m*6 predictions with mean mineralization rate values (Table 2) $l = -0.4\ d^{-1}$ and $r = -0.014\ d^{-1}$ and the P'_L and P_S fittings are shown in Figs. 1–3. The accord with data series remained valuable with $r^2 > 99.5\%$ for seven series, $99 < r^2 < 99.5$ for five series, $98 < r^2 < 99$ for two series and $93 < r^2 < 98$ for the three animal products Guano, Featm and Nfeat. Tests *F* (Eq. 6, Table 3) showed no significant difference between model *m*5 and model *m*6 predictions for five data series. However, significantly better predictions were found for model *m*5 compared to model *m*6 at 5% risk for one data series and at 1% risk for eight other data series. As mentioned above, the three-compartment models were less appropriate than two-compartment models for the animal products Guano, Gnofer and Nfeat.

Despite satisfactory data fittings, residual checks (Table 3) showed that model *m*6 did not explain the whole information in data series, contrarily to model *m*5. Durbin Watson tests gave significant autocorrelation except for one composted matter (Compo e).

Precision of model *m*6 predictions was found close to the precision of model *m*4 (or *m*1 or *m*3) ones. Tests *F* (Eq. 6, Table 3) showed that predictions with model *m*6 were better than model *m*4 ones for nine data series, with significant difference for three data series only (two at 5% risk and one at 1% risk.). Model *m*4 predictions were better than model *m*6 ones for eight data series but differences were significant only for five data series (at 1% risk). For nine data series, the model *m*6 and *m*4 precisions were equivalent.

3.5. Conclusion

This work dealt with the mineralization kinetics of various AOM and not of soil organic matter (SOM). The higher proportion of mineralized AOM-C (~65–90% added C) was found in the animal-originated AOM rich in N. That from composts was of a lesser importance (~12–33% added C), and depended on their composting time. The majority of the plant-originated AOM had an intermediary C mineralization behavior, with a great discrepancy between that of animal-originated AOM and composts. The values of the very labile fractions P'_L, stable fractions P_S (Table 4) and resistant fractions ($1-P'_L-P_S$) illustrated these mineralization behaviors.

For the wide variety of AOM tested in this experiment, the CO_2-C mineralization were not predicted very well by the single compartment models. Additionally, this data did not justify the choice for the consecutive models for their more complex formulation than parallel ones.

In general, a better simulation was provided by the three-compartment model *m*5 as compared to model *m*4 (two compartments); furthermore, the correlations between the *m*5 parameters were less significant than between the *m*4 ones. Model *m*6 was adapted by simplification of model *m*5. Under controlled conditions, the mineralization rate of the very labile compounds was found approximately constant (half life 1.8 days), as was the mineralization rate of the resistant ones (half life 49 days). The simplified model *m*6 gave satisfactory predictions with only two parameters: the very labile AOM fraction and the very stable one. This did not affect negatively the quality of the predictions since the predictions of *m*6 were not very different than those of model *m*5, and sometimes better than those of *m*4. From the eight models tested, *m*4, *m*5 and *m*6 could be recommended at this time-scale. The *m*5 model with four parameters must be useful in fluctuating conditions, over longer time-scale. The *m*6 model was powerful and simple enough to be chosen but the *m*4 one could not be completely rejected. This work shows that it is possible to find accurate and simple parameters to describe the C mineralization kinetics of AOM with very different C mineralization behavior.

Acknowledgements

This work was partly granted by a CIFRE convention. The authors thank the CivamBio (organic farming French national association) and Dr M. Viel (R&D Department, Phalippou-Frayssinet© S.A., France) for the AOM choice and helpful discussions, Dr P. Bottner (Cefe-Cnrs, Montpellier, France) for the experimental advice, Dr C.M. Arshad, (Agriculture and Agri-Food Canada, Edmonton, Canada) and Dr M.C. Larré-Larrouy (IRD, Montpellier, France) for comments on an early version of the manuscript.

References

Andrén, O., Kätterer, T., 1997. ICBM: The introductory carbon balance model for exploration of soil carbon balances. Ecological Applications 7, 1226–1236.

Andrén, O., Paustian, K., 1987. Barley straw decomposition in the field: a comparison of models. Ecology 68, 1190–1200.

Bernal, M.P., Sanchez-Monedero, M.A., Paredes, C., Roig, A., 1998. Carbon mineralization from organic wastes at different composting stages during their incubation with soil. Agriculture Ecosystems and Environment 69, 175–189.

Blet-Charaudeau, C., Muller, J., Laudelout, H., 1990. Kinetics of carbon dioxide evolution in relation to microbial biomass and temperature. Soil Science Society of America Journal 54, 1324–1328.

Bradbury, N.J., Whitmore, A.P., Hart, P.B.S., Jenkinson, D.S., 1993. Modelling the fate of nitrogen in crop and soil in the years following application of ^{15}N labelled fertilizer to winter wheat. Journal of Agricultural Science 121, 363–379.

FAO-UNESCO-ISRIC, 1988. FAO-UNESCO soil map of the world: revised legend. World soil resources report. Rome, Italy, 119 pp.

Gilmour, J.T., Mauromoustakos, A., Gale, P.M., Norman, R.J., 1998. Kinetics of crop residue decomposition: variability among crops and years. Soil Science Society of America Journal 62, 750–755.

Hadas, A., Portnoy, R., 1994. Nitrogen and carbon mineralization rates of composted manures incubated in soil. Journal of Environmental Quality 23, 1184–1189.

Hadas, A., Portnoy, R., 1997. Rates of decomposition in soil and release of available nitrogen from cattle manure and municipal waste composts. Compost Science and Utilization 5, 48–54.

Hansen, S., Jensen, H.E., Nielsen, N.E., Svendsen, H., 1991. Simulation of nitrogen dynamics and biomass production in winter wheat using the Danish simulation model Daisy. Fertilizer Research 27, 245–259.

Hartz, T.K., Mitchell, J.P., Giannini, C., 2000. Nitrogen and carbon mineralization dynamics of manures and composts. Hort Science 35, 209–212.

Hébert, M., Karam, A., Parent, L.E., 1991. Mineralization of nitrogen and carbon in soils amended with composted manure. Biological Agriculture and Horticulture 7, 349–361.

Hénin, S., Monnier, G., Turc, L., 1959. Un aspect de la dynamique des matières organiques du sol. Comptes Rendus de l'Académie d'Agriculture Française 248, 138–141.

Henriksen, T.M., Breland, T.A., 1999. Nitrogen availability effects on carbon mineralization, fungal and bacterial growth, and enzyme activities during decomposition of wheat straw in soil. Soil Biology & Biochemistry 31, 1121–1134.

Hess, T.F., Schmidt, S.K., 1995. Improved procedure for obtaining statistically valid parameter estimates from soil respiration data. Soil Biology & Biochemistry 27, 1–7.

Janzen, H.H., Kucey, R.M.N., 1988. C, N and S mineralization of crop residue as influenced by crop species and nutrient regime. Plant and Soil 100, 35–41.

Kaboneka, S., Sabbe, W.E., Mauromoustakos, A., 1997. Carbon decomposition kinetics and nitrogen mineralization from corn, soybean, and wheat residues. Communications in Soil Science and Plant Analysis 28, 1359–1373.

Kirchmann, H., Bernal, M.P., 1997. Organic waste treatment and C stabilization efficiency. Soil Biology & Biochemistry 29, 1747–1753.

Levi-Minzi, R., Riffaldi, R., Saviozzi, A., 1990. Carbon mineralization in soil amended with different organic material. Agriculture, Ecosystems and Environment 31, 325–335.

Lomander, A., Kätterer, T., Andrén, O., 1998. Modelling the effects of temperature and moisture on CO_2 evolution from top- and sub-soil using a multi-compartment approach. Soil Biology & Biochemistry 30, 2023–2030.

Mary, B., Fresneau, C., Morel, J.L., Mariotti, A., 1993. C and N cycling during decomposition of root mucilage, roots and glucose in soil. Soil Biology & Biochemistry 25, 1005–1014.

McGill, W.B., Hunt, H.W., Woodmansee, R.G., Reuss, J.O., Paustian, K.H., 1981. Formulation, process controls, parameters and performance of PHOENIX: a model of carbon and nitrogen dynamics in grassland soils. In: Frissel, M.J., van Veen, J.A. (Eds.). Simulation of Nitrogen Behaviour of Soil Plant Systems. Wageningen, The Netherlands, pp. 171–191.

Mòlina, J.A.E., Clapp, C.E., Shaffer, M.J., Chichester, F.W., Larson, W.E., 1983. NCSOIL, a model of nitrogen and carbon transformations in soils: description, calibration, and behavior. Soil Science Society of America Journal 47, 85–91.

Mueller, T., Jensen, L.S., Nielsen, N.E., Magid, J., 1998. Turnover of carbon and nitrogen in a sandy loam soil following incorporation of chopped maize plants, barley straw and blue grass in the field. Soil Biology & Biochemistry 30, 561–571.

N'Dayegamiye, A., Royer, R., Audesse, P., 1997. Nitrogen mineralization and availability in manure composts from Quebec biological farms. Canadian Journal of Soil Science 77, 345–350.

NFU 44160, 1985. Détermination de la matière organique totale, méthode par calcination. In: AFNOR (Ed.), Normes et Réglementation: Matières Fertilisantes et Supports de Culture, Tome 1, Normalisation. AFNOR, Paris, France, p. 648.

Pansu, M., Gautheyrou, J., Loyer, J.Y., 1998a. L'analyse du Sol: échantillonnage, Instrumentation et Contrôle. Masson, Paris, France, p. 512.

Pansu, M., Sallih, Z., Bottner, P., 1998b. Modelling of soil nitrogen forms after organic amendments under controlled conditions. Soil Biology & Biochemistry 30, 19–29.

Pansu, M., Sidi, H., 1987. Cinétique d'humification et de minéralisation de mélanges sols-résidus végétaux. Science du sol 25, 247–265.

Paré, T., Dinel, H., Schnitzer, M., Dumontet, S., 1998. Transformations of carbon and nitrogen during composting of animal manure and shredded paper. Biology and Fertility of Soils 26, 173–178.

Parton, W.J., Schimel, D.S., Cole, C.V., Ojima, D.S., 1987. Analysis of factors controlling soil organic matter levels in Great Plains grasslands. Soil Science Society of America Journal 51, 1173–1179.

Paul, J.W., Beauchamp, E.G., 1994. Short-term nitrogen dynamics in soil amended with fresh and composted cattle manures. Canadian Journal of Soil Science 74, 147–155.

Quemada, M., Cabrera, M.L., 1995. Carbon and nitrogen mineralized from leaves and stems of four cover crops. Soil Science Society of America Journal 59, 471–477.

Recous, S., Robin, D., Darwis, D., Mary, B., 1995. Soil inorganic N availability: effect on maize residue decomposition. Soil Biology & Biochemistry 27, 1529–1538.

Saggar, S., Parshotam, A., Sparling, G.P., Feltham, C.W., Hart, P.B.S., 1996. ^{14}C-labelled ryegrass turnover and residence times in soils varying in clay content and mineralogy. Soil Biology & Biochemistry 28, 1677–1686.

Sallih, Z., Pansu, M., 1993. Modelling of soil carbon forms after organic amendment under controlled conditions. Soil Biology & Biochemistry 25, 1755–1762.

Saviozzi, A., Levi-Minzi, R., Riffaldi, R., 1993. Mineralization parameters

from organic materials added to soil as a function of their chemical composition. Bioresource Technology 45, 131–135.

Servat, E., Callot, G., 1966. Notice Explicative de la Carte des sols du Roussillon. ENSA-Montpellier, Montpellier, France, p. 68.

Sørensen, P., Jensen, E.S., 1995. Mineralization of carbon and nitrogen from fresh and anaerobically stored sheep manure in soils of different texture. Biology and Fertility of Soils 19, 29–35.

Thuriès, L., Arrufat, A., Dubois, M., Feller, C., Herrmann, P., Larré-Larrouy, M.-C., Pansu, M., Rémy, J.-C., Viel, M., 2000a. Influence d'une fertilisation organique et de la solarisation sur la productivité maraîchère et les propriétés d'un sol sableux sous abri. Etude et Gestion des Sols 7, 215–229.

Thuriès, L., Larré-Larrouy, M.-C., Pansu, M., 2000b. Evaluation of three incubation designs for mineralization kinetics of organic materials in soil. Communications in Soil Science and Plant Analysis 31, 289–304.

USDA, 1975. Soil taxonomy. A basic system of soil classification for making and interpreting soil surveys. Agric. Handbook no. 436, USDA, 754 pp.

Vanlauwe, B., Dendooven, L., Merckx, R., 1994. Residue fractionation and decomposition—The significance of the active fraction. Plant and Soil 158, 263–274.

Verberne, E.L.J., Hassink, J., de Willingen, P., Groot, J.J.R., van Veen, J.A., 1990. Modelling organic matter dynamics in different soils. Netherlands Journal of Agricultural Science 328, 221–238.

Whitmore, A.P., 1996. Describing the mineralization of carbon added to soil in crop residues using second-order kinetics. Soil Biology & Biochemistry 28, 1435–1442.

La Transformation du carbone des Apports Organiques (modèle TAO-C)

Composition biochimique de l'apport et transformation du carbone

PERGAMON

Soil Biology & Biochemistry 34 (2002) 239–250

Soil Biology & Biochemistry

www.elsevier.com/locate/soilbio

Biochemical composition and mineralization kinetics of organic inputs in a sandy soil

L. Thuriès[a], M. Pansu[b,*], M-C. Larré-Larrouy[b], C. Feller[b]

[a]*Phalippou-Frayssinet S.A., Organic fertilizers, 81240 Rouairoux, France*
[b]*IRD (formerly ORSTOM), BP 5045, 34032 Montpellier Cedex 1, France*

Received 17 October 2000; received in revised form 25 July 2001; accepted 27 August 2001

Abstract

The carbon mineralization of added organic materials (AOM) in soil was assessed by combining laboratory and modeling approaches. The AOM used in the organic fertilizer industry included: plant residues from agri-food origin, animal wastes, manures, composts, and organic fertilizers. They were fractionated by sequential analyses of fibers and analyzed for C, N and ash contents. A previous kinetic study permitted to select two predictive models for AOM C mineralization in a sandy soil. These models, *m*4 and *m*6, were respectively defined by (i) two compartments (labile L and very resistant R) with three parameters: P_L (proportion of L), and k_{mL}, k_{mR} (kinetic constants of L and R); (ii) three compartments (very labile L′, resistant R′ and stable S), with two parameters: P'_L and P_S (proportions of L′ and S) with fixed kinetic constants at 28 °C, 75% WHC. We tested for the best prediction of the above parameters with the analytical data. These predictions were significant for the whole AOM set, but to a lesser degree for the C mineralization of AOM with contrasted characteristics. A Principal Component Analysis (PCA) was used to classify the AOM according to their biochemical contents into two groups: (+) ligneous ones with relatively high C and low N contents (mostly plant-originated AOM), and (−) more nitrogenous ones, poorer in organic C and ligno–cellulosic fibers (mostly animal-originated or partially composted AOM). The classification improved the predictive equations, which use one to three biochemical variables in agreement with the conceptual definition of the parameters. P'_L, P_L and P_S were more accurately estimated than k_{mL} and k_{mR}. For most of the AOM, *m*6 gave better simulations than *m*4. From *m*6 equations, the conceptual compartments L′, R′ (with $P'_R = 1 - P'_L - P_S$) and S appeared to correspond to (i) parts of soluble, nitrogenous and hemicellulosic compounds, (ii) cellulose and the remaining fraction of hemicelluloses, (iii) the ligneous fraction, respectively. © 2002 Published by Elsevier Science Ltd.

Keywords: Modeling; Organic fertilizers; Composts; Biochemical analysis; Added organic material; Organic carbon; Mineralization kinetics; Sandy soil

1. Introduction

For several decades, there has been a great interest in decomposition studies of soil organic inputs in relation with their biochemical characteristics. Indeed, since the early works of Wollny (1902), Waksman and Tenney (1927) and Tenney and Waksman (1929), the organic matter (OM) decomposition rate was believed to be influenced by the OM quality, as defined by the chemical composition and relative proportions of its constitutive organic compounds. Rubins and Bear (1942) referred to the decomposition of organic fertilizers in soil as a function of their quality, firstly their C-to-N ratio. Other scientists reported similar work on forest litters (Melillo et al., 1982; Ågren and Bosatta, 1996; Heal et al., 1997; Coûteaux et al., 1998; Sanger et al., 1998), and crop residue decomposition (Amato et al., 1984; Angers and Recous, 1997; Mary et al., 1996; Quemada and Cabrera, 1995).

With the revival of organic farming, a large range of organic fertilizers led some researchers to pay more attention to these products. The major aim of their work was to define quality criteria for organic fertilizers in relation to their potential C and/or N mineralization in soil (Cheneby et al., 1992; Linères and Djakovitch, 1993; Robin, 1997). The determination of quality criteria is of theoretical interest for combining measurable pools of added organic materials (AOM, Mueller et al., 1998) with conceptual pools of decomposition models. Quality has been the object of a theory applied to AOM constituents as a continuum (Bosatta and Ågren, 1985). More commonly, the decomposition of discrete classes of organic compounds in AOM has been presented as a constitutive part of soil organic matter (SOM) decomposition models, the AOM being split in two (Molina et al., 1983; Van Veen et al., 1984; Parton et

* Corresponding author. Tel.: +33-4-67-41-62-28; fax: +33-4-67-41-62-94.
E-mail address: pansu@mpl.ird.fr (M. Pansu).

0038-0717/02/$ - see front matter © 2002 Published by Elsevier Science Ltd.
PII: S0038-0717(01)00178-X

al., 1987; Sallih and Pansu, 1993; Bradbury et al., 1993) or three (Hansen et al., 1991; Verberne et al., 1990) compartments with a specific decay rate.

One of the most considered quality criteria was the C-to-N ratio of the AOM (Rubins and Bear, 1942; McGill et al., 1981), but this simple criterion appeared sometimes inadequate for predicting the decomposition kinetics (Recous et al., 1995; Paré et al., 1998). Thus, other quality criteria seemed necessary; such criteria can be provided by the sequential analysis of Van Soest (1963) and Van Soest et al. (1991), which attempts to divide AOM into soluble-, hemicellulose-, cellulose- and lignin-like substances. Nowadays some modelers utilize these fractions (Linères and Djakovitch, 1993; Robin, 1997; Henriksen and Breland, 1999a,b,c; Trinsoutrot et al., 2000) or their combinations as the lignin-to-N ratio (Melillo et al., 1982; Parton et al., 1987).

This study was conducted in conjunction with a manufacturer of organic fertilizers and a French national association for organic farming. The aim was to relate the mineralization kinetics of different AOM to their chemical (C, N) and biochemical (soluble, hemicelluloses, cellulose, lignin) characteristics. We thus studied, under laboratory conditions, the mineralization of raw AOM or their combinations into complex admixtures (composts), and modeled their kinetics (Thuriès et al., 2001). In the present study, we then attempted to define the model parameters as a function of the AOM composition.

When matching measurable OM fractions with conceptual pools in models of C turnover, Christensen (1996) concluded that the challenge of modelers is to "keep the balance between structural simplicity, explanatory capability and predictive power". Our objective was to combine laboratory and discrete modeling approaches in order to find a simple and accurate way of predicting AOM-C mineralization.

2. Materials and methods

2.1. Added organic materials

Different kinds of AOM from agri-food industry wastes and industrial-processed fertilizers (organic amendments and fertilizers) were tested (Table 1). The raw materials were from (i) plant origin: wet and dry grape berry pellicle cakes (Wgrap, Dgrap), coffeecake (Coffk), cocoacake (Kokoa), olivecake (Olivp) (ii) animal origin: hydrolyzed feather meal (Featm), native fine feather (Nfeat), guano (Guano) (iii) plant and animal origin: sheep manure (Shepm), chicken manure (Chicm), and (iv) fertilizers: composted organic amendments (Compo series), and organic fertilizers (Gnofer, Comfer). The composted organic amendments (Compo) were made from Shepm and Coffk, periodically turned and aerated during a 10-month composting period. Samples were taken before the composting process (Compo a), and at 40 (Compo b), 120 (Compo p), and 305 (Compo e) days. Compo + was a mixture of 75% Compo e and 25% Dgrap (used for lowering moisture). Gnofer was a guano-based organic fertilizer, whereas Comfer was a Compo-based fertilizer supplemented with Chicm.

The AOM were air-dried, then ground to pass a 1-mm sieve for a sequential analysis of fibers, or finely ground (<200 μm, in order to reduce the AOM sampling heterogeneity) for the incubation tests and total C and N analyses. Angers and Recous (1997) found an increase then a slight decrease of C mineralization when the particle size decreases, in the early and latter incubation stages, respectively.

2.2. Biochemical characterization of AOM

Each AOM sample (six replicates) was successively extracted for NDF (neutral detergent fiber), ADF (acid detergent fiber) and ADL (acid detergent lignin) by sequential analysis of fibers (Table 2), after Van Soest et al. (1991). At each extraction step, the products obtained were filtered, dried at 40 °C, weighed, and either (i) analyzed for C and N by dry combustion (Fisons NA2000), or (ii) dried at 105 °C for determining residual moisture, then ignited gradually at 525 °C for ash content. The data used in this paper (Table 1) were calculated according to Table 2:

Sol (neutral detergent soluble), Hem (hemicelluloses-like), Cel (cellulose-like), and Lig (lignin-like) represented the different organic fractions (ash free) as defined by Van Soest (1967),

C_{Sol}, N_{Sol}, C_{Hem}, N_{Hem}, C_{Cel}, N_{Cel}, C_{Lig}, and N_{Lig} were the respective carbon and nitrogen contents of fractions Sol, Hem, Cel and Lig,

Ash_{AOM} represented the inorganic part of AOM.

2.3. Mineralization kinetics

The experiment was described in detail in Thuriès et al. (2000). Briefly, 125–500 mg AOM were incorporated homogeneously in 50 g air-dried soil (<2 mm) and incubated in the dark at 28 °C and 75% WHC. These experimental AOM amounts corresponded to realistic inputs under field conditions: 7 or 14 t ha^{-1} for animal materials or fertilizers, 28 t ha^{-1} for plant-originated materials, manures, and composts. Carbon mineralization was measured as respired CO_2–C in closed chambers on 17 sampling occasions across a six-month period. The sandy soil used (11.5% clay, 69.3% sand; 4.98 g C kg^{-1}) has been classified as fluvisol (FAO–UNESCO–ISRIC, 1988) or Udifluvent (USDA, 1975).

Two models for AOM-C mineralization have been selected after Thuriès et al. (2001): (*m*4), a parallel 1st order two-compartment model with labile (L) and very resistant (R) organic compounds, (*m*6), a simplified parallel

Table 1
Parameters estimated by Thuriès et al. (2001) for the predictive C-mineralization of AOM according to models *m*4 (P_L, k_{mL}, k_{mR}, Eq. (1)) and *m*6 (P'_L, P_S, Eq. (2)) related to measured chemical and biochemical characteristics in g g^{-1} d.w. (× 100; Sol + Hem + Cel + Lig + Ash_{AOM} = 1) of the AOM (see text for explanation of P_L, k_{mL}, k_{mR}, P'_L, P_S and Sol, Hem, Cel, Lig)

AOM		g g^{-1} d.w. (× 100)							C g g^{-1} d.w. (× 100)				N g g^{-1} d.w. (× 100)				Model *m*4			Model *m*6	
Origin	Name	Ash	C	N	Sol	Hem	Cel	Lig	Sol	Hem	Cel	Lig	Sol	Hem	Cel	Lig	P_L	k_{mL}	k_{mR}	P'_L	P_S
Plant	Coffk	3.1	53.7	2.0	24.0	9.7	38.0	25.2	16.8	7.4	18.4	11.1	0.29	0.49	0.09	1.10	0.114	0.164	0.0041	0.055	0.394
	Wgrap	8.9	52.9	2.7	11.3	4.7	17.6	57.5	7.0	2.5	11.2	29.9	0.39	0.66	0.06	1.62	0.165	0.082	0.0014	0.070	0.624
	Dgrap	7.1	49.4	2.2	29.2	10.5	23.0	30.2	16.3	3.6	13.0	16.4	0.70	0.48	0.19	0.88	0.177	0.053	0.0008	0.058	0.670
	Olivp	8.8	46.9	2.0	24.6	13.7	24.1	28.8	12.5	6.1	13.1	15.2	0.63	0.07	0.19	1.08	0.197	0.044	0.0019	0.048	0.531
	Kokoa	9.1	43.7	4.5	53.8	9.3	15.5	12.4	24.7	4.2	8.7	6.1	2.71	0.61	0.61	0.61	0.333	0.245	0.0016	0.278	0.482
Manure	Shepm	28.1	37.9	2.2	22.3	28.6	10.2	10.7	9.0	14.8	5.9	8.2	1.07	0.63	0.2	0.33	0.428	0.028	0.0006	0.064	0.422
	Chicm	32.3	37.6	6.1	33.5	15.8	10.8	7.5	16.9	11.8	5.5	3.4	5.24	0.12	0.48	0.22	0.338	0.375	0.0041	0.309	0.304
Animal	Nfeat	3.8	54.5	14.6	4.5	27.2	20.6	43.9	3.3	20.2	10.6	20.4	1.08	4.00	2.51	6.97	0.231	0.045	0.0001	0.068	0.697
	Featm	2.8	47.1	15.2	32.9	55.0	5.2	4.0	18.6	24.2	3.2	1.1	7.81	6.23	0.88	0.26	0.668	0.136	0.0033	0.450	0.089
	Guano	43.3	17.5	15.6	54.4	0.1	0.1	2.1	17.0	0.0	0.0	0.4	15.5	0.01	0.00	0.06	0.599	0.668	0.0066	0.637	0.130
Fertilizer	Gnofer	40.4	27.3	9.5	25.6	22.9	6.7	4.4	9.1	12.4	5.0	0.8	4.62	3.83	0.90	0.16	0.479	0.227	0.0065	0.394	0.108
	Comfer	25.5	36.9	3.7	32.4	4.3	20.4	17.5	14.3	2.1	10.8	9.7	2.62	0.11	0.39	0.62	0.285	0.334	0.0008	0.261	0.613
Compost	Compo a	32.2	36.2	2.9	20.2	7.3	23.0	16.8	11.2	4.7	11.9	9.7	1.52	0.20	0.53	0.62	0.191	0.13	0.0012	0.117	0.634
	Compo b	34.4	36.3	2.5	19.9	5.8	21.2	18.7	11.2	3.3	10.9	10.8	1.07	0.17	0.50	0.72	0.148	0.161	0.0011	0.097	0.680
	Compo e	40.4	28.8	2.7	18.7	7.1	10.7	23.0	7.3	2.1	7.1	12.3	1.33	0.04	0.18	1.15	0.057	0.139	0.0004	0.034	0.869
	Compo +	32.1	33.9	2.6	21.3	8.0	13.8	24.8	9.7	2.4	8.5	13.3	1.11	0.01	0.27	1.19	0.125	0.144	0.0008	0.079	0.750
	Compo p	40.2	34.2	2.4	6.4	9.9	9.8	33.7	6.4	2.7	6.7	18.5	0.83	0.07	0.18	1.33	0.102	0.058	0.0007	0.032	0.776

Table 2
Sequential procedure for biochemical fractionation of the AOM into NDF, ADF, ADL, after Van Soest et al. (1991) (NDS, ADS = neutral detergent solution, acid detergent solution, respectively (Van Soest et al., 1991); AOM_o, NDF_o, ADF_o, ADL_o = organic part of AOM, NDF, ADF and ADL residues, respectively; w_{ct} = sample weight on a 105 °C basis; C_{AOM}, N_{AOM}, C_{NDF}, N_{NDF}, C_{ADF}, N_{ADF}, C_{ADL}, N_{ADL} = carbon and nitrogen contents of AOM, NDF, ADF, ADL, respectively; Ash_t, Ash_{NDF}, Ash_{ADF}, Ash_{ADL} = ash contents of AOM, NDF, ADF, ADL, respectively; Sol, Hem, Cel, Lig = dry masses of soluble, hemicelluloses, cellulose and lignine fractions, respectively; C_{Sol}, N_{Sol}, C_{Hem}, N_{Hem}, C_{Cel}, N_{Cel}, C_{Lig}, N_{Lig} = carbon and nitrogen contents of Sol, Hem, Cel and Lig fractions, respectively; Ash_{AOM} = inorganic part of AOM)

Extractions	Weight (40 °C)	C (%)	N (%)	Weight (105 °C)	Correction factor f_w	Ash content (525 °C)	Fibrous product	Calculation	Final data (%)
AOM 6 replicates	w_{1AOM}	C_{total}	N_{total}	w_{2AOM}	$f_{wAOM} = w_{2AOM}/w_{1AOM}$	Ash_t	AOM	$w_{1AOM} f_{wAOM}$	w_{ct}
								C_{total}/f_{wAOM}	C_{AOM}
								N_{total}/f_{wAOM}	N_{AOM}
							AOM_o	$w_{ct} - Ash_t$	
NDS → Sol	w_{1NDF}	C_{NDF}	N_{NDF}	w_{2NDF}	$f_{wNDF} = w_{2NDF}/w_{1NDF}$	Ash_{NDF}	NDF	$w_{1NDF} f_{wNDF}$	
							NDF_o	$w_{1NDF} f_{wNDF} - Ash_{NDF}$	
NDF 6 replicates								$(AOM_o - NDF_o)/w_{ct}$	Sol
								$(C_{AOM} w_{1AOM} - C_{NDF} w_{1NDF})/w_{ct}$	C_{Sol}
								$(N_{AOM} w_{1AOM} - N_{NDF} w_{1NDF})/w_{ct}$	N_{Sol}
ADS → Hem	w_{1ADF}	C_{ADF}	N_{ADF}	w_{2ADF}	$f_{wADF} = w_{2ADF}/w_{1ADF}$	Ash_{ADF}	ADF	$w_{1ADF} f_{wADF}$	
							ADF_o	$w_{1ADF} f_{wADF} - Ash_{ADF}$	
ADF 4 replicates								$(NDF_o - ADF_o)/w_{ct}$	Hem
								$(C_{NDF} w_{1NDF} - C_{ADF} w_{1ADF})/w_{ct}$	C_{Hem}
								$(N_{NDF} w_{1NDF} - N_{ADF} w_{1ADF})/w_{ct}$	N_{Hem}
H_2SO_4 → Cel	w_{1ADL}	C_{ADL}	N_{ADL}	w_{2ADL}	$f_{wADL} = w_{2ADL}/w_{1ADL}$	Ash_{ADL}	ADL	$w_{1ADL} f_{wADL}$	
							ADL_o	$w_{1ADL} f_{wADL} - Ash_{ADL}$	
ADL 2 replicates								$(ADF_o - ADL_o)/w_{ct}$	Cel
								$(C_{ADF} w_{1ADF} - C_{ADL} w_{1ADL})/w_{ct}$	C_{Cel}
								$(N_{ADF} w_{1ADF} - N_{ADL} w_{1ADL})/w_{ct}$	N_{Cel}
525°C → Lig								ADL_o/w_{ct}	Lig
								$C_{ADL} w_{1ADL}/w_{ct}$	C_{Lig}
								$N_{ADL} w_{1ADL}/w_{ct}$	N_{Lig}
								Ash_t/w_{ct}	Ash_{AOM}

1st order three-compartment model with very labile (L′), resistant (R′) and stable (S) organic compounds. More complex model including exchanges between compartments (humification from L to R, decomposition from R to L) was not retained after statistical analysis.

The three parameters of model *m*4 are classically used to regulate organic inputs in many SOM models: P_L (no dimension) is the proportion of labile compounds in AOM, k_{mL} and k_{mR} (d^{-1}) are the mineralization kinetic constants for the compartments L and R, respectively. The mineralized AOM fraction (*MAOMF*, cumulative CO_2–C expressed as a fraction of added C) at a given incubation time *t* (d) was:

$$\text{MAOMF} = 1 - P_L\, e - k_{mL}t - (1 - P_L)e - k_{mR}t \qquad (1)$$

Model *m*6 is also used to regulate organic inputs in other SOM models. The complete version utilizes generally five parameters: the proportions P'_L and P_S (no dimension) of very labile and stable compounds, respectively, (P'_R is obtained by the difference $1 - P'_L - P_S$) and the kinetic constants k'_{mL}, k'_{mR}, and k_{mS} (d^{-1}) of each compartment. Here, in the simplified version, k_{mS} was set to zero as the mineralization of this stable compartment was not noticeable during the six-month experiment. The k'_{mL}, and k'_{mR} values fitted for each AOM (model *m*5 in Thuriès et al., 2001) were found less variable than k_{mL} and k_{mR} (*m*4) and close to their mean value. The increase from two (*m*4) to three (*m*6) discrete classes of compounds in AOM logically displayed more homogeneous products in each class with analogous decomposition rate. Thus *m*6 could be defined with only two parameters P'_L and P_S (k'_{mL} and k'_{mR} set at their mean values: $k'_{mL} = 0.40\ d^{-1}$, $k'_{mR} = 0.012\ d^{-1}$). The MAOMF (28 °C, 75% WHC) at a given incubation time *t* was thus calculated as:

$$\text{MAOMF} = 1 - P'_L\, e^{-0.4t} - (1 - P'_L - P_S)e^{-0.012t} - P_S \qquad (2)$$

The values of the parameters (Eqs. (1) and (2)) obtained for the 17 AOM are reported in Table 1.

2.4. Calculations

In the present work, a stepwise regression was used to determine the relationships between the parameters of Eqs. (1) and (2) (Table 1), and the characteristics of the measured biochemical fractions: C_{AOM}, N_{AOM}, Ash_{AOM}, Sol, Hem, Cel, Lig, C_{Sol}, N_{Sol}, C_{Hem}, N_{Hem}, C_{Cel}, N_{Cel}, C_{Lig}, N_{Lig}. The variables synthesized were also taken into account from the former fractions: C-to-N, labile (*lab* = Sol + Hem) and stable (*stab* = Cel + Lig) fractions, labile organic fraction *flab* = lab/(lab + stab), labile/stable ratio *flabr* = lab/stab, soluble organic fraction (cellular content) *fsol* = Sol/(lab + stab), soluble/insoluble ratio fsolr = Sol/(Hem + Cel + Lig), soluble fraction in labile organic compounds fsoll = Sol/lab, cellulose fraction in the stable compounds *fces* = Cel/stab, lignin/nitrogen ratio (Lig/N_{AOM}), C and N in labile (C_{lab}, N_{lab}) and stable (C_{stab}, N_{stab}) fractions.

A stepwise regression procedure using partial *F*-test and sequential *F*-test, controlled by Mallows Cp statistic (Draper and Smith, 1980) was used in order to remove or to enter biochemical variables in the models describing each parameter of *m*4 (Eq. (1)) and *m*6 (Eq. (2)). The resulting equations (Table 3) were then associated to Eq. (1) or Eq. (2) in order to give biochemical prediction of C-mineralization with *m*4 and *m*6 model, with or without classification.

In each case, the efficiency of these predictions was assessed by the residual sum of squares *RSS* and graphic visualization. The best simulation must have the lowest RSS; let RSS*a* and RSS*b* be the residual sum of squares of simulations *a* and *b*, respectively; if RSS*a* > RSS*b*, comparisons with *F*-test must be performed as follows:

$$F = \frac{\text{RSS}a}{\text{RSS}b} = \frac{\sum(y_i - \hat{y}_{ia})^2/(p-m)_a}{\sum(y_i - \hat{y}_{ib})^2/(p-m)_b} \qquad \text{otherwise, if}$$

$$\text{RSS}b > \text{RSS}a,\quad F = \frac{\text{RSS}b}{\text{RSS}a} \qquad (3)$$

where *p* is the number of sampling occasions, *m* the number of model parameters, y_i, $\hat{y}_{ia}$, $\hat{y}_{ib}$ is the measured and predicted values with models *a* and *b*, respectively, at sampling *i*. A *F* value (Eq. (3)) higher than bilateral $F^{0.05}_{(p-m)_a(p-m)_b}$ (statistical table) implies that the hypothesis of equality must be rejected at $p < 0.05$: RSS*a* is greater than RSS*b*, *b* simulation is thus better than *a*.

When necessary, Principal Component Analysis (PCA) was also used to classify the AOM before the simulations.

3. Results

3.1. Predictions of CO_2–C mineralization for the AOM set

The best relationships found between the parameters and the biochemical characteristics (Table 1) were reported in Table 3, Eqs. (4) (P_L), (5) (k_{mL}) and (6) (k_{mR}) for *m*4 and Eqs. (7) (P'_L) and (8) (P_R) for *m*6.

For 11 AOM among the 17 tested, the *F*-tests (Eq. (3), columns 'no' in Table 4) showed that Eqs. (2), (7) and (8) (simplified three-compartment model) gave better mineralization predictions than Eqs. (1), (4)–(6) (two-compartment model). However, the differences were only significant for four AOM: Nfeat, Chicm, and Dgrap at $p < 0.01$, Coffk at $p < 0.05$. The carbon mineralization for six AOM was best predicted by Eqs. (1), (4)–(6), but the differences were only significant for three of them: Wgrap and Kokoa at $p < 0.01$, and Guano at $p < 0.05$.

Despite the significant predictions of the parameters ($85.7 < r^2 < 97.1$), the modeling of MAOMF with Eqs. (1), (4)–(6), or (2), (7) and (8), was not always satisfactory for some contrasted N-rich (e.g. Guano) and

Table 3
Predictive equations of parameters of the two models (*m*4 Eq. (1) and *m*6 Eq. (2)) by biochemical data, without (all) and with (−, +Co values, Eq. (9)) classification of AOM (r^2 = % of the explained total variation, significant at $p < 0.01$ for Eq. (14), at $p < 0.001$ for Eqs. (15) and (18), at $p < 0.0001$ for other Equations) (Sol, Hem, Cel, Lig, Ash_{AOM} = mass fraction of the organic extracts: soluble, hemicelluloses, cellulose, lignin in AOM, and inorganic part of AOM, respectively, C_{Sol}, C_{Hem}, C_{Cel}, C_{Lig} = carbon in Sol, Hem, Cel and Lig fractions; N_{Sol}, N_{Hem}, N_{Cel}, N_{Lig}, N_{AOM} = nitrogen in Sol, Hem, Cel, Lig fractions and whole AOM; $N_{lab} = N_{Sol} + N_{Hem}$; flab = (Sol + Hem)/(Sol + Hem + Cel + Lig), fsol = Sol/(Sol + Hem + Cel + Lig); fsoll = Sol/(Sol + Hem), fces = Cel/(Cel + Lig))

Class	Model Eq.	Eq. No	Parameter	Equation	r^2
All	1	(4)	P_L	0.38 flab + 1.8 N_{lab}	97.1
All	1	(5)	k_{mL}	0.53 Sol − 0.32 Hem + 2.6 N_{Sol}	93.2
All	1	(6)	k_{mR}	0.025 C_{Cel} − 0.015 C_{Lig} + 0.045 N_{Sol}	85.7
All	2	(7)	P'_L	0.24 flab + 2.8 N_{Sol} − 0.31 C_{Lig}	96.3
All	2	(8)	P_S	3.55 C_{Lig} + 0.61 Ash_{AOM}	96.0
−	1	(10)	P_L	0.66 flab − 0.67 Lig	97.8
−	1	(11)	k_{mL}	0.50 fsol − 0.45 Hem + 1.3 N_{AOM}	96.9
−	1	(12)	k_{mR}	0.023 N_{AOM} − 0.023 C_{Lig} + 0.009 Ash_{AOM}	96.3
+	1	(13)	P_L	0.25 flab + 0.54 Hem	99.1
+	1	(14)	k_{mL}	0.13 fsoll	78.5
+	1	(15)	k_{mR}	0.014 fces − 0.013 lab	97.7
−	2	(16)	P'_L	0.35 fsol + 2.2 N_{AOM} − 0.010 Lig/N_{AOM}	98.7
−	2	(17)	P_S	3.60 Lig	98.9
+	2	(18)	P'_L	0.099 flab + 0.14 Hem	97.2
+	2	(19)	P_S	1.61 Lig + 0.62 Ash_{AOM}	99.0

N-poor (e.g. Wgrap) AOM (curves not shown). Additionally, Eqs. (4)–(8) required the utilization of C and N data from biochemical fractions, not as easily collectable as fraction masses (Table 2). The improvement of MAOMF simulations was thus assessed by classifying the AOM.

3.2. Classification of AOM

A PCA was applied on the set of quality indices: C_{AOM}, N_{AOM}, Ash_{AOM}, Sol, Hem, Cel, Lig, C_{Sol}, N_{Sol}, C_{Hem}, N_{Hem}, C_{Cel}, N_{Cel}, C_{Lig}, N_{Lig}, or the previously defined ratios (C-to-N, flab, flabr, fsol, fsolr, fsoll, fces, Lig/N_{AOM}). We then explored for the most discriminant variables in order to express the maximum variability on the 1st axis. Finally, the ratio Lig/N_{AOM} and the variable C_{AOM} explained more than 70% of the variability on axis 1. Equation of the 1st principal component was: 0.71(C_{AOM} + Lig/N_{AOM}). The PCA variables being standardized, the coordinate of each variable on the 1st axis was calculated by:

$$Co = 0.71\left(\frac{C_{AOM} - \bar{C}_{AOM}}{SC_{AOM}} + \frac{Lig/N_{AOM} - \overline{Lig/N}_{AOM}}{SLig/N_{AOM}}\right)$$

$$= 7.18C_{AOM} + 0.14Lig/N_{AOM} - 3.84 \quad (9)$$

Calculations of the PCA component 1 (*Co*, Eq. (9)) allowed to classify easily the AOM (Table 4). Indeed, the fertilizers and the AOM of animal origin had negative Co values ranging from −0.41 for Feath to −2.49 for Guano. On the opposite, the AOM of plant origin had positive Co values ranging from 1.54 for Olivp to 1.98 for Wgrap, except the atypical Kokoa (fertilizer-like mineralization behavior with C-to-N = 10 against $20 <$ C-to-N < 27 for other plant-originated AOM). In accordance with their partially animal character and their C mineralization behavior, Shepm and Chicm presented negative Co values. Most of the composts had negative Co values but these were no lower than −0.55. Compo p, which had high lignin content, had a positive Co value like the plant-originated AOM. It could be noticed that upon the addition of Dgrap (Co = +1.55) to Compo e (Co = −0.55), the Co value of the obtained mixture Compo + increased (Co = −0.04).

Other methods of cluster analysis, hierarchical and non-hierarchical classifications were tested. However in that case, results were not as clear as the ones obtained by the PCA method; indeed it allowed to separate markedly, ligneous materials with relatively high C and low N contents (Co > 0) from the more nitrogenous ones with lower C and stable fiber (Cel + Lig) contents (Co < 0).

3.3. Simulations for the classified AOM

The *m*4 parameters (Eq. (1)) for the AOM classified ' − ' (Table 4, Co < 0) were simulated by Eqs. (10), (11) and (12) (Table 3, r^2 = 97.8, 96.9 and 96.3) more accurate than Eqs. (4)–(6) (r^2 = 97.1, 93.2, 85.7) for all the AOM. For the AOM classified ' + ' (Co > 0), two *m*4 parameters (P_L and k_{mR}) were better simulated by Eqs. (13) and (15) (r^2 = 99.1 and 97.7) after classification. The *m*6 parameter simulations were improved by classification, for P'_L (r^2 = 98.7 in Eq. (16) and 97.2 in Eq. (18) against r^2 = 96.3 in Eq. (7)) as for P_S (r^2 = 98.9 in Eq. (17) and 99.0 in Eq. (19) against r^2 = 96.0 in Eq. (8)).

The comparisons of the AOM simulated mineralization were made by using *F*-test on residuals (Eq. (3); Table 4)

Table 4
Comparison of models *m*4 (Eq. (1)) and *m*6 (Eq. (2)) predictions (*F*-test, Eq. (3)), with ('yes', Eqs. (10)–(19) in Table 3) or without ('no', Eqs. (4)–(8) in Table 3) classification of the AOM by means of PCA (Co, Eq. (9)) (symbols represent the level of significance for *F*-test (Eq. (3)): **($p < 0.01$), *($p < 0.05$), ns (no significant))

	Classification	No				No/yes		Yes/no		No/yes		Yes/no		Yes			
	Co	*m4/m6*		*m6/m4*		*m4/m4*		*m4/m4*		*m6/m6*		*m6/m6*		*m4/m6*		*m6/m4*	
Coffk	1.76	3.76	*			3.14	*			< 1		1.83	ns	< 1		1.53	ns
Wgrap	1.98	< 1		9.42	**	1.69	ns			6.44	**			< 1		2.47	ns
Dgrap	1.56	4.12	**			6.65	**			< 1		7.50	**	< 1		12.10	**
Olivp	1.54	2.05	ns			1.18	ns			5.36	**			9.33	**		
Kokoa	−0.31	< 1		5.90	**	< 1		1.41	ns	22.26	**			5.32	*		
Shepm	−0.43	< 1		1.55	ns	< 1		1.16	ns	< 1		2.26	ns	1.70	ns		
Chicm	−0.94	4.88	**			< 1		4.84	**	< 1		2.26	ns	10.45	**		
Nfeat	0.48	> 100	**			> 100	**			2.34	ns			> 100	**		
Featm	−0.41	< 1		2.18	ns	< 1		2.06	ns	< 1		1.08	ns	< 1		1.14	ns
Guano	−2.49	< 1		3.64	*	1.83	ns			1.57	ns			< 1		4.24	**
Gnofer	−1.76	< 1		1.49	ns	20.97	**			4.66	**			< 1		6.69	**
Comfer	−0.52	1.31	ns			< 1		1.14	ns	1.33	ns			1.31	ns		
Compo a	−0.42	1.93	ns			10.44	**			7.04	**			1.93	ns		
Compo b	−0.16	1.42	ns			9.08	**			16.29	**			2.56	*		
Compo e	−0.55	1.08	ns			< 1		1.09	ns	7.91	**			9.30	**		
Compo +	−0.05	1.10	ns			1.01	ns			34.37	**			37.38	**		
Compo p	1.26	1.82	ns			6.00	**			50.63	**			15.37	**		

and graphically (Figs. 1–3) in order to: (i) compare models *m*4 (Eqs. (1), (4)–(6)) and *m*6 (Eqs. (2), (7) and (8)) without AOM classification (see description earlier) (ii) show the effect of classification on *m*4 (Eqs. (1), (4)–(6) vs (1), (10)–(15)) and *m*6 simulations (Eqs. (2), (7) and (8) vs (2), (16)–(19)) (iii) compare *m*4 (Eqs. (1), (10)–(15)) and *m*6 (Eqs. (2), (16)–(19)) simulations after classification of AOM.

For the model *m*4, the classification improved the simulations for 11 AOM (Table 4), but only significantly

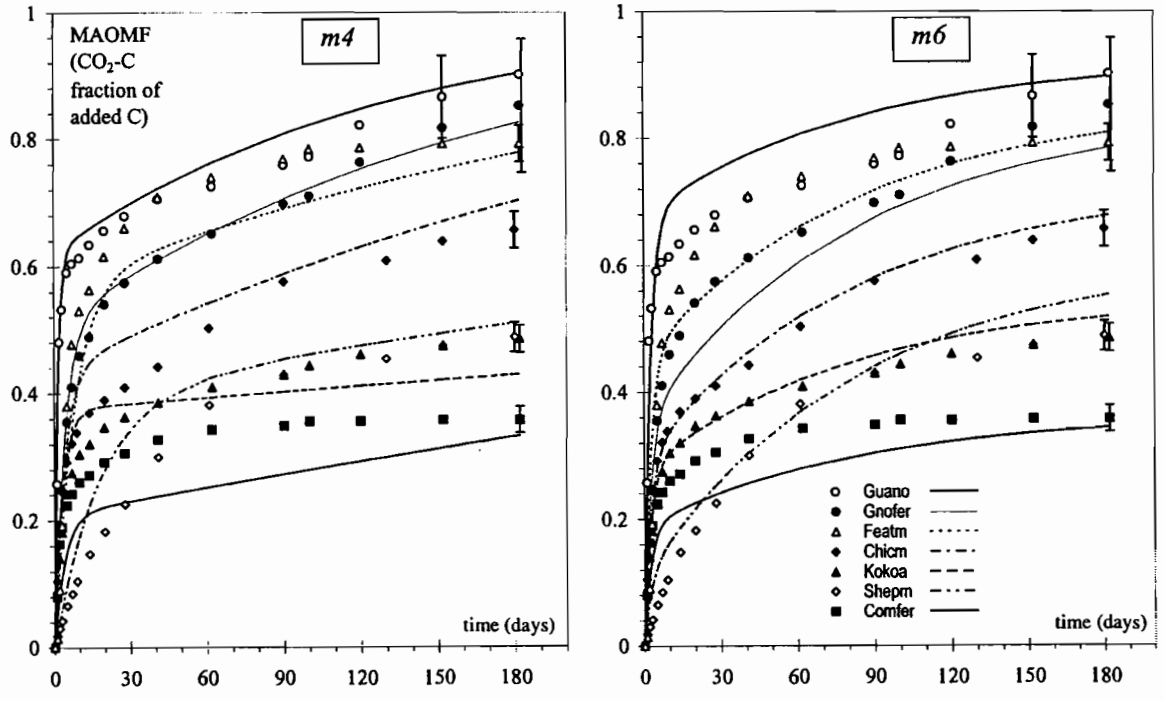

Fig. 1. Mineralized added organic material fraction (MAOMF) of the AOM from animal origin (Guano: ○; Featm: △), manures (Chicm: ◆; Shepm: ◇), fertilizers (Gnofer: ●; Comfer: ■) or with a fertilizer-like behavior (Kokoa: ▲). Symbols represent experimental data ($n = 3$), and lines represent the predictions according to *m*4 (Eqs. (1), (10)–(12)) and *m*6 (Eqs. (2), (16) and (17)) models after classification of the AOM (Co < 0, Eq. (9)). Vertical bars represent the maximum of cumulative confidence intervals at 95%.

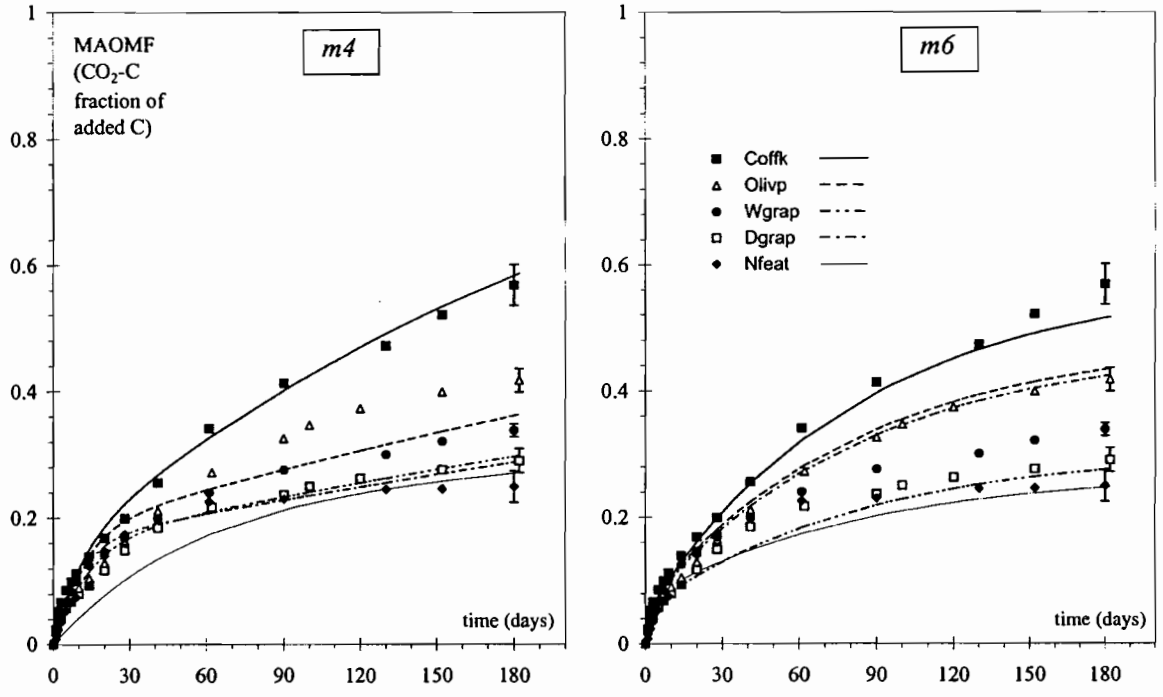

Fig. 2. Mineralized added organic material fraction (MAOMF) of the AOM from plant origin (Coffk: ■; Olivp: △; Wgrap: ●; Dgrap: □) or with a plant-AOM-behavior (Nfeat: ◆). Symbols represent experimental data ($n = 3$), and lines represent the predictions according to $m4$ (Eqs. (1), (13)–(15)) and $m6$ (Eqs. (2), (18) and (19)) models after classification of the AOM (Co > 0, Eq. (9)). Vertical bars represent the maximum of cumulative confidence intervals at 95%.

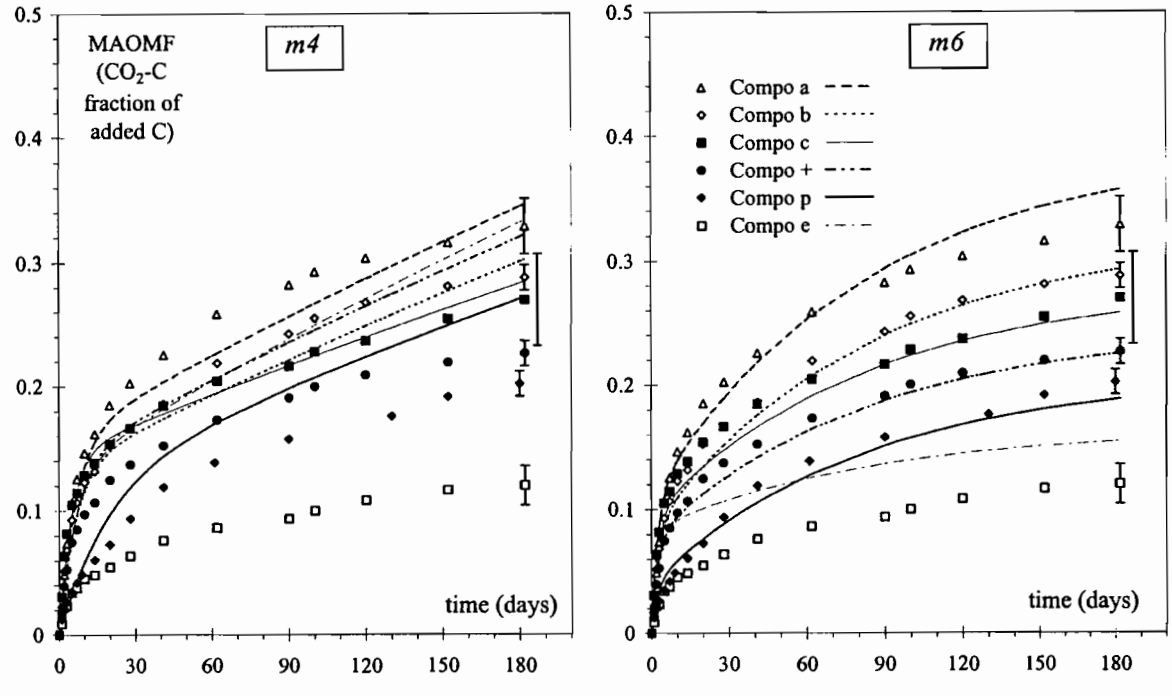

Fig. 3. Mineralized added organic material fraction (MAOMF) of the initial mixture of AOM (uncomposted Compo a: △), and the obtained composts at different composting times (Compo b: ◇; Compo c: ■; Compo p: ◆; Compo e: □), or compost supplemented with Dgrap (Compo +: ●). Symbols represent experimental data ($n = 3$), and lines represent the predictions according to $m4$ (Eqs. (1), (10)–(15)) and $m6$ (Eqs. (2), (16)–(19)) models after classification of the AOM (Co < 0 except Co > 0 for Compo p). Vertical bars represent the maximum of cumulative confidence intervals at 95%.

for 7 AOM: Dgrap, Nfeat, Gnofer, Compo a, Compo b, Compo p at $p < 0.01$, and Coffk at $p < 0.05$. For 6 AOM, the classification resulted in poorer simulations compared to unclassified data, but only significantly ($p < 0.01$) for Chicm.

For *m*6, the classification improved the simulations for 12 AOM (Table 4), but only significantly ($p < 0.01$) for 9 AOM: Wgrap, Olivp, Kokoa, Gnofer, Compo a, Compo b, Compo e, Compo +, and Compo p. For 5 AOM, the classification resulted in poorer simulations compared to unclassified data, but only significantly ($p < 0.01$) for Dgrap.

After classification, the *m*6 simulations (Eqs. (2), (16)–(19)) were better than the *m*4 ones (Eqs. (1), (10)–(15)) for 11 AOM, but only significantly for 8 AOM: Olivp, Chicm, Nfeat, Compo e, Compo +, Compo p at $p < 0.01$, and Kokoa, Compo b at $p < 0.05$. Inversely, the *m*4 simulations were better for 6 AOM, but only significantly ($p < 0.01$) for 3 AOM: Dgrap, Guano and Gnofer.

Fig. 1 shows the C mineralization data and their simulations by models *m*4 (Eqs. (1), (10)–(12)) and *m*6 (Eqs. (2), (16) and (17)) for AOM classified ' − ' (animal-originated AOM and Kokoa). Guano and Gnofer *m*4 simulations were better than *m*6 ones from 15 to 150 d of incubation and similar at the beginning and the end of the incubation. Since Guano and Gnofer had very low Lig contents (Table 1), a three-compartment model was obviously not necessary to describe their mineralization. However, the calculation of P_S from Eq. (2) gave a low but no null value (Table 1); Guano and Gnofer represented borderline cases for *m*6, but still acceptable since the predictions were close to experimental data at the end of incubation. During the first 90 d, Shepm mineralization was better simulated with *m*6, but better with *m*4 afterwards (ns *F*-test). The overestimation observed with *m*6 at the end of the experiment could be explained by the low content of Lig in Shepm.

Fig. 2 shows the C mineralization data and their simulations by models *m*4 (Eqs. (1), (13)–(15)) and *m*6 (Eqs. (2), (18) and (19)) for AOM classified ' + ' (plant-originated AOM and Nfeat). Good simulations were observed with both models for Coffk (ns *F*-test), and with *m*6 for Nfeat (***F*-test). The Olivp simulated mineralization was close to the experimental data with *m*6 but not with *m*4 (***F*-test). Inversely, Dgrap mineralization was better simulated with *m*4 (***F*-test). These differences between Dgrap and Olivp simulations were difficult to explain since the biochemical characteristics of the two AOM were almost similar (Table 1). The major difference concerned Hem, a term of Eq. (18). The Wgrap simulations were slightly underestimated by both models.

The C mineralization data and their simulations for composts classified ' − ' (Eqs. (1), (10)–(12) and (2), (16), (17)) and Compo p classified ' + ', (Eqs. (1), (13)–(15) and (2), (18), (19)) are displayed in Fig. 3. Compo c was added in Fig. 3 for validating the model but it was not used for calculations nor discussed there. For all the composts, *m*6 simulations were close to experimental data, but slightly overestimated for Compo e (greatly overestimated with *m*4, see Section 4.3). All the *m*6 simulations were better than the *m*4 ones; however, the latter seemed still valid for Compo a (ns difference between *m*4 and *m*6) and Compo b (with a better *m*6 prediction, **F*-test).

4. Discussions

4.1. Simulations for the AOM set

Equations in Table 3 highlight the relationships between the kinetic parameters and contrasted biochemical characteristics of the AOM set. The conceptual labile fraction P_L in Eq. (1) was mostly linked to the measured labile organic fraction flab (Eq. (4)). But P_L was not strictly equivalent to the flab value as it represented 0.38 flab. The three-compartment model (Eq. (2)) defined L' as a part (the most labile compounds) of compartment L (Eq. (1)). As for P_L, the conceptual very labile fraction P'_L (Eqs. (2) and (7)) was first linked to the measured labile organic fraction flab, but to a lesser extent (0.24 flab against 0.38 flab). P'_L was also linked to the most labile nitrogenous compounds ($N_{sol} = N_{lab} - N_{Hem}$), like P_L was to N_{lab} (Eq. (4)). The very stable fraction P_S (Eqs. (2) and (8)) was strongly linked to the carbon content of ligneous compounds (C_{Lig}). It is generally accepted that lignin is one of the least degradable part of an AOM (Melillo et al., 1982; Heal et al., 1997). The weaker relationship between P_S and Ash_{AOM} could be explained by the high ash contents of some humified products (composts, manure, Table 1).

The kinetic constants k_{mL} (Eq. (5)) and k_{mR} (Eq. (6)) were less strongly linked to the biochemical characteristics. The k_{mL} and k_{mR} values were positively related to the most decomposable compounds (Sol and N_{Sol} for k_{mL}, Cel for k_{mR}), and negatively to the less decomposable ones (Hem for k_{mL}, C_{Lig} for k_{mR}) in the labile (lab = Sol + Hem) and the stable (Stab = Cel + Lig) fractions, respectively.

4.2. Simulations for the classified AOM

The conceptual labile fraction P_L was always linked to the measured labile organic fraction flab (0.66 flab in Eq. (10), 0.25 flab in Eq. (13), 0.38 flab in Eq. (4). The equations differed in their second term: P_L was negatively linked with Lig in Eq. (10), positively linked to Hem in Eq. (13). The AOM classified ' + ' included mostly plant-originated AOM, non-composted, and containing hemicellulosic constitutive parts of plant cell walls.

The conceptual very labile fraction P'_L (a part of labile fraction P_L) was principally related to the soluble organic fraction fsol (the more labile part of the labile fraction flab) for the AOM classified ' − ' (Eq. (16) in Table 3) or to flab for the AOM classified ' + ' (Eq. (18) in Table 3). For AOM

classified ' + ', P'_L was secondarily linked to Hem (Eq. (18)) as P_L in Eq. (13). For AOM classified ' − ', P'_L was secondarily positively linked to N_{AOM}, and to a small extent negatively linked to the ratio Lig/N_{AOM} as the metabolic fraction of Parton et al. (1987). The very stable conceptual fraction P_S was logically firstly linked to Lig (Eqs. (17) and 19) like P_S to C_{Lig} in Eq. (8). To a lesser extent, P_S of the AOM ' + ' was related to Ash_{AOM} (Eq. (19)) as P_S in Eq. (8) for all the AOM.

In Eq. (11) as in Eq. (5), k_{mL} was: (i) positively linked to the more decomposable compounds of the labile fractions Sol (Eq. (5), soluble fraction of AOM) and fsol (Eq. (11), soluble fraction of AOM organic part), (ii) negatively linked to Hem, and (iii) positively linked to N_{Sol} (Eq. (5)) or N_{AOM} (Eq. (11)). The prediction of the kinetic constant k_{mL} (Eq. (14)) was positively related to the ratio fsoll, the soluble fraction from the labile organic part of the AOM (the most labile part). Sol is generally represented by polysaccharidic and soluble nitrogen metabolites more readily degradable than structural saccharides of Hem (Chesson, 1997).

Predictions of k_{mR} with Eqs. (6) and (12) were less accurate than P_L and k_{mL} ones. In both equations, k_{mR} was negatively linked to C_{Lig} (the more stable C). In Eq. (15), k_{mR} was positively linked to the ratio fces, the cellulosic fraction of the stable compounds, and negatively linked to the labile fraction lab. Eqs. (14) and (15), as Eqs. (5), (6), (11) and (12), did not give predictions of k_{mL} and k_{mR} kinetic constants as satisfactory as those of P_L, P'_L and P_S fractions.

4.3. Simulation for very composted materials

The overestimation of Compo e carbon mineralization by both models (see Section 3.3 and Fig. 3) can be explained by its composting duration: 10 months for Compo e, 0–6 months for the others. Yet, Compo e presented a lower Lig and a higher Sol contents (Table 1) than expected. A prolonged composting time may result indeed in artifacts of the biochemical profiles, with Lig degradation into soluble fulvo-humic molecules (Govi et al., 1995; Horwath and Elliott, 1996) resistant to microbial attack. In this manner, the Sol fraction generally represented by polysaccharides and soluble proteins (Chesson, 1997) was particular in Compo e as compared to Sol of other composts. Consequently, Eqs. (10) and (16) could overestimate P_L (positively linked to flab, negatively to Lig) and P'_L (positively linked to fsol and N_{AOM}, and negatively to Lig/N_{AOM}).

4.4. Model applications

The mineralization data of Compo c -not used in this experiment- are shown in Fig. 3. We measured the following biochemical characteristics of this AOM: C_{AOM} = 0.2961, N_{AOM} = 0.0226, Ash_{AOM} = 0.3460, Sol = 0.2479, Hem = 0.0269, Cel = 0.1804, Lig = 0.1988, C_{Lig} = 0.1162 g g^{-1}. From this data, Eq. (9) gave Co = −0.5. As Co had a negative value, the predictive mineralization of Compo c must be calculated according to Eqs. (1), (10)–(12) (*m*4) or Eqs. (2), (16) and (17) (*m*6). For both models, the results were in good accordance with mineralization data (Fig. 3).

Compo+ was a mixture of 75% Compo e (classified ' − ') and 25% Dgrap (classified ' + '). The biochemical profile of the mixture was calculated according to the measured biochemical characteristics of Compo e and Dgrap: for example, $Lig_{Compo+} = 0.75\ Lig_{Compo\ e} + 0.25\ Lig_{Dgrap}$. From the calculated profile, Eq. (9) gave Co = −0.05. With such an ambiguous classification (Co ~ 0), the simulations (not shown) were underestimated with Eqs. (1), (10)–(12) (*m*4) or (2), (16) and (17) (*m*6), and overestimated with Eqs. (1), (13)–(15) (*m*4) or (2), (18) and (19) (*m*6). It was hypothesized that the calculated biochemical profile was not the real one. Indeed, Dgrap was a distillery by-product and contained tannins, which can react with nitrogenous products (Metche and Girardin, 1980) in the highly composted Compo e. The other way to predict Compo+ mineralization was to calculate each parameter like the biochemical profile was. For example, $P'_{L(Compo+)} = 0.75\ P'_{L(Compo\ e)} + 0.25\ P'_{L(Dgrap)}$ with $P'_{L(Compo\ e)}$ calculated with Eq. (16), and $P'_{L(Dgrap)}$ with Eq. (18). In this manner, *m*6 gave a very good prediction of mineralization, whereas that of *m*4 was overestimated (Fig. 3). Despite this interesting result, one should be cautious in generalizing this kind of calculation. Indeed, a good prediction was obtained for the mixture (Compo+) whereas Compo e and Dgrap predictions were slightly overestimated (Figs. 2 and 3).

5. Conclusions

This work has highlighted correspondences between conceptual parameters and their laboratory estimations, but the theoretical parameters did not correspond exactly to the measured ones. Differences could have originated from the method since the sequential analysis of fibers did not give exactly the real biochemical entities. However, few (one to three) biochemical characteristics were sufficient to give significant and logical estimations of each conceptual parameter. The C mineralization simulations obtained from the entire AOM set were not always satisfactory for contrasted N-rich and N-poor AOM. The predictive equations have been recalculated and improved after a classification of the AOM by means of a PCA. The classification was based on the total C content and the lignin-to-N ratio. It allowed to discriminate (i) ligneous and relatively N-poor AOM (mostly plant-originated), from (ii) the more nitrogenous AOM with lower C and fiber contents (mostly animal-originated or composts). After classification, the C mineralizations were quite well simulated for all AOM.

The labile and stable fractions were always more accurately estimated than the kinetic constants. Moreover, for most of the AOM, the simplified three-compartment model *m*6 (two parameters) gave better predictions than the two-compartment one (*m*4, three parameters): *m*6 can

thus be recommended. Henriksen and Breland (1999a,b,c) defined a three-compartment model with (i) Sol, (ii) Hem + Cel, and (iii) Lig. But Hem is generally defined by a relatively large range of molecules more or less degradable (Heal et al., 1997); indeed, Hem represents an heterogeneous group of linear or branched polysaccharides with a degree of polymerisation of about 100–200 while Cel represents mostly a homopolymer of β 1–4 D-glucose with a degree of polymerisation of about 14,000 (Breznak and Brune, 1994). From our equations, the contents of the very labile, resistant and stable compartments could be defined by: (i) parts of soluble, nitrogenous and hemicellulosic compounds, (ii) cellulose and the remaining fraction of hemicelluloses, (iii) the ligneous fraction, respectively.

This study has shown the possibility to simulate AOM-C mineralization from a simple analytical approach including sequential extraction and mass measurements. The calculations can be easily managed through a spreadsheet. The kinetic constants (0.4 and 0.012 d^{-1} for *m*6) obtained under these experimental conditions (28 °C, 75% WHC) must be adjusted with classical laws to varying pedoclimatic conditions.

Acknowledgements

This work was partly granted by a CIFRE convention. The authors gratefully acknowledge Prof J.C. Rémy and Prof P. Herrmann (ENSA-Montpellier, France), Dr M. Viel (Phalippou-Frayssinet S.A., Rouairoux, France), and Dr P. Bottner (CEFE-CNRS-Montpellier, France) for helpful discussions. We thank D. Beunard for technical assistance with fiber analyses.

References

Ågren, G.I., Bosatta, E., 1996. Quality: a bridge between theory and experiment in soil organic matter studies. Oikos 76, 522–528.

Amato, M., Jackson, R.B., Butler, J.H.A., Ladd, J.N., 1984. Decomposition of plant material in Australian soils. II. Residual organic ^{14}C and ^{15}N from legume plant parts decomposing under field and laboratory conditions. Australian Journal of Soil Research 22, 331–341.

Angers, D.A., Recous, S., 1997. Decomposition of wheat straw and rye residues as affected by particle size. Plant and Soil 189, 197–203.

Bosatta, E., Ågren, G.I., 1985. Theoretical analysis of decomposition of heterogeneous substrates. Soil Biology and Biochemistry 17, 601–610.

Bradbury, N.J., Whitmore, A.P., Hart, P.B.S., Jenkinson, D.S., 1993. Modelling the fate of nitrogen in crop and soil in the years following application of ^{15}N labelled fertilizer to winter wheat. Journal of Agricultural Science 121, 363–379.

Breznak, J.A., Brune, A., 1994. Role of microorganisms in the digestion of lignocellulose by termites. Annual Review of Entomology 39, 453–487.

Cheneby, D., Nicolardot, B., Linères, M., 1992. Estimation de la valeur agronomique de produits organiques au moyen de cinétiques de minéralisation déterminées au laboratoire. Ministère de l'Agriculture, INRA Dijon.

Chesson, A., 1997. Plant degradation by ruminants: parallels with litter decomposition in soils. In: Cadisch, G., Giller, K.E. (Eds.). Driven by Nature, Plant Litter Quality and Decomposition. CAB International, Wallingford, pp. 3–30.

Christensen, B.T., 1996. Matching measurable soil organic matter fractions with conceptual pools in simulation models of carbon turnover: revision of model structure. In: Powlson, D.S., Smith, P., Smith, J.U. (Eds.). Evaluation of Soil Organic Matter Models. Springer, Berlin, pp. 143–159.

Coûteaux, M.M., McTiernan, K.B., Berg, B., Szuberla, D., Dardenne, P., Bottner, P., 1998. Chemical composition and carbon mineralization potential of scots pine needles at different stages of decomposition. Soil Biology and Biochemistry 30, 583–595.

Draper, N.R., Smith, H., 1980. Applied Regression Analysis. 2nd ed. Wiley, New York.

FAO–UNESCO–ISRIC, 1988. FAO–UNESCO Soil Map of the Word: revised legend. World Soil Resources Report. Rome.

Govi, M., Ciavatta, C., Sitti, L., Gessa, C., 1995. Evaluation of the stabilization level of pig organic waste: influence of humic-like compounds. Communications in Soil Science and Plant Analysis 26, 425–439.

Hansen, S., Jensen, H.E., Nielsen, N.E., Svendsen, H., 1991. Simulation of nitrogen dynamics and biomass production in winter wheat using the Danish simulation model Daisy. Fertilizer Research 27, 245–259.

Heal, O.W., Anderson, J.M., Swift, M.J., 1997. Plant litter quality and decomposition: an historical overview. In: Cadisch, G., Giller, K.E. (Eds.). Driven by Nature, Plant Litter Quality and Decomposition. CAB International, Wallingford, pp. 47–66.

Henriksen, T.M., Breland, T.A., 1999a. Nitrogen availability effects on carbon mineralization, fungal and bacterial growth, and enzyme activities during decomposition of wheat straw in soil. Soil Biology and Biochemistry 31, 1121–1134.

Henriksen, T.M., Breland, T.A., 1999b. Evaluation of criteria for describing crop residue degradability in a model of carbon and nitrogen turnover in soil. Soil Biology and Biochemistry 31, 1135–1149.

Henriksen, T.M., Breland, T.A., 1999c. Decomposition of crop residues in the field: evaluation of a simulation model developed from microcosm studies. Soil Biology and Biochemistry 31, 1423–1434.

Horwath, W.R., Elliott, L.F., 1996. Ryegrass straw component decomposition during mesophilic and thermophilic incubations. Biology and Fertility of Soils 21, 227–232.

Linères, M., Djakovitch, J.L., 1993. Caractérisation de la stabilité biologique des apports organiques par l'analyse biochimique. In: Decroux, J., Ignazi, J.C., (Eds.), Matières Organiques et Agricultures. Quatrièmes Journées de l'Analyse de Terre et Cinquième Forum de la Fertilisation Raisonnée. Gemas-Comifer, Blois, pp. 159–168.

Mary, B., Recous, S., Darwis, D., Robin, D., 1996. Interactions between decomposition of plant residues and nitrogen cycling in soil. Plant and Soil 181, 71–82.

McGill, W.B., Hunt, H.W., Woodmansee, R.G., Reuss, J.O., Paustian, K.H., 1981. Formulation, process controls, parameters and performance of PHOENIX: a model of carbon and nitrogen dynamics in grassland soils. In: Frissel, M.J., Van Veen, J.A. (Eds.). Simulation of Nitrogen Behaviour of Soil Plant Systems. Centre for Agricultural Publishing and Documentation. Wageningen, The Netherlands, pp. 171–191.

Melillo, J.M., Aber, J.D., Muratore, J.F., 1982. Nitrogen and lignin control of hardwood leaf litter decomposition dynamics. Ecology 63, 621–626.

Metche, M., Girardin, M., 1980. Les tanins végétaux. In: Monties, B. (Ed.), Les Polymères Végétaux, Polymères Pariétaux et Alimentaires non Azotés. Bordas, Paris, pp. 252–288.

Molina, J.A.E., Clapp, C.E., Shaffer, M.J., Chichester, F.W., Larson, W.E., 1983. NCSOIL, a model of nitrogen and carbon transformations in soils: description, calibration, and behavior. Soil Science Society of America Journal 47, 85–91.

Mueller, T., Jensen, L.S., Nielsen, N.E., Magid, J., 1998. Turnover of carbon and nitrogen in a sandy loam soil following incorporation of chopped maize plants, barley straw and blue grass in the field. Soil Biology and Biochemistry 30, 561–571.

Paré, T., Dinel, H., Schnitzer, M., Dumontet, S., 1998. Transformations of

carbon and nitrogen during composting of animal manure and shredded paper. Biology and Fertility of Soils 26, 173–178.

Parton, W.J., Schimel, D.S., Cole, C.V., Ojima, D.S., 1987. Analysis of factors controlling soil organic matter levels in Great Plains grasslands. Soil Science Society of America Journal 51, 1173–1179.

Quemada, M., Cabrera, M.L., 1995. Carbon and nitrogen mineralized from leaves and stems of four cover crops. Soil Science Society of America Journal 59, 471–477.

Recous, S., Robin, D., Darwis, D., Mary, B., 1995. Soil inorganic N availability: effect on maize residue decomposition. Soil Biology and Biochemistry 27, 1529–1538.

Robin, D., 1997. Intérêt de la caractérisation biochimique pour l'évaluation de la proportion de matière organique stable après décomposition dans le sol et la classification des produits organominéraux. Agronomie 17, 157–171.

Rubins, E.J., Bear, F.E., 1942. Carbon–nitrogen ratios in organic fertilizer materials in relation to the availability of their nitrogen. Soil Science 54, 411–423.

Sallih, Z., Pansu, M., 1993. Modelling of soil carbon forms after organic amendment under controlled conditions. Soil Biology and Biochemistry 25, 1755–1762.

Sanger, L.J., Cox, P., Splatt, P., Whelan, M., Anderson, J.M., 1998. Variability in the quality and potential decomposability of *Pinus sylvestris* litter from sites with different soil characteristics: acid detergent fibre (ADF) and carbohydrate signatures. Soil Biology and Biochemistry 30, 455–461.

Tenney, F.G., Waksman, S.A., 1929. Composition of natural organic materials and their decomposition in soil: IV. The nature and rapidity of decomposition of the various organic complexes in different plant materials, under aerobic conditions. Soil Science 28, 55–84.

Thuriès, L., Larré-Larrouy, M.C., Pansu, M., 2000. Evaluation of three incubation designs for mineralization kinetics of organic materials in soil. Communications in Soil Science and Plant Analysis 31, 289–304.

Thuriès, L., Pansu, M., Feller, C., Herrmann, P., Rémy, J.C., 2001. Kinetics of added organic matter decomposition in a Mediterranean sandy soil. Soil Biology and Biochemistry 33, 997–1010.

Trinsoutrot, I., Recous, S., Bentz, B., Linères, M., Chèneby, D., Nicolardot, B., 2000. Biochemical quality of crop residues and carbon and nitrogen mineralization kinetics under nonlimiting nitrogen conditions. Soil Science Society of America Journal 64, 918–926.

USDA, 1975. Soil Taxonomy. A Basic System of Soil classification for Making and Interpreting Soil Surveys. USDA Soil Survey Staff, Washington.

Van Soest, P.J., 1963. Use of detergents in the analysis of fibrous feeds. II. A rapid method for the determination of fiber and lignin. Journal of the AOAC 46, 829–835.

Van Soest, P.J., 1967. Use of detergents in the analysis of fibrous feeds. IV. Determination of plant cell-wall constituents. Journal of the AOAC 50, 50–55.

Van Soest, P.J., Robertson, J.B., Lewis, B.A., 1991. Symposium: carbohydrate methodology, metabolism, and nutritional implications in dairy cattle. Methods for diatery fiber, neutral detergent fiber, and nonstarch polysaccharides in relation to animal nutrition. Journal of Dairy Science 74, 3583–3597.

Van Veen, J.A., Ladd, J.N., Frissel, M.J., 1984. Modelling C and N turnover through the microbial biomass in soil. Plant and Soil 76, 257–274.

Verberne, E.L.J., Hassink, J., de Willingen, P., Groot, J.J.R., Van Veen, J.A., 1990. Modelling organic matter dynamics in different soils. Netherlands Journal of Agricultural Science 328, 221–238.

Waksman, S.A., Tenney, F.G., 1927. Composition of natural organic materials and their decomposition in soil: II. Influence of age of plant upon the rapidity and nature of its decomposition—rye plants. Soil Science 24, 317–334.

Wollny, E., 1902. La Décomposition des Matières Organiques et les Formes d'Humus dans leurs Rapports avec l'Agriculture. Translated from the 1896 German edition by Henry, E., Berger-Levrault, Paris.

La Transformation de l'azote des Apports Organiques (modèle TAO-N)

Cinétique de transformation de l'azote

PERGAMON

Soil Biology & Biochemistry 35 (2003) 37–48

Soil Biology & Biochemistry

www.elsevier.com/locate/soilbio

Kinetics of C and N mineralization, N immobilization and N volatilization of organic inputs in soil

M. Pansu[a,*], L. Thuriès[b]

[a]IRD (ORSTOM), BP 64501, 34394 Montpellier Cedex 5, France
[b]Phalippou-Frayssinet S.A., Organic Fertilizers, 81240 Rouairoux, France

Received 5 February 2002; received in revised form 1 August 2002; accepted 3 September 2002

Abstract

C and N mineralization data for 17 different added organic materials (AOM) in a sandy soil were collected from an incubation experiment conducted under controlled laboratory conditions. The AOM originated from plants, animal wastes, manures, composts, and organic fertilizers. The C-to-N_{AOM} ratios (η_{AOM}) ranged from 1.1 to 27.1. Sequential fibre analyses gave C-to-N ratios of soluble (η_{Sol}), holocellulosic (η_{Hol}) and ligneous compounds (η_{Lig}) ranging from 1.1 to 57.2, 0.8 to 65.2, and 3.5 to 25.3, respectively. Very different patterns of net AOM-N mineralization were observed: (i) immobilization for four plant AOM; (ii) moderate mineralization (4–15% AOM-N) for composts; (iii) marked mineralization (11–27% AOM-N) for 1 animal AOM, 1 manure and 2 organic fertilizers; and (iv) high rates of transformations with possible gaseous losses for some N-rich AOM.

The Transformation of Added Organics (TAO) model proposed here, described AOM-C mineralization (28 °C, 75% WHC) from three labile (L′), resistant (R) and stable (S) compartments with the sole parameters P'_L and P_S = fractions of very labile and stable compounds of AOM, respectively. Dividing the C-compartments by their C-to-N estimates supplied the remaining N_{AOM} fraction (RAONF). A P_{im} parameter split the TAO nitrogen fraction (TAONF = added N-RAONF) into two compartments, immobilized (imN) and inorganic (inorgN) N. A $P_{im} > 0$ value meant that all the TAONF plus a fraction ($P_{im} - 1$) of native soil inorganic N was immobilized. Additional N mineralization was predicted when necessary from imN by first order kinetics (constant k_{remin}). The TAO version with two parameters P_{im} and k_{remin} allowed us to predict very different patterns of N mineralization and N immobilization. In a few cases, a further first order kinetic law (constant k_v) was added to predict N volatilization from inorgN. Two hypotheses were tested: (i) $\eta_{L'}$, η_R, η_S (C-to-N of L′, R and S) = η_{Sol}, η_{Hol}, η_{Lig}, respectively, (ii) $\eta_{L'} = \eta_R = \eta_S = \eta_{AOM}$. The first hypothesis was validated by these data, and the second was a good approximation of the former one. In all the cases, predictions were in good agreement with measured values.

Keywords: Modelling; Kinetics; Carbon and nitrogen turnover; N mineralization; N immobilization; Organic fertilizers

1. Introduction

Despite a large collection of experimental data, the fate of nitrogen (N) of organic inputs in soils remains difficult to interpret. Inorganic N can be produced by mineralization or immobilized by microbial biomass; it can be assimilated by plants, partially fixed within clays, leached in water or volatilized as NH_3, N_2O, NO_x or N_2. Tracer experiments illustrate the complexity of the fluxes (Mary et al., 1998), with a high turnover of ammonium (NH_4^+) largely re-immobilized by microbial biomass (Yevdokimov and Blagodatsky, 1993), and partly nitrified according to a growth law (Pansu et al., 1998a).

In most soil organic matter (SOM) models, N kinetics are derived from those of carbon (C). The initial input material is generally defined by two (Molina et al., 1983; Van Veen et al., 1984; Parton et al., 1987; Bradbury et al., 1993; Pansu et al., 1998b) or three (Verberne et al., 1990; Hansen et al., 1991) compartments. Some mineralization data have been used directly with SOM models (Hadas and Portnoy, 1994; Jans-Hammermeister and McGill, 1997; Trinsoutrot et al., 2000a) or have been adjusted to different specific models. In simplified systems with artificial extraction of inorganic N, a one-compartment model has been proposed by Stanford and Smith (1972). Other functions have been then tested: linear (Addiscott, 1983), parabolic (Broadbent, 1986),

* Corresponding author. Tel.: +33-4674-16100; fax: +33-4674-16294.
E-mail address: pansu@mpl.ird.fr (M. Pansu).

0038-0717/03/$ - see front matter © 2003 Elsevier Science Ltd. All rights reserved.
PII: S0038-0717(02)00234-1

exponential plus constant (Bernal et al., 1998), or double exponential (Deans et al., 1986; Matus and Rodriguez, 1994). In other studies, double exponential expressions failed to estimate organic N pools (Dendooven et al., 1997) or were used for C- but not for N-pools (Bloemhof and Berendse, 1995; Trinsoutrot et al., 2000b).

Another option is to propose mechanistic models in order to follow specifically the decomposition of added organic matter (AOM) to the SOM part. The model of Bosatta and Ågren (1985) defined a quality theory applied to AOM constituents as a continuum. In the model of Henriksen and Breland (1999a), AOM was split into three biochemical compartments, and then assimilated into five soil compartments. Nicolardot et al. (2001) proposed one AOM compartment assimilated into three soil compartments. From a comparative statistical study on C mineralization, Thuriès et al. (2001) proposed splitting AOM into three compartments with only two descriptive parameters. In this paper, we aimed to extend this AOM-C to an AOM-N model in order to predict the C- and N-transformations of AOM.

Although pioneer studies on inorganic-N evolution from incubation experiments took into account a large diversity of AOM (Rubins and Bear, 1942), most of these can be classified in two large groups corresponding to homogeneous materials: (i) plant residues (Nordmeyer and Richter, 1985; Janzen and Kucey, 1988; Jensen, 1994; Bloemhof and Berendse, 1995; Quemada and Cabrera, 1995; Kaboneka et al., 1997; Dendooven et al., 1997; Mueller et al., 1998; Trenbath and Diggle, 1998; Henriksen and Breland 1999a,b; Trinsoutrot et al., 2000a,b; Nicolardot et al., 2001), and (ii) animal manures or composts (Leclerc, 1990; Thiénot, 1991; Hébert et al., 1991; Hadas and Portnoy, 1994; Mahimairaja et al., 1995; Jedidi et al., 1995; Sørensen and Jensen, 1995; Hadas and Portnoy, 1997; Bernal et al., 1998; Paré et al., 1998). Our objective was to model AOM-C and -N transformations of a large collection of AOM from plant, animal manure or compost origins.

2. Materials and methods

2.1. Added organic materials (AOM)

Different kinds of AOM from agri-food industry wastes and industrial-processed fertilizers (organic amendments and fertilizers) were tested (Table 1). The materials originated from (a) plant residues: wet and dry grape berry pellicle cakes (Wgrap, Dgrap), coffee cake (Coffk), cocoa cake (Kokoa), olive pulp (Olivp), (b) animal wastes: hydrolysed feather meal (Featm), native fine feather (Nfeat), guano (Guano), (c) animal manures from sheep (Shepm), and chickens (Chicm), and (d) industrial organic fertilizers: composted amendments (Compo series), and combined fertilizers (Gnofer, Comfer). A full description of these organic materials and their biochemical characterization by the Van Soest et al. (1991) method were given in Thuriès et al. (2001, 2002). The data used in this paper (Table 1) were: η_{AOM}, η_{Sol}, η_{Hol}, η_{Lig} = C-to-N ratios of AOM, soluble, holocellulosic (= hemicellulosic + cellulosic), and ligneous AOM fractions, respectively.

2.2. Incubation experiment

The incubation test using a sandy soil (top 0–20 cm layer; sand = 69.3%, clay = 11.5%, $pH_{(H2O)}$ 6.6, CEC = 5.5 cmol c^+ kg^{-1}, total C = 4.98 g kg^{-1}, total N = 0.59 g kg^{-1}) was previously described by Thuriès et al. (2001). 125 to 500 mg AOM in 50 g air-dried soil (AOM-C ranged from 8 to 102% of initial soil C, AOM-N from 26 to 93% of initial soil N) were incubated at 28 °C and 75% WHC. CO_2–C titrimetric measurements were made on 17 sampling occasions during six months. Organic C and total N in soil, AOM and soil + AOM mixtures were determined by dry combustion on a Fisons Instruments elemental analyser (Fisons, Crawley, UK).

Inorganic-N measurements were made at days 0, 1, 2, 5, 10, 21, 41, 90, 182 (when soil + AOM or control soil samples were removed from the incubation) according to the reference method NF–ISO 14256 (2000): (i) extraction by a KCl 1 mol l^{-1} solution, (ii) filtration through a 0.2-μm membrane and storage of filtrates at −20 °C, and (iii) determination of nitrate + nitrite and ammonium by spectrophotometric methods. In this paper, we considered total inorganic N (= ammonium + nitrate + nitrite). An aliquot of each soil + AOM sample was air dried and analysed for total N content in order to be able to estimate possible gaseous losses of N.

2.3. Data calculation and control

The inorganic N due to AOM at sampling occasion i can be written:

$$\mathrm{inorgN}_i = \frac{1}{n}\sum_{\alpha=1}^{n}(\mathrm{inorgN}_{i\alpha}^{s} - \overline{\mathrm{inorgN}_i^{c}}) \quad (1)$$

where $\mathrm{inorgN}_{i\alpha}^{s}$ and $\overline{\mathrm{inorgN}_i^{c}}$ are inorganic N at sampling occasion i and replication α for sample (soil + AOM) and mean value of soil control, respectively; n = three replicates. Net N mineralization gives a mN_i positive value, whereas N immobilization gives a negative one. All units (Remaining Added Organic C Fraction RAOCF in Eq. (3), $\mathrm{inorgN}_{i\alpha}^{s}$, $\overline{\mathrm{inorgN}_i^{c}}$, inorgN_i and total-N) were expressed as a fraction of C input (Mary et al., 1996; Whitmore and Handayanto, 1997; Henriksen and Breland, 1999b; Trinsoutrot et al., 2000b), in order to facilitate the interpretation of N fluxes from AOM by using C-to-N ratios.

For p sampling occasions with n replicates, the pooled variance of inorgN_i was:

$$s_{\mathrm{inorgN}}^2 = \frac{1}{np-p}\sum_{i=1}^{p}\sum_{\alpha=1}^{n}(\mathrm{inorgN}_{i\alpha} - \mathrm{inorgN}_i)^2 \quad (2)$$

Table 1
AOM-C application rates in the incubation experiment, TAO-C parameter values (Thuriès et al., 2001), measured C-to-N data for AOM (η_{AOM}), soluble (η_{Sol}), holocellulosic (η_{Hol}), ligneous (η_{Lig}) AOM fractions, and parameters obtained for TAO-N with Eqs. (4) and (10) hypotheses

AOM origin	AOM	g kg^{-1} soil added C	TAO-C parameters Eq. (3)		C-to-N data				TAO-N parameters with C-to-N L′, R′, S Eqs. (4)–(6)			TAO-N parameters with C-to-N AOM Eqs. (5), (6) and (10)			F test	
			P'_L	P_S	η_{AOM}	η_{Sol}	η_{Hol}	η_{Lig}	P_{im}	k_{remin}	k_v	P_{im}	k_{remin}	k_v	Eq. (11)	Eq. (11a)
Plant	Coffk	4.999	0.055	0.394	27.13	57.21	39.35	18.00	1.170	0.00099	0	1.109	0.00064	0	1.001 NS	
	Wgrap	4.667	0.070	0.624	19.64	23.92	21.56	18.46	1.156	0.00209	0	1.136	0.00181	0	1.000 NS	
	Dgrap	4.605	0.058	0.670	21.99	23.29	39.43	18.56	1.713	0.00522	0	1.514	0.00410	0		1.299 NS
	Olivp	4.426	0.048	0.531	23.78	19.97	65.22	16.00	1.814	0.00419	0	1.505	0.00337	0		1.087 NS
	Kokoa	4.072	0.278	0.482	9.62	9.14	9.53	9.97	0.981	0.00246	0.00896	0.979	0.00257	0.00890		1.001 NS
Manure	Shepm	3.230	0.064	0.422	16.99	8.43	14.87	25.27	0.900	0	0	0.871	0	0	1.010 NS	
	Chicm	3.360	0.309	0.304	6.20	2.40	31.59	14.96	0.820	0.00163	0.0120	0.572	0.00404	0.0184		1.054 NS
Animal wastes	Nfeat	1.205	0.068	0.697	3.74	3.07	5.08	3.50	0.835	0.04850	0	0.487	0.00982	0		4.310 *
	Featm	1.064	0.450	0.089	3.10	2.38	4.13	4.17	0.703	0.00466	0.00694	0.611	0.00117	0.00316		1.016 NS
	Guano	0.392	0.637	0.130	1.12	1.10	0.80	6.60	0.497	0.0413	0.05270	0.484	0.04040	0.04840		1.001 NS
Fertilizer	Gnofer	0.617	0.394	0.108	2.87	1.96	3.94	5.08	0.665	0	0	0.601	0	0		1.345 NS
	Comfer	1.735	0.261	0.613	9.87	5.45	8.78	15.66	0.772	0.00208	0	0.601	0.00475	0		1.295 NS
Compost	Compo a	2.709	0.117	0.634	12.40	5.19	13.18	16.17	0.889	0.00054	0	0.787	0.00045	0		1.005 NS
	Compo b	3.434	0.097	0.680	14.74	8.00	21.60	14.98	1.084	0.00151	0	1.116	0.00202	0		1.029 NS
	Compo e	2.505	0.034	0.869	10.66	5.45	15.18	10.70	0.532	0	0	0.448	0	0		1.027 NS
	Compo +	3.035	0.079	0.750	13.12	8.64	57.89	11.70	1.145	0.00231	0	1.168	0.00246	0	1.005 NS	
	Compo p	2.816	0.032	0.776	14.16	1.40	30.63	18.70	0.760	0.00075	0	0.208	0	0		1.124 NS

Coffk, coffee cake; Wgrap, wet grape berry pellicle cake; Dgrap, dry grape berry pellicle cake; Olivp, olive pulp; Kokoa, cocoa cake; Shepm, sheep manure; Chicm, chicken manure; Nfeat, native fine feather; Featm, feather meal; Guano, bird guano; Gnofer, guano-based industrial fertilizer; Comfer, compost-based industrial fertilizer; Compo, industrial composted amendments.

with the corresponding confidence interval: $\text{inorgN}_i \pm t^{np-p}_{0.975} s_{\text{inorgN}}$.

2.4. Mathematical model

In order to predict C mineralization, Thuriès et al. (2001) selected two models amongst the seven tested: a parallel first order two-compartment model with three parameters (*m*4), and a parallel first order three-compartment model with four parameters (*m*5). Additionally, a simplification of *m*5 was proposed: the kinetic constants of very labile (k'_{mL}) and resistant (k'_{mR}) compartments could be considered as being independent of the AOM origin. Under the controlled conditions of the incubation (28 °C, 75% WHC), the following mean values were retained: $k'_{\text{mL}} = 0.4 \pm 0.15\ \text{d}^{-1}$ (half life $T_{1/2} = 1.7$ d), $k'_{\text{mR}} = 0.012 \pm 0.003\ \text{d}^{-1}$ ($T_{1/2} = 58$ d). Thus the proposed model *m*6 needed two parameters only: the fraction P'_{L} of very labile compounds, and the fraction P_{S} of very stable ones (with a mineralization constant fixed to 0 for this six-month experiment). The fraction of intermediary resistant compounds was $P_{\text{R}} = 1 - P'_{\text{L}} - P_{\text{S}}$, and RAOCF (remaining C_{AOM} plus AOM-C transformed into microbial biomass and humus) at a given time t from input time t_0 (d) can be written:

$$\text{RAOCF} = P'_{\text{L}}\, e^{-0.4(t-t_0)} + (1 - P'_{\text{L}} - P_{\text{S}})e^{-0.012(t-t_0)} + P_{\text{S}} \quad (3)$$

Among the 17 AOMs tested in the experiment, Eq. (3) with P'_{L} and P_{S} values from Table 1, allowed us to predict RAOCF with determination coefficients of $r^2 > 99.5$ for seven series, $99 < r^2 < 99.5$ for five series, $98 < r^2 < 99$ for two series, and $93 < r^2 < 98$ for the three animal AOMs, i.e. Guano, Featm and Nfeat (best predicted with *m*4).

Let η_{L}, η_{R}, η_{S} be the C-to-N ratios of very labile, resistant and stable AOM-compartments, respectively; the remaining added organic N fraction (RAONF) can be expressed as:

$$\text{RAONF} = \frac{P'_{\text{L}}}{\eta_{\text{L}}} e^{-0.4(t-t_0)} + \frac{1 - P'_{\text{L}} - P_{\text{S}}}{\eta_{\text{R}}} e^{-0.012(t-t_0)} + \frac{P_{\text{S}}}{\eta_{\text{S}}} \quad (4)$$

The transformed (mineralized or immobilized) added organic N fraction (TAONF) can then be expressed from the total C (= 1 in this data, all values of C and N expressed as a fraction of initial C content) and C-to-N ratio of AOM (η_{AOM}) by:

$$\text{TAONF} = \frac{1}{\eta_{\text{AOM}}} - \text{RAONF} \quad (5)$$

In the proposed TAO model (Fig. 1), the fraction P_{im} splits the TAONF into 2 compartments: immobilized N (imN = P_{im} TAONF) and mineralized N (inorgN = $(1 - P_{\text{im}})$ TAONF). Additionally, imN could be re-mineralized

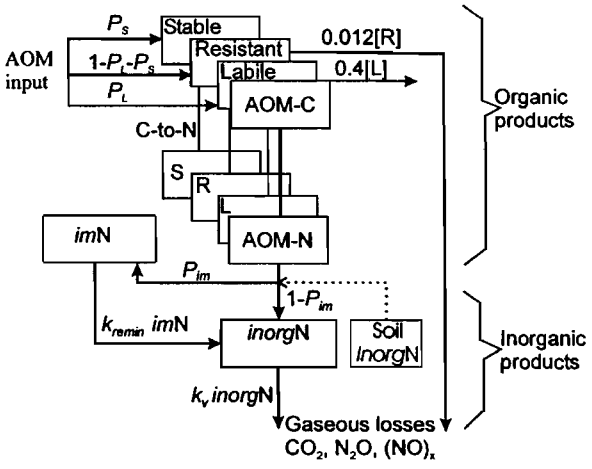

Fig. 1. The model TAO (Transformation of Added Organics, *Transformation des Apports Organiques*) for C mineralization, N mineralization, N immobilization and N volatilization of Added Organic Matters (AOM) in soil: inorgN, inorganic N from AOM; imN, immobilized N from AOM (and Soil-Inorg N if $P_{\text{im}} > 1$).

(decomposition of microbial cells) and inorgN could be partly volatilized according to first order kinetics, the complete equations become:

$$\text{inorgN} = (1 - P_{\text{im}})\text{TAONF} + \int_{t_0}^{t} \text{imN}\, k_{\text{remin}}\, dt - \int_{t_0}^{t} \text{inorgN}\, k_v\, dt \quad (6)$$

$$\text{imN} = P_{\text{im}}\,\text{TAONF} - \int_{t_0}^{t} \text{imN}\, k_{\text{remin}}\, dt \quad \text{for } t > t_0 \quad (6a)$$

otherwise inorgN = initial $\text{inorgN}_{\text{AOM}}$ and imN = 0 for $t = t_0$

When $k_{\text{remin}} = k_v = 0$, the system is entirely governed by the fraction P_{im}, and the two fractions P'_{L} and P_{S} from C mineralization curves. The curves TAONF, imN and inorgN are thus parallel. If the inorgN slope becomes greater than the TAONF slope, then k_{remin} must be greater than 0. If the inorgN slope becomes lower than the TAONF one, then N losses occur and k_v becomes greater than zero. A system where P_{im}, k_{remin} and k_v have simultaneously positive values is in active transformation with a phase of gaseous N losses from inorgN and maintenance of inorgN level from imN and organic N_{AOM}. By these transfer processes, losses of inorgN give losses of total N from AOM. Conversely, a system where $P_{\text{im}} = k_{\text{remin}} = k_v = 0$ is a system where only N mineralization occurs from initial AOM without any N immobilization or N volatilization. In a system where $P_{\text{im}} = 1$, the AOM organic N is entirely re-organized into SOM which mineralizes according to the k_{remin} value. In a system where $P_{\text{im}} > 1$, N immobilization is greater than TAONF; this system immobilizes all TAONF plus a part ($P_{\text{im}} - 1$) of the inorganic N from soil origin (expressed in the AOM-N unit).

Sensitivity analysis showed a linear response of predicted inorgN to change of parameters P_{im}, k_{remin} or k_v (data not shown). The P_{im} parameter had the greatest influence on inorgN, especially when P_{im} was used alone ($k_{remin} = k_v = 0$). For example, in the Shepm prediction with P_{im} alone ($P_{im} = 0.87$, Table 1), a random normal distribution of P_{im} with a relative standard deviation of 1% gave a random normal distribution of inorgN at 210 d with 10% RSD. A less accurate simulation could be performed with a positive value for the three parameters ($P_{im} = 0.81$, $k_{remin} = 0.0021$, $k_v = 0.016$), but the model predictions were more stable: a 1% RSD for P_{im} gave 5% and <1% RSD for inorgN predictions at 90 and 210 d, respectively. The fluctuations of inorgN predictions to P_{im} changes were the greatest for the maximum or minimum values of inorgN curves. The predictions were less sensitive to k_{remin} or k_v fluctuations, with the greatest changes at the end of the incubation.

2.5. Model calculations

The P'_L and P_S parameters (Eqs. (3) and (4); Table 1) were given by Thuriès et al. (2001). As a first step, we calculated RAONF Eq. (4) with $\eta_{L'}$, η_R, η_S assimilated to C-to-N data η_{Sol}, η_{Hol}, and η_{Lig}, respectively. These data must be checked (and if necessary η_{Hol} recalculated) according to the balance Eq. (7):

$$\frac{1}{\eta_{AOM}} = \frac{P'_L}{\eta'_L} + \frac{P_R}{\eta_R} + \frac{P_S}{\eta_s} \tag{7}$$

TAONF was then calculated according to Eq. (5). The prediction of inorgN required the optimization of P_{im} only and, if necessary, k_{remin} and/or k_v (Eq. (6)). It was performed by Powell's method with the minimized criterion:

$$RSS = \sum_j (y_j - \hat{y}_j)^2 \tag{8}$$

where y_j and $\hat{y}_j$ were data measurement and prediction of inorgN, respectively, at sampling occasion j. The alternative consisted of considering total N data with the minimized criterion:

$$RSSt = \sum_{k=1}^{2} p_k^2 \sum_j (y_{kj} - \hat{y}_{kj})^2 \tag{9}$$

where k identified the data series (inorgN or total added N) associated with a weight coefficient p_k. The two possibilities were tested, and the first (Eq. (8)) then retained (similar accuracy; inorgN measurements more repeatable than total N ones). Although total added N data were not taken into account in the calculations, the predictions obtained were in accordance with these data. Hence, total added N data was used to validate the TAO approach.

In a second step, RAONF was calculated without the use of η_L, η_R, η_S determinations, C-to-N ratios of compartments L, R, S being equal to η_{AOM}. Eq. (4) became:

$$RAONF = \frac{1}{\eta_{AOM}}(P'_L\, e^{-0.4(t-t_0)} + (1 - P'_L - P_S)e^{-0.012(t-t_0)} + P_S) \tag{10}$$

with the other calculations remaining unchanged. Comparisons of the two methods were made by the test:

$$F = \frac{RSS_4}{RSS_{10}} \quad \text{if } RSS_4 > RSS_{10} \tag{11}$$

$$\text{else } F = \frac{RSS_{10}}{RSS_4} \quad \text{if } RSS_{10} > RSS_4, \tag{11a}$$

RSS_4 and RSS_{10} being RSS (Eq. (8)) with first (Eq. 4) and second (Eq. (10)) calculations, respectively.

3. Results

3.1. Classification of inputs according to inorganic-N production

Fig. 2 presents N-rich AOM incubation data showing net positive mineralization flux and positive rates of mineralization (slope). After six months of incubation, net mineralized N represented about 27% of total AOM-N for the two organic fertilizers Gnofer (C-to-N = 2.9) and Comfer (C-to-N = 9.9), 22% for Nfeat (animal waste, C-to-N = 3.7), and 11% for Shepm (manure = plant + animal origin, C-to-N = 17). The mineralized N decreased whereas C-to-N ratios increased, but there was no significant relationship. In contrast with the results of Thiénot (1991) and Corbeels et al. (1999), Shepm did not show a net N immobilization. The fraction of mineralized N was almost the same for the two organic fertilizers, and was higher than that for Nfeat and Shepm. The expected difference between the two fertilizers was shown. The guano-based fertilizer (Gnofer) mineralized 26% of its N during the first month of incubation, this level remaining stable during the following five months. The compost-based fertilizer (Comfer) mineralized about 10% of its N contact during the first week, the mineralization increasing afterwards linearly with the incubation time.

Fig. 3 shows the inorganic N immobilization by N-poor plant debris which has often been observed (Quemada and Cabrera, 1995; Trenbath and Diggle, 1998; Mueller et al., 1998; Henriksen and Breland, 1999b; Trinsoutrot et al., 2000b). From this incubation data at 180 d, the C-to-N threshold for mineralization/immobilization (Whitmore and Handayanto, 1997) was found to be ca. 19. All the AOM in Fig. 3, with C-to-N ranging from 19.6 (Wgrap) to 27.1 (Coffk), induced a marked N immobilization. The particular behaviour of Kokoa (Fig. 5), an AOM of plant origin, could be partly explained by its low C-to-N value (Table 1). Negative values of inorgN were observed during

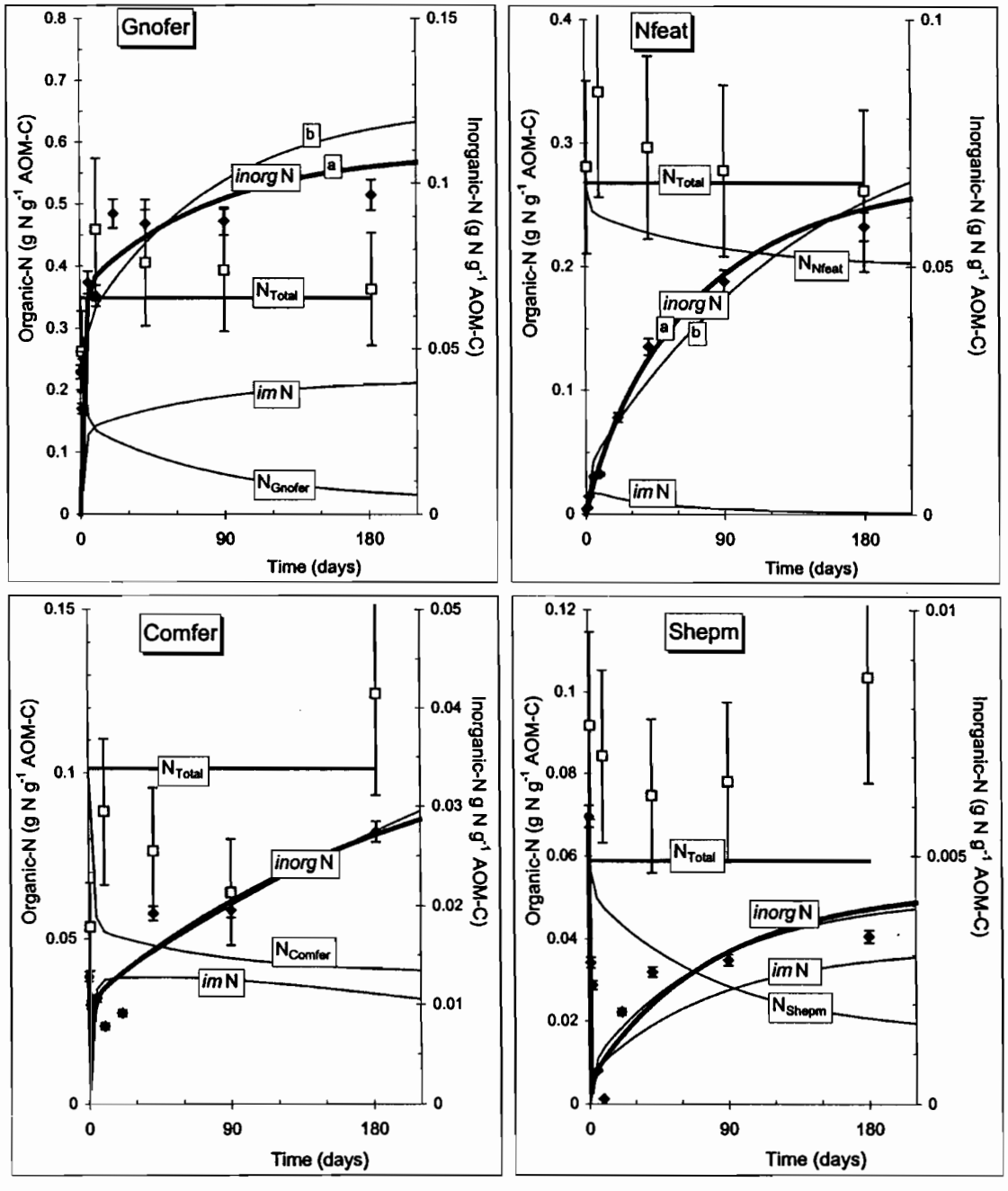

Fig. 2. Mineralization and immobilization of N from guano-based fertilizer (Gnofer), native fine feather (Nfeat), compost-based fertilizer (Comfer), sheep manure (Shepm). Points = experimental data with 95% confidence intervals (◆, inorgN from AOM; □, total N from AOM) continuous lines = TAO predictions of inorgN (bold lines: a, prediction with C-to-N of fractions; b, predictions with C-to-N_{AOM}), remaining N_{AOM} and immobilized N (thin lines).

6 months for Olivp and Coffk, 4 months for Wgrap and 5 months for Dgrap, respectively. All the inorganic N (from soil + AOM, Tot.inorg.N in Fig. 3) was immobilized within 3 months for Olivp and Coffk, and 1.5 months for Wgrap and Dgrap. In comparison, immobilization for the olive pulp studied by Thomson and Nogales (1999) lasted 3 months.

At 180 d, mineralized-N from composts (Fig. 4) represented 9% of total AOM-N for Compo a (mixture at composting time ct = 0), 4% for Compo b (ct = 41 d), 7% for Compo e (ct = 305 d), and 15% for Compo p (ct = 185 d). Immobilization of N is known to depend on the degree of composting (Bernal et al., 1998) but no clear relationship was found. Compo b and Compo + (mixture of

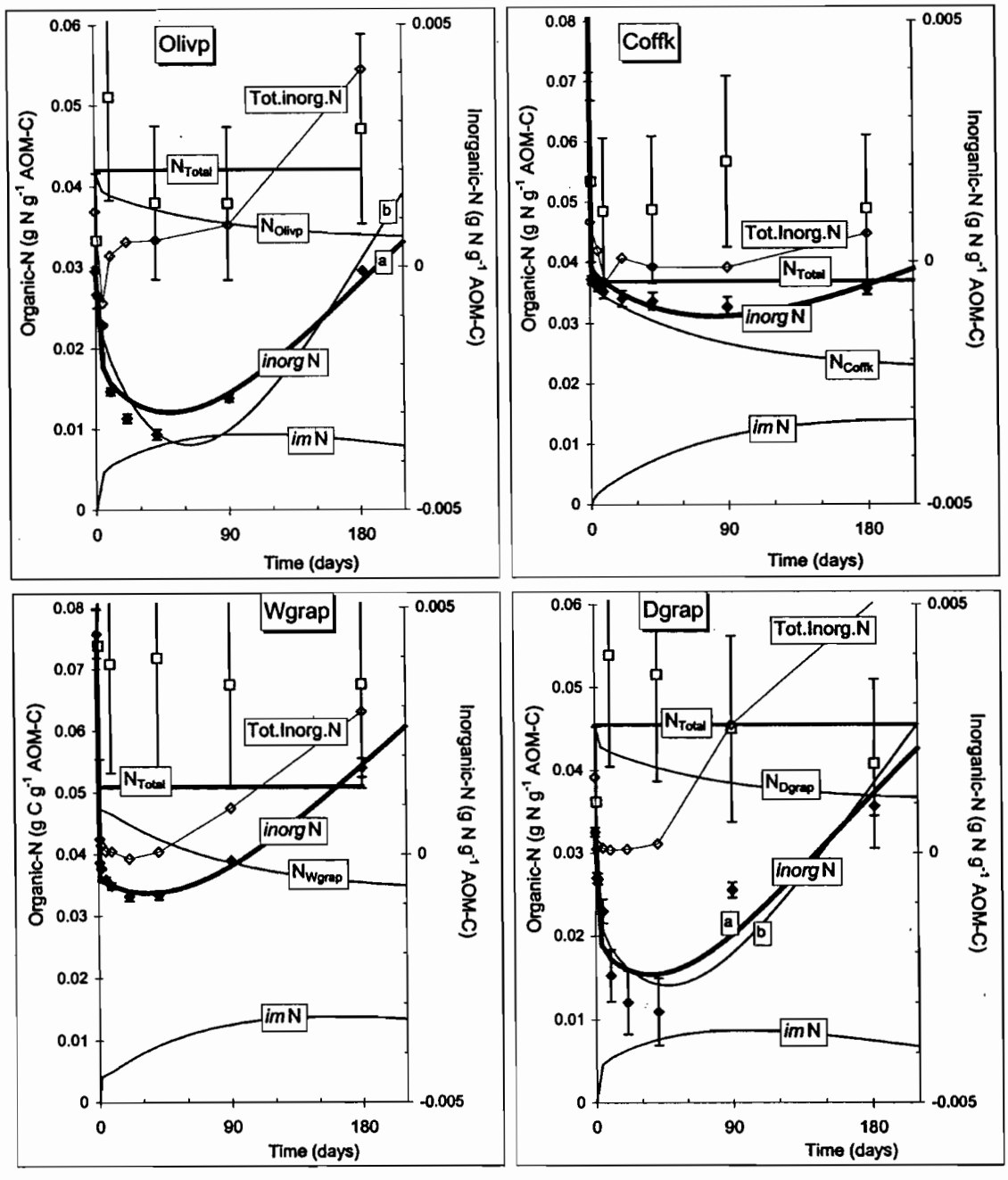

Fig. 3. Mineralization and immobilization of nitrogen from plant-originated AOM: olive pulp (Olivp), coffee cake (Coffk), wet grape berry pellicle cake (Wgrap) and dry grape berry pellicle cake (Dgrap). Points = experimental data with 95% confidence intervals (◆, inorgN from AOM; ◇, total (soil + AOM) inorganic N; □, total N from AOM) continuous lines = TAO predictions of inorgN (bold lines: a, prediction with C-to-N of fractions; b, predictions with C-to-N_{AOM}), immobilized N (imN) and remaining N_{AOM} (thin lines).

75% Compo e and 25% Dgrap, curve not shown) induced an inorgN immobilization during the first two months followed by a net inorgN production.

Fig. 5 shows the inorgN curves of three N-rich animal AOM (Guano, Featm and Chicm), and an atypical N-rich plant residue (Kokoa) which could have lost gaseous N during the experiment. Estimated gaseous losses were particularly evident for Guano: 30% of its N mineralized during the first month of incubation, with only 1% remaining as inorganic N after 6 months (Fig. 5). Rubins and Bear

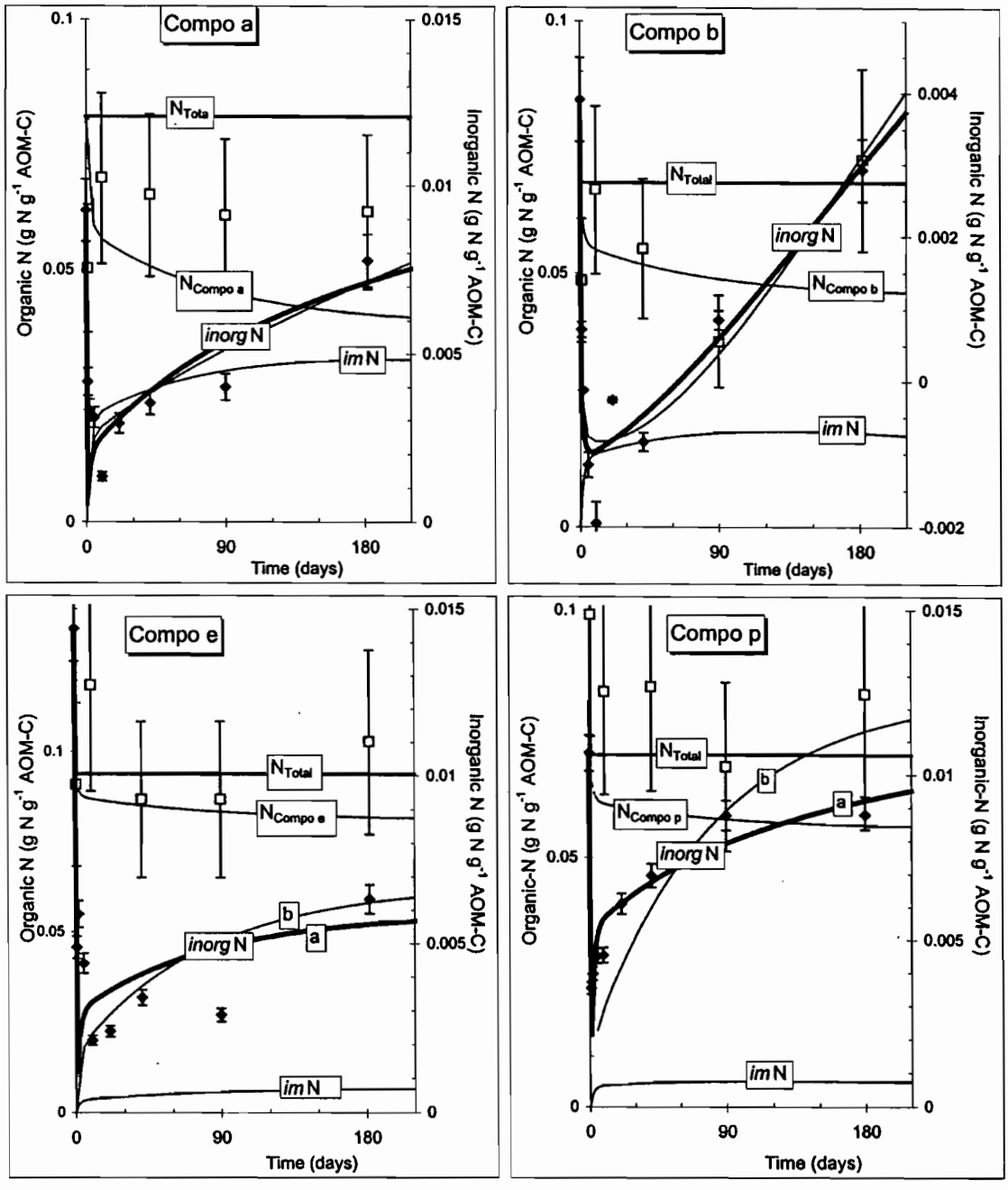

Fig. 4. Mineralization and immobilization of N from composts. Points = experimental data with 95% confidence intervals (◆, inorgN; □, total N from AOM) continuous lines = TAO predictions of inorgN (bold lines: a, prediction with C-to-N of fractions; b, predictions with C-to-N_{AOM}), immobilized N (imN) and remaining N_{AOM} (thin lines).

(1942) and Leclerc (1990) showed that 80 and 60–93% guano-N, respectively, were transformed in NO_3-N in leachates. The removal of NO_3 by leaching was not studied in this experimental design. Total gaseous losses estimated by difference from N_{Total} analyses were about 90% of added N for Guano, and 30% for Chicm. Similar losses for chicken manure were observed by Mahimairaja et al. (1994) and Gagnon and Simard (1999). Gaseous N loss was not demonstrated for Kokoa (quantified to about 10%, i.e. within experimental error) and Featm (about 20%). This experiment highlighted the stabilization effect of the industrial process used to produce the organic fertilizer Gnofer (Fig. 2) by

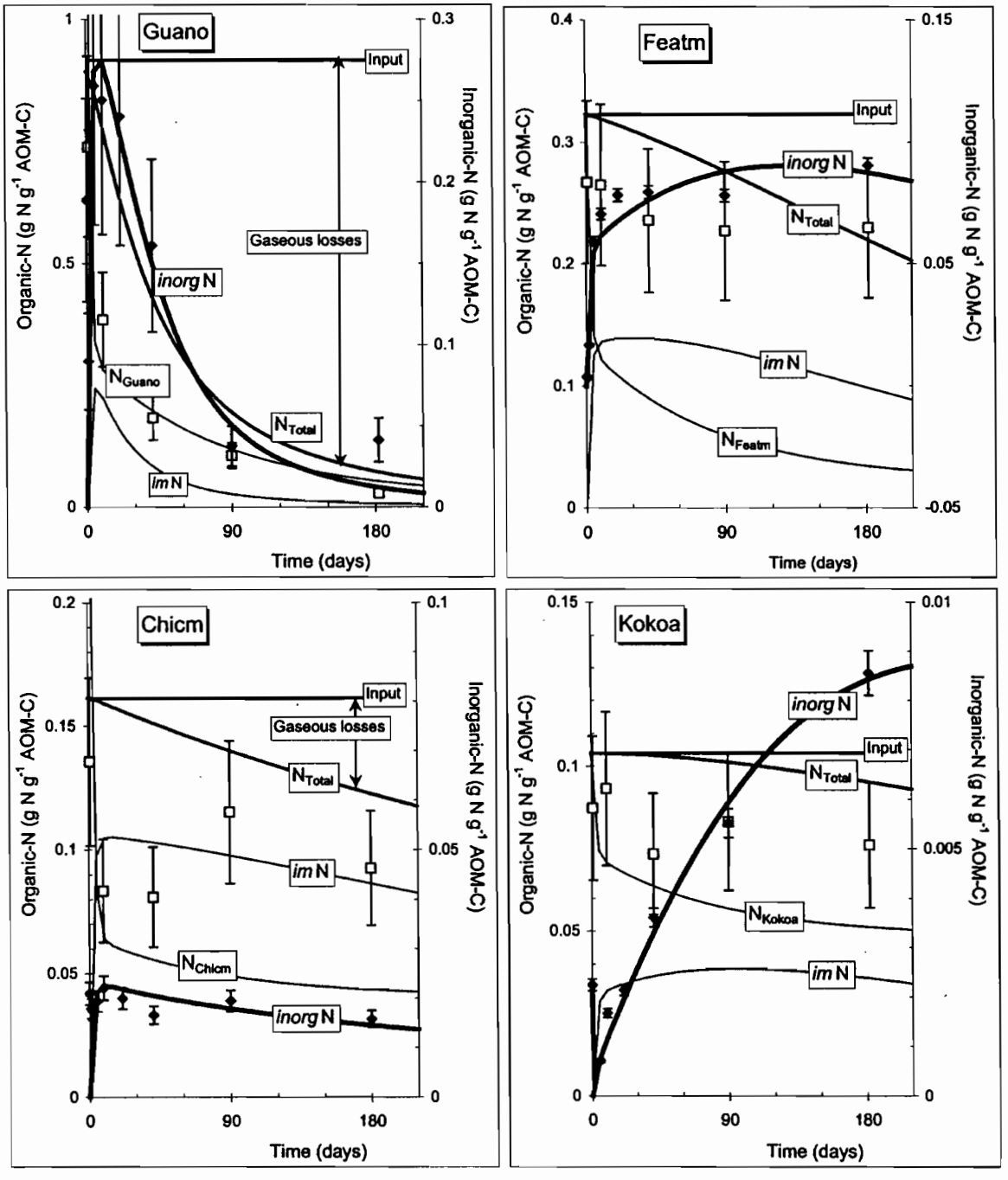

Fig. 5. Mineralization, immobilization and gaseous losses of N from (i) animal-originated AOM: guano (Guano), feather meal (Featm), chicken manure (Chicm), and (ii) plant-originated AOM: cocoa cake (Kokoa). Points = experimental data with 95% confidence intervals (◆, inorgN; □, total N from AOM) continuous lines = TAO predictions of inorgN (bold lines), remaining N_{AOM}, immobilized N (imN) and N_{Total} from AOM (thin lines).

the addition of N-poor plant residues (Wgrap and Olivp) to Guano. The same effect was observed by Mahimairaja et al. (1994) when mixing chicken manure with wheat straw. These are usefull processes for avoiding N volatilization (compare Gnofer, Fig. 2, and Guano, Fig. 5).

3.2. Predictions made with C-to-N ratios of biochemical fractions

All the TAO-inorgN predictions were in good accordance with the data (Figs. 2–5). AOM-N transformations

could be predicted for 4 materials using P_{im} only (Table 1): Shepm, Gnofer, Compo e, Compo p. Let N_{AOM} be the remaining untransformed N in AOM (N_{Nfeat} and N_{Shepm} in Fig. 2, $N_{Compo\ e}$ and $N_{Compo\ p}$ in Fig. 4) and N_{Total} the N input from AOM, at any incubation time the curves were plotted in accordance with the balance equation:

$$N_{Total} - N_{AOM} = inorgN + imN \quad (12)$$

N transformations were predicted for 9 AOM, only with the two N-parameters P_{im} and k_{remin} (Table 1): four plant residues (Fig. 3), the animal residue Nfeat, the fertilizer Comfer (Fig. 2) and three composts (Fig. 4). In these cases, the slope of imN decreased when k_{remin} increased. In this experiment, the highest k_{remin} value was found for Nfeat which explained the strong decrease of imN for this AOM (Fig. 2); after three months of incubation, the balance relationship (Eq. (12)) became: $inorgN = N_{Total} - N_{Nfeat}$. All transformed N was mineralized.

The four other AOM required the three TAO parameters P_{im}, k_{remin} and k_v: three animal N-rich residues Guano, Featm and Chicm, and the atypical plant residue Kokoa (Fig. 5). The highest k_v value was found for Guano with also a high k_{remin} value. Guano presented the highest fraction of very labile compounds and a small fraction of stable compounds (see P'_L and P_S values, Table 1). It was thus rapidly decomposed (see N_{Guano} in Fig. 5) into unstable N forms. Important gaseous N-losses occurred from inorgN, this compartment being supplied by further mineralization of imN. By these transfer processes, almost all N was lost under gaseous forms at the end of the incubation (Fig. 5), although Guano represented the highest N-input.

3.3. Predictions using C-to-N ratios of AOM

For 13 of the 17 AOM tested, F tests (Table 1, Eqs. (11) and (11a)) showed $RSS_{10} > RSS_4$. The predictions with C-to-N ratios of biochemical fractions thus tended to be better than predictions made with C-to-N_{AOM} solely, the difference being significant for Nfeat only. In the four other cases ($RSS_4 > RSS_{10}$), there were no significant differences. The inorgN predictions by the two methods were plotted in Figs. 2–5. The two simulations were almost similar for Comfer and for Shepm, but slightly different for Gnofer and for Nfeat (Fig. 2). There was only a significant difference for Nfeat because the predictions with biochemical fractions were very close to the data. The two simulations were identical for Coffk and for Wgrap and slightly different for Olivp and for Dgrap (Fig. 3), but the differences were not significant and did not modify the predicted duration and amounts of inorgN immobilization. As for composts, the two methods gave almost the same predictions except for Compo p (Fig. 4), but the difference was not significant. For the four AOM with N-losses, the predictions made with the two methods were identical (Fig. 5).

4. Discussion

4.1. Decomposition and immobilization

Decomposition of AOM was based on C evolution (Eqs. 3 and 4): P_S (Table 1) defined the stable non-transformed N_{AOM}, the rate of transformation (slope of N_{AOM} curve) was related to P'_L and P_R (Table 1, $P'_R = 1 - P'_L - P_S$). The lowest P_S values, for Featm, Guano and Gnofer, showed the lowest remaining N_{AOM} and a high value of imN (only during the first stage, before volatilization for Guano). Most AOM from plant origin, composts and Nfeat displayed high P_S values together with high remaining N_{AOM} levels and low N immobilization. Compo e and Compo p, with the longest composting times, presented the highest P_S value, high N_{AOM} and low imN levels. The fertilizer Gnofer mineralized more rapidly than Comfer during the early stages ($P'_L = 0.39$ and 0.26, respectively). During the later stages, further Gnofer mineralization and immobilization occurred, resulting from the decomposition of the N_{Gnofer} resistant compounds ($P'_R = 0.49$, $k_{remin} = 0$). A more constant mineralization of Comfer from imN ($P'_R = 0.12$, $k_{remin} = 0.0048$) displayed a more regular pattern.

4.2. C-to-N ratios and transformations of AOM

Predictions made with η_L, η_R and η_S of the first hypothesis (Eq. (4)) were close to those made with η_{AOM} of the second hypothesis (Eq. (10)). This represented a technical advantage since the later required C-to-N_{AOM} ratios only. Significant correlations were often reported between mineralized-N and C-to-N_{AOM} ratios (Frankenberger and Abdelmagid, 1985; Quemada and Cabrera, 1995; Trinsoutrot et al., 2000a). The model proposed by Nicolardot et al. (2001) was also based on C-to-N_{AOM} data. Although the first hypothesis was more logical (Eq. (4)), the correspondences between theoretical and measured fractions (labile-soluble, resistant-holocellulosic, stable-ligneous) remained to be proved. Chesson (1997) considered the soluble fraction as a sum of polysaccharides (poor in N) plus soluble proteins of low molecular weight (very rich in N). On the other hand, as lignin is known to be the least biodegradable plant polymer (Melillo et al., 1982; Heal et al., 1997), ligno-protein N should represent the most recalcitrant part of N_{AOM}.

In order to explain how the two hypotheses were linked (Eqs. (4) and (10)), one should consider the relationships existing between all the C-to-N values. First, these values were linked by the balance Eq. (7). Three significant relationships were computed from Table 1: $\eta_{Sol} \cong 0.05 \times \eta^2_{AOM}$, $\eta_{Hol} \cong 2\eta_{AOM}$, $\eta_{Lig} \cong 1.8\eta_{AOM} - 0.04\,\eta^2_{AOM}$. From these relationships (curves not shown), $\eta_{Sol} < \eta_{AOM}$ for $\eta_{AOM} < 20$ ($\eta_{Sol} \leq 5$ for $\eta_{AOM} \leq 10$, $\eta_{Sol} \leq 10$ for $\eta_{AOM} \leq 20$), otherwise $\eta_{Sol} > \eta_{AOM}$ for $\eta_{AOM} > 20$. Most soluble compounds were probably proteinaceous molecules for N-rich AOM, and polysaccharides for N-poor ones.

The curvature of η_{Lig} predictions was inverse to that of η_{Sol} (not shown). For $\eta_{AOM} < 15$, $\eta_{Lig} \cong \eta_{AOM}$ otherwise for $\eta_{AOM} > 15$, the slope of η_{Lig} predictions decreased, and η_{Lig} tended to $\cong 18$. This maximum value occurred with plant-originated AOM of C-to-N $\cong$ 19–27. It could be indicative of the minimum N content required for stabilizing ligno-proteinaceous macromolecules. Trinsoutrot et al. (2000b) reported a lignin C-to-N $\cong$ 21 for C-to-$N_{AOM} \cong 22–26$. The η_{Hol} values showed the greatest variability but were generally higher than η_{Sol} and η_{Lig}, in accordance with their hemicellulose- and cellulose-like molecular structures.

For the calculation of the stable N fraction, the two predictive methods (Eqs. (4) and (10)) used P_S (Eq. (3)) first. The stable fractions were P_S/η_{Lig} and P_S/η_{AOM} in Eqs. (4) and (10), respectively. Since these two fractions were not very different, the predicted level of TAONF was similar with the two methods. The main differences concerned the slopes of the predictive curves governed by the relative values of P'_L/η_L and P'_L/η_{AOM} on one hand, P'_R/η_R and P'_R/η_{AOM} on the other hand. Although the F-test (Eqs. (11) and (11a)) was only significant for Nfeat (Table 1), Figs. 2–5 showed a good agreement with the shape of measured data by the first method ('a' in Figs. 2–4) for some AOM: Gnofer, Nfeat, Olivp, Dgrap, Compo p. The first hypothesis was therefore validated and the second hypothesis was a good approximation of the former one in all the cases tested.

4.3. Conclusions

The TAO (Transformation of Added Organics) model was proposed in this paper as a predictive tool for C mineralization, N mineralization, N immobilization, and N volatilization from added AOM, without taking into account the native SOM. The interest of this work was to relate the TAO-N version to the TAO-C one, which employs the C-to-N ratio of the AOM. The transformed N_{AOM} fraction (TAONF) was higher than the mineralized AOM. In TAO, the split parameter P_{im} allowed us to partition TAONF between mineralized N and immobilized N. A value $P_{im} > 1$ indicated a total immobilization of TAONF, plus a further immobilization ($P_{im} - 1$) of soil inorganic N. The first order kinetic parameter k_{remin} was used according to the AOM type, for regulating a further mineralization from immobilized N. The two parameters P_{im} and k_{remin} were sufficient for predicting various properties of a large range of organic fertilizers. For some AOM with high N content (animal wastes), another first order kinetic parameter k_v was sometimes introduced for predicting a volatilization from N_{AOM}. All the predictions were in good agreement with the data collected from very different AOM: plant residues, manures, animal wastes, organic fertilizers, and amendments.

Acknowledgements

This work was partly granted by a CIFRE convention. The authors gratefully acknowledge Prs J.C. Rémy and P. Herrmann (ENSA-Montpellier, France), Dr M. Viel (Phalippou-Frayssinet S.A., Rouairoux, France), Dr P. Bottner (CNRS Montpellier, France), Drs M.C. Larré-Larrouy and C. Feller (IRD Montpellier, France) for helpful discussions.

References

Addiscott, T.M., 1983. Kinetics and temperature relationships of mineralization and nitrification in Rothamsted soils with differing histories. Journal of Soil Science 34, 343–353.

Bernal, M.P., Navarro, A.F., Sanchez-Monedero, M.A., Roig, A., Cegarra, J., 1998. Influence of sewage sludge compost stability and maturity on carbon and nitrogen mineralization in soil. Soil Biology & Biochemistry 30, 305–313.

Bloemhof, H.S., Berendse, F., 1995. Simulation of the decomposition and nitrogen mineralization of aboveground plant material in two unfertilized grassland ecosystems. Plant and Soil 177, 157–173.

Bosatta, E., Ågren, G.I., 1985. Theoretical analysis of decomposition of heterogeneous substrates. Soil Biology & Biochemistry 17, 601–610.

Bradbury, N.J., Whitmore, A.P., Hart, P.B.S., Jenkinson, D.S., 1993. Modelling the fate of nitrogen in crop and soil in the years following application of ^{15}N labelled fertilizer to winter wheat. Journal of Agricultural Science 121, 363–379.

Broadbent, F.E., 1986. Empirical modelling of soil nitrogen mineralization. Soil Science 141, 208–213.

Chesson, A., 1997. Plant degradation by ruminants: parallels with litter decomposition in soils. In: Cadish, G., Giller, K.E. (Eds.), Driven by Nature, Plant Litter Quality and Decomposition, CAB International, Wallingford, pp. 47–66.

Corbeels, M., Hofman, G., Van Cleemput, O., 1999. Simulation of net N immobilization and mineralization on substrate-amended soils by the NCSOIL computer model. Biology and Fertility of Soils 28, 422–430.

Deans, J.R., Molina, J.A.E., Clapp, C.E., 1986. Models for predicting potentially mineralizable nitrogen and decomposition rate constants. Soil Science Society of America Journal 50, 323–326.

Dendooven, L., Merckx, R., Verstraeten, L.M.J., Vlassak, K., 1997. Failure of an iterative curve-fitting procedure to successfully estimate two organic N pools. Plant and Soil 195, 121–128.

Frankenberger, W.T., Abdelmagid, H.M., 1985. Kinetic parameters of nitrogen mineralisation rate of leguminous crops incorporated into soil. Plant and Soil 87, 257–271.

Gagnon, B., Simard, R.R., 1999. Nitrogen and phosphorus release from on-farm and industrial composts. Canadian Journal of Soil Science 79, 481–489.

Hadas, A., Portnoy, R., 1994. Nitrogen and carbon mineralization rates of composted manures incubated in soil. Journal of Environmental Quality 23, 1184–1189.

Hadas, A., Portnoy, R., 1997. Rates of decomposition in soil and release of available nitrogen from cattle manure and municipal waste composts. Compost Science and Utilization 5, 48–54.

Hansen, S., Jensen, H.E., Nielsen, N.E., Svendsen, H., 1991. Simulation of nitrogen dynamics and biomass production in winter wheat using the Danish simulation model Daisy. Fertilizer Research 27, 245–259.

Heal, O.W., Anderson, J.M., Swift, M.J., 1997. Plant litter quality and decomposition: an historical overview. In: Cadish, G., Giller, K.E. (Eds.), Driven by Nature, Plant Litter Quality and Decomposition, CAB International, Wallingford, pp. 3–30.

Hébert, M., Karam, A., Parent, L.E., 1991. Mineralization of nitrogen and carbon in soils amended with composted manure. Biological Agriculture and Horticulture 7, 349–361.

Henriksen, T.M., Breland, T.A., 1999a. Nitrogen availability effects on carbon mineralization, fungal and bacterial growth, and enzyme activities during decomposition of wheat straw in soil. Soil Biology & Biochemistry 31, 1121–1134.

Henriksen, T.M., Breland, T.A., 1999b. Evaluation of criteria for describing crop residue degradability in a model of carbon and nitrogen turnover in soil. Soil Biology & Biochemistry 31, 1135–1149.

Jans-Hammermeister, D.C., McGill, W.B., 1997. Evaluation of three simulation models used to describe plant residue decomposition in soil. Ecological Modelling 104, 1–13.

Janzen, H.H., Kucey, R.M.N., 1988. C, N and S mineralization of crop residue as influenced by crop species and nutrient regime. Plant and Soil 100, 35–41.

Jedidi, N., Van Cleemput, O., Mhiri, A., 1995. Quantification of nitrogen mineralization and immobilization in soil in the presence of organic amendments. Canadian Journal of Soil Science 75, 85–91.

Jensen, E.S., 1994. Mineralization immobilization of nitrogen in soil amended with low C–N ratio plant residues with different particle sizes. Soil Biology & Biochemistry 26, 519–521.

Kaboneka, S., Sabbe, W.E., Mauromoustakos, A., 1997. Carbon decomposition kinetics and nitrogen mineralization from corn, soybean, and wheat residues. Communications in Soil Science and Plant Analysis 28, 1359–1373.

Leclerc, B., 1990. Vitesse de minéralisation de l'azote des fertilisants organiques. Proceedings Les journées techniques de l'agriculture biologique, 12–14 December Avignon, ACB-GRAB, pp. 172–177.

Mahimairaja, S., Bolan, N.S., Hedley, M.J., Macgregor, A.N., 1994. Losses and transformation of nitrogen during composting of poultry manure with different amendments–An incubation experiment. Bioresource Technology 47, 265–273.

Mahimairaja, S., Bolan, N.S., Hedley, M.J., 1995. Denitrification losses of N from fresh and composted manures. Soil Biology & Biochemistry 27, 1223–1225.

Mary, B., Recous, S., Darwis, D., Robin, D., 1996. Interactions between decomposition of plant residues and nitrogen cycling in soil. Plant and Soil 181, 71–82.

Mary, B., Recous, S., Robin, D., 1998. A model for calculating nitrogen fluxes in soil using N-15 tracing. Soil Biology & Biochemistry 30, 1963–1979.

Matus, F.J., Rodriguez, J., 1994. A simple model for estimating the contribution of nitrogen mineralization to the nitrogen supply of crops from a stabilized pool of soil organic matter and recent organic input. Plant and Soil 162, 259–271.

Melillo, J.M., Aber, J.D., Muratore, J.F., 1982. Nitrogen and lignin control of hardwood leaf litter decomposition dynamics. Ecology 63, 621–626.

Molina, J.A.E., Clapp, C.E., Shaffer, M.J., Chichester, F.W., Larson, W.E., 1983. NCSOIL, a model of nitrogen and carbon transformations in soils: description, calibration, and behavior. Soil Science Society of America Journal 47, 85–91.

Mueller, T., Jensen, L.S., Nielsen, N.E., Magid, J., 1998. Turnover of carbon and nitrogen in a sandy loam soil following incorporation of chopped maize plants, barley straw and blue grass in the field. Soil Biology & Biochemistry 30, 561–571.

NF-ISO 14256, 2000. Dosage des nitrates, des nitrites et de l'ammonium dans les sols humides par extraction avec une solution de chlorure de potassium. Qualité des Sols. AFNOR, Paris, X31-423-2.

Nicolardot, B., Recous, S., Mary, B., 2001. Simulation of C and N mineralisation during crop residue decomposition: a simple dynamic model based on the C:N ratio of the residues. Plant and Soil 228, 83–103.

Nordmeyer, H., Richter, J., 1985. Incubation experiments on nitrogen mineralization in loess and sandy soils. Plant and Soil 83, 433–445.

Pansu, M., Sallih, Z., Bottner, P., 1998. A process-based model for carbon and nitrogen transfers in soil organic matter. Proceedings of the 16th World Congress of Soil Science, 20–26 August 1998, Montpellier, France, ISSS-AISS-IBG-SICS-AFES (CD-ROM), Symp. 7, 883-t.pdf, 7 pp.

Pansu, M., Sallih, Z., Bottner, P., 1998b. Modelling of soil nitrogen forms after organic amendments under controlled conditions. Soil Biology & Biochemistry 30, 19–29.

Paré, T., Dinel, H., Schnitzer, M., Dumontet, S., 1998. Transformations of carbon and nitrogen during composting of animal manure and shredded paper. Biology and Fertility of Soils 26, 173–178.

Parton, W.J., Schimel, D.S., Cole, C.V., Ojima, D.S., 1987. Analysis of factors controlling soil organic matter levels in Great Plains grasslands. Soil Science Society of America Journal 51, 1173–1179.

Quemada, M., Cabrera, M.L., 1995. Carbon and nitrogen mineralized from leaves and stems of four cover crops. Soil Science Society of America Journal 59, 471–477.

Rubins, E.J., Bear, F.E., 1942. Carbon-nitrogen ratios in organic fertilizer materials in relation to the availability of their nitrogen. Soil Science 54, 411–423.

Sørensen, P., Jensen, E.S., 1995. Mineralization of carbon and nitrogen from fresh and anaerobically stored sheep manure in soils of different texture. Biology and Fertility of Soils 19, 29–35.

Stanford, G., Smith, S.J., 1972. Nitrogen mineralization potentials of soils. Soil Science Society of America Proceedings 36, 465–472.

Thiénot, F., 1991. Etude de la minéralisation de l'azote de différents fertilisants organiques. Proceedings Les journées techniques de l'agriculture biologique, 28–29 November, Agen, GRAB-ITAB-CIVAMBIO, pp. 78–83.

Thompson, R.B., Nogales, R., 1999. Nitrogen and carbon mineralization in soil of vermi-composted and unprocessed dry olive cake (orujo seco) produced from two-stage centrifugation for olive oil extraction. Journal of Environmental Science and Health 34, 917–928.

Thuriès, L., Pansu, M., Feller, C., Herrmann, P., Rémy, J.-C., 2001. Kinetics of added organic matter decomposition in a Mediterranean sandy soil. Soil Biology & Biochemistry 33, 997–1010.

Thuriès, L., Pansu, M., Larré-Larrouy, M.-C., Feller, C., 2002. Biochemical composition of organic materials in relation with their mineralization in a sandy soil. Soil Biology & Biochemistry 34, 239–250.

Trenbath, B.R., Diggle, A.J., 1998. An interpretative model of carbon and nitrogen transformations applied to a residue incubation experiment. Australian Journal of Agricultural Research 49, 537–553.

Trinsoutrot, I., Recous, S., Bentz, B., Linères, M., Chèneby, D., Nicolardot, B., 2000a. Biochemical quality of crop residues and carbon and nitrogen mineralization kinetics under nonlimiting nitrogen conditions. Soil Science Society of America Journal 64, 918–926.

Trinsoutrot, I., Recous, S., Mary, B., Nicolardot, B., 2000b. C and N fluxes of decomposing C-13 and N-15 *Brassica napus* L.: effects of residue composition and N content. Soil Biology and Biochemistry 32, 1717–1730.

Van Soest, P.J., Robertson, J.B., Lewis, B.A., 1991. Symposium: carbohydrate methodology, metabolism, and nutritional implications in dairy cattle. Methods for dietary fiber, neutral detergent fiber, and nonstarch polysaccharides in relation to animal nutrition. Journal of Dairy Science 74, 3583–3597.

Van Veen, J.A., Ladd, J.N., Frissel, M.J., 1984. Modelling C and N turnover through the microbial biomass in soil. Plant and Soil 76, 257–274.

Verberne, E.L.J., Hassink, J., de Willingen, P., Groot, J.J.R., Van Veen, J.A., 1990. Modelling organic matter dynamics in different soils. Netherlands Journal of Agricultural Science 328, 221–238.

Whitmore, A.P., Handayanto, E., 1997. Simulating the mineralization of N from crop residues in relation to residue quality. In: Cadish, G., Giller, K.E. (Eds.), Driven by Nature, Plant Litter Quality and Decomposition, CAB International, Wallingford, pp. 337–348.

Yevdokimov, I.V., Blagodatsky, S.A., 1993. Nitrogen immobilization and remineralization by microorganisms and nitrogen uptake by plants: Interactions and rate calculations. Geomicrobiology Journal 11, 185–193.

La Transformation de l'azote des Apports Organiques (modèle TAO-N)

Composition biochimique de l'apport et transformation de l'azote

Available online at www.sciencedirect.com
SCIENCE DIRECT®
PERGAMON
Soil Biology & Biochemistry 35 (2003) 353–363
Soil Biology & Biochemistry
www.elsevier.com/locate/soilbio

Predicting N transformations from organic inputs in soil in relation to incubation time and biochemical composition

M. Pansu[a,*], L. Thuriès[b], M.C. Larré-Larrouy[a], P. Bottner[c]

[a]*IRD (ORSTOM), BP 64501, 34394 Montpellier Cedex 5, France*
[b]*Phalippou-Frayssinet S.A., Organic fertilizers, 81240 Rouairoux, France*
[c]*Cefe-CNRS, 1919 route de Mende 34293 Montpellier Cedex 5, France*

Received 24 April 2002; received in revised form 22 October 2002; accepted 26 November 2002

Abstract

Seventeen different added organic materials (AOM) in a sandy soil were incubated under controlled laboratory conditions (28 °C, 75% WHC), and examined for C and N mineralisation. The transformation of added organics (TAO) model has been presented in previous work for predicting C mineralisation. The two variables (very labile and stable fractions of AOM) used in TAO have been related to the biochemical characteristics of the AOM. The transformed added organic N fraction (TAONF) was estimated from the remaining C_{AOM} and N_{AOM} linked by the C-to-N ratios. TAONF was split (P_{im} parameter) into immobilised N (imN) and inorganic N (inorgN). When necessary, an additional N mineralisation of imN was predicted by first order kinetics (constant k_{remin}). The TAO version with the two parameters P_{im} and k_{remin} allowed us to predict very different dynamics of N mineralisation and N immobilisation from the AOM. In a few cases, another first order kinetic law (constant k_v) was used to predict N volatilisation from inorgN.

Biochemical characteristics of AOM were used for predicting N transformations. First, at each incubation date, inorgN was approximated to inorgNa = α(N-to-C_{AOM}) + β by linear regression. The α, β and $-\beta/\alpha$ (C-to-N_{AOM} threshold for mineralisation/immobilisation) were related to time. The TAO expression $(1 - P_{im})$TAONF was then replaced by the proposed approximation inorgNa as a function of incubation time and C-to-N_{AOM}. Secondly, significant relationships were computed between k_{remin} and organic fibre content of AOM. Finally, a TAO approximation was proposed for predicting the simultaneous transformations of C and N, only using biochemical data (plus the k_v parameter in a few cases of N volatilisation). For all AOMs, the validity of the approximation and its borderline cases were examined by comparing the two TAO versions.

Keywords: Modelling; N mineralisation; N immobilisation; Organic residues; Biochemical characteristics

1. Introduction

It is a challenge to develop accurate tools for predicting (i) C sequestration in soil from added organic materials (AOM) and its influence on soil properties, and (ii) nutrient (N, especially) transformations from AOM to meet the optimum crop N-demand and avoid N-losses by volatilisation and leaching.

AOM inputs in the decomposition models of soil organic matter (SOM) are generally defined by two (Molina et al., 1983; Van Veen et al., 1984; Parton et al., 1987; Bradbury et al., 1993; Sallih and Pansu, 1993) or three (Verberne et al., 1990; Hansen et al., 1991) initial AOM pools. Other mechanistic models considered AOM constituents as a continuum (Bosatta and Ågren, 1985) or split AOM and their decomposition products into SOM compartments (Henriksen and Breland, 1999; Nicolardot et al., 2001) according to their quality. Indeed, the decomposition of AOM has been known for a long time to depend upon their quality (Wollny, 1902), often on their C-to-N ratio (Jensen, 1929; Rubins and Bear, 1942; Nicolardot et al., 2001). The method of Van Soest et al. (1991) fractionates AOM into soluble, hemicelluloses-, cellulose- and lignin-like initial substances. To define AOM quality, these fractions can be used directly (Linères and Djakovitch, 1993; Robin, 1997; Henriksen and Breland, 1999; Trinsoutrot et al., 2000) or in combination (e.g. lignin/N ratio; Melillo et al., 1982).

This paper examines the modelling of C and N transformation kinetics of various AOM in a Mediterranean

* Corresponding author. Tel.: +33-4674-16228; fax: +33-4674-16294.
E-mail address: pansu@mpl.ird.fr (M. Pansu).

0038-0717/03/$ - see front matter © 2003 Elsevier Science Ltd. All rights reserved.
doi:10.1016S0038-0717(02)00285-7

sandy soil with low C content. In previous works (Thuriès et al., 2001) comparing several models, a first order, three-compartment model with four parameters was selected to describe CO_2-C mineralisation processes. Under controlled conditions (28 °C, 75% WHC), this model was simplified with two parameters only: P'_L (fraction of very labile AOM) and P_S (fraction of stable AOM). New equations then related P'_L and P_S to biochemical characteristics of AOM, and hence predicted CO_2-C mineralisation from these data (Thuriès et al., 2002). The C results were then extended to simulate N transformations, and the transformation of added organics (TAO, Transformation des Apports Organiques) model was proposed (Pansu and Thuriès, 2002). The TAO-N model required, in most cases, one or two additional parameters: P_{im} (immobilised fraction of transformed N) and, if necessary, k_{remin} (first order kinetic constant of re-mineralisation from immobilised N). In some cases, when N volatilisation occurred, another first order kinetics (constant k_v) was added. The aim of the present work was to simulate both C and N transformations with AOM biochemical data.

2. Materials and methods

2.1. Added organic materials (AOM)

Different kinds of AOM from the agri-food industry and industrially-processed fertilisers (organic amendments and fertilisers) were tested (Table 1). They originated from (i) plant residues: wet and dry grape skin cakes (Wgrap, Dgrap), coffee cake (Coffk), cocoa cake (Kokoa), olive pulp (Olivp); (ii) animal residues: hydrolyzed feather meal (Featm), native fine feather (Nfeat), guano (Guano); (iii) sheep and chicken manures (Shepm, Chicm); (iv) industrial organic fertilisers: composted amendments (Compo series), and combined fertilisers (Gnofer, Comfer). A more complete description of these products was given in Thuriès et al. (2001, 2002). The AOM were air-dried and ground for total C and N analyses, sequential analysis of fibres, and the incubation tests.

2.2. Biochemical characterization of AOM

Each AOM sample (six replicates) was successively extracted for NDF (neutral detergent fibre), ADF (acid detergent fibre) and ADL (acid detergent lignin) by sequential analysis of fibres, after Van Soest et al. (1991). At each extraction step, the products obtained were filtered, dried at 40 °C, weighed, and either (i) analysed for C and N by dry combustion (autoanalyser Fisons NA2000), or (ii) dried at 105 °C for determining residual moisture, then ignited gradually at 525 °C for ash content. The contents of neutral detergent soluble, hemicelluloses-, cellulose-, lignin-like compounds and ashes (Sol, Hem, Cel, Lig, Ash, respectively) were then calculated. The data used in this paper (Table 1) were:

(i) the mass of ash-free fractions of the AOM,
labile, flab = (Sol + Hem)/(Sol + Hem + Cel + Lig),
soluble, fsol = Sol/(Sol + Hem + Cel + Lig), and
cellulose-like, fcel = Cel/(Sol + Hem + Cel + Lig);
(ii) C_{AOM}, N_{AOM}, Lig, i.e. the C and N contents and the lignin-like fraction of AOM, respectively;
(iii) η_{Sol}, η_{Hol}, η_{Lig}, i.e. C-to-N ratios of soluble, holocellulosic, and ligneous AOM fractions, respectively.

2.3. Incubation experiment

The incubation test using a sandy soil (0–20 cm depth, sand = 69.3%, clay = 11.5%, $pH_{(H2O)} = 6.6$, CEC = 5.5 cmol c^+ kg^{-1}, total C = 4.98 g kg^{-1}, total N = 0.59 g kg^{-1}) was previously described in Thuriès et al. (2001). The CO_2-C release (28 ± 1 °C) was measured in closed chambers (Thuriès et al., 2000). Organic C, total and inorganic N (inorgN = ammonium + nitrate + nitrite) of soil, AOM and 'soil + AOM' mixtures were determined as reported by Thuriès et al. (2001, 2002) and Pansu and Thuriès (2002).

2.4. Modelling

At 28 °C and 75% WHC, the selected model (Thuriès et al., 2001) described the remaining AOM-C fraction (RAOCF) as a function of incubation time t, time of application t_0, fraction of very labile P'_L and stable (P_S) compounds, respectively:

$$\mathrm{RAOCF} = P'_L\, e^{-0.4(t-t_0)} + (1 - P'_L - P_S)\, e^{-0.012(t-t_0)} + P_S \quad (1)$$

If η_L, η_R, η_S are the C-to-N ratios of very labile, resistant and stable AOM-compartments, respectively, the remaining added organic nitrogen fraction (RAONF) is:

$$\mathrm{RAONF} = \frac{P'_L}{\eta_L} e^{-0.4(t-t_0)} + \frac{1 - P'_L - P_S}{\eta_R} e^{-0.012(t-t_0)} + \frac{P_S}{\eta_S} \quad (2)$$

From Pansu and Thuriès (2002), Eq. (2) can be approximated to:

$$\mathrm{RAONF} = \frac{1}{\eta_{AOM}}(P'_L\, e^{-0.4(t-t_0)} + (1 - P'_L - P_S) \times e^{-0.012(t-t_0)} + P_S) \quad (3)$$

The transformed (mineralised or immobilised) added organic nitrogen fraction (TAONF) was calculated from the initial total C of the AOM (= 1 in this data set, all values of C and N being expressed as a fraction of initial C content) and C-to-N of AOM (η_{AOM}) by:

$$\mathrm{TAONF} = \frac{1}{\eta_{AOM}} - \mathrm{RAONF} \quad (4)$$

Table 1
Biochemical characteristics of added organic matters (AOM). PCA = AOM classification according to the principal component analysis method (Thuriès et al., 2002), k^a_{remin} and k^a_v are the optimised values of parameters from TAO initial version (Pansu and Thuriès, 2002), k^b_{remin} is recalculated from Eqs. (9) and (10), k^b_v is the reoptimised values of volatilisation parameter in predictions from biochemical data, * AOM where an adjustment of C-to-N_{AOM} value improved the predictions (see Fig. 3 and Section 4)

Origin	AOM	PCA	Laboratory data (100 g g^{-1})							C-to-N of fractions			C-to-N_{AOM}			Initial parameters		Re-calculated parameters	
			Ash	C	N	Sol	Hem	Cel	Lig	η_{Sol}	η_{Hol}	η_{Lig}	Direct	Mixture	Adjust	k^a_{remin}	k^a_v	k^b_{remin}	k^b_v
Plant	Coffk	+	3.1	53.71	1.98	24.0	9.7	38.0	25.2	57.21	39.35	18.00	27.13	19.61	17.52*	0.00059	0	0.00037	0
	Wgrap	+	8.9	52.85	2.69	11.3	4.7	17.6	57.5	23.92	21.56	18.46	19.64	14.20	16.37*	0.00178	0	0.00063	0
	Dgrap	+	7.1	49.40	2.25	29.2	10.5	23.0	30.2	23.29	39.43	18.56	21.99	21.92	21.99	0.00401	0	0.0016	0
	Olivp	+	8.8	46.86	1.97	24.6	13.7	24.1	28.8	19.97	65.22	16.00	23.78	24.15	21.24*	0.00324	0	0.0024	0
	Kokoa	−	9.1	43.68	4.54	53.8	9.3	15.5	12.4	9.14	9.53	9.97	9.62	12.14	14.04*	0.00250	0.00860	0.0012	0
Manure	Shepm	−	28.1	37.91	2.23	22.3	28.6	10.2	10.7	8.43	14.87	25.27	16.99	11.55	16.99	0	0	0.0011	0
	Chicm	−	32.3	37.59	6.06	33.5	15.8	10.8	7.5	2.40	31.59	14.96	6.20	7.41	6.20	0.00401	0.0183	0.0010	0.00813
Animal	Nfeat	+	3.8	54.48	14.57	4.5	27.2	20.6	43.9	3.07	5.08	3.50	3.74	3.45	3.74	0.00951	0	0	0
	Featm	−	2.8	47.13	15.18	32.9	55.0	5.2	4.0	2.38	4.13	4.17	3.10	4.09	3.10	0.00076	0.00274	0.00034	0
	Guano	−	43.3	17.50	15.61	54.4	0.1	0.1	2.1	1.10	0.80	6.60	1.12	1.35	0.82*	0.03410	0.04610	0.00013	0.0201
Fertilizer	Gnofer	−	40.4	27.28	9.51	25.6	22.9	6.7	4.4	1.96	3.94	5.08	2.87	2.66	2.87	0	0	0.00070	0
	Comfer	−	25.5	36.88	3.74	32.4	4.3	20.4	17.5	5.45	8.78	15.66	9.87	12.32	9.87	0.00476	0	0.0024	0
Compost	Compo a	−	32.2	36.19	2.92	20.2	7.3	23.0	16.8	5.19	13.18	16.17	12.40	16.34	14.67*	0.00050	0	0.0030	0
	Compo b	−	34.4	36.29	2.46	19.9	5.8	21.2	18.7	8.00	21.60	14.98	14.74	17.92	18.37*	0.00200	0	0.0031	0
	Compo e	−	40.4	28.76	2.70	18.7	7.1	10.7	23.0	5.45	15.18	10.70	10.66	10.27	12.95*	0	0	0.0028	0
	Compo +	−	32.1	33.92	2.58	21.3	8.0	13.8	24.8	8.64	57.89	11.70	13.12	13.51	16.78*	0.00244	0	0.0028	0
	Compo p	+	40.2	34.18	2.41	6.4	9.9	9.8	33.7	1.40	30.63	18.70	14.16	12.25	11.32*	0	0	0.00020	0

The TAO equations for inorganic N (inorgN) and immobilised N (imN) are:

$$\text{inorgN} = (1 - P_{\text{im}})\text{TAONF} + \int_{t_0}^{t} \text{imN}\, k_{\text{remin}}\, dt - \int_{t_0}^{t} \text{inorgN}\, k_v\, dt \quad (5)$$

$$\text{imN} = P_{\text{im}}\, \text{TAONF} - \int_{t_0}^{t} \text{imN}\, k_{\text{remin}}\, dt \qquad \text{for } t > t_0 \quad (5')$$

otherwise, inorgN = initial inorg*N* and imN = 0 for $t = t_0$, where P_{im} is the fraction of immobilised TAONF, k_{remin} and k_v are first order kinetic constants for mineralisation of immobilised TAONF and possible volatilisation of inorgN, respectively. For most of the samples, k_v was equated to zero and the third term of Eq. (5) was not necessary.

The objective of this work was to transform Eqs. (5) and (5′) to predict inorgN and imN only with biochemical data. For a complete decomposition of uniformly decomposable residues, inorgN can be approximated to inorgNa in the balance equation (Whitmore and Handayanto, 1997):

$$\text{inorgNa} = C_0\left(\frac{1}{\eta_{\text{AOM}}} - \frac{E}{Y}\right) \quad (6)$$

where C_0 represents the initial C content of the AOM (= 1 in this data), E is a microbial efficiency factor (can be estimated as being ca. 0.4 after Whitmore and Handayanto (1997)), Y is the C-to-N ratio of the end product of the decomposition process (ca. 10 for humic materials). For not complete decompositions but limited to a fraction α of AOM we chose to study the following linear relationship:

$$\text{inorgNa} = \alpha\left(\frac{1}{\eta_{\text{AOM}}}\right) + \beta \quad (6')$$

In a second way, a stepwise regression procedure using partial and sequential *F*-tests (Draper and Smith, 1980) was used in order to enter or remove biochemical variables and finally obtain a significant descriptive biochemical approximation of k_{remin}. If necessary, the AOM were classified by the principal component analysis method used by Thuriès et al. (2002) before calculations.

3. Results

3.1. Approximation of inorgN data with Eq. (6′)

At each incubation time, linear relationships were calculated according to Eq. (6′) for the AOM set, except the atypical Guano (great N-loss). The C-to-N limits ($\eta^{\text{lim}}_{\text{AOM}}$) were deduced from Eq. (6′) when inorgNa = 0 and $\eta^{\text{lim}}_{\text{AOM}} = -\alpha/\beta$ i.e. when the net production of inorganic N of a given AOM = 0 (the threshold for immobilisation of soil inorganic N). The results are reported in Table 2 and illustrated in Fig. 1 at four incubation times.

Table 2
Estimation of α and β parameters for Eq. (6′) (with associated standard deviations s_α and s_β) and determination of $\eta^{\text{lim}}_{\text{AOM}}$ and E/Y ratio (Eq. (6)) at each incubation time t. F test indicates significance of Eq. (6′) fit (* at $p < 0.01$, ** at $p < 10^{-4}$, ns not significant)

t (day)	α	s_α	β	s_β	F	$\eta^{\text{lim}}_{\text{AOM}}$	E/Y
0	0.054	0.023	0.0027	0.0034	6 ns	−19.92	
1	0.052	0.017	−0.0013	0.0025	10 *	40.31	0.03
2	0.096	0.018	−0.0049	0.0027	27 **	19.65	0.05
5	0.193	0.024	−0.0126	0.0036	64 **	15.34	0.07
10	0.207	0.026	−0.0145	0.0038	64 **	14.29	0.07
21	0.262	0.027	−0.0180	0.0040	97 **	14.56	0.07
41	0.270	0.021	−0.0175	0.0031	170 **	15.46	0.06
90	0.272	0.015	−0.0163	0.0023	321 **	16.65	0.06
182	0.314	0.019	−0.0169	0.0029	266 **	18.55	0.05

The variations of α and β (Eq. (6′), Table 2) with incubation time t were reported in Fig. 2(a) and (b) and showed a strong inverse correlation between α and β. Consequently, the ratio $-\alpha/\beta$ ($= \eta^{\text{lim}}_{\text{AOM}}$) was approximately constant during the course of the incubation (see Section 4.2 for constant values from the literature). However, the ratio increased to a slight extent, following a significant linear relationship with time (Fig. 2(c)), except between 0 and 5 days, where substantial variations occurred (Fig. 2(d)). Except for $t = 0$, the parameters α and β were closely linked to $t^{-1/2}$ equations (see Fig. 2(a) and (b)). These equations predicted the $-\alpha/\beta$ ratio ($= \eta^{\text{lim}}_{\text{AOM}}$) as being close to the fitted linear relationship and the measured data in the initial stages of incubation (see Fig. 2(d) and Section 4.2). The predictive Eq. (6′) became:

$$\text{inorgNa} = -0.0198 + \frac{0.313}{\eta_{\text{AOM}}} + \left(0.0187 - \frac{0.278}{\eta_{\text{AOM}}}\right)\frac{1}{\sqrt{t - t_0}} \quad (7)$$

for $t > t_0$

otherwise, inorgN = initial inorgN and imN = 0 for $t = t_0$.

The combination of Eq. (7) with Eqs. (5) and (5′) gave:

$$\text{inorgN} = \text{inorgNa} + \int_{t_0}^{t} \text{imN}\, k_{\text{remin}}\, dt - \int_{t_0}^{t} \text{inorgN}\, k_v\, dt \quad (8)$$

$$\text{imN} = \text{TAONF} - \text{inorgNa} - \int_{t_0}^{t} \text{imN}\, k_{\text{remin}}\, dt \quad (8')$$

for $t > t_0$

otherwise, inorgN = initial inorgN and imN = 0 for $t = t_0$.

The parameter P_{im} was then eliminated from the calculations.

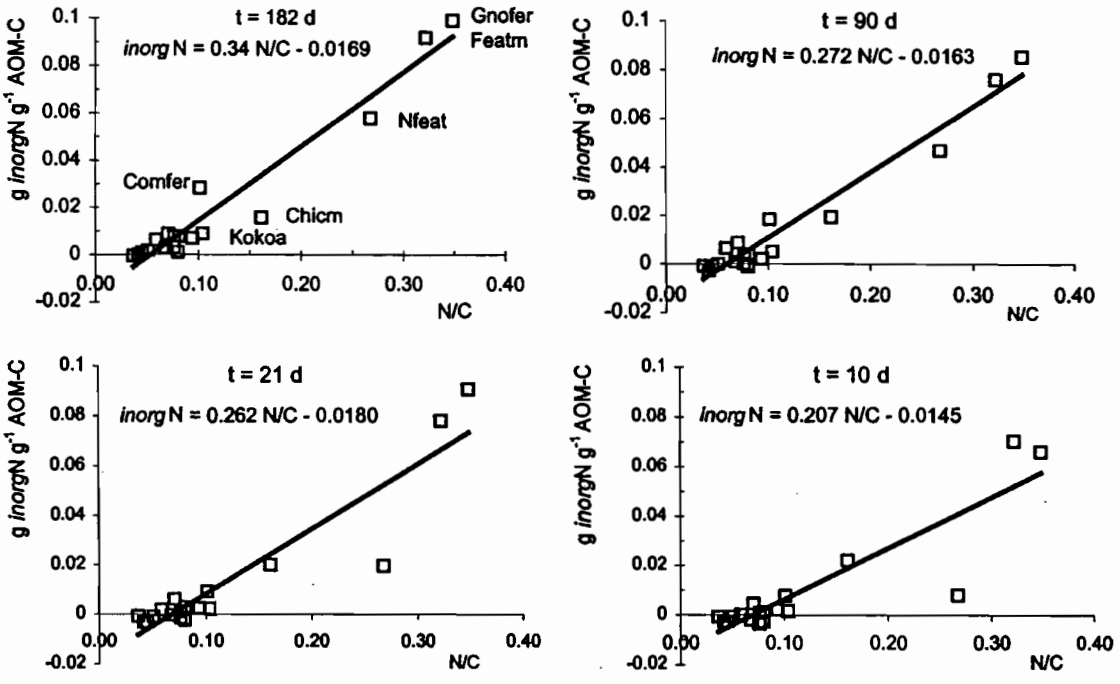

Fig. 1. Estimation (solid line) of N mineralisation by Eq. (6′) ($N/C = 1/\eta_{AOM}$) at four incubation times.

3.2. Predicting re-mineralisation of immobilised N

Predictions of inorganic N with time Eq. (7) gave similar curves (not shown) with a high absolute value for the slope (positive for mineralisation, negative for immobilisation) during the first 10 days of incubation, a strong inflexion for 10–30 days and a slight increase for 30–180 days. In a few cases, the predictions were close to the inorganic N measured data (Gnofer, Featm) and in general they provided approximate estimates of the total inorganic N production or immobilisation. In the case of net immobilisation of N, Eq. (7) did not take into account the production of inorganic

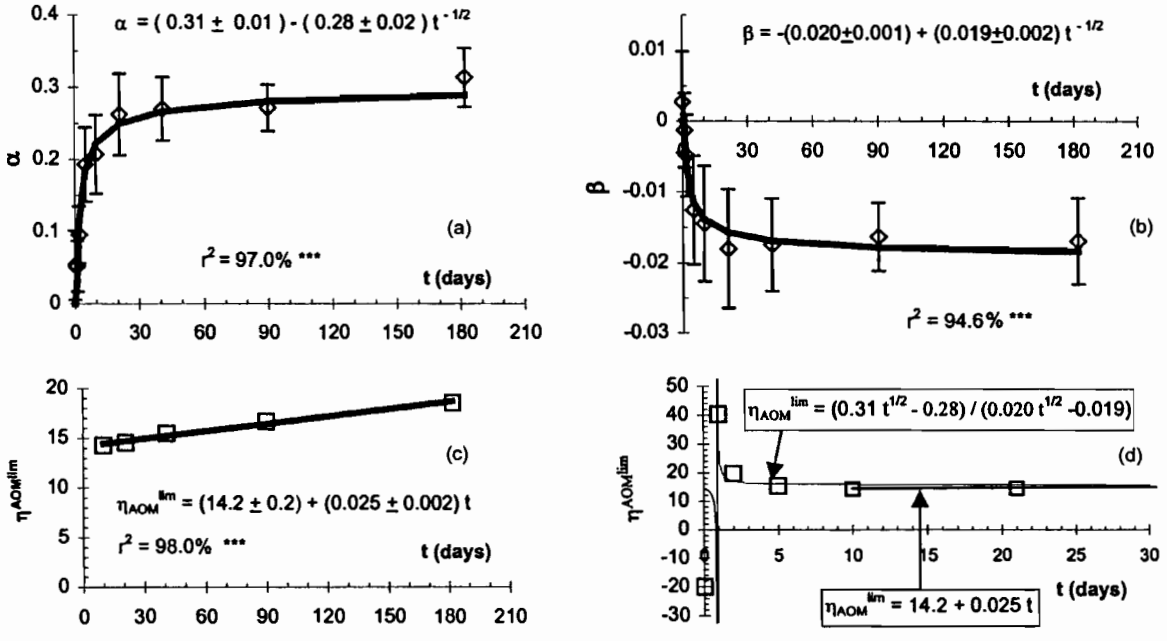

Fig. 2. Evolution of Eq. (6′) parameters (above) and η^{lim}_{AOM} (below) as functions of incubation time (from initial input time $t_0 = 0$).

N from immobilised N; the predicted inorganic N remained at a negative value whereas a re-mineralisation was often observed. In the case of net mineralisation, Eq. (7) did not simulate the different shapes of inorganic N releases related to the specific properties of the tested products.

The k_{remin} values obtained from Eqs. (5) and (5′) (Pansu and Thuriès, 2002) were re-optimized with Eqs. (8) and (8′) (Table 1). The relationships between optimised k_{remin} values and biochemical characteristics of the AOM were then examined. As pointed out for the C mineralisation studies (Thuriès et al., 2002), it was difficult to obtain a satisfactory relationship for the whole AOM set. The same method of Principal Component Analysis (PCA) was used in order to discriminate the AOM into two groups: (+) ligneous ones with relatively high C-to-N ratio, mostly plant-originated AOM (PCA + in Table 1), and (−) more nitrogenous ones, with lower C-to-N and ligno-cellulosic fibre contents, mostly animal-originated or partially-composted AOM (PCA − in Table 1). For each group, the k_{remin} values could then be fitted to the following equations:

$$k_{remin} = -(0.0034 \pm 0.0003)\ln(\text{flab}) \quad (\text{PCA}-) \tag{9}$$

$$k_{remin} = -(0.008 \pm 0.002)\text{fcel} + (0.014 \pm 0.003)\text{fsol} \quad (\text{PCA}+) \tag{10}$$

with determination coefficients $r^2 = 93.6$ and 95.7% for Eqs. (9) and (10), respectively.

3.3. Biochemical predictions of C and N transformations

The simultaneous C and N transformations were then predicted with the biochemical data only (in g g^{-1}, Table 1): Eqs. (7), (9) and (10) combined with Eqs. (8) and (8′), and Eqs. (1), (3) and (4) with the following equations originated from Thuriès et al. (2002). For PCA −

$$P'_L = 0.35\text{fsol} + 2.2N_{AOM} - 0.010\text{Lig}/N_{AOM} \tag{11}$$

$$P_S = 3.60\text{Lig} \tag{12}$$

or for PCA +

$$P'_L = 0.099\text{flab} + 0.14\text{Hem} \tag{13}$$

$$P_S = 1.61\text{Lig} + 0.62\text{Ash}_{AOM} \tag{14}$$

Additionally, the k_v value was re-optimized for N volatilisation. The k_v parameter was not adjusted by biochemical data since volatilisation clearly occurred on only two (Guano and Chicm) occasions ($k_v = 0$ for the 15 other AOM). The biochemical predictions were satisfactory for seven AOM. For the remaining AOM (* in Table 1), a correction, assuming a possible variability in C and N_{AOM} measurements, improved the predictions (see Fig. 3 and Section 4.3). The results are shown in Figs. 4–7 .

4. Discussion

4.1. About α and β values

Except for d 0–1, the relationships for Eq. (6′) were highly significant ($p < 10^{-4}$ for d 2–182 in Table 2). For a complete mineralisation of N-AOM, the slope α Eq. (6′) might be equal to 1. The value $\alpha = 0.31$ (at d 182) indicates that about one third of AOM-N was mineralised during the 182-day experiment. Consequently, 0.69 AOM-N could be

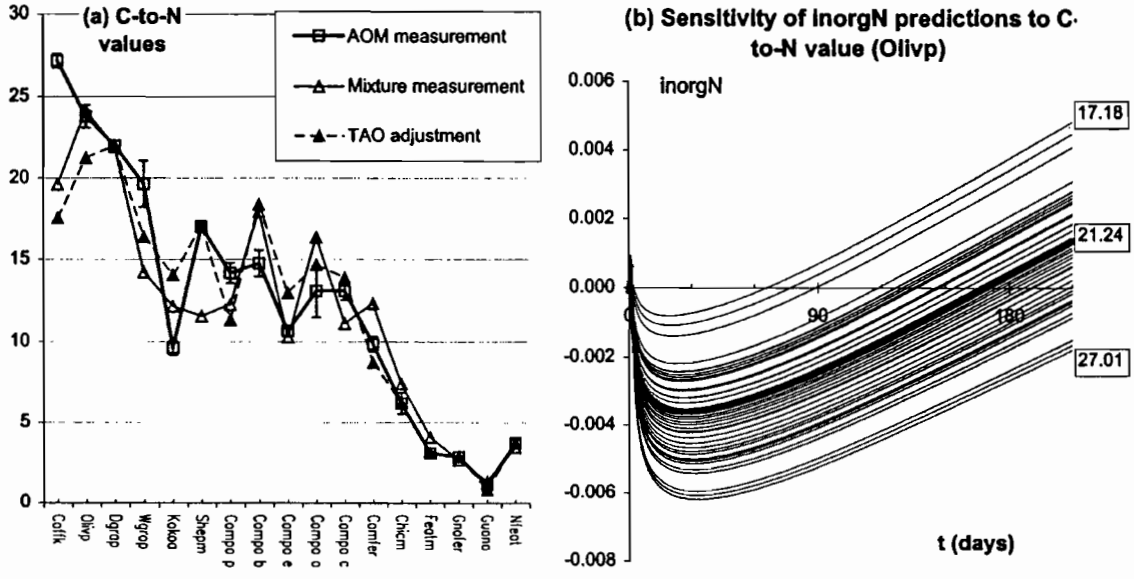

Fig. 3. (a) Values of C-to-N obtained by: (□) direct measurement on AOM (with 95% confidence intervals, three replicates), (△) measurement from soil + AOM sample, (▲) model adjustment. (b) Sensitivity of inorgN predictions vs. changes in C-to-N values following a random normal distribution with 10% RSD (minimum, mean and maximum values in box).

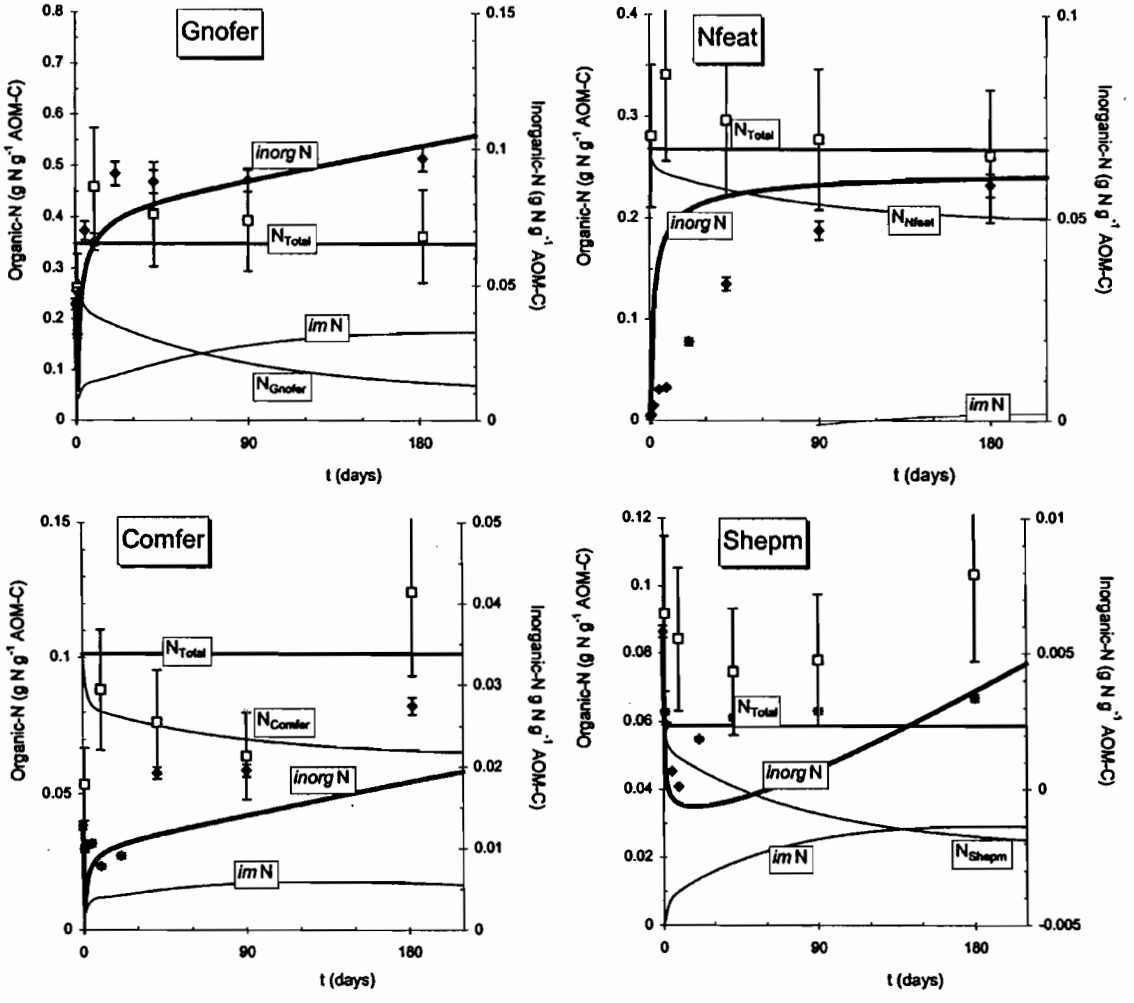

Fig. 4. Mineralisation and immobilisation of N from guano-based fertiliser (Gnofer), native fine feather (Nfeat), compost-based fertiliser (Comfer), sheep manure (Shepm). Points, experimental data with 95% confidence intervals ((◆, inorgN from AOM; □, N_{Total} from AOM); solid lines, TAO biochemical predictions of inorgN (bold lines), immobilised N (imN) and remaining N_{AOM} (thin lines).

considered as being stable. The mean value of P_S (the very stable fraction of the AOM, Thuriès et al., 2001) for the 17 AOM was 0.53. Thus ca. 0.16 AOM-N could originate from immobilisation or from the undecomposed resistant R fraction ($P_R = 1 - P'_L - P_S$).

The comparison of Eq. (6) and (6′) gave an interpretation of β values: α being the decomposed fraction, β must be equal to $-\alpha E/Y$, then $E/Y = -\beta/\alpha$. The obtained E/Y values (Table 2) are very close to those given by Whitmore and Handayanto (1997) with $Y \approx 10$ and $E \approx 0.4$.

4.2. About η^{lim}_{AOM} values and $\alpha, \beta, \eta^{lim}_{AOM}$ predictions

In a pioneer study, Jensen (1929) found a C-to-N ratio limit 'above which no nitrification occurred' reaching about 13 in an acid soil and 26 in an alkaline one. In the present experiment with a sandy soil ($pH_{H2O} = 6.6$), the values η^{lim}_{AOM} (Table 2) ranged between 14.3 (d 10) and 18.6 (d 182). These values were consistent with other found in the literature. The C-to-N ratio threshold for mineralisation/immobilisation has been variously assumed to be 20–25 (Haynes, 1986), about 25 (Whitmore and Handayanto, 1997), 24 (Trinsoutrot et al., 2000), about 20 (Stevenson, 1986), 17.5 (Hue and Sobieszczyk, 1999), and 11.5 (Gagnon and Simard, 1999).

There was wide variation in the experimental values of inorganic N at the early incubation times following the quick immobilisation after the addition of AOM at t_0. Nevertheless, the parameters α and β were very well predicted by the $t^{-1/2}$ equations as the incubation proceeded (Fig. 2(a) and (b)). From these equations, the ratio $-\alpha/\beta$ ($= \eta^{lim}_{AOM}$) was an hyperbole with an asymptote parallel to the η^{lim}_{AOM} axis at $t \cong 1$, and values very close to the experimental ones at the early incubation stages (Fig. 2(d)).

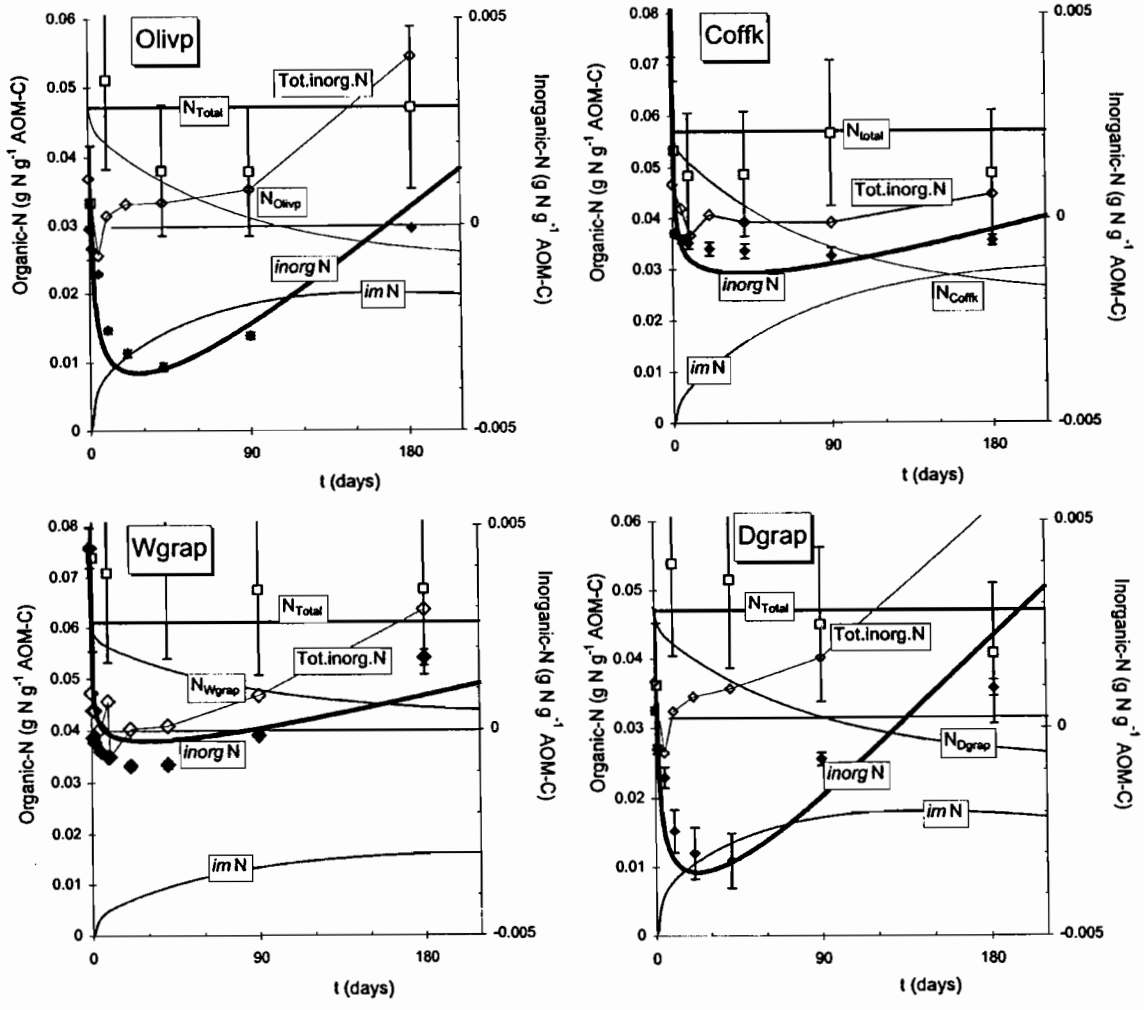

Fig. 5. Mineralisation and immobilisation of N from crop residues: olive pulp (Olivp), coffee cake (Coffk), wet grape skin cake (Wgrap) and dry grape skin cake (Dgrap). Points, experimental data with 95 % confidence intervals (◆, inorgN from AOM; ◇, total (AOM + soil) inorganic N; □, N_{Total} from AOM); solid lines, TAO biochemical predictions of inorgN (bold lines), immobilised N (imN) and remaining N_{AOM} (thin lines).

A slight difference appeared at later incubation times (Fig. 2(c)). In the $-\alpha/\beta$ equation (Fig. 2(d)), when $t \rightarrow \infty$, $\eta_{AOM}^{lim} \rightarrow 15.5$. In reality, after d 10, η_{AOM}^{lim} increased weakly but significantly according to the linear relationship in Fig. 2(c). The precision found for α and β was satisfactory (see confidence intervals of the data in Figs. 4–7) and the proposed Eq. (7) need not be more complicated.

4.3. Sensitivity to C-to-N_{AOM} ratios

Among the biochemical data used in modelling the N mineralisation dynamics (Corbeels et al., 1999; Henriksen and Breland, 1999), the importance of C-to-N_{AOM} ratio was emphasized by Trinsoutrot et al. (2000) and Nicolardot et al. (2001).

In the first TAO version Eqs. (1), (3), (4), (5) and (5′), the fitting of P_{im} and k_{remin} permitted correction of the variability of C and N measurements. As shown in Fig. 3(b), the present TAO version was very sensitive to C-to-N values. The error in C-to-N determination is linked to the propagation of random and systematic errors on C and N measurements (Pansu et al., 2001). The relative variance (RV) is the sum RV on C and RV on N. In this study, each AOM was measured in triplicate, and the corresponding 95% confidence intervals were plotted in Fig. 3(a). For Dgrap, Shepm, Chicm, Nfeat, Featm, Gnofer and Comfer, the measured C-to-N values gave good predictions. For Compo a, Compo c and Guano, the adjusted C-to-N values were within the confidence intervals of measured C-to-N. In the seven other cases, the predictions were not explained by the random errors. There were probably systematic errors confirmed by differences between direct AOM measurements and the 'soil + AOM' ones $[1/(N_{soil+AOM} - N_{soil})]$. They could originate from two sources. First, the 'soil +

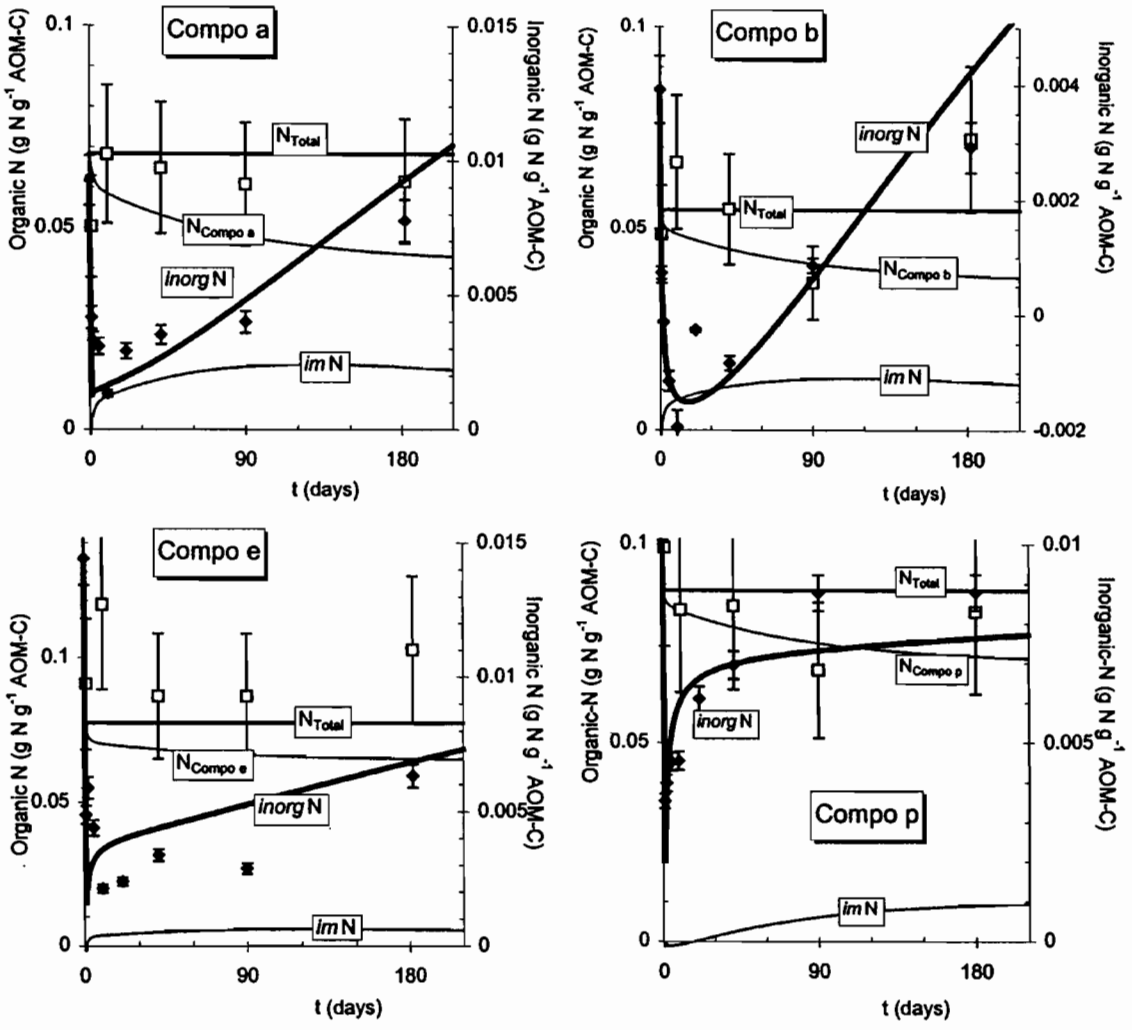

Fig. 6. Mineralisation and immobilisation of N from composts. Points, experimental data with 95 % confidence intervals (◆, inorgN from AOM; □, N_{Total} from AOM); solid lines, TAO biochemical predictions of inorgN (bold lines), immobilised N (imN) and remaining N_{AOM} (thin lines).

AOM' mixtures were obtained from air-dried materials while the direct C and N_{AOM} measurements were made on samples dried at 40 °C. Even at this low temperature, a partial N volatilisation may occur. Secondly, active N-rich sites could induce a micro-heterogeneity in AOM. For Coffk, Wgrap, Kokoa, Compo a, Compo b and Compo p, the C-to-N_{AOM} adjustments by TAO were closer to the values measured on the 'soil + AOM' mixtures than to those determined on the sole AOM before addition to soil (Fig. 3(a)).

4.4. Modelling N transformations

Figs. 4–7 displayed biochemical predictions as accurate as those presented in the kinetic adjustment of Figs. 2–5 of Pansu and Thuriès (2002) for Gnofer (Fig. 4), Olivp, Coffk, Wgrap, Dgrap (Fig. 5), Compo a, Compo b, Compo e, and Compo p (Fig. 6). For Guano, Featm, Chicm, and Kokoa (Fig. 7), the inorganic N predictions were accurate with both approaches, but the biochemical method underestimated N volatilisation (too high a value of predicted N_{Total}). In Pansu and Thuriès (2002), the optimisation method gave $k_v > 0$ for these four AOM. This study showed $k_v > 0$ only for Guano and Chicm. Even for these AOM, the present predicted volatilisations of N were lower than those in Pansu and Thuriès (2002). Total-N was overestimated. The k_{remin} values were underestimated (especially for Guano, Table 1) by Eqs. (9) and (10). The transfers of imN to inorgN and to volatile N were thus low. These AOM were borderline cases for Eqs. (9) and (10).

In Nfeat and Comfer (Fig. 4) the shape of inorganic N prediction curve differed from the data measured. At d 180 the prediction of Nfeat inorgN was correct but the slope of the curve was different from the data. The C mineralisation

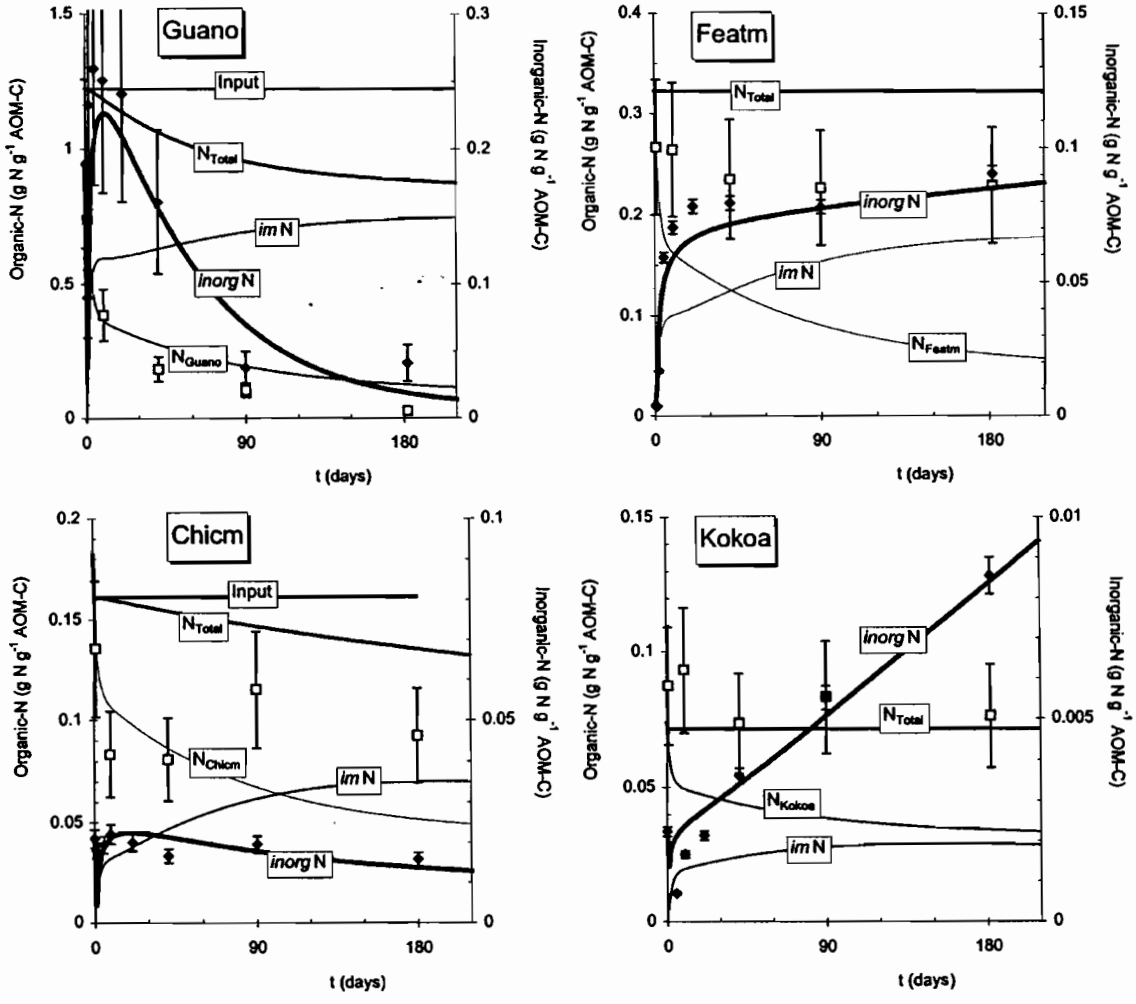

Fig. 7. Mineralisation, immobilisation and gaseous losses of N from animal residues guano (Guano), feather meal (Featm), chicken manure (Chicm) and crop residue cocoa cake (Kokoa). Points, experimental data with 95% confidence intervals (◆, inorgN from AOM; □, N_{Total} from AOM); solid lines, TAO biochemical predictions of inorgN (bold lines), immobilised N (imN) and remaining N_{AOM} (thin lines), N_{Total} from AOM.

rate of Nfeat was low (Thuriès et al., 2001, 2002) despite a high N content. Nfeat had a high P_S fraction and a k_{remin} value poorly predicted by Eqs. (9) and (10). The inorgN curve was more in accordance with the CO_2-C– than with the inorgN-data. Comfer (Fig. 4) was also a borderline case of Eqs. (9) and (10). The k_{remin} value and the regular production of inorganic N were underestimated (by 30% during the 1–6 month incubation time).

4.5. Conclusion

Eq. (7) is proposed as a means of estimating the production of inorganic N in soil as a function of incubation time and C-to-N_{AOM} ratio. The threshold for mineralisation/immobilisation ($= \eta^{lim}_{AOM}$) has been related to the incubation time. Eq. (7) was used to replace the P_{im} term in the previous TAO-C and –N kinetic model. The k_{remin} values were then re-optimised and Eqs. (9) and (10) were suggested as a means of predicting k_{remin} based on biochemical characteristics. In a few cases where N volatilisation clearly occurred (Guano and Chicm), TAO needed the integration of the first order volatilisation kinetics (k_v constant) of Pansu and Thuriès (2002). Despite some cautions linked to the variability of C and N measurements, a few borderline cases in k_{remin} determination, and classical corrections needed for field and soil type conditions, this TAO version appears as a valuable tool for predicting both C and N transformations of AOM in soil.

Acknowledgements

This work was partly granted by a CIFRE convention. The authors gratefully acknowledge Dr C. Feller (IRD Montpellier, France), Dr M. Viel (Phalippou-Frayssinet

S.A., Rouairoux, France), Prs J.C. Rémy and P. Herrmann (ENSA-Montpellier, France) for helpful discussions.

References

Bosatta, E., Ågren, G.I., 1985. Theoretical analysis of decomposition of heterogeneous substrates. Soil Biology & Biochemistry 17, 601–610.

Bradbury, N.J., Whitmore, A.P., Hart, P.B.S., Jenkinson, D.S., 1993. Modelling the fate of nitrogen in crop and soil in the years following application of ^{15}N labelled fertilizer to winter wheat. Journal of Agricultural Science 121, 363–379.

Corbeels, M., Hofman, G., Van Cleemput, O., 1999. Simulation of net N immobilisation and mineralisation in substrate-amended soils by the NCSOIL computer model. Biology and Fertility of Soils 28, 422–430.

Draper, N.R., Smith, H., 1980. Applied Regression Analysis, second ed., Wiley, New York.

Gagnon, B., Simard, R.R., 1999. Nitrogen and phosphorus release from on-farm and industrial composts. Canadian Journal of Soil Science 79, 481–489.

Hansen, S., Jensen, H.E., Nielsen, N.E., Svendsen, H., 1991. Simulation of nitrogen dynamics and biomass production in winter wheat using the Danish simulation model Daisy. Fertilizer Research 27, 245–259.

Haynes, R.J., 1986. Mineral nitrogen in the soil–plant system. In: Haynes, R.J., (Ed.), Mineral Nitrogen in the Soil–Plant System, Academic Press, Orlando, pp. 52–126.

Henriksen, T.M., Breland, T.A., 1999. Evaluation of criteria for describing crop residue degradability in a model of carbon and nitrogen turnover in soil. Soil Biology & Biochemistry 31, 1135–1149.

Hue, N.V., Sobieszczyk, B.A., 1999. Nutritional values of some biowastes as soil amendments. Compost Science and Utilization 7, 34–41.

Jensen, H.L., 1929. On the influence of the carbon:nitrogen ratios of organic material on the mineralisation of nitrogen. Journal of Agricultural Science 19, 71–82.

Linères, M., Djakovitch, J.L., 1993. Caractérisation de la stabilité biologique des apports organiques par l'analyse biochimique. In: Decroux, J., Ignazi, J.C. (Eds.), Matières Organiques et Agricultures, Quatrièmes Journées de l'Analyse de Terre et Cinquième Forum de la Fertilisation Raisonnée, Gemas-Comifer, Blois, pp. 159–168.

Melillo, J.M., Aber, J.D., Muratore, J.F., 1982. Nitrogen and lignin control of hardwood leaf litter decomposition dynamics. Ecology 63, 621–626.

Molina, J.A.E., Clapp, C.E., Shaffer, M.J., Chichester, F.W., Larson, W.E., 1983. NCSOIL, a model of nitrogen and carbon transformations in soils: description, calibration, and behavior. Soil Science Society of America Journal 47, 85–91.

Nicolardot, B., Recous, S., Mary, B., 2001. Simulation of C and N mineralisation during crop residue decomposition: a simple dynamic model based on the C:N ratio of the residues. Plant and Soil 83, 83–103.

Pansu, M., Gautheyrou, J., Loyer, J.Y., 2001. Soil Analysis—Sampling, Instrumentation and Quality Control, Balkema, Lisse.

Pansu, M., Thuriès, L., 2003. Kinetics of C and N mineralization, N immobilization and N volatilization of organic inputs in a sandy soil. Soil Biology & Biochemistry 35, 37–48.

Parton, W.J., Schimel, D.S., Cole, C.V., Ojima, D.S., 1987. Analysis of factors controlling soil organic matter levels in Great Plains grasslands. Soil Science Society of America Journal 51, 1173–1179.

Robin, D., 1997. Intérêt de la caractérisation biochimique pour l'évaluation de la proportion de matière organique stable après décomposition dans le sol et la classification des produits organominéraux. Agronomie 17, 157–171.

Rubins, E.J., Bear, F.E., 1942. Carbon-nitrogen ratios in organic fertilizer materials in relation to the availability of their nitrogen. Soil Science 54, 411–423.

Sallih, Z., Pansu, M., 1993. Modelling of soil carbon forms after organic amendment under controlled conditions. Soil Biology & Biochemistry 25, 1755–1762.

Stevenson, F.J., 1986. Cycles of Soil. Carbon, Nitrogen, Phosphorus, Sulfur, Micronutrients, Wiley, New York, 637 pp.

Thuriès, L., Larré-Larrouy, M.-C., Pansu, M., 2000. Evaluation of three incubation designs for mineralization kinetics of organic materials in soil. Communications in Soil Science and Plant Analysis 31, 289–304.

Thuriès, L., Pansu, M., Feller, C., Herrmann, P., Rémy, J.C., 2001. Kinetics of added organic matter decomposition in a Mediterranean sandy soil. Soil Biology & Biochemistry 33, 997–1010.

Thuriès, L., Pansu, M., Larré-Larrouy, M.-C., Feller, C., 2002. Biochemical composition and mineralization kinetics of organic inputs in a sandy soil. Soil Biology & Biochemistry 34, 239–250.

Trinsoutrot, I., Recous, S., Bentz, B., Linères, M., Chèneby, D., Nicolardot, B., 2000. Biochemical quality of crop residues and carbon and nitrogen mineralization kinetics under non-limiting nitrogen conditions. Soil Science Society of America Journal 64, 918–926.

Van Soest, P.J., Robertson, J.B., Lewis, B.A., 1991. Symposium: carbohydrate methodology, metabolism, and nutritional implications in dairy cattle. Journal of Dairy Science 74, 3583–3597.

Van Veen, J.A., Ladd, J.N., Frissel, M.J., 1984. Modelling C and N turnover through the microbial biomass in soil. Plant and Soil 76, 257–274.

Verberne, E.L.J., Hassink, J., de Willingen, P., Groot, J.J.R., Van Veen, J.A., 1990. Modelling organic matter dynamics in different soils. Netherlands Journal of Agricultural Science 328, 221–238.

Whitmore, A.P., Handayanto, E., 1997. Simulating the mineralization of N from crop residues in relation to residue quality. In: Cadisch, G., Giller, K.E. (Eds.), Driven by Nature: Plant Litter Quality and Decomposition, CAB International, Wallingford, pp. 337–348.

Wollny, E., 1902. La Décomposition des Matières Organiques et les Formes d'Humus dans leurs Rapports avec l'Agriculture. Translated from the 1896 German edition by E. Henry. Berger-Levrault, Paris.

Le rôle de la biomasse microbienne (modèle MOMOS-6)

GLOBAL BIOGEOCHEMICAL CYCLES, VOL. 18, GB4022, doi:10.1029/2004GB002230, 2004

Comparison of five soil organic matter decomposition models using data from a ^{14}C and ^{15}N labeling field experiment

Marc Pansu,[1] Pierre Bottner,[2] Lina Sarmiento,[3] and Klaas Metselaar[4]

Received 30 January 2004; revised 15 July 2004; accepted 12 August 2004; published 24 November 2004.

[1] Five alternatives of the previously published MOMOS model (MOMOS-2 to -6) are tested to predict the dynamics of carbon (C) and nitrogen (N) in soil during the decomposition of plant necromass. ^{14}C and ^{15}N labeled wheat straw was incubated over 2 years in fallow soils of the high Andean Paramo of Venezuela. The following data were collected: soil moisture, total ^{14}C and ^{15}N and microbial biomass (MB)-^{14}C and -^{15}N, daily rainfall, air temperature and total radiation. Daily soil moisture was predicted using the SAHEL model. MOMOS-2 to -4 (type 1 models) use kinetic constants and flow partitioning parameters. MOMOS-2 can be simplified to MOMOS-3 and further to MOMOS-4, with no significant changes in the prediction accuracy and robustness for total-^{14}C and -^{15}N as well as for MB-^{14}C and -^{15}N. MOMOS-5 (type 2 models) uses only kinetic constants: three MB-inputs (from labile and stable plant material and from humified compounds) and two MB-outputs (mortality and respiration constants). MOMOS-5 did not significantly change the total-^{14}C and -^{15}N predictions but markedly improved the predictive quality and robustness of MB-^{14}C and -^{15}N predictions (with a dynamic different from the predictions by other models). Thus MOMOS-5 is proposed as an accurate and ecologically consistent description of decomposition processes. MOMOS-6 extends MOMOS-5 by including a stable humus compartment for long-term simulations of soil native C and N. The improvement of the predictions is not significant for this 2-year experiment, but MOMOS-6 enables prediction of a sequestration in the stable humus compartment of 2% of the initially added ^{14}C and 5.4% of the added ^{15}N. *INDEX TERMS:* 1045 Geochemistry: Low-temperature geochemistry; 1055 Geochemistry: Organic geochemistry; 1615 Global Change: Biogeochemical processes (4805); 3210 Mathematical Geophysics: Modeling; *KEYWORDS:* decomposition, modeling, tracer experiment, soil organic matter, carbon, nitrogen, ^{14}C, ^{15}N, microbial biomass

Citation: Pansu, M., P. Bottner, L. Sarmiento, and K. Metselaar (2004), Comparison of five soil organic matter decomposition models using data from a ^{14}C and ^{15}N labeling field experiment, *Global Biogeochem. Cycles*, *18*, GB4022, doi:10.1029/2004GB002230.

1. Introduction

[2] Extending the knowledge of soil carbon and nitrogen cycles and improving its modeling remain a major challenge for land use management and prediction of the global C and N flows. The kinetics are generally described by assigning fractions of the soil organic matter (SOM) into compartments that are supposed to be qualitatively homogeneous and by quantifying C and N flows between these compartments. Natural or artificial isotopic tracer techniques are an essential tool to understand and model SOM systems. The tracer is generally introduced in a particular compartment, and is followed through the other compartments, assumed to behave as ideally mixed reservoirs. Then the pathways of the tracer reflect the functioning of the system. Sensitivity analysis (SA) is a complementary tool that was more recently used to analyze complex SOM systems [e.g., *Knorr and Heimann*, 2001; *Chimner et al.*, 2002; *Paul et al.*, 2003].

[3] A pioneer SOM decomposition model (a simple two compartment model) was proposed by *Hénin et al.* [1959]. Among the further published models, many were too complex to be easily validated, because theoretical compartments were often not measurable. The numerous physical, chemical and biological SOM fractionation procedures seldom allowed identification of theoretically defined compartments. A major step was achieved when *Jenkinson and Powlson* [1976] and *Anderson and Domsch* [1978] proposed new procedures to measure the microbial biomass pool (MB), a keystone to describe the SOM system. However, the structural identifiability analysis [*Cobelli et al.*, 1979] of the complex theoretical schemes remains a

[1]Institut de Recherche pour le Développement, Montpellier, France.
[2]Centre d'Ecologie Fonctionnelle et Evolutive, Centre National de la Recherche Scientifique, Montpellier, France.
[3]Instituto de Ciencias Ambientales y Ecológicas, Facultad de Ciencias, Universidad de los Andes, Mérida, Venezuela.
[4]Crop and Weed Ecology, Wageningen University and Research Centre, Wageningen, Netherlands.

0886-6236/04/2004GB002230$12.00

difficult task. The models are often tested by estimating their predictive quality using long-term experiments. This approach is explored by, for example, *Moorhead et al.* [1999], who compared four models, or by *Smith et al.* [1997], who compared the following 10 models: Roth-C [*Jenkinson*, 1990; *Jenkinson and Rayner*, 1977], Ncsoil [*Molina et al.*, 1983], Century [*Parton et al.*, 1987], Hurley pasture [*Thornley and Verberne*, 1989], Verberne/MOTOR [*Verberne et al.*, 1990], ITE forest [*Thornley*, 1991], Daisy [*Hansen et al.*, 1991], DNDC [*Li et al.*, 1994], Candy [*Franko et al.*, 1995], and SOMM [*Chertov and Komarov*, 1997]. The authors identified two groups, but for most of the compared models the prediction errors did not differ significantly. Thus, the model performance seems to be independent of their conceptual content, suggesting that some of them may be overparameterized.

[4] Data from a former ^{14}C and ^{15}N labeling experiment performed under controlled laboratory conditions enabled construction of an initial MOMOS-C [*Sallih and Pansu*, 1993] and MOMOS-N [*Pansu et al.*, 1998] models. The aim of the present work was to validate and improve the initial MOMOS model with data from a new ^{14}C and ^{15}N experiment performed under natural field conditions. This paper compares the predictive quality and analyzes the sensitivity of five new versions (Momos-2 to -6) derived from the initial proposal (1) through successive simplifications of the model structure (the models more complex or more parameterized than MOMOS-2 are not taken into account in this study) by suppressing some compartments or some decomposition pathways and (2) by highlighting the key functional role of the microbial biomass compartment.

2. Materials and Methods

2.1. Site of the Experiment

[5] The experiment was conducted at the paramo site of Gavidia (8°35′N–8°45′N, 70°52′W–70°57′W) in the Andes of Mérida (Mérida State, Venezuela) at an altitude of 3400 m. The mean annual precipitation is 1329 mm, with a dry season between November and March and a rainy season between April and October. The mean annual temperature is 8.5°C differing only by 1.5°C between the coldest and the warmest months but with a mean daily thermal amplitude of 10.5°C. The experiment was set up in (1) a 2-year-old fallow plot (F2y data series) with an estimated soil cover = 0.85 of mainly perennial herbs and (2) in a 7-year-old fallow plot (F7y data series) covered by the characteristic paramo giant rosettes and by shrubs (height = 1 to 1.5 m, estimated soil cover = 0.9, differing markedly from grassland). The soil (*humitropepts*, USA Soil Taxonomy) is loamy and well drained. In the 0- to 10-cm layer, sand = 54%, silt = 31%, clay = 15%, pH(H_2O) = 4.5, water-holding capacity (v/v) = 0.52 (mean values of the two experimental plots), C = 9.4% (plot F2y) and 8.8% (plot F7y), and N = 0.55% (F2y) and 0.56% (F7y). The high organic matter content explains the high water-holding capacity. The cultivation system is based on a long fallow period used for extensive grazing (generally lasting from 5 to 10 years) alternating with a short (1 to 3 years) potato and cereal cropping period.

2.2. ^{14}C and ^{15}N Labeled Plant Material

[6] A low N-requiring old cultivar of spring wheat (Florence Aurore) was grown from seed to maturity in a labeling chamber with controlled $^{14}CO_2$ atmosphere (0.03% v/v, 0.86 kBq mg^{-1} C), temperature, radiation, and alternate lighting conditions. The plants, which were cultivated in pure sand, were periodically flooded with a complete nutrient solution containing $Ca(^{15}NO_3)_2$ (10% atomic ratio) as the sole N source. At ear emergence the wheat was dried at 40°C. Only the stems and leaves were used in the experiment. They were ground into particles between 2 and 7 mm long and mixed to obtain a homogeneous material. The C content of the material was 43.0 ± 0.39% (0.821 ± 0.022 kBq mg^{-1} C), the N content was 1.60 ± 0.05% (^{15}N isotopic ratio = 9.250 ± 0.451%), and the C/N ratio was 26.9 ± 0.9. The biochemical fractions of the straw [*van Soest et al.*, 1991] were as follows: neutral detergent soluble = 0.36, hemicelluloses = 0.25, cellulose = 0.26, lignin = 0.03, and ashes = 0.10. The N content of the straw used in the present part of the experiment was relatively high, but the behavior of the model from a litter with low N content will be discussed elsewhere (work in preparation).

2.3. Field Incubation

[7] For each plot (F2y and F7y series), homogenized air-dried soil, sampled from the 5- to 10-cm layer, was divided into 40 samples of 150.0 g soil each. Then 3.260 g of labeled straw were homogeneously added to each sample, corresponding to 9.0% (F2y) and 9.6% (F7y) of total C (soil native C + plant material C) and 5.9% (F2y) and 5.8% (F7y) of total N (soil native N + plant N). The mixture was placed in 10 × 8 cm sealed polyester bags made from 0.5-mm mesh tissue. The bags were placed horizontally in the 5- to 10-cm layer and covered with the upper 0- to 5-cm layer soil. The experiment lasted from 13 November 1998 to 11 November 2000. For each series, nine samplings (+1 at time 0) were performed, collecting four replicates at each sampling (see Figures 2 and 3 in section 3 for sampling dates).

2.4. Data Acquisition

[8] At sampling, the wet sample was homogenized and 3 × 5 g wet soil was dried at 105°C for the measurement of the moisture content. The remaining wet soil was sub-sampled for analyses of (1) microbial biomass-^{14}C and -^{15}N (four field replicates × two analysis replicates for MB-^{14}C, four field replicates for MB-^{15}N), and (2) total-^{14}C, (four × eight replicates) and -^{15}N (four × two replicates). Microbial biomass was measured according to the fumigation-extraction method of *Brookes et al.* [1985]: 20 g soil, 150 mL 1 mol($^1/_2K_2SO_4$)L^{-1} extractant, ^{14}C measurement on the extracts by liquid scintillation counting (Tricarb 1500, Packard), measurement of N and ^{15}N by Kjeldahl procedure and isotope mass spectrometry (Finnigan delta S), k_{eC} (the microbial biomass-C correcting factor) = 0.45 [*Joergensen*, 1996], and k_{EN} (N correcting factor) = 0.54 [*Joergensen and Mueller*, 1996]. Total C and ^{14}C were measured simultaneously using Carmograph 12A

(Wösthoff, Bochum, Germany), according to *Bottner and Warembourg* [1976]. Total N and ^{15}N were measured using coupled CHN/isotope mass spectrometry.

[9] Climatic parameters (daily precipitation, mean air temperature, and total radiation) were recorded using an automatic Campbell weather station at the site throughout the experiment period.

2.5. Predictive Models

[10] The five models tested with Vensim software (Ventana Systems, Inc., Harvard, Massachusetts) are presented in Figure 1. Three compartments are present in all the models: labile (VL), stable (VS) fractions of necromass (NC = VL + VL) and microbial biomass (MB). MOMOS-3, -4, and -5 contain a compartment for humified compounds (H). MOMOS-2 and -6 contain compartments for labile (HL) and stable (HS) humified compounds. MOMOS-2 is the model already presented by *Sallih and Pansu* [1993] using data from a labeling experiment performed under laboratory conditions, with measurements of total ^{14}C, microbial biomass ^{14}C and not yet decomposed plant fragments ^{14}C. MOMOS-3 results from the simplification of MOMOS-2, with an equation system analogous to the Roth-C model [*Jenkinson*, 1990], but without the inert organic matter compartment of Roth-C (not necessary for this short-term ^{14}C and ^{15}N experiment). MOMOS-4 offers a further simplification of MOMOS-3: The recycling part of H and MB compartments are removed. MOMOS-5 explores two new modifications: (1) the whole outputs from plant material (VL+VS) and humus (H) compartments are the inputs of MB, and (2) the outputs of MB are defined by a respiration quotient (q_{CO2}) and a microbial mortality rate (k_{MB}). The equation system of MOMOS-5 is similar to that of the CANDY model [*Franko et al.*, 1995] and to that used by *Saggar et al.* [1996] to calculate ^{14}C turnover and residence times in soils. However, MOMOS-5 differs from the former models in the following aspects: (1) fractionation of NC inputs into VL and VS, (2) change of kinetic calculation of the microbial respiration (see below, equations (9) and (10)), and (3) elimination of the flow fractionation between necromass and MB used in CANDY (in MOMOS-5 the whole flow from the NC substrate enters into MB). MOMOS-6 attempts to improve MOMOS-5 by introducing a stable humus compartment (HS) that results from the slow maturation of HL and supplies the dormant MB with maintenance energy, when the fresh C input is exhausted. MOMOS-5 and -6 are only regulated by first-order kinetic constants (k parameters, dimension t^{-1}), without the dimensionless parameters (efficiency factors) often used in SOM models to fractionate the flows between the compartments (P parameters in MOMOS-2 to -4, or, e.g., *Jenkinson and Rayner* [1977], *Parton et al.* [1987], or *Franko et al.* [1995]).

[11] For each model, the initial necromass (NC) was partitioned over VL and VR on the basis of its biochemical characteristics using the equations proposed by *Thuriès et al.* [2001, 2002], which give for this labeled straw the stable fraction of NC: $f_s = 0.107$.

[12] The general equation of the models is

$$\dot{x} = \mathbf{A}\,\mathbf{x}, \tag{1}$$

where $\mathbf{x}$ is the vector of the state variables (compartments), $\dot{x}$ is the vector of the rates variables, and $\mathbf{A}$ is the parameter matrix of each model. $\mathbf{A}$ and $\mathbf{x}$ are written, for MOMOS-2,

$$\mathbf{A} = \begin{vmatrix} -k_{VL} & 0 & 0 & 0 & 0 \\ 0 & -k_{VS} & 0 & 0 & 0 \\ P_{MB}k_{VL} & P_{MB}k_{VS} & (P_{MB}-1)\,k_{MB} & P_{MB}k_{HL} & P_{MB}k_{HS} \\ P_{HL}k_{VL} & P_{HL}k_{VS} & P_{HL}k_{MB} & (P_{HL}-1)\,k_{HL} & P_{HL}k_{HS} \\ P_{HS}k_{VL} & P_{HS}k_{VS} & P_{HS}k_{MB} & P_{HS}k_{HL} & (P_{HS}-1)\,k_{HS} \end{vmatrix}$$

$$\mathbf{x} = \begin{vmatrix} VL \\ VS \\ MB \\ HL \\ HS \end{vmatrix}, \tag{2}$$

for MOMOS-3,

$$\mathbf{A} = \begin{vmatrix} -k_{VL} & 0 & 0 & 0 \\ 0 & -k_{VS} & 0 & 0 \\ P_{MB}k_{VL} & P_{MB}k_{VS} & (P_{MB}-1)k_{MB} & P_{MB}k_{H} \\ P_{H}k_{VL} & P_{H}k_{VS} & P_{H}k_{MB} & (P_{H}-1)k_{H} \end{vmatrix}$$

$$\mathbf{x} = \begin{vmatrix} VL \\ VS \\ MB \\ H \end{vmatrix}, \tag{3}$$

for MOMOS-4,

$$\mathbf{A} = \begin{vmatrix} -k_{VL} & 0 & 0 & 0 \\ 0 & -k_{VS} & 0 & 0 \\ P_{MB}k_{VL} & P_{MB}k_{VS} & -k_{MB} & 0 \\ P_{H}k_{VL} & P_{H}k_{VS} & 0 & -k_{H} \end{vmatrix} \quad \mathbf{x} = \begin{vmatrix} VL \\ VS \\ MB \\ H \end{vmatrix}, \tag{4}$$

for MOMOS-5,

$$\mathbf{A} = \begin{vmatrix} -k_{VL} & 0 & 0 & 0 \\ 0 & -k_{VS} & 0 & 0 \\ k_{VL} & k_{VS} & -(q_{CO_2}+k_{MB}) & k_{H} \\ 0 & 0 & k_{MB} & -k_{H} \end{vmatrix} \quad \mathbf{x} = \begin{vmatrix} VL \\ VS \\ MB \\ H \end{vmatrix}, \tag{5}$$

and for MOMOS-6,

$$\mathbf{A} = \begin{vmatrix} -k_{VL} & 0 & 0 & 0 & 0 \\ 0 & -k_{VS} & 0 & 0 & 0 \\ k_{VL} & k_{VS} & -(q_{CO_2}+k_{MB}) & k_{HL} & k_{HS} \\ 0 & 0 & k_{MB} & -(k_{HL}+k_{HLS}) & 0 \\ 0 & 0 & 0 & k_{HLS} & -k_{HS} \end{vmatrix}$$

$$\mathbf{x} = \begin{vmatrix} VL \\ VS \\ MB \\ HL \\ HS \end{vmatrix}, \tag{6}$$

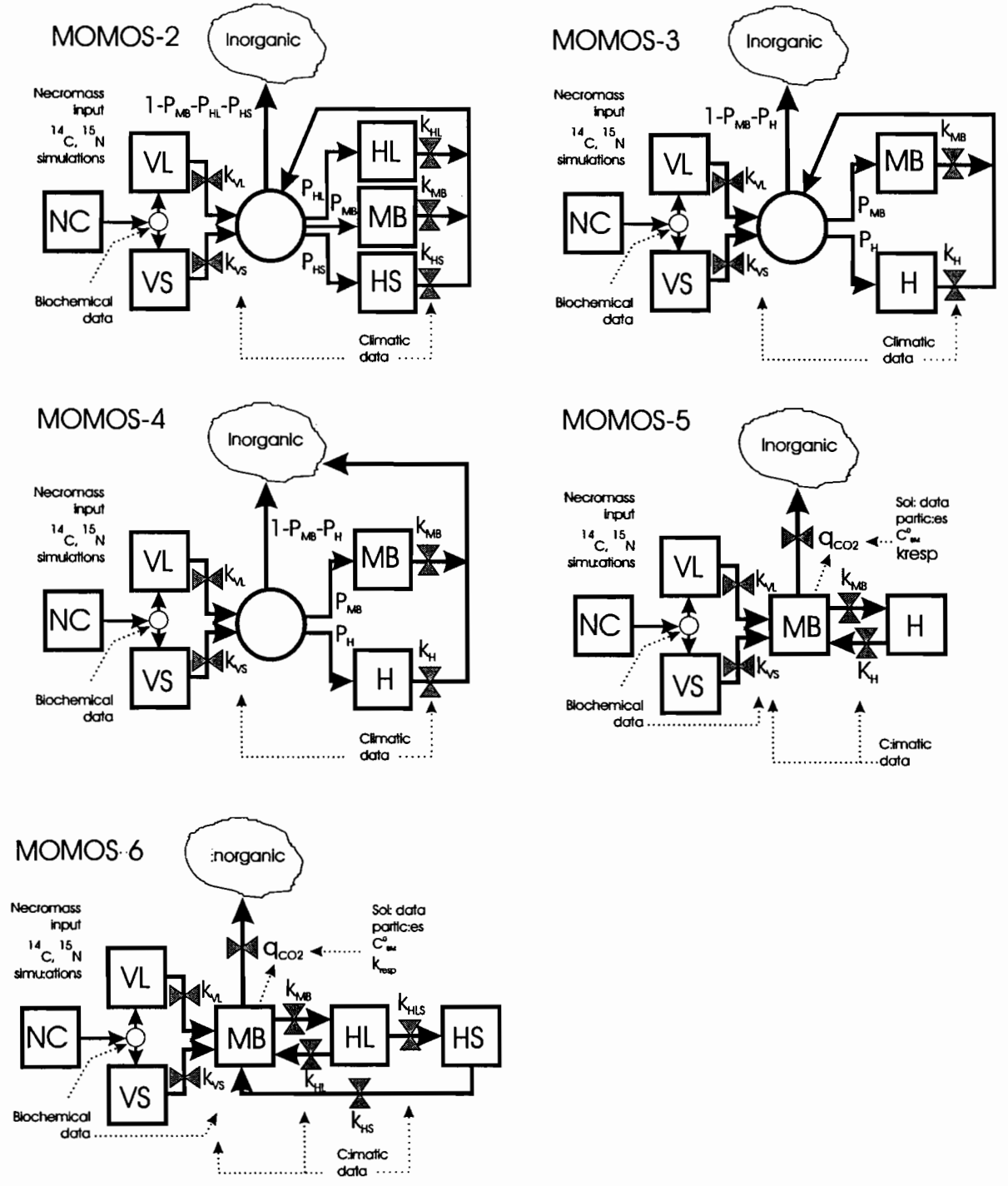

Figure 1. Flow diagram's of the five versions of the MOMOS model compared. NC, total necromass; VL, labile necromass; VS, stable necromass; MB, microbial biomass; H, humified compounds (humus); HL, labile humus; HS, stable humus.

For the labeling experiment described in this paper (one single initial input of dead matter and an initial amount C_0 of ^{14}C with a stable fraction f_S), the initial conditions are given by

$$\begin{aligned} VL(0) &= (1 - f_S)C_0, \\ VS(0) &= f_S C_0, \\ MB(0) &= 0, \\ H(0) &= 0, \\ HL(0) &= 0, \\ HS(0) &= 0, \\ CO_2(0) &= 0. \end{aligned} \tag{7}$$

[13] At each incubation time, the total ^{14}C evolution $\dot{c}$ from the n compartments ($n = 4$ for MOMOS-3, -4, -5; $n = 5$ for MOMOS-2, -6) is given by

$$\dot{c} = \sum_{i=1}^{n} \dot{x}_i \qquad c(0) = C_0. \tag{8}$$

[14] In the case of MOMOS-5 and -6, equation (8) becomes particularly simple,

$$\dot{c} = -q_{CO2}\,MB, \tag{9}$$

where q_{CO2} is the metabolic quotient of the microbial biomass [*Anderson and Domsch*, 1993]. Another condition is necessary to ensure correct performance of MOMOS-5 and -6: q_{CO2} must be controlled by the amount of MB. The q_{CO2} increases when MB is growing (particularly in response to the initial high supply from VL) and decreases when MB decreases or becomes inactive (dormant MB). Then $\dot{c}$ is linked to MB by a second-order kinetics. In order to allow use of MOMOS-5 or -6 in different situations, we suggest (1) the introduction of a respiratory coefficient k_{resp} (dimension t^{-1}) and (2) the weighting of the k_{resp} values by the ratio of the actual level of MB in the studied soil and its equilibrium value (C^0_{MB} measured in biologically stable soil, i.e., a long time after the former inputs of substrate). For the present labeling experiment, $C^0_{MB} = 0.15$ g kg^{-1}, the level of MB-^{14}C measured at the end of the experiment. The q_{CO2} is given by

$$q_{CO2} = k_{resp}\frac{MB}{C^0_{MB}}. \tag{10}$$

[15] The N calculation of MOMOS-2 to -6 is simplified compared to the initial MOMOS-N model (MOMOS-1 [*Pansu et al.*, 1998]). Ammonia and nitrate pools are combined in a single pool of inorganic-N. For each of the five models, the N state variables are derived from the C model, using the C-to-N ratios of the compartments. If $\boldsymbol{\eta}$ is the vector of the C-to-N ratios and $\mathbf{y}$ is the vector of N contents, the simulation of organic N status at a given incubation time is governed by

$$\mathbf{y} = \frac{\mathbf{x}}{\boldsymbol{\eta}}. \tag{11}$$

If η_0 is the initial ^{14}C-to-^{15}N ratio of the plant material, the inorganic ^{15}N (iN) is

$$iN = \frac{C_0}{\eta_0} - \sum_{i=1}^{n} y_i. \tag{12}$$

In this labeling experiment, the values η_0, η_t (remaining total ^{14}C-to- remaining total ^{15}N), and η_{MB} (^{14}C-to-^{15}N of microbial biomass) were measured. The η_{VL} value is linked to η_0 and η_{VS} by

$$\eta_{VL} = \frac{(1 - f_S)}{\left(\frac{1}{\eta_0} - \frac{f_S}{\eta_{VS}}\right)}. \tag{13}$$

The η_H or η_{HL} values are linked to the other data by

$$\eta_H = \frac{x_H}{\frac{C_t}{\eta_t} - \frac{x_{VL}}{\eta_{VL}} - \frac{x_{VS}}{\eta_{VS}} - \frac{x_{MB}}{\eta_{MB}}} \tag{14}$$

$$\eta_{HL} = \frac{x_{HL}}{\frac{C_t}{\eta_t} - \frac{x_{VL}}{\eta_{VL}} - \frac{x_{VS}}{\eta_{VS}} - \frac{x_{MB}}{\eta_{MB}} - \frac{x_{HS}}{\eta_{HS}}}. \tag{15}$$

Thus the only η values that have to be estimated are η_{VS} (^{14}C-to-^{15}N of the stable fraction of NC) in MOMOS-3 to -5 or η_{VS} and η_{HS} (^{14}C-to-^{15}N of the stable fraction of humus) in MOMOS-2 and -6. In order to avoid irregularities in predictions, the values calculated for η_H or η_{HL} are smoothed in the interval $[\eta_{MB}, \frac{2}{5}(\eta_0 + \eta_{MB})]$ with $\eta_{HS} = 6\,\eta_{MB}/5$ for MOMOS-6.

[16] During the simulations, the kinetic constants are daily corrected by two functions, one for temperature $f(T)$ and one for moisture $f(w)$; $f(T)$ is a law with Q10 = 2 for a reference temperature of 20°C assumed to be valid for these mountain soils [*Kätterer et al.*, 1998]; $f(w)$ is a linear function of the actual soil moisture scaled by moisture content at field capacity ($f(w) = 0$ for $w = 0$). For the 5- to 10-cm soil layer, the actual moisture was calculated by the SAHEL model [*Penning de Vries et al.*, 1989]. With the corrective factor $f(T) \times f(w)$ in [0, 1] interval, the general formulation (equation (1)) of the models becomes

$$\dot{x} = f(T)f(w)\mathbf{A}\,\mathbf{x}. \tag{16}$$

2.6. Comparison of the Predictive Quality and Sensitivity of the Models

[17] The four vectors of measured data were:

- $\mathbf{x}_t$ = total ^{14}C (nine sampling occasions (so) during 2 years of incubation), corresponding to the predicted values $\hat{\mathbf{x}}_t = \sum_{i=1}^{n} \mathbf{x}_i$,

Table 1. Estimated Values of the Parameters for the Five Tested Models[a]

	Parameter Values												
Model	k_{VL}	k_{VS}	k_{MB}	k_{HL}	k_H	k_{HS_u}	k_{HLS}	k_{resp}	P_{MB}	P_H	P_{HS}	η_{VS}	η_H	η_{HS}
MOMOS-2	0.54	0.004	0.01	k_{VL}		k_{VS}			0.014		0.08	500		10.5
MOMOS-3	0.13	0.004	0.01		k_{VS}				0.06	0.36		450	10.9	
MOMOS-4	0.13	0.002	0.007		k_{VS}				0.06	0.36		500	10.5	
MOMOS-5	0.6	0.003	0.45		0.05			0.03				27	Cal	
MOMOS-6	0.6	0.003	0.45	0.05		$5\ 10^{-5}$	$3\ 10^{-4}$	0.03				46	Cal	9.9
	Sensitivity Analysis (S_{sv}, Equation (19)) of MOMOS-4 (Type 1) Model													
SV	k_{VL}	k_{VS}	k_{MB}	k_{HL}	k_H	k_{HS_u}	k_{HLS}	k_{resp}	P_{MB}	P_H	P_{HS}	η_{VS}	η_H	η_{HS}
Tot-^{14}C 3 m	0.17	0.17	0.05		0.17				0.17	1.5				
Tot-^{14}C 24 m	0.03	1.0	0.14		1.0				0.09	1.7				
Tot-^{15}N 3 m	0.04	0.09	0.05		0.09				0.27	1.9				
Tot-^{15}N 24 m	0.03	0.9	0.2		0.9				0.14	2				
MB-^{14}C 3 m	0.17	0.08	0.3		0.08				2.5	0				
MB-^{14}C 24 m	0.07	0.15	3.2		0.15				2.4	0				
MB-^{15}N 3 m	0.16	0.07	0.2		0.07				2.4	0				
MB-^{15}N 24 m	0.05	0.12	3.8		0.12				2.3	0				
	Sensitivity Analysis (S_{sv}, Equation (19)) of MOMOS-6 (type 2) Model													
SV	k_{VL}	k_{VS}	k_{MB}	k_{HL}	k_H	k_{HS_u}	k_{HLS}	k_{resp}	P_{MB}	P_H	P_{HS}	η_{VS}	η_H	η_{HS}
Tot-^{14}C 3 m	0.3	0.02	1.2	0.5		<0.01	0.01	0.7						
Tot-^{14}C 24 m	0.2	0.16	2.3	2.0		<0.01	0.16	1.1						
Tot-^{15}N 3 m	0.4	0.02	1.2	0.5		<0.01	0.01	0.9						
Tot-^{15}N 24 m	0.2	0.16	2.2	2.0		<0.01	0.2	1.2						
MB-^{14}C 3 m	0.4	0.04	0.20	1.4		<0.01	0.02	1.1						
MB-^{14}C 24 m	0.2	0.15	0.43	0.43		<0.01	0.09	1.5						
MB-^{15}N 3 m	0.4	0.04	0.35	1.4		<0.01	0.02	1.1						
MB-^{15}N 24 m	0.3	0.09	0.56	0.56		<0.01	0.06	1.5						

[a]Abbreviations: k, first-order kinetic constants (day^{-1}); P, fraction of flow (dimensionless); η, estimated ^{14}C-to-^{15}N ratio. Sensitivity analysis to parameter fluctuations of the four-state variable Total-^{14}C, Total-^{15}N, MB-^{14}C, and MB-^{15}N is at 3 and 24 m of incubation.

$-\mathbf{y}_t$ = total ^{15}N (nine so) corresponding to the predicted values $\hat{\mathbf{y}}_t = \sum_{i=1}^{n} \mathbf{y}_i$,

$-\mathbf{x}_{MB}$ = MB-^{14}C (nine so) corresponding to the predicted values $\hat{\mathbf{x}}_{MB}$,

$-\mathbf{y}_{MB}$ = MB-^{15}N (nine so) corresponding to the predicted values $\hat{\mathbf{y}}_{MB}$,

For each model, four residual sums of square (RSS) were calculated for the m so,

$$\begin{aligned} RSS_{xt} &= \sum_{j=1}^{m} (\mathbf{x}_t - \hat{\mathbf{x}}_t)^2, \\ RSS_{yt} &= \sum_{j=1}^{m} (\mathbf{y}_t - \hat{\mathbf{y}}_t)^2, \\ RSS_{xMB} &= \sum_{j=1}^{m} (\mathbf{x}_{MB} - \hat{\mathbf{x}}_{MB})^2, \\ RSS_{yMB} &= \sum_{j=1}^{m} (\mathbf{y}_{MB} - \hat{\mathbf{y}}_{MB})^2. \end{aligned} \tag{17}$$

[22] The smallest RSS corresponds to the best fit. In addition, the comparison should take the number of model parameters p into account. The best model has the smallest RSS and also the smallest p. MOMOS-5 has five parameters: k_{VL}, k_{VS}, k_{MB}, k_{HL}, and k_{resp}. MOMOS-3 and -4 have six parameters: k_{VL}, k_{VS}, k_{MB}, k_H, P_{MB}, and P_H. However, the specific parameterization of this experiment takes $k_{VS} = k_H$ and reduces MOMOS-3 and -4 to five parameter models. MOMOS-2 has eight parameters: k_{VL}, k_{VS}, k_{HL}, k_{HS}, k_{MB}, P_{HL}, P_{MB}, and P_{HS}. However, again, the parameterization of this experiment takes $k_{VL} = k_{HL}$, $k_{VS} = k_{HS}$, and $P_{HL} = 0.77$ (value found by *Sallih and Pansu* [1993]) and also reduces MOMOS-2 to a five-parameter model.

[23] Thus the predictive quality of the models MOMOS-2–-5 can be pairwise compared by the F tests,

$$F_{(m-1,m-1)} = \begin{cases} RSS_{MOMOS-t}/RSS_{MOMOS-u} & \text{if } RSS_{MOMOS-t} > RSS_{MOMOS-u} \\ RSS_{MOMOS-u}/RSS_{MOMOS-t} & \text{if } RSS_{MOMOS-u} > RSS_{MOMOS-t} \end{cases}, \tag{18}$$

(u, $t \in [2-5]$, $t \neq u$, m sampling occasions, for each of the four models applied to each of the four series total-^{14}C and -^{15}N, MB-^{14}C, and -^{15}N.

[24] For a given state variable (SV), a scaled dimensionless sensitivity to a parameter (PA) can be defined by

$$S_{SV} = \frac{\Delta_{SV}\ SV^{-1}}{\Delta_{PA}\ PA^{-1}} \tag{19}$$

for the SV total-^{14}C, total-^{15}N, MB-^{14}C, and MB-^{15}N from 13 November 1998 to 11 November 2000 at a daily time step. The values of the parameters were randomly sampled (200 simulations) from a normal distribution. For each parameter, the mean of the distribution is presented in Table 1; the relative standard deviation (sd) was 10%.

3. Results

3.1. Parameters and Sensitivity of the Models

[25] Since there was no significant difference between the results from series F2y and F7y, all the predictions for each

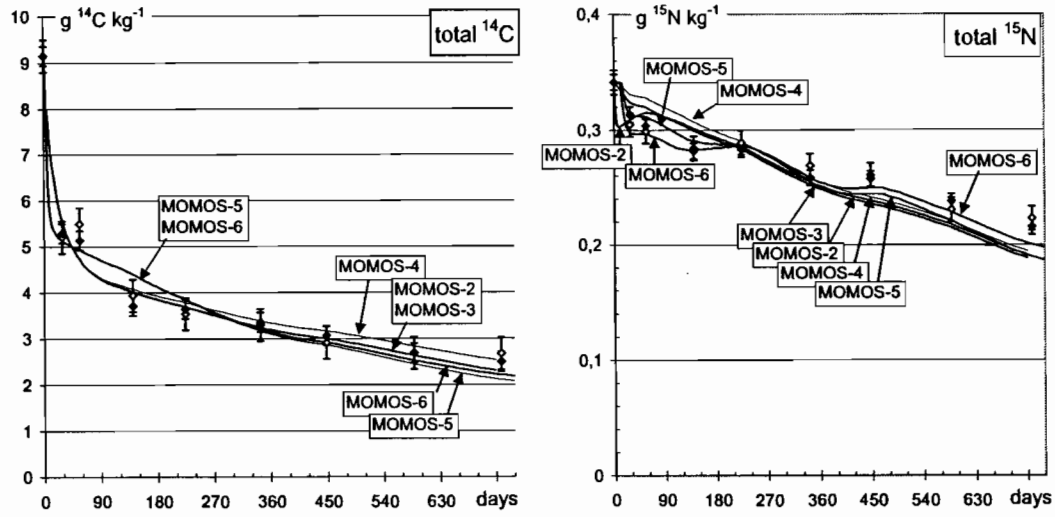

Figure 2. Model predictions (lines) and measured data of total-^{14}C and -^{15}N for the two series (solid diamonds, F2y; open diamonds, F7y) with pooled 95% confidence interval (nine sampling occasions × four field replicates × two to eight analysis replicates). Day 0 is 13 November 1998.

model are based on only one set of parameters (the mean value from F2y and F7y calculations, Table 1). The results of sensitivity analysis of the five models show (1) a similar behavior of MOMOS-2 to -4 and (2) a similar behavior of MOMOS-5 and -6. Therefore MOMOS-4 was chosen in Table 1 as being representative of MOMOS-2 to -4 (type 1 models), and MOMOS-6 was chosen as being representative of the type 2 models. Type 1 defines models with two types of parameters: kinetic constants and flow fractionation (efficiency factors). Type 2 defines models with only kinetic constants as parameters; consequently, all the parameters of type 2 models are linked to climatic variations.

3.2. Total ^{14}C and ^{15}N Predictions

[26] The predictions of the five models and the measured F2y and F7y values are plotted in Figure 2. Tables 2 and 3 compare the predictive quality (equation (18)) of the models for total ^{14}C and ^{15}N, respectively.

[27] For total ^{14}C, the MOMOS-2 and MOMOS-3 predictions were almost identical. For the other models the predictions were slightly different (Figure 2), but all the results were statistically equivalent (Table 2). The MOMOS-5 and -6 predictions were also almost identical during the first 9 months, as long as the HS content (MOMOS-6) was low. At the end of the experiment, MOMOS-6 predicted slightly higher values, closer to the measured data than MOMOS-5, indicating a ^{14}C-sequestration in the HS compartment.

[28] For total ^{15}N predictions, slight differences appeared between the models (Figure 2), but they were again all statistically equivalent (Table 3). The MOMOS-2 to -4 predictions were overestimated during the first 6 months of incubation and underestimated during the last year. The MOMOS-5 and especially the MOMOS-6 predictions were the closest to the measured values throughout the whole incubation period. The slight underestimation observed during the last year could be explained by a slight overestimation of the measured ^{15}N; total-^{15}N is defined in MOMOS as organic-^{15}N, whereas the measurements include small amounts of inorganic ^{15}N remaining in the soil.

[29] The sensitivity analysis (Table 1) shows that the total ^{14}C and total ^{15}N predicted by the type 1 models are mainly influenced by the P_H values, that is, the fraction of materials transformed in stable humus. In type 2 models, the effect of the parameters fluctuation on total ^{14}C and total ^{15}N predictions is better balanced. The most active parameters are the mortality constant of MB (k_{MB}), the respiration constant of MB (k_{resp}), the MB input from HL (K_{HL}),

Table 2. *F* Tests (Equation (18)) Applied to the Comparison of the Residual Sums of Squares (RSS) of Total ^{14}C Predictions for the Two Data Series F2y and F7y[a]

	MOMOS-3		MOMOS-4		MOMOS-5		MOMOS-6	
Model	F2y	F7y	F2y	F7y	F2y	F7y	F2y	F7y
MOMOS-2	$1.00^{2,\ NS}$	$1.13^{2,\ NS}$	$1.06^{2,\ NS}$	$1.10^{2,\ NS}$	$2.17^{2,\ NS}$	$1.16^{2,\ NS}$	$1.83^{2,\ NS}$	$1.00^{6,\ NS}$
MOMOS-3			$1.06^{3,\ NS}$	$1.02^{4,\ NS}$	$2.16^{3,\ NS}$	$1.02^{3,\ NS}$	$1.83^{3,\ NS}$	$1.13^{6,\ NS}$
MOMOS-4					$2.05^{4,\ NS}$	$1.05^{4,\ NS}$	$1.73^{4,\ NS}$	$1.10^{6,\ NS}$
MOMOS-5							$1.18^{6,\ NS}$	$1.16^{6,\ NS}$

[a]Exponent close to *F* value is MOMOS number with the smallest RSS; NS denotes not significant.

Table 3. F Tests (Equation (18)) Applied to the Comparison of the Residual Sums of Squares (RSS) of Total ^{15}N Predictions for the Two Data Series F2y and F7y[a]

	MOMOS-3		MOMOS-4		MOMOS-5		MOMOS-6	
Model	F2y	F7y	F2y	F7y	F2y	F7y	F2y	F7y
MOMOS-2	$1.34^{2,\ NS}$	$1.36^{2,\ NS}$	$1.36^{2,\ NS}$	$1.38^{2,\ NS}$	$1.28^{2,\ NS}$	$1.14^{5,\ NS}$	$1.74^{6,\ NS}$	$1.53^{6,\ NS}$
MOMOS-3			$1.02^{3,\ NS}$	$1.01^{3,\ NS}$	$1.04^{5,\ NS}$	$1.77^{5,\ NS}$	$1.81^{6,\ NS}$	$2.09^{6,\ NS}$
MOMOS-4					$1.06^{5,\ NS}$	$1.79^{5,\ NS}$	$1.85^{6,\ NS}$	4.35^{6}
MOMOS-5-s							$1.74^{6,\ NS}$	$2.43^{6,\ NS}$

[a]Exponent close to F value is MOMOS number with the smallest RSS; NS denotes not significant.

especially at the end of incubation, and the MB input from VL (k_{VL}), especially at 3 months of incubation.

3.3. Predictions of MB-^{14}C and -^{15}N

[30] The predicted and measured values of MB in the F2y and F7y series are plotted in Figure 3. Tables 4 and 5 compare the predictive quality (equation (18)) of the models for MB-^{14}C and -^{15}N, respectively. The MOMOS-2 and -3 predictions were almost identical and were close to the MOMOS-4 predictions. In all cases the results show clearly a significant improvement of the MB predictions by MOMOS-5 compared to those by MOMOS-2 to -4. For MB-^{14}C, the improvement was significant at 5% risk in five cases and at 2% risk in one case. For MB-^{15}N, the improvement was significant at 10% risk in two cases and at 5% in the four other cases. During the first 5 months the MOMOS-5 and -6 predictions were again similar. After this time the MOMOS-6 predictions were slightly closer to the measured values of MB-^{14}C and -^{15}N.

[31] The sensitivity analysis (Table 1) shows that MB-^{14}C and MB-^{15}N predicted by the type 1 models are mostly controlled by the P_{MB} values (the fraction of materials transformed in microbial biomass) during the whole incubation period. At the end of experiment, these MB-^{14}C and MB-^{15}N predictions are also very sensitive to k_{MB} values (the kinetic constant of the MB output), but during the whole incubation the predictions do not depend on the P_H value; symmetrically, the H-^{14}C and H-^{15}N predictions do not depend on the P_{MB} values. The MB-^{14}C and MB-^{15}N predictions are more stable in type 2 than in type 1 models: The maximum S_{SV} value is 2.5 in type 1 models and 1.5 in type 2 models (Table 1). These predictions are most sensitive to the k_{resp} values (the respiratory coefficient of MB) and, second, at the beginning of incubation, to the k_{HL} (the input into MB from HL) and k_{VL} (the input into MB from VL) values.

4. Discussion

4.1. Comparison of MOMOS-2 and MOMOS-3

[32] MOMOS-3 differs from MOMOS-2 by the absence of the labile humus compartment (HL, Figure 1). This results in very different values of the first-order kinetic constants of VL: $k_{VL} = 0.54$ ($t^{1/2} = 1.3$ days) for MOMOS-2 and $k_{VL} = 0.13$ ($t^{1/2} = 5.3$ days) for MOMOS-3 (Table 1). In MOMOS-2 the labile metabolites are subsequently transferred to the transient HL compartment. The predictions of the two models are similar for total-^{14}C and MB-^{14}C, as

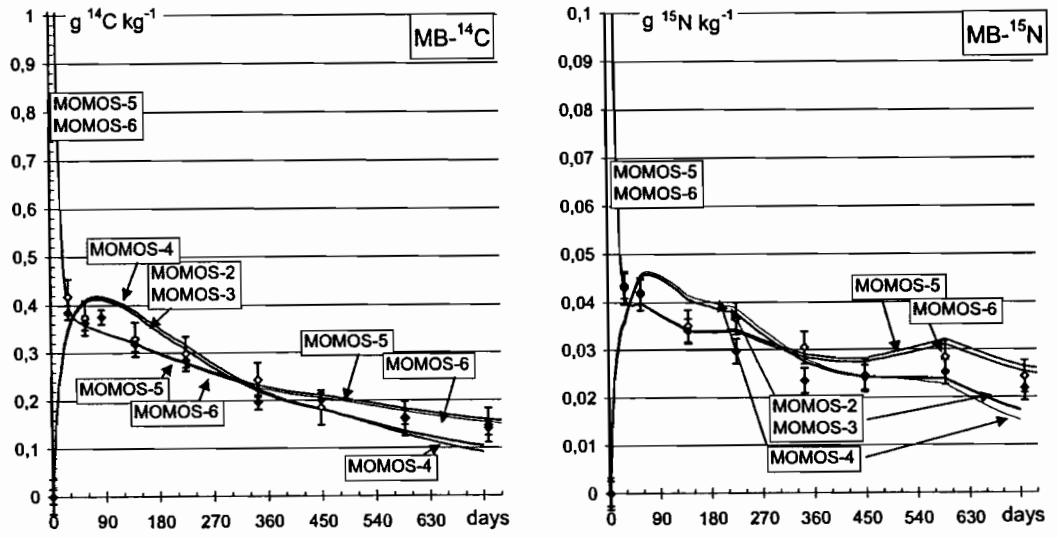

Figure 3. Model predictions (lines) and measured data of MB-^{14}C and -^{15}N for the two series (solid diamonds, F2y; open diamonds, F7y) with pooled 95% confidence interval (nine sampling occasions × four field replicates). Day 0 is 13 November 1998.

Table 4. *F* Tests (Equation (18)) Applied to the Comparison of the Residual Sums of Squares (RSS) of MB-^{14}C Predictions for the Two Data Series F2y and F7y[a]

	MOMOS-3		MOMOS-4		MOMOS-5		MOMOS-6	
Model	F2y	F7y	F2y	F7y	F2y	F7y	F2y	F7y
MOMOS-2	$1.02^{3,\ NS}$	$1.09^{3,\ NS}$	$1.31^{2,\ NS}$	$1.20^{2,\ NS}$	$4.51^{5,\ A}$	$5.22^{5,\ A}$	6.60^{6}	5.80^{6}
MOMOS-3			$1.33^{3,\ NS}$	$1.22^{3,\ NS}$	$4.43^{5,\ A}$	$5.12^{5,\ A}$	6.48^{6}	5.69^{6}
MOMOS-4					$5.88^{5,\ A}$	$6.26^{5,\ B}$	8.61^{6}	6.97^{6}
MOMOS-5							1.46^{6}	1.11^{6}

[a]Exponent close to *F* value is MOMOS number with the smallest RSS; A, B, and NS denote RSS significant difference at 5% and 2% risk and not significant, respectively.

well as for MB-^{15}N (Figures 2 and 3). The slight but not significant differences observed for total-^{15}N resulted from the estimated C-to-N ratio (equation (15)) of the HL compartment. Thus the two models are clearly equivalent in predicting the total SOM dynamics. The MOMOS-2 decay rate of HL and VL are identical ($k_{HL} = k_{VL}$). Both VL and HL compartments are quickly and almost completely exhausted after 90–120 days of incubation; at that time, MB reaches its maximum values and begins also to decline; this highlights the role of labile compounds in the MB dynamics. In MOMOS-3, the VL compartment represents the sum VL + HL of MOMOS-2 and is exhausted at the same time. Thus MOMOS-3, with an equation system analogous to the Roth-C model [*Jenkinson*, 1990], is a valuable simplification of MOMOS-2. Nevertheless, the need of the HL compartment was supported from another labeling experiment [*Sallih and Pansu*, 1993] performed under controlled laboratory conditions where, in addition to the MB measurement, the not yet decomposed plant fragments-^{14}C (NC) remaining in the soil were also measured: HL-^{14}C = total-^{14}C minus (MB-^{14}C + plant fragments-^{14}C). The HL compartment describes a real transient decomposition step. Nevertheless, in modeling the total C and N dynamics from long field experiments with this type of model, HL can be eliminated. Thus MOMOS-3, with an equation system analogous to the Roth-C model [*Jenkinson*, 1990], is a valuable simplification of MOMOS-2.

4.2. Comparison of MOMOS-3 and MOMOS-4

[33] MOMOS-4 is a further simplification derived from MOMOS-3 by suppressing the recycling loop of MB and H outputs (Figure 1). MOMOS-4 is a parallel decomposition model in which a part P_{MB} of the flow from VL and VS becomes MB and another part P_H becomes H. In the mathematical description of MOMOS-4, this simplification eliminates the *P* parameters from the diagonal terms (see matrix equation (3)). In the matrix of equation (4), the diagonal terms become first-order kinetic constants; all the terms above the diagonal become zero. The calculated MOMOS-3 and -4 parameters are similar, except the slightly lower first-order kinetic constants k_{VS} (and $k_H = K_{VS}$) and k_{MB} in MOMOS-4. This is in accordance with the removal of the recycling part in MOMOS-4.

[34] In Tables 3, 4, and 5, RSS-3 was always lower than RSS-4, indicating a tendency of more accurate predictions for MOMOS-3 than for MOMOS-4, but the differences were never significant. Given the RSS ratios (Tables 2–5), the models 3 and 4 predictions are never significantly different. Consequently, MOMOS-4 is preferable because of its simpler structure.

4.3. Comparison of MOMOS-4 (Type 1 Models) and MOMOS-5 (Type 2)

[35] In MOMOS-5, the estimated first-order kinetic constant k_{VL} is higher than in MOMOS-3 and -4 and close to the MOMOS-2 value (Table 1). However, in MOMOS-5, the VL labile plant material is entirely assimilated by MB, while in MOMOS-2, VL becomes, for the P_{HL} part, labile humus (HL). Consequently, MOMOS-5 and MOMOS-2 to -4 generate different MB curves. In MOMOS-5, the predicted MB increased sharply during the 3 initial days, reaching for MB-^{14}C 20 to 30% of Total-^{14}C, and for MB-^{15}N over 80% of Total-^{15}N for all treatments (not shown in Figure 3). After this initial quick peak, MB-^{14}C and -^{15}N decreased rapidly, giving significantly better predictions than MOMOS-2 to -4 from day 30 until the end of the incubation.

[36] In this experiment, the first measurement occurred at day 30, i.e., at the end of the MB initial peak (Figure 3). The shape of the MOMOS-5 MB curve agrees with literature data: The response time of MB to the addition of labile organic substrate is generally on the order from a few hours

Table 5. *F* Tests (Equation (18)) Applied to the Comparison of the Residual Sums of Squares (RSS) of MB-^{15}N Predictions for the Two Data Series F2y and F7y[a]

	MOMOS-3		MOMOS-4		MOMOS-5-s		MOMOS-5	
Model	F2y	F7y	F2y	F7y	F2y	F7y	F2y	F7y
MOMOS-2	1.02^{NS}	$1.09^{3,\ NS}$	$1.36^{2,\ NS}$	$1.22^{2,\ NS}$	$3.94^{5,\ A}$	$4.46^{5,\ B}$	6.23^{6}	5.70^{6}
MOMOS-3			$1.39^{3,\ NS}$	$1.33^{3,\ NS}$	$3.85^{5,\ A}$	$4.07^{5,\ B}$	6.08^{6}	5.21^{6}
MOMOS-4					$5.35^{5,\ B}$	$5.42^{5,\ B}$	8.46^{6}	6.93^{6}
MOMOS-5-s							1.58^{6}	1.28^{6}

[a]Exponent close to *F* value is MOMOS number with the smallest RSS; A, B, and NS denote RSS significant difference at 10% and 5% risk and not significant, respectively.

[*Anderson and Domsch*, 1978] to a few days. The maximum size of MB is often observed at the first measurement, i.e., about 7–10 days after the substrate addition [*Henriksen and Breland*, 1999; *Lundquist et al.*, 1999; *Ocio et al.*, 1991; *Trinsoutrot et al.*, 2000]. An immediate N microbial immobilization was measured from the beginning of the incubation using various substrates by *Pansu and Thuriès* [2003], *Pansu et al.* [2003], and *Trinsoutrot et al.* [2000]. Conversely, for MOMOS-2 to -4, the predicted MB curve increases slowly, reaching the maximum level only after about 2 months of incubation. Thus MOMOS-2 to -4 underestimate MB at the first measurements, overestimate it during the following few months, and again underestimate it during the second year. A similar discrepancy between the predicted and measured MB has already been observed by *Sallih and Pansu* [1993], using the MOMOS-1 model. Despite the more complex equation describing MB dynamics in type 2 models as compared to type 1, the sensitivity analysis shows a greater stability in type 2 than in type 1 models for MB-^{14}C and -^{15}N predictions. The responses are also more consistent with the ecological definition of the parameters in type 2 than in type 1 models. In type 1, the productions of MB and H are independent (they depend mainly on P_{MB} and P_H, respectively); the two compartments run in parallel without interaction. The type 2 models show a more coherent link between compartments; the total-C and -N and MB-C and -N are better equilibrated in response to the fluctuations of the most acting parameters of the model.

[37] In MOMOS-5 the H compartment has the same input (k_{MB}) and output (k_H) kinetic constants as HL in MOMOS-6. Indeed, H and HL represent labile metabolites, like HL in MOMOS-2. However, H and HL should be interpreted differently. As used in MOMOS-2, HL consists of labile metabolites resulting from decomposing plant material. In MOMOS-5, H consists of metabolites resulting from microbial cadavers or byproducts of microbial activity. Both materials are used (for MOMOS-2 HL) or reused (for MOMOS-5 H) as substrates for microorganisms, but HL in MOMOS-2 is rapidly used and exhausted ($k_{HL} = k_{VL} = 0.54$ day^{-1}), explaining the above-mentioned failures in MB predictions. In contrast, H in MOMOS-5 represents a large reserve of ^{14}C and ^{15}N that persists for the whole incubation period ($k_H = 0.05$ day^{-1}) and sustains the relatively high level of MB until the end of the experiment. This agrees with the conclusions of *Mueller et al.* [1998]: "a part of the decomposed plant material is immobilized both in soil MB as well as in a considerable amount of microbial residual products."

4.4. Improvement of MOMOS-5 by MOMOS-6

[38] MOMOS-6, which results from the improvement of MOMOS-5 by adding a stable humus compartment (HS, Figure 1), shows a tendency toward better RSS for all predicted variables (Tables 2–5). However, MOMOS-6 needs two additional parameters (k_{HLS} and k_{HS}), and the improvement in terms of RSS over MOMOS-5 is not significant. Thus, for the ^{14}C and ^{15}N experiment presented here, the largest improvement in predictive quality is achieved by MOMOS-5. However, the simulation of the dynamics of soil native total-C and -N including slow sequestration and accumulation of C with a long turnover time (work in preparation) required the introduction of the stable humus compartment. In this 2-year experiment, MOMOS-6 predicted an amount of stabilized HS-^{14}C = 0.18 g kg^{-1}, i.e., 2.0% of the total added ^{14}C, and an amount of stabilized HS-^{15}N = 0.018 g kg^{-1}, i.e., 5.4% of added ^{15}N. The HS compartment is also the most important reservoir of stable soil native N.

[39] Figures 2 and 3 show the ecological consistency of the MOMOS-6 improvement. During the second year of incubation, the MOMOS-6 predictions were closer to the measured data than the MOMOS-5 ones. For MB-^{14}C and -^{15}N, the MOMOS-6 predictions were lower than the MOMOS-5 ones, as a response to stabilization in HS. During the same time, total-^{14}C and -^{15}N predictions were higher in MOMOS-6 than in MOMOS-5, logically reflecting a lower microbial mineralization. In contrast, the MOMOS-2 to -4 predictions were less consistent, because lower total-^{14}C values also corresponded to lower MB-^{14}C values (fraction P_{MB}) and vice versa.

5. Conclusions and Recommendations

[40] The five-compartment MOMOS-2 model was initially developed on the basis of a laboratory labeling experiment in which most of the predicted compartments were measured [*Sallih and Pansu*, 1993]. In the present field experiment, under natural climate conditions, with less intensive sampling and a simpler procedure of chemical analysis, the aim was to test the predictive quality and sensitivity of successively simpler versions. The first step was to reduce the number of compartments (MOMOS-2 to -3) and to suppress a recycling process (MOMOS-3 to -4). The successive simplifications did not significantly modify the prediction accuracy for total ^{14}C and ^{15}N, nor for microbial biomass. Thus the simplification of MOMOS-2 to -3 is considered to be valid, as is the further simplification of MOMOS-3 to MOMOS-4. The second step focused on the processes associated with the microbial activity as a key stone compartment. It allowed elimination of the dimensionless parameters used for flow partitioning. As a result, MOMOS-5 only uses (1) the three first-order kinetic constants k_{VL}, k_{VS}, and k_H, which control the inputs into MB, (2) the first-order kinetic constant k_{MB}, which defines the production of microbial cadavers and metabolites, and (3) the metabolic quotient q_{CO2}, which regulates MB respiration. The modifications leading to MOMOS-5 did not change the accuracy of total ^{14}C and ^{15}N predictions, but noticeably improved the predictive quality and stability of MB-^{14}C and -^{15}N. Therefore, among the tested versions, the present paper proposes MOMOS-5 as the most accurate and the most consistent to describe labeling experiments during the first years of incubation. Modifications leading to MOMOS-6 were essentially carried out in order to model longer-term processes, including those associated with soil native organic matter (work in preparation). For that purpose, a stable humus compartment (HS) was introduced, which results from the slow stabilization of a small fraction of HL (H in MOMOS-5). In the paramo soils, MOMOS-6 HS includes a high amount of sequestered soil native C and

N. This labeling incubation allowed quantification of the ^{14}C and ^{15}N that has been sequestrated over a period of 2 years. This comparative study allows recommendation of the MOMOS-6 concept as a basis for simulating added and native SOM turnover in soil.

[41] **Acknowledgments.** TROPANDES INCO-DC program of the European Union (ERBIC18CT98-0263) supported this work. We are grateful to T. Carballas, CSIC-IIAG, Santiago de Compostela Spain, coordinator of the program, to A. Olivo, ICAE Mérida Venezuela, for her help in the field experiment, and to B. Buatois, CEFE-CNRS, Montpellier France and N. Marquez of the ICAE for the analysis of ^{14}C and ^{15}N.

References

Anderson, J. P. E., and K. H. Domsch (1978), A physiological method for the quantitative measurement of microbial biomass in soils, *Soil Biol. Biochem.*, *10*, 215–221.

Anderson, T. H., and K. H. Domsch (1993), The metabolic quotient for $CO_2(q_{CO2})$ as a specific activity parameter to assess the effect of environmental conditions such as pH on the microbial biomass of forests soil, *Soil Biol. Biochem.*, *25*, 393–395.

Bottner, P., and F. Warembourg (1976), Method for simultaneous measurement of total and radioactive carbon in soils, soil extracts and plant materials, *Plant Soil*, *45*, 273–277.

Brookes, P. C., J. F. Kragt, D. S. Powlson, and D. S. Jenkinson (1985), Chloroform fumigation and the release of soil nitrogen: The effects of fumigation time and temperature, *Soil Biol. Biochem.*, *17*, 831–835.

Chertov, O. G., and A. S. Komarov (1997), SOMM: A model of soil organic matter dynamics, *Ecol. Modell.*, *94*, 177–189.

Chimner, R. A., D. J. Cooper, and W. J. Parton (2002), Modeling carbon accumulation in Rocky Mountain fens, *Wetlands*, *22*, 100–110.

Cobelli, C., A. Lepschy, and G. Romanin-Jacur (1979), Structural identifiability of linear compartmental models, in *Theoretical Systems Ecology*, pp. 239–258, Academic, San Diego, Calif.

Franko, U., B. Oelschlägel, and S. Schenk (1995), Simulation of temperature-, water- and nitrogen dynamics using the model CANDY, *Ecol. Modell.*, *81*, 213–222.

Hansen, S., H. E. Jensen, N. E. Nielsen, and H. Svendsen (1991), Simulation of nitrogen dynamics and biomass production in winter wheat using the Danish simulation model DAISY, *Fertil. Res.*, *27*, 245–259.

Hénin, S., G. Monnier, and L. Turc (1959), Un aspect de la dynamique des matières organiques du sol, *C. R. Acad. Sci.*, *248*, 138–141.

Henriksen, T. M., and T. A. Breland (1999), Nitrogen availability effects on carbon mineralization, fungal and bacterial growth, and enzyme activities during decomposition of wheat straw in soil, *Soil Biol. Biochem.*, *31*, 1121–1134.

Jenkinson, D. S. (1990), The turnover of organic carbon and nitrogen in soil, *Philos. Trans. R. Soc. London, Ser. B.*, *329*, 361–368.

Jenkinson, D. S., and D. S. Powlson (1976), The effects of biocidal treatments on metabolism in soil: V. A method for measuring soil biomass, *Soil Biol. Biochem.*, *8*, 209–213.

Jenkinson, D. S., and J. H. Rayner (1977), The turnover of soil organic matter in some of the Rothamsted classical experiments, *Soil Sci.*, *123*, 298–305.

Joergensen, R. G. (1996), The fumigation-extraction method to estimate soil microbial biomass: Calibration of the k(EC) value, *Soil Biol. Biochem.*, *28*, 25–31.

Joergensen, R. G., and T. Mueller (1996), The fumigation-extraction method to estimate soil microbial biomass: Calibration of the k(EN) value, *Soil Biol. Biochem.*, *28*, 33–37.

Kätterer, T., M. Reichstein, O. Andrén, and A. Lomander (1998), Temperature dependence of organic matter decomposition: A critical review using literature data analyzed with different models, *Biol. Fertil. Soils*, *27*, 258–262.

Knorr, W., and M. Heimann (2001), Uncertainties in global terrestrial biosphere modeling: 1. A comprehensive sensitivity analysis with a new photosynthesis and energy balance scheme, *Global Biogeochem. Cycles*, *15*(1), 207–225.

Li, C., S. Frolking, and R. C. Harriss (1994), Modeling carbon biogeochemistry in agricultural soils, *Global Biogeochem. Cycles*, *8*(3), 237–254.

Lundquist, E. J., L. E. Jackson, K. M. Scow, and C. Hsu (1999), Change in microbial biomass and community composition, and soil carbon and nitrogen pools after incorporation of rye into three California agricultural soils, *Soil Biol. Biochem.*, *31*, 221–238.

Molina, J. A. E., C. E. Clapp, M. J. Shaffer, F. W. Chichester, and W. E. Larson (1983), NCSOIL, a model of nitrogen and carbon transformations in soil: Description, calibration and behavior, *Soil Sci. Soc. Am. J.*, *47*, 85–91.

Moorhead, D. L., W. S. Currie, E. B. Rastetter, W. J. Parton, and M. E. Harmon (1999), Climate and litter quality controls on decomposition: An analysis of modeling approaches, *Global Biogeochem. Cycles*, *13*, 575–589.

Mueller, T., L. S. Jensen, N. E. Nielsen, and J. Magid (1998), Turnover of carbon and nitrogen in a sandy loam soil following incorporation of chopped maize plants, barley straw and blue grass in the field, *Soil Biol. Biochem.*, *30*, 561–571.

Ocio, J. A., P. C. Brookes, and D. S. Jenkinson (1991), Field incorporation of straw and its effects on soil microbial biomass and soil inorganic N, *Soil Biol. Biochem.*, *23*, 171–176.

Pansu, M., and L. Thuriès (2003), Kinetics of C and N mineralization, N immobilization and N volatilization of organic inputs in soil, *Soil Biol. Biochem.*, *35*, doi:10.1016/S0038-0717(02)00234-1.

Pansu, M., Z. Sallih, and P. Bottner (1998), Modelling of soil nitrogen forms after organic amendments under controlled conditions, *Soil Biol. Biochem.*, *30*, 19–29.

Pansu, M., L. Thuriès, M. C. Larré-Larrouy, and P. Bottner (2003), Predicting N transformations from organic inputs in soil in relation to incubation time and biochemical composition, *Soil Biol. Biochem.*, *35*, doi:10.1016/S0038-0717(02)00285-7.

Parton, W. J., D. S. Schimel, C. V. Cole, and D. S. Ojima (1987), Analysis of factors controlling soil organic matter levels in great plains grasslands, *Soil Sci. Soc. Am. J.*, *51*, 1173–1179.

Paul, K. I., P. J. Polglase, and G. P. Richards (2003), Sensitivity analysis of predicted change in soil carbon following afforestation, *Ecol. Modell.*, *164*, 137–152.

Penning de Vries, F. W. T., D. M. Jansen, H. F. M. ten Berge, and A. Bakema (1989), *Simulation of Ecophysiological Processes of Growth in Several Annual Crops*, 271 pp., Pudoc, Wageningen, Netherlands.

Saggar, S., A. Parshotam, G. P. Sparling, C. W. Feltham, and P. B. S. Hart (1996), ^{14}C-labelled ryegrass turnover and residence times in soils varying in clay content and mineralogy, *Soil Biol. Biochem.*, *28*, 1677–1686.

Sallih, Z., and M. Pansu (1993), Modelling of soil carbon forms after organic amendment under controlled conditions, *Soil Biol. Biochem.*, *25*, 1755–1762.

Smith, P., et al. (1997), A comparison of the performance of nine soil organic matter models using datasets from seven long-term experiments, *Geoderma*, *81*, 153–225.

Thornley, J. H. M. (1991), A transport-resistance model of forest growth and partitioning, *Ann. Bot.*, *68*, 211–226.

Thornley, J. H. M., and E. L. Verberne (1989), A model of nitrogen flows in grassland, *Plant Cell Environ.*, *12*, 863–886.

Thuriès, L., M. Pansu, C. Feller, P. Herrmann, and J. C. Rémy (2001), Kinetics of added organic matter decomposition in a Mediterranean sandy soil, *Soil Biol. Biochem.*, *33*, doi:10.1016/S0038-0717(02)00003-7.

Thuriès, L., M. Pansu, M. C. Larré-Larrouy, and C. Feller (2002), Biochemical composition and mineralization kinetics of organic inputs in a sandy soil, *Soil Biol. Biochem.*, *34*, doi:10.1016/S0038-0717(02)00178-X.

Trinsoutrot, I., S. Recous, B. Mary, and B. Nicolardot (2000), C and N fluxes of decomposing C-13 and N-15 Brassica napus L.: Effects of residue composition and N content, *Soil Biol. Biochem.*, *32*, 1717–1730.

van Soest, P. J., J. B. Robertson, and B. A. Lewis (1991), Symposium: Carbohydrate methodology, metabolism, and nutritional implications in dairy cattle, *J. Dairy Sci.*, *74*(10), 3583–3597.

Verberne, E. L., J. Hassink, P. De Willigen, J. J. R. Groot, and J. A. Van Veen (1990), Modelling organic matter dynamics in different soils, *Neth. J. Agric. Sci.*, *38*, 221–238.

P. Bottner, Centre d'Ecologie Fonctionnelle et Evolutive, Centre National de la Recherche Scientifique, 1919 Route de Mende, F-34293 Montpellier Cedex 05 France. (bottner.pierre@wanadoo.fr)

K. Metselaar, Crop and Weed Ecology, Wageningen University and Research Centre, P.O. Box 430, NL-6700 AK, Wageningen, Netherlands. (henriette.drenth@wur.nl)

M. Pansu, Institut de Recherche pour le Développement, BP 64501, F-34394 Montpellier Cedex 05 France. (pansu@mpl.ird.fr)

L. Sarmiento, Instituto de Ciencias Ambientales y Ecológicas, Facultad de Ciencias, Universidad de los Andes, Mérida 5101, Venezuela. (lsarmien@ula.ve)

Modélisation du fonctionnement d'écosystèmes

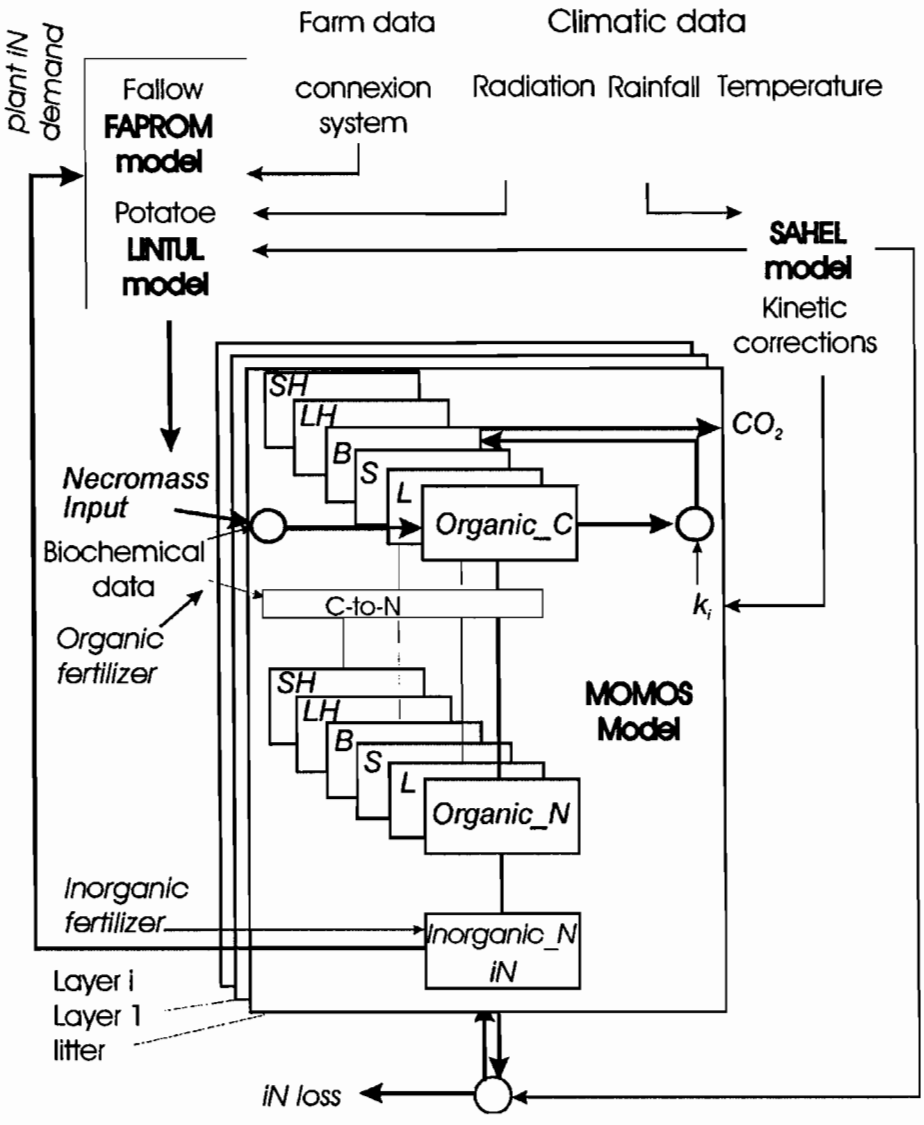

Figure 5. Coupling of MOMOS decomposition model with fallow production model (FAPROM), potatoes production model (LINTUL) and soil water model (SAHEL). The system operate with one litter layer and three (Bolivia) or four (Venezuela) soil layer, five organic C compartments (L,S = labile and stable OM from necromass, B = microbial biomass, LH and SH = labile and stable humified compounds) and two sources of OM (above ground and below ground).

Modélisation de: production primaire aérienne et souterraine, eau de la litière et des horizons organiques du sol, évolution C et N des cinq compartiments organiques et de l'azote minéral dans la litière et les mêmes horizons de sol (programme européen Tropandès).

Bilan et perspective

Les principaux acquis

MOMOS-6 (Fig. 7) est la concrétisation modélisée du cycle des matières organiques représenté Fig. 6 en introduction de ce mémoire. Sa mise au point a nécessité trois groupes de travaux représentés par les trois rectangles gris de la figure 7.

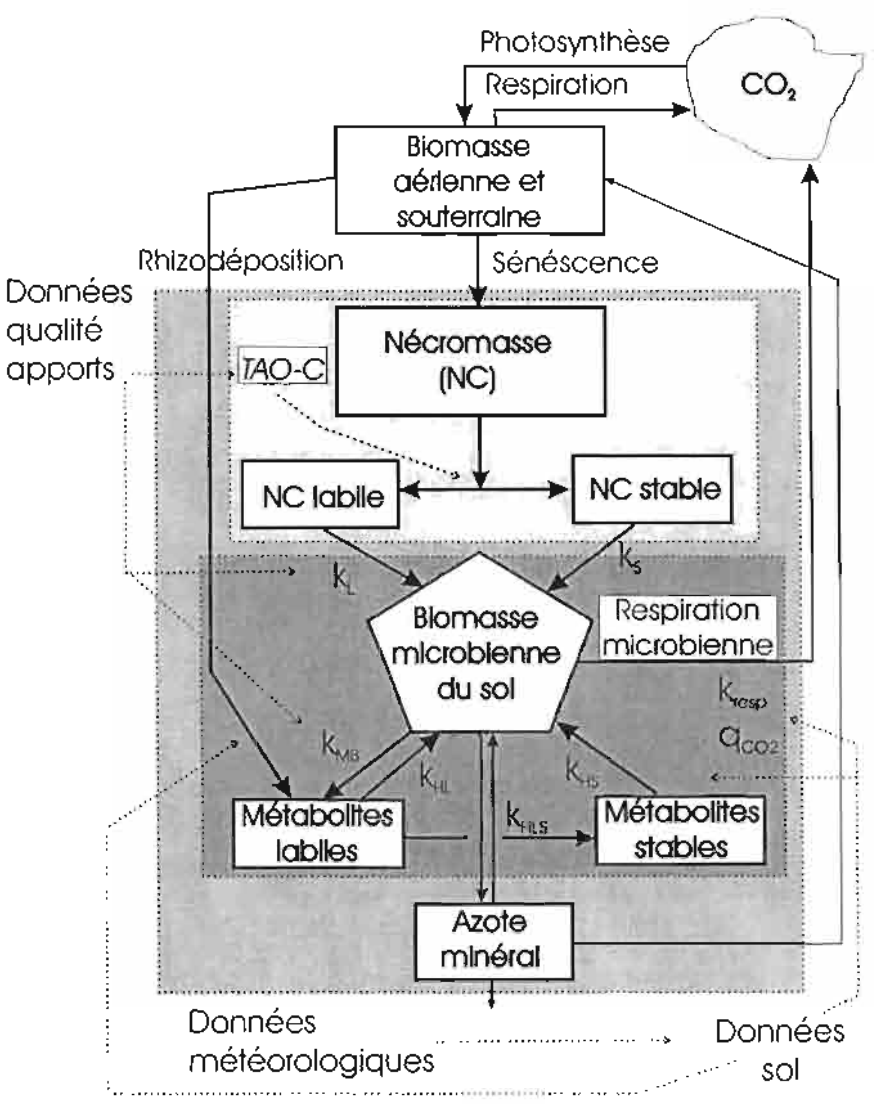

Fig. 7. Le modèle MOMOS-6 de la dynamique du cycle C et N : flèches pleines épaisses = flux de matières, flèches fines pointillé = contrôle des flux depuis les données biochimiques, météorologiques et édaphiques ; k_L, k_S = taux de décroissance des compartiments NC labile et NC stable par unité de temps, k_{HL}, k_{HS} = taux de décroissance des métabolites labiles et stables par unité de temps, k_{MB} = taux de mortalité de la biomasse microbienne, k_{HLS} = taux de maturation des métabolites labiles en humus stable, k_{resp} = coefficient de respiration de BM par unité de temps, q_{CO2} = quotient métabolique de la biomasse microbienne.

Le petit rectangle gris clair de la Fig. 7 correspond aux études sur la Transformation des Apports Organiques (modèle TAO) qui permet maintenant de prédire la minéralisation des apports d'après une connaissance élémentaire de leur composition biochimique (contenu en matières soluble, hémicellulosique, cellulosique, ligneuse, minérale et azote). MOMOS-6

n'utilise que le modèle TAO-C alors que le modèle TAO-N permet aussi de prédire les transformations plus complexes de l'azote en provenance de l'apport. En effet, selon ses caractéristiques biochimiques, particulièrement son rapport C/N, l'apport organique provoque soit une immobilisation de l'azote minéral du sol soit une libération d'azote minéral (pour les plantes mais aussi pour des pertes possibles vers les nappes phréatiques) ou encore dans certains cas une perte d'azote par volatilisation dans l'atmosphère. On voit donc tout l'intérêt que présente TAO (Fig. 8) pour une pratique raisonnée de la fertilisation organique : éviter les pertes d'azote minéral dans l'atmosphère et l'hydrosphère, optimiser la croissance des plantes en faisant correspondre les besoins en azote minéral liés à leur croissance et la fourniture d'azote minéral de l'apport prédite par TAO-N.

Des travaux complémentaires sont en cours ou à venir d'une part pour quantifier la réponse du modèle TAO à des variations édaphiques et climatiques, d'autre part pour associer ce modèle à des données spectrographiques d'acquisition plus aisée que le fractionnement biochimique.

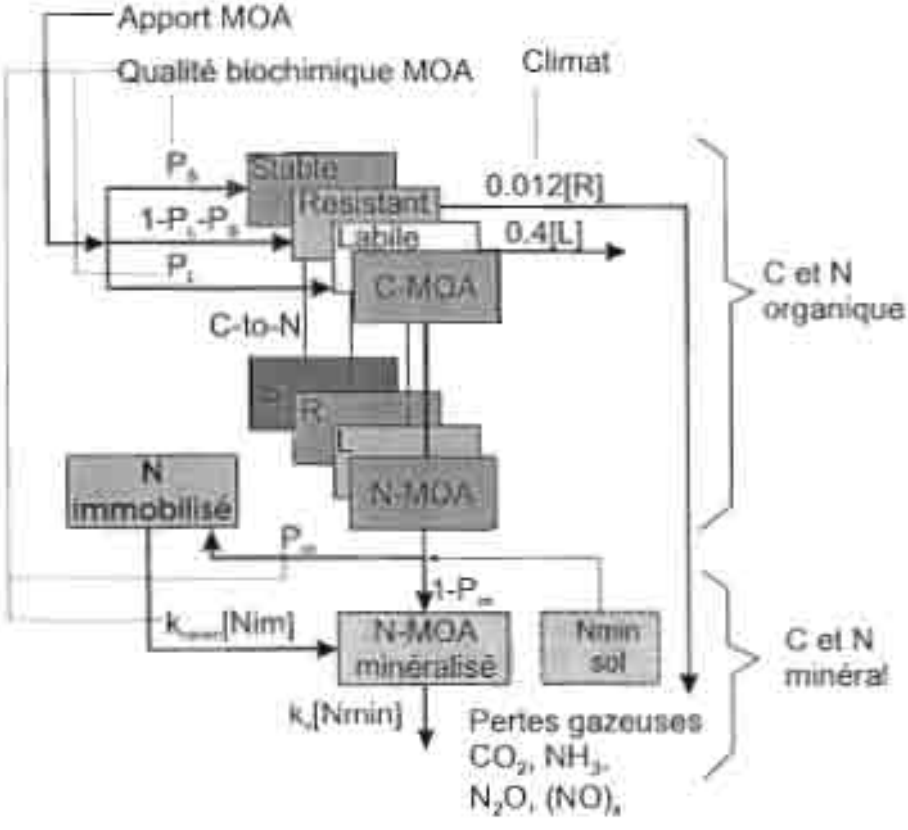

Fig. 8 – Le modèle de transformation des apports organiques TAO : MOA = matière organique apportée, P_L = fraction très labile de MOA, P_S = fraction stable de MOA, P_{im} = paramètre d'immobilisation de N minéral, k_{nmin} = taux de minéralisation de N immobilisé, k_v = taux de volatilisation de N minéral. Les paramètres P_L, P_S, P_{im} et k_{nmin} sont estimés d'après la qualité biochimique des MOA.

Le petit rectangle gris foncé de la figure 7 correspond aux travaux plus récents sur la comparaison de modèles de décomposition qui ont conduit à la version 6 du modèle MOMOS centré sur la biomasse microbienne. MOMOS-6 fonctionne uniquement avec des constantes de vitesse du premier ordre (dimension t^{-1}), sans paramètre de partage des flux (FF, voir

section 1.3 de l'introduction). Tous les paramètres fonctionnels de ce modèle sont donc liés à la température et à l'humidité du sol par l'intermédiaire de données météorologiques et de modèles de propagation de la chaleur et de l'eau. Dans les études actuelles, la température du sol dans la couche 5-10 cm est assimilée à la température de l'air. L'humidité du sol est estimée par le modèle de bilan hydrique SAHEL[1]. La mise au point de MOMOS-6 a nécessité une loi régissant la respiration de la biomasse microbienne. Le quotient respiratoire q_{CO2} de la BM (CO_2 respiré par unité de BM et de temps) est proportionnel au coefficient de respiration k_{resp} (dimension t^{-1}) et au rapport BM actuelle : BM basale à l'équilibre. En d'autres termes plus BM croît sous l'effet de l'apport de matière labile, plus le quotient respiratoire des microorganismes croît. Inversement lorsque diminue le flux d'entrée de matière labile, BM diminue rapidement et les microorganismes restants deviennent moins actifs. Le modèle simule à la fois des pics à croissance et décroissance rapide de BM et q_{CO2} en début d'incorporation des matériaux et une dynamique de décroissance lente liée à la consommation microbienne des résidus végétaux résistants et des métabolites microbiens formés lors des phases d'intense activité minéralisatrice. L'équation décrivant ce fonctionnement microbien est relativement complexe, mais les analyses de sensibilité ont démontré la robustesse et la cohérence écologique des prédictions du modèle.

Une méthode d'utilisation du modèle MOMOS-1 pour la quantification des flux de C à la rhizosphère des plantes actives a été proposée. Jusqu'ici la plupart des travaux de ce type utilisent des expérimentations de cultures de plantes en atmosphère contrôlée avec marquage isotopique du CO_2 pour la photosynthèse, puis mesure du C marqué de la respiration racinaire (difficile à distinguer de la respiration de la rhizosphère). Notre méthode utilise un marquage préalable du sol par apport de nécromasse marquée sur sol nu et cultivé. Le modèle est d'abord ajusté sur sol nu avec le traceur isotopique, puis l'expérience sur sol cultivé permet de quantifier l'apport de C non marqué depuis les racines vivantes. La nouvelle version MOMOS-6 sera aussi utilisée pour ce type d'étude (travail en préparation).

Les outils disponibles

Les deux modèles TAO et MOMOS-6 sont programmés actuellement sur la plateforme de modélisation VENSIM (Ventana systems, 60 Jacob Gates Road, Harvard MA 01451 USA ; ATN, 15 rue du Louvre, 75001 Paris). Ils sont disponibles sur demande auprès de l'auteur (Marc Pansu, UR SeqBio, IRD Montpellier, pansu@mpl.ird.fr).

Modèle TAO

But

Fournir une prédiction de la transformation du C et N des apports organiques et de leur effet agronomique et environnemental. C'est un outil de choix, relativement simple d'emploi, pour les techniciens et ingénieurs de l'agriculture et de l'environnement, ainsi que pour les fabricants et utilisateurs de fertilisants organiques

Données d'entrée

Pourcentages massiques en C et N et en fibres de l'apport (méthode van Soest, 1991)[2] : fraction soluble au détergent neutre (Sol), fraction hemicellulosique (Hem), fraction cellulosique (Cel), fraction ligneuse (Lig), fraction minérale (Cendres).

---

[1] Penning de Vries, F.W.T., Jansen, D.M., ten Berge, H.F.M. and Bakema, A., 1989. Simulation of ecophysiological processes of growth in several annual crops. Pudoc, Wageningen, 271 pp.

[2] van Soest, P.J., J.B. Robertson, and B.A. Lewis. 1991. Symposium: carbohydrate methodology, metabolism, and nutritional implications in dairy cattle. Journal of Dairy Science 74:3583-3597.

Données de sortie

Courbe prédite de minéralisation C en fraction du C apporté pendant les 6 mois suivant l'apport.

Courbes prédites de minéralisation N, immobilisation N et N organique non transformé en fraction du C apporté pendant les 6 mois suivant l'apport.

Modèle MOMOS-6

But

Prédire l'évolution des formes du C et N du sol et des agro/écosystèmes durant quelques années, décennies ou siècles. Selon la version et les besoins, les prédictions peuvent concerner l'ensemble des stocks du sol, ou bien fractionner l'évolution des stocks de la litière au-dessus du sol et de divers horizons humifères du sol.

Données d'entrée

Apports organiques : selon les versions du modèle, estimation manuelle d'après des données, estimateurs simplifiés liés aux données climatiques de la production de biomasse et nécromasse, estimation de la production en systèmes plus complexe comme les jachères par couplage avec le modèle FAPROM[4], possible différentiation des apports aériens et racinaires.
Qualité des apports : voir modèle TAO ci-dessus.
Données édaphiques : taux de biomasse microbienne dormante du sol (en l'absence d'apport organique, mesure par la méthode de fumigation-extraction de Brookes et al., 1985[3] ou estimation approximative d'après le type de sol et le taux de matière organique), taux de fraction fine du sol (argile + limon) ; pour le couplage avec SAHEL : teneur en eau à la capacité au champ, teneur en eau au point de flétrissement, humidité à 105°C.
Données météorologiques : au minimum température et pluviométrie journalières moyennes ; pour version plus précise avec version couplée incluant le modèle FAO d'évapotranspiration, collecter en plus : vitesse du vent, latitude et altitude.

Données de sortie

Carbone et azote total du sol, carbone et azote des résidus végétaux non décomposés, carbone et azote de BM, quotient métabolique de BM, azote minéral, carbone et azote des métabolites microbiens labiles, carbone et azote des composés humifiés stables.

Travaux en cours et perspectives

La figure 7 est simplificatrice en ce qui concerne le cycle de l'azote (voir section 1.2 de l'introduction de ce mémoire) et ne représente pas tous les échanges avec l'atmosphère, l'hydrosphère et la géosphère. MOMOS-6 couplé avec le modèle de bilan hydrique SAHEL et de production végétale des jachères FAPROM[4] (labo. d'écophysiologie, université d'Orsay) a permis de comprendre le processus de restauration de la fertilité azotée par la mise en jachère. La fixation symbiotique des plantes amélioratrices était prise en compte dans les taux d'azote des nécromasses restituées au sol, l'entraînement des nitrates par lixiviation était pris en compte par une modification du modèle SAHEL. Alors que les analyses de sol au laboratoire n'ont pas permis de déceler de changement significatif lié à la jachère, la restauration de la fertilité était simulée par un accroissement des stocks en C et N des compartiments

[3] Brookes, P.C., A. Landman, G. Pruden, and D.S. Jenkinson. 1985. Chloroform fumigation and the release of soil nitrogen : a rapid direct extraction method to measure microbial biomass nitrogen in soil. Soil Biology & Biochemistry 17:837-842.

[4] Martineau, Y., and B. Saugier. 2006. Comportement contre-intuitif d'un modèle mécaniste de succession végétale. Comptes Rendus de l'Académie des Sciences (section Biologie Ecologie), France 329:21–30.

Martineau, Y. and Saugier, B., 2006. A process-based model of old-field succession linking ecosystem and community ecology. Ecological Modelling, Submitted.

« Biomasse microbienne » et « Métabolites labiles » du modèle (Fig. 7), ce dernier compartiment accumulant la principale réserve azotée disponible pour la mise en culture (Fig.9). Le maximum d'accumulation observé vers 7-10 ans correspond aux temps de jachère effectivement pratiqués par les agriculteurs dans ces systèmes de montagne.

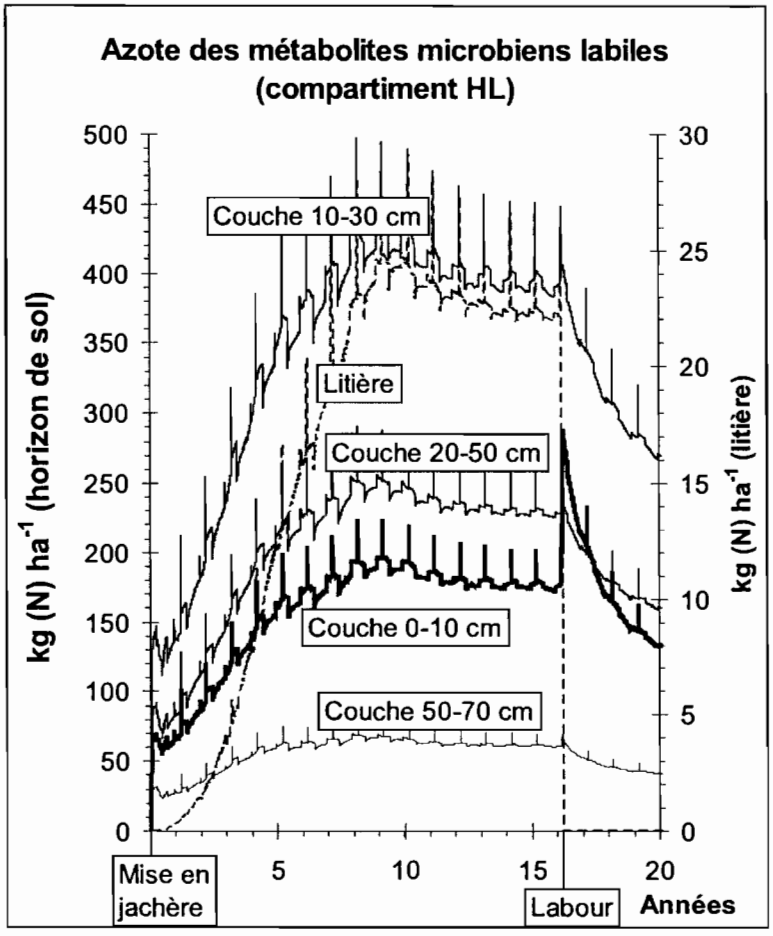

Figure 9 – Simulation de la restauration de la fertilité par la jachère et l'enfouissement de biomasse dans le paramo vénézuélien. La litière et les diverses couches de sol appauvries lors de l'utilisation agricole réaccumulent progressivement des métabolites microbiens pour atteindre un maximum vers 8 à 10 ans de mise en jachère. L'enfouissement de la litière à la mise en culture (labour à l'araire) procure un apport supplémentaire d'azote dans la couche 0-10 cm. L'ensemble des réserves azotées d'origine microbienne décroît ensuite progressivement durant la phase ultérieure de mise en culture

Ce travail en cours prend en compte une simulation des compartiments aérien et racinaire des différentes espèces végétales en compétition pour la lumière, l'eau et l'azote disponible (modèle FAPROM). Il simule les restitutions organiques et leur transformation dans la litière et les principaux horizons organiques des sols étudiés. Il prend en compte l'effet des différences entre les caractéristiques édaphiques des deux sites (Puna bolivienne et

Paramo vénézuélien) et leur influence sur la respiration de la biomasse microbienne[5] ainsi que l'effet du contenu biochimique de l'apport sur d'autres paramètres de fonctionnement du modèle MOMOS-6[6]. L'outil sera ensuite validé et testé sur d'autres sites. Sa spatialisation fournira un outil précis de gestion simultanée de la fertilité des sols et des flux de C et N au niveau de la planète.

Le champ d'application de nos prochaines études concernera :

- la validation et complémentation des travaux en cours,
- l'intégration de données spectrographiques dans les modèles,
- l'acquisition de données supplémentaires concernant la volatilisation de l'azote,
- l'application à la simulation d'écosystèmes et agrosystèmes sur sites expérimentaux comportant des suivis organiques de longue durée, la comparaison et la recherche de synergies avec d'autres démarches prédictives,
- l'application à l'agriculture de précision utilisant la fertilisation organique,
- l'application à la transformation de déchets,
- l'intégration dans les modèles de changement global.

[5] Pansu, M., Sarmiento, L., Metselaar, K., Hervé, D. and Bottner, P., 2006. Modelling the transformations and sequestration of soil organic matter in two contrasting ecosystems of the Andes. European Journal of Soil Science, en correction.

[6] Bottner, P. et al., 2006. Factors controlling decomposition of soil organic matter in fallow systems of the high tropical Andes: a field simulation approach using ^{14}C and ^{15}N labelled plant material Soil Biology & Biochemistry, sous presse.

Publications

Publications

Marc Pansu

Revues à comité de lecture

P. Guillet, Coz J., Sannier C., Barathe J., Mustapha A., Pansu M., J.Itard, 1979 - Etude de la sensibilité à quelques insecticides, OMS 1998, OMS 1821, OMS 2, OMS 185, OMS 595, OMS 570 de glossines d'élevage, *Cah. ORSTOM, Ser. Ent. Med. et Parasito.* XVII, 81-87.

M. Pansu, M.H. Dhouibi, M. Pinta, 1981 - Détermination des traces de pyréthrinoïdes dans les substats biologiques par chromatographie en phase gazeuse, *Analusis*, 9, 55-59.

M. Pansu, S. Tostain, M. Pinta, 1981 - Etude par chromatographie en phase gazeuse de la variabilité des acides gras des graines de mil, *Journal of chromatography*, 204, 377-383.

M. Pansu, M.N. Al Salti, H. Aubert, J. Gry, 1981 - Contribution à l'étude de l'activité systémique du carbofuran par chromatographie en phase gazeuse, *Phytiatrie phytopharmacie*, 30, 203-214.

M. Pansu et F. Abo, 1985 - Application d'un progiciel de chimiométrie (SPCLAS) à l'étude de l'incidence du Bore et du Manganèse sur la fertilisation du blé (triticum aestivum L.), *Analusis*, 13, 443-451.

M.Pansu et H.Sidi, 1987 - Cinétique d'humification et de minéralisation des mélanges sols-résidus végétaux, *Sciences du sol*, 25, 4, 247-265.

M.Pansu, 1988 - Proposition de modèles descriptifs de la dynamique des matières organiques des sols, *Cah. ORSTOM Ser. Pédol.*, XXIV, 4, 361-362.

H. Sidi et M. Pansu, 1990 - Effets d'apports organiques et de gypse sur la stabilité structurale de deux sols méditerranéens, *Science du Sol*, 28, 237-255.

M. Pansu, 1991 - Détermination de quelques paramètres caractéristiques de la cinétique d'humification et de minéralisation des amendements organiques dans les sols, *Cah. Orstom Ser. Pédol.*, XXVI, 2 : 131-144.

Z. Sallih et M. Pansu, 1993 - Modelling of soil carbon forms after organic amendments under controlled conditions. *Soil Biology & Biochem*istry, 25, 1755-1762.

M. Pansu, Z. Sallih et P. Bottner, 1996. - Modélisation des formes du carbone organique dans les sols. *Compte Rendus de l'Acad. des Sciences*, Série IIa, 322, 401-406.

M. Pansu, Z. Sallih et P. Bottner, 1998 - Modelling of soil nitrogen forms after organic amendments under controlled conditions. *Soil Biology & Biochemistry*, 30, 19-29.

P. Bottner, M. Pansu et Z. Sallih, 1999. - Modelling the effect of active roots on soil organic matter turnover, *Plant and Soils,* 216, 15-25.

L. Thuriès, M. -C. Larré-Larrouy et M. Pansu, 2000. - Evaluation of three incubation designs for mineralization kinetics of organic materials in soil. *Communications in Soil Science and Plant Analysis*, 31, 289-304

L. Thuries, A. Arrufat, M. Dubois, C. Feller, P. Herrmann, M.C. Larre-Larrouy, C; Martin, M. Pansu, J.C. Remy et M. Viel, 2000. – Influence d'une fertilisation organique et de la solarisation sur la productivité maraîchère et les propriétés d'un sol sableux sous abri. *Etude et Gestion des sols*, 7, 73-88.

L. Thuriès, M. Pansu, C. Feller, P. Hermann, et J.C. Rémy. 2001 – Kinetics of added organic matter decomposition in a mediterranean sandy soil. *Soil Biology & Biochemistry* 33, 997-1010.

L. Thuriès, M. Pansu, M.C. Larre-Larrouy et C. Feller. 2002 – Biochemical composition and mineralization kinetics of organic inputs in a sandy soil. *Soil Biology & Biochemistry* 34, 239-250.

M. Pansu et L. Thuriès 2003 – Kinetics of C and N mineralization, N immobilization and N volatilization of organic inputs in soil. *Soil Biology & Biochemistry*, 35, 37-48.

M. Pansu, L. Thuriès, M.C. Larré-Larrouy et P. Bottner, 2003 – Predicting N transformations from organic inputs in soil in relation to incubation time and biochemical composition. *Soil Biology & Biochemistry*, 35, 353-363.

M. Pansu, P. Bottner, L. Sarmiento and K. Metselaar, 2004 - Comparison of five soil organic matter decomposition models using data from a ^{14}C and ^{15}N labeling field experiment, *Global Biogeochemical Cycles,* 18, GB4022, doi: 10.1029/2004GB002230.

L. Thuriès, D. Bastianelli, F. Davrieux, L. Bonnal, R. Oliver, M. Pansu and C. Feller, 2005 - Prediction by NIRS of the composition of plant raw materials from the organic fertiliser industry and of crop residues from tropical agrosystems. *J. of Near Infrared Spectroscopy*, 13, 187-199.

P. Bottner, M. Pansu, R. Callisaya, K. Metselaar, D. Hervé, 2006 - Modelización de la evolución de la materia orgánica en suelos en descanso (Altiplano seco boliviano). *Ecologia Boliviana*, sous presse.

M. Pansu, L. Sarmiento, D. Hervé, K. Metselaar and P. Bottner, 2006 -Modelling the transformations and sequestration of soil organic matter in two contrasting ecosystems, *Eur. J. of Soil Science*, en correction.

P. Bottner, M. Pansu, L. Sarmiento, D. Hervé, R. Callisaya-Bautista, K. Metselaar, 2006 - Factors controlling decomposition of soil organic matter in the fallow systems of the high tropical Andes: a field simulation approach using ^{14}C and ^{15}N labelled plant material, *Soil Biology & Biochemistry*, sous presse.

Livres

M. Pansu, J. Gautheyrou et J.Y. Loyer, 1998 - *L'analyse du sol - échantillonnage, instrumentation et contrôle*, Masson, Paris, Milan, Barcelone, 512 p.

M. Pansu, J. Gautheyrou et J.Y. Loyer, 2001 - *Soil analysis* - sampling, *instrumentation and quality control*, translated from French by V.A.K. Sarma, Balkema, Lisse Abingdon, Exton, Tokyo, New Delhi, Calcutta, 489 p.

M. Pansu et J. Gautheyrou, 2003 - *L'analyse du sol* – minéralogique, organique et minérale, Springer, Paris, Berlin, Heidelberg, New York, Hong Kong, Londres, Milan, Tokyo, 995 p.

M. Pansu et J. Gautheyrou, 2006 – Soil analysis – mineralogical, organic and inorganic, Springer, sous presse, 1000 p.

Communication à congrès internationaux

M. Pansu, Sallih Z. et Bottner P., 1998. - *A process-based model for carbon and nitrogen transfers in soil organic matter.* Un modèle mécaniste des flux de C et N dans la matière organique du sol. Actes *16° Congrès mondial de science du sol*, Montpellier août 1998.

L. Thuriès and M. Pansu, 2001. - Classification and modelling of added organic matter decomposition in a sandy soil. Proceeding of 11 Nworkshop, Reims, France, 9-12 Sept. 2001.

M. Pansu, L. Thuriès, M.C. Larré-Larrouy et C. Feller, 2002 – Kinetics of organic inputs in soil carbon model. Proceeding of 17th World Congress of soil science, Bangkok, 14-21 August 2002, Oral communication 1502, symposium10.

D. Blavet, J.C. Leprun, E. Mathe et M. Pansu, 2002 – Soil colour variables as simple indicators of the duration of soil waterlogging in a west African catena. Proceeding of 17th World Congress of soil science, Bangkok, 14-21 August 2002, Poster 1333, Symposium 32.

M. Pansu et P. Bottner, 2002 – Modélisation de l'effet des racines actives sur les transferts de C organique dans les sols. Proceeding of congress Gestion de la biomasse, erosion et sequestration du carbone, Agropolis Montpellier, 23-28 Septembre 2002.

L. Thuriès et M. Pansu, 2002 – Classification et modélisation de la décomposition de matières organiques ajoutées au sol. Proceeding of congress Gestion de la biomasse, erosion et sequestration du carbone, Agropolis Montpellier, 23-28 Septembre 2002.

Communication à congrès nationaux

M. Pansu et F. Abo, 1986 - L'outil informatique au service des analyses chimiques et agronomiques, *Actes 26ème semaine scientifique de Latakié-Syrie.*

M. Pansu, 1987 - La gestion des données des laboratoires d'analyses physico-chimiques. Exemple d'application : MIDAS, *Actes SEMINFOR1 "premier séminaire informatique ORSTOM"*, 203-219.

M.Pansu, 1988 - Cinétique chimique et modèles compartimentaux : application à l'étude de l'évolution du stock organique des sols. In *actes séminaire SEMINFOR "la modélisation : aspects pratiques et méthodologie"*, ORSTOM Coll. et séminaires, 46-61.

M. Pansu et P. de Boissezon, 1990 - Dynamique du carbone organique dans les mélanges sols-résidus végétaux ; influence sur la capacité d'échange cationique. *Actes GEMOS (Groupe d'étude des matières organiques des sols), INRA-Bordeaux 18-19 avril 1989*).

M. Pansu, 1990 - Modélisation appliquée à l'étude du stock organique et de la stabilité structurale de sols méditerranéens, *Actes séminaire de Tiaret (Algérie) "Les sols céréaliers"*, Tiaret, sept 1989.

M. Pansu, R. Gavinelli et P. Espiau, 1990 - Etude de précision appliquée à la détermination de l'acidité d'échange des sols, *Actes Journées des laboratoires 18..20 septembre 1990 ORSTOM Bondy.*

M. Pansu, Z. Sallih et P. Bottner, 1991 - Cinétique d'évolution des formes du carbone organique dans les sols. In *actes séminaire SEMINFOR5 "Statistiques impliquées"*, ORSTOM Coll. et séminaires.

M. Pansu, 1994 - Modélisation des formes du carbone organique dans les sols. *Actes 4emes journées d'études des sols-AFES (Association Française d'Etude des Sols), Lille* 19-21 avril 1994.

M. Pansu and P. Bottner, 2001. – Modélisation de l'effet des racines actives sur les transferts de carbone organique dans les sols. Actes 3° colloque rhizosphère, Dijon, 26-28 Nov. 2001

M. Pansu, L. Thuriès, MC Larre-Larrouy et C. Feller, 2002. – Dynamique de minéralisation d'apports organiques dans les modèles carbone du sol. *Actes Journées Nationales d'Etude des Sols AFES* d'Orléans, France, 22-24 Octobre 2002.

Marc Pansu et Pierre Bottner, 2004 - Comparaison de modèles de décomposition de matière organique du sol à l'aide de données expérimentales *in situ* de traceurs ^{14}C et ^{15}N. Communication orale aux *Journées Nationales d'étude des sols AFES* de Bordeaux, France, 26-28 Octobre 2004

Marc Pansu et Pierre Bottner, 2004 - Dynamique des matières organiques du sol. Séminaire, IFR Ecosystems, Agropolis international, Montpellier, 16 Décembre 2004.

Marc Pansu et Pierre Bottner, 2005 - Marquage isotopique 14C et 15N *in situ* et modèles de décomposition de matière organique du sol. Journée des isotopes stables, Vendredi 21 Octobre 2005, Muséum d'histoire naturelle, Paris.

M. Pansu, P. Bottner et L. Thuriès, 2006 - Modélisation de la dynamique des matières organiques du sol. Actes séminaire « Les matières organiques en France. Etat de l'art et prospectives », 22-24 Janvier 2006, Carqueiranne, France. Réseau matières organiques et groupe français de l'IHSS.

L. Thuriès, R. Oliver, F. Davrieux, D. Bastianelli et M. Pansu, 2006 - Transformations des apports organiques : application du modèle TAO à des matières de l'agro-industrie à partir de leur analyse biochimique mesurée ou estimée par Spectrométrie Proche Infra-Rouge (SPIR). Carquairanne (France), 22-24 Janvier 2006, Réseau Matière Organique et groupe français de l'IHSS.

Publications IRD, logiciels

M. Pansu, 1983 - SPCLAS - *Un logiciel basic pour le calcul, le classement, la gestion des résultats d'un laboratoire d'analyses physico-chimiques*, ORSTOM (60 p.).

M. Pansu, 1985 - Le logiciel SPCLAS, *Fiches techniques Agence Nationale du logiciel*-Vandoeuvre les Nancy.

M. Pansu 1985 - OPTIMI - Optimisation des mesures par utilisation de plans d'expériences et méthodologie des surfaces de réponse, *Fiches techniques Agence Nationale du Logiciel*-Vandoeuvre les Nancy. In *Logiciels pour la chimie*, Société Française de chimie.

M. Pansu 1985, HUMUS - Extension du logiciel SPCLAS à la gestion personnalisée d'un laboratoire, *Fiches techniques Agence nationale du Logiciel*-Vandoeuvre les Nancy.

M. Pansu et B. Loustalan, 1990 - *Le logiciel MIDAS : Management Informatique des Données Analytiques : manuel d'utilisation (70 pages) et disquettes programmes compilés*, aide en ligne et exemples, LogORSTOM.

M. Pansu, 1992 - *Les sucres neutres dans les sols : opportunité et tentatives d'amélioration de leur détermination*, Document ORSTOM Montpellier, n°4 : 24 p.

Rapports, conférences, information scientifique

Mémoire de Doctorat

M. Pansu, 2005 – Chimie du sol et cycle du carbone et de l'azote. Soutenu le 28 Janvier 2005, Université de Montpellier II, Procédure Validation des Acquis de l'Expérience.

Programmes et expertise

P. Bottner, M.M. Couteaux, D. Hervé et M. Pansu, 2003 - INCO-DC ERBIC18CT98-0263,. Final report of Tropandes program. T. Carballas ed., CESGA, Santiago de Compostella, Spain, Part 5 and 7.

M. Pansu et D. Hervé, 2000. – El analysis de suelo en laboratorios de Peru y Bolivia (Lima, Puno, La Paz, Cochabamba). IRD et Consortium pour le développement de l'écorégion andine (CONDESAN), 18 p.

Rapports divers

M. Pansu, 1985, 1986, et 1987 - Rapports d'activités du laboratoire "Matières organiques", ORSTOM-BONDY.

M. Pansu, 1986 - Influence de la préparation des échantillons sur la précision des analyses de sols, ORSTOM-BONDY.

M. Pansu, 1986 - Plan d'essai de précision inter-laboratoires ORSTOM, Comité des moyens analytiques-ORSTOM

P. Baujard et M. Pansu, 1987 - Analyse des problèmes liés à l'utilisation du dibromochloropropane dans les sols de la zône sahélienne Ouest-Africaine, Labo de nématologie ORSTOM-DAKAR-SENEGAL.

M. Pansu et Y.Jacob, 1988 - Installation d'une unité d'analyses de résidus de nématicides au laboratoire de nématologie ORSTOM-DAKAR.

M. Pansu, 1990 - Compte rendu de mission à l'I.N.E.S. agro-vétérinaire de Tiaret (Algérie), 17-22 Mars 1990.

M. Pansu, N.Elissa, 1990 - Cinétique de dégradation de solutions diluées de deltaméthrine en relation avec leur pouvoir insecticide.

M. Pansu, 1990 - Modélisation de l'évolution des compartiments organiques des sols, Rapport d'activités Juillet 1990.

M. Pansu, 1991- 2000. - 10 Rapports de secrétariat de l'ouvrage " Analyse du sol ".

M. Pansu, 1999. – Rapport de mission Pérou et Bolivie du 6 au 29 Novembre 1999, 15 p., 4 photos (avec traduction en espagnol pour les partenaires)

Conférences

-La programmation des microrordinateurs, le langage Basic et son utilisation au laboratoire, GAMS PARIS, cycle "l'outil informatique en chimie analytique", 1984, 1985, 1986, 1987.

-Gestion de fichiers de données : exemples d'applications au laboratoire, GAMS PARIS, cycle "l'outil informatique en chimie analytique", 1984, 1985, 1986, 1987.

-Méthodes d'optimisation des conditions expérimentales en spectrométrie atomique : principes, informatisation, applications, CNRS-formation-IVRY, cycle "Spectrométrie atomique par émission et absorption : application à l'analyse", 1986.

-Optimisation des conditions expérimentales en spectrométrie atomique : plans d'expériences et méthodologie des surfaces de réponse", CNRS-Formation-BONDY, cycle "Spectrométrie d'émission et d'absorption atomique", 1986, 1987, 1988, 1989, 1990, 1991, 1992, 1993, 1994, 1995, 1996, 1997.

-Caractérisation des matières organiques des sols en liaison avec leur dynamique d'évolution, Faculté d'agronomie, DAMAS, 1986.

-Utilisation du logiciel de gestion de bases de données DBASE III, ORSTOM-DIVA-formation BONDY, 1986, 1987.

-Initiation à la programmation en langage BASIC, ORSTOM-DIVA-formation BONDY, 1986, 1987.

-La mesure chimique, son intervalle de confiance et quelques tests liés à l'étude de sa précision, ORSTOM-DIVA-Formation, cycle "Valorisation informatique des données des laboratoires d'analyses physico-chimiques", 1987.

-Aperçu des méthodes d'optimisation en physico-chimie analytique, ORSTOM-DIVA-Formation, cycle "Valorisation informatique des données des laboratoires d'analyses physico-chimiques", 1987.

-Gestion de l'information physico-chimique : exemples d'application, ORSTOM-DIVA-Formation, cycle "Valorisation informatique des données des laboratoires d'analyses physico-chimiques, 1987.

M. Pansu, 1999. El analysis de suelo. Université de Lima, Puno, La Paz, Cochabamba. 20 transparents, 1 h de conférence + 1 h de discussions. Collaboration avec Dominique Hervé pour la traduction préalable du texte en espagnol et pour la traduction des questions.

M. Pansu, 2001. Le sol - formation, fonctions, composition, dégradation. Grand public, 5° Festival « L'avenir au naturel » L'Albenc Isère, 1 Sept. 2001.

M. Pansu, 2001. Le sol - formation, fonctions, composition, dégradation. Public BTS, Fête de la science, 16 Oct. 2001.

M. Pansu, 2001. Modélisation des transferts de carbone et azote dans les sols. Public scientifique et enseignement supérieur, séminaires Agropolis, M. Pansu, organisateur

M. Pansu, 2002. Modélisation de la transformation des apports de carbone dans les sols. Public scientifique et enseignement supérieur, étudiants INA-PG, 4 Décembre 2002.

L. Thuriès et M. Pansu, 2006. La fertilisation organique et sa modélisation. Etudiants master2 pro, DEA Fennec, ENSAM Montpellier, 30 Janvier 2006, 5 h.

Information scientifique,

M. Pansu, 2000. – Le sol et son analyse. *Fréquence Chimie*, 28, 2-9.

M. Pansu et F. Doumenge, 2000. – Modélisation des transferts de carbone et d'azote dans les sols, poster fête de la science.

M. Pansu, 2001. – Le sol : formation, fonctions et composition. In Encyclopédie francophone sur Internet Webencyclo http://webencyclo.com, rubrique « sol », editions Atlas

M. Pansu, 2001. – Le sol : méthodes d'analyse. In Encyclopédie francophone sur Internet Webencyclo http://webencyclo.com, rubrique « sol », editions Atlas

Chimie du sol et modélisation du cycle du carbone et de l'azote

Ce mémoire synthétise vingt ans de travaux de chimie du sol principalement sur les méthodes d'analyse et la modélisation du cycle du carbone et de l'azote. Deux livres de synthèse ont été édités en Français (Masson, 1998 et Springer, 2003), un en Anglais (Balkema, 2001) et un quatrième est sous presse en Anglais (Springer, 2006). La communauté scientifique a bien accueilli ces livres, les deux éditions en Français sont épuisées chez les éditeurs et une réédition française est à l'étude chez Springer. La recherche expérimentale s'est inscrite depuis 1985 dans la préoccupation mondiale sur le cycle du carbone et de l'azote pour les problèmes agronomiques et environnementaux d'échange du compartiment sol avec la biosphère, l'atmosphère, l'hydrosphère et la géosphère. Une première publication permettait de valider en 1987 le modèle théorique de Hénin et al. (1959) à deux compartiments et de proposer un modèle à trois compartiments. Deux publications annexes ouvraient une voie vers la prédiction de propriétés chimique (capacité d'échange cationique) et physique (stabilité structurale) du sol liées aux matières organiques. En 1993 des expériences de traceurs isotopiques conduisaient à proposer le modèle MOMOS-1 proche du modèle Roth-C (Jenkinson, 1990) mais comportant en plus un compartiment métabolites labiles. En 1998 ce modèle était étendu au cycle de l'azote. En 1999, il servait à quantifier par une nouvelle approche de modélisation, l'influence des racines actives sur les flux de carbone. Une recherche était entreprise pour préciser les cinétiques de décomposition des matières organiques apportées au sol (MOA). En 2001 après sélection d'un modèle parmi sept propositions de la littérature, la minéralisation C était trouvée dépendante de deux paramètres essentiels : la fraction très labile et la fraction stable des MOA. Ces paramètres étaient liés en 2002 avec les données analytiques. Le modèle résultant TAO-C permet de prédire la minéralisation d'une MOA au moyen de son analyse biochimique (contenu en fibres et rapport C :N). En 2003 le modèle était étendu au cycle de l'azote avec ajout de trois paramètres régulant : l'immobilisation de N minéral, la minéralisation de N immobilisé et la volatilisation de N minéral. Des relations étaient montrées entre les deux premiers paramètres et les données analytiques permettant la prédiction des transformations N liées au seul contenu biochimique de l'apport (TAO-N). Les résultats TAO-C étaient intégrés dans MOMOS puis une recherche était conduite sur l'autre partie de ce modèle gérant la dynamique des microorganismes et métabolites microbiens. Des données de traceur isotopiques in situ ainsi que des analyses de sensibilité conduisaient à la proposition du nouveau modèle MOMOS-6 centré sur la respiration et la dynamique de la biomasse microbienne. MOMOS-6 ne comporte comme paramètre que des constantes de vitesse du 1er ordre liées à la température et l'humidité ainsi qu'à la qualité des intrants et aux propriétés texturales du sol. Les recherches actuelles et à venir visent à intégrer nos propositions à l'étude des écosystèmes, l'agriculture organique, le devenir des déchets et le changement global.